

THE UNIVERSITY OF HULL

**PARTICLES AT FLUID INTERFACES:
BEHAVIOUR AND DERIVED MATERIALS**

being a Thesis submitted for the Degree of Doctor of Philosophy
in the University of Hull

by

Anaïs Rocher
M.Sc. Chimie (Université Bordeaux 1)

April 2011

ACKNOWLEDGEMENTS

First and foremost, I would like to thank my academic supervisor, Prof. Bernard P. Binks, for his excellent supervision and guidance. I am sincerely grateful to have had the opportunity of learning from you, and am appreciative of all the knowledge you helped me gain.

I also thank the University of Hull for financial support in providing me a Scholarship for this project, and a bursary for presenting a poster on my work at the ECIS 2010.

I would like to thank Tony Sinclair and Ann Lowry from the University of Hull for the high-quality SEM and TEM images, respectively. Likewise, I would like to thank Mark Kirkland of Unilever for the cryo-SEM measurements, which provided lovely images. I must also thank my project students, Julia Zhu and Matthew Kibble for undertaking some of the experimental work.

I would like to show my gratitude to the Surfactant & Colloid Group, both past and present, for their support and friendship. I thank Dr Jhonny A. Rodrigues for his help at the beginning of my research. I thank especially Karl Reed, my colleague and friend, who helped me go through the Ph.D, by means of quite a few coffee breaks and conversations. I also thank Michael Thompson for his support and for being such a pleasant distraction in the lab with his songs and dances. I also thank Dr Mika Kohonen, Dr Theoni Georgiou and Dr Andrew Campbell, for the scientific and non-scientific discussions during the past three years.

Finally, for my other friends and my family, I will thank in French. Je souhaite remercier toute ma famille pour leur soutien et encouragements tout au long de ces trois ans. Tout spécialement mes sœurs, Tatiana et Caroline Rocher, qui m'ont données la volonté de leur prouver qu'elles pouvaient être fière de moi. Je remercie aussi mes parents, Dr Eric Rocher et Corinne Vivez, d'avoir eu confiance en moi et d'avoir fait l'effort d'écouter mes explications compliquées. Je souhaite aussi remercier ma grand-mère, Cécile Plumaugat, pour ses emails qui m'ont soutenus durant ma thèse. Enfin, mes remerciements les plus profonds vont à Dr Benjamin Holt, qui m'a instruite durant trois ans de thèse, avant de me faire succomber à son charme: Merci pour ta patience, ton aide et tes encouragement.

PUBLICATIONS AND PRESENTATIONS

The work contained within this thesis has given rise to the following publications and presentations:

1. B. P. Binks and A. Rocher, "Effects of temperature on water-in-oil emulsions stabilised solely by wax microparticles", *J. Colloid Interf. Sci.*, **335**, 94 (2009) DOI: 10.1016/j.jcis.2009.03.089
2. B. P. Binks and A. Rocher, "Stabilisation of liquid-air surfaces by particles of low surface energy", *Phys. Chem. Chem. Phys.*, **12**, 9169 (2010) DOI: 10.1039/c0cp00777c
3. B. P. Binks, A. Rocher and Mark Kirkland, "Oil foams stabilised solely by particles", *Soft Matter*, **7**, 1800 (2011) DOI: 10.1039/C0SM01129K.
4. B.P. Binks, A.N. Boa, M.A. Kibble, G. Mackenzie, A. Rocher, "Sporopollenin capsules at fluid interfaces: particle-stabilised emulsions and liquid marbles", *Soft Matter*, **7**, 4017 (2011) DOI: 10.1039/c0sm01516d.
5. Oral presentation: "Effects of temperature on water-in-oil emulsions stabilised solely by wax microparticles", European Student Colloid Conference, 15-18th July 2009, Almeria, Spain.
6. Poster presentation: "Temperature responsive water-in-oil emulsions stabilised by wax microparticles", UK Polymer Colloid Forum, 14-16th September 2009, University of Hull, UK.
7. Poster presentation: "Sporopollenin particles from natural *Lycopodium clavatum* at fluid interfaces", European Colloid and Interface Society, 5-10th September 2010, Prague, Czech Republic.

ABSTRACT

The objectives of this thesis are to enhance the understanding of the particle behaviour at fluid interfaces using novel and stimuli responsive particles, and how their adsorption at these interfaces affect the emulsions, foams or other materials that they are stabilising. Materials stabilised solely by particles are of great interest due to long-term stability, generally low emulsifier content and also in order to replace surfactant molecules, which are often potentially harmful with relatively inert solid materials. The adsorption/desorption of a particle from an interface depends on the particle wettability, which can be affected by the temperature, the pH or the liquid type used, to cite only a few examples. This is investigated through six different sections encompassing particle-stabilised emulsions, particle-stabilised foams and dry liquids.

The synthesis of stimuli-responsive particles and their use for production of stimuli-responsive materials is a recent area of interest particularly for bio-medical applications. It is shown in this thesis that temperature has a strong effect on the stability of water-in-oil emulsions stabilised by microwax particles. Separation of wax-stabilised emulsions can be controlled by changing the storing temperature of these emulsions: increasing the temperature results in melting of the wax, destabilising the emulsions. Conversely, the same wax particles give really stable emulsions at elevated temperature, due to potential release from the particles of surface-active molecules. Although it is observed more as a time than as a temperature effect, emulsions stabilised with biodegradable polymer particles undergo analogous separation. The initially high stability oil-in-water emulsions destabilise over time, most likely because of degradation of the polymer particles. It is observed that modification of the polymer particle surface, by grafting pH-sensitive groups on their surface, hinders emulsion separation. It is also shown that sporopollenin particles, originated from natural *Lycopodium clavatum* spores, show a change in charge and wettability with pH. This leads to emulsion inversion from oil-in-water at their high natural pH to water-in-oil at low pH. Interestingly, the sporopollenin particles also exhibit preferred orientation around water droplets: the

anisotropic sporopollenins orientate with their hemispherical side toward the oil either for a better packing geometry or due to a wettability difference.

The production of new particle-stabilised materials is another concern for this study. The production of novel emulsion drop architectures by using emulsion heteroaggregation has been attempted. Although aggregation of opposite-charge emulsion drops has been found difficult to obtain, the importance of pH, method used for mixing and excess of free particle in the continuous phase is discussed. It is also shown that the number ratio of small to large drops affects the drop aggregation. Another new material produced in this study is particle-stabilised non-aqueous foam. Fluoroethylene microparticles are observed to disperse in low surface tension oil, to stabilise air bubbles when aerated with intermediate surface tension oil, and to form a powder like material with high surface tension liquids. The effect of particle type, oil type and particle concentration on these foams are described, and freeze fracture electron microscopy is used in order to observe the close-packed arrangement of particles at the air-oil surface. Finally, production of a powdered emulsion is attempted in order to encapsulate low volume fraction of oils in a dry material. For this purpose, particle-stabilised oil-in-water emulsions were produced, before being blended with hydrophobic particles, resulting in an encapsulation of emulsion drops into particles. It is shown that the particle type, both for the initial emulsions and production of the powdered emulsions, the particle concentration, the blending time and the oil volume fraction affect the nature of the material obtained.

PARTICLES AT FLUID INTERFACES

CONTENTS

CHAPTER 1	INTRODUCTION	1
1.1	Colloidal dispersions	1
1.1.1	<i>DLVO forces</i>	1
1.1.2	<i>Non-DLVO forces</i>	5
1.2	Particles at fluid interfaces	6
1.2.1	<i>Energy of particle detachment</i>	6
1.2.2	<i>Forces between particles at fluid interfaces</i>	8
1.3	Emulsions	11
1.3.1	<i>Emulsion stability</i>	13
1.3.2	<i>Emulsions stabilised by solid particles</i>	16
1.3.3	<i>Effect of particle concentration on emulsions</i>	17
1.3.4	<i>Transitional phase inversion</i>	18
1.3.5	<i>Effect of oil type on emulsions</i>	20
1.3.6	<i>Mixture of particles and surfactant in emulsions</i>	21
1.4	Heteroaggregation in emulsions	21
1.5	Foams	24
1.5.1	<i>Foam formation and stability</i>	24
1.5.2	<i>Foams stabilised with solid particles</i>	26
1.5.3	<i>Non-aqueous foams</i>	28
1.5.4	<i>Dry water</i>	29
1.6	Presentation of thesis	30
1.7	References	32

CHAPTER 2	EXPERIMENTAL	41
2.1	Materials	41
2.1.1	<i>Water</i>	41
2.1.2	<i>Oils and other liquids</i>	41
2.1.3	<i>Particles</i>	46
2.1.3.1	Waxes and fat	47
2.1.3.2	Poly(lactic-co-glycolic) acid	49
2.1.3.3	Ludox HS-30 and Ludox CL	50
2.1.3.4	Sporopollenin	51
2.1.3.5	Teflon	52
2.1.3.6	Fumed silica	54
2.1.4	<i>Other chemicals</i>	55
2.2	Methods	56
2.2.1	<i>Surface tension of oil</i>	56
2.2.2	<i>Characterisation of particles</i>	56
2.2.2.1	Microscopy : optical, SEM and TEM	56
2.2.2.2	Light scattering	57
2.2.2.3	Differential scanning calorimetry	58
2.2.2.4	Attenuated Total Reflection Fourier Transform Infrared Spectroscopy	59
2.2.2.5	Contact angles	59
2.2.2.6	Powder wetting	60
2.2.2.7	pH titration	60
2.2.3	<i>Preparation of particle dispersions</i>	61
2.2.3.1	Wax particle dispersions	61

2.2.3.2	Fumed silica particle dispersions	61
2.2.3.3	Other particle dispersions	62
2.2.4	<i>Preparation of emulsions</i>	62
2.2.4.1	Ultra turrax homogenisation	62
2.2.4.2	Handshaking	62
2.2.4.3	Magnetic stirring	63
2.2.4.4	Temperature studies	63
	2.2.4.4.1. <i>Emulsions made at room temperature</i>	63
	2.2.4.4.2. <i>Emulsions made at different temperatures</i>	63
2.2.5	<i>Characterisation of emulsions</i>	64
2.2.5.1	Drop test	64
2.2.5.2	Conductivity	64
2.2.5.3	Stability	64
2.2.5.4	Optical microscopy	65
2.2.5.5	Zeta potential	66
2.2.6	<i>Preparation of emulsion mixtures</i>	66
2.2.7	<i>Characterisation of emulsion mixtures</i>	67
2.2.8	<i>Preparation of liquid marbles</i>	67
2.2.9	<i>Characterisation of liquid marbles</i>	67
	2.2.9.1 Static and dynamic stability	67
	2.2.9.2 Evaporation and buckling	67
2.2.10	<i>Preparation of foams</i>	68
2.2.11	<i>Characterisation of foams</i>	68
2.2.12	<i>Preparation and characterisation of powdered emulsions</i>	69
2.3	References	71

CHAPTER 3	INFLUENCE OF TEMPERATURE ON EMULSIONS STABILISED BY WAX OR FAT PARTICLES	73
3.1	Introduction	73
3.2	Wax particle characterisation	75
3.2.1	<i>DSC measurements</i>	75
3.2.2	<i>Contact angle measurements</i>	79
3.2.3	<i>ATR-FTIR measurements</i>	80
3.3	Effect of particle type	82
3.3.1	<i>Large spherical wax</i>	82
3.3.1.1	Dispersion	83
3.3.1.2	Emulsification	83
3.3.1.3	Addition of surfactant	85
3.3.2	<i>Triglyceride crystals</i>	87
3.3.2.1	Dispersion	87
3.3.2.2	Emulsification	88
3.3.3	<i>Non-spherical wax particles</i>	88
3.3.3.1	Dispersion	88
3.3.3.2	Emulsification	89
3.4	Effect of particle concentration	90
3.4.1	<i>Triglyceride crystals</i>	90
3.4.2	<i>Wax particles</i>	95
3.5	Effect of temperature	103
3.5.1	<i>Effect of temperature increase after emulsification</i>	103
3.5.1.1	Handshaking	103
3.5.1.2	Ultra turrax homogenisation	107

3.5.2	<i>Effect of temperature during emulsification</i>	109
3.5.2.1	Wax particles	109
3.5.2.1.1.	<i>Preparation and storage at high temperature</i>	109
3.5.2.1.2.	<i>Preparation at high temperature and storage at room temperature</i>	114
3.5.2.2	Triglyceride crystals	118
3.6	Conclusions	120
3.7	References	121
CHAPTER 4	EMULSIONS STABILISED BY BIODEGRADABLE PARTICLES	123
4.1	Introduction	123
4.2	Particle characterisation	125
4.2.1	<i>Dynamic light scattering</i>	125
4.2.2	<i>Contact angles</i>	129
4.3	Effect of particle type on emulsions	130
4.4	Effect of particle concentration on emulsions	132
4.4.1	<i>Variable surface chemistry</i>	132
4.4.2	<i>Variable lactic/glycolic acid ratio</i>	134
4.5	Effect of pH on emulsions	138
4.5.1	<i>Variable surface chemistry</i>	138
4.5.2	<i>Variable lactic/glycolic acid ratio</i>	143
4.6	Effect of time on emulsion degradation	145
4.7	Conclusions	151
4.8	References	153

CHAPTER 5	HETEROAGGREGATION OF EMULSIONS STABILISED BY CHARGED COLLOIDAL SILICA PARTICLES	155
5.1	Introduction	155
5.2	Zeta potential measurements of aqueous particle dispersions	157
5.3	Emulsions with dodecane	159
5.3.1	<i>Effect of pH in Ludox HS-30 systems</i>	159
5.3.2	<i>Effect of pH in Ludox CL systems</i>	163
5.4	Emulsions with isopropyl myristate	167
5.4.1	<i>Effect of pH in Ludox HS-30 systems</i>	167
5.4.2	<i>Effect of pH in Ludox CL systems</i>	171
5.4.3	<i>Effect of oil volume fraction</i>	174
5.5	Mixing of oppositely charged emulsion drops	179
5.5.1	<i>Effect of mixing method</i>	179
5.5.2	<i>Dodecane-in-water emulsions</i>	180
5.5.3	<i>Isopropyl myristate-in-water emulsions</i>	183
5.5.3.1	Effect of excess particles	185
5.5.3.2	Effect of drop number ratio	190
5.5.3.3	Effect of drop size	193
5.6	Conclusions	195
5.7	References	196
CHAPTER 6	NATURAL SPOROPOLLENIN PARTICLES: TRANSITIONAL INVERSION OF EMULSIONS AND LIQUID MARBLES	198
6.1	Introduction	198
6.2	Sporopollenin particle characterisation	201

6.2.1	<i>Powdered particles</i>	201
6.2.2	<i>Particle dispersions</i>	202
6.2.3	<i>Particles at planar fluid interfaces</i>	206
6.3	Emulsification with sporopollenin particles	208
6.3.1	<i>Effect of initial particle location</i>	208
6.3.2	<i>Effect of particle concentration</i>	210
6.3.3	<i>Effect of pH</i>	213
6.3.4	<i>Effect of oil type</i>	220
6.3.4.1	Tricaprylin	220
6.3.4.2	Dodecane	226
6.4	Liquid marbles with sporopollenin particles at the air-water interface	231
6.4.1	<i>Effect of pH</i>	231
6.4.2	<i>Evaporation and buckling</i>	232
6.4.3	<i>Effect of salt concentration</i>	236
6.5	Conclusions	238
6.6	References	239
CHAPTER 7	NON-AQUEOUS FOAMS STABILISED SOLELY BY TEFLON PARTICLES	241
7.1	Introduction	241
7.2	Tetrafluoroethylene particle characterisation	243
7.2.1	<i>SEM imaging</i>	243
7.2.2	<i>Light scattering</i>	243
7.2.3	<i>Powder immersion tests</i>	246
7.2.4	<i>Contact angles</i>	248
7.3	Non-aqueous foams with TFE particles	251

7.3.1	<i>Effect of mixing method on foams</i>	251
7.3.1.1	Blender homogenisation	251
7.3.1.2	Ultra-turrax homogenisation	253
7.3.1.3	Handshaking	255
7.3.1.4	Diffuser aeration	257
7.3.2	<i>Effect of liquid type on foams</i>	258
7.3.3	<i>Effect of particle type on foams</i>	264
7.3.4	<i>Effect of particle concentration on foams</i>	267
7.4	Dry powder with PTFE particles	271
7.5	Conclusions	274
7.6	References	275
CHAPTER 8	POWDERED EMULSIONS STABILISED BY FUMED SILICA PARTICLES	278
8.1	Introduction	278
8.2	Oil-in-water emulsions	279
8.2.1	<i>Effect of particle hydrophobicity on emulsions</i>	279
8.2.2	<i>Effect of particle concentration on emulsions</i>	280
8.3	Oil-in-water-in-air powdered emulsions	284
8.3.1	<i>Effect of particle hydrophobicity on powdered emulsions</i>	284
8.3.2	<i>Effect of blending time on powdered emulsions</i>	287
8.3.3	<i>Effect of initial oil fraction on powdered emulsions</i>	290
8.4	Conclusions	294
8.5	References	295

CHAPTER 9	SUMMARY OF CONCLUSIONS AND FUTURE WORK	296
9.1	Conclusions	296
9.2	Future work	298
9.3	References	301
APPENDIX		

LIST OF SYMBOLS AND ABBREVIATIONS

r	radius of the particle
g	acceleration due to gravity
ϵ	permittivity of free space
γ	surface tension or interfacial tension
η	shear viscosity
θ	contact angle
ϕ	volume fractions
κ	reciprocal of the Debye length
ρ	density
ζ	zeta potential
K	conductivity
Ψ_0	particle surface potential
[]	concentration
A_H	Hamaker constant
f_{aq} (or f_{oil})	fraction of water (or oil) resolved
K_a	acid dissociation constant
pK_a	$-\log K_a$
v_f, v_l and v_t	volumes of foam, liquid and total volume
wt. %	weight percentage
%SiOH	silanol content
1-D/2-D/3-D	1 dimension/2 dimensions/3 dimensions
L:G	lactic-glycolic acid ratio
S:L	number ratio of small to large drops
ATR-FTIR	Attenuated Total Reflection Fourier Transform Infrared Spectroscopy
AOT	sodium di(2-ethylhexyl) sulfosuccinate (Aerosol-OT)
Cryo-SEM	Freeze-fracture Scanning Electron Microscopy

DLVO	Derjaguin and Landau, and Verwey and Overbeek
DSA	Drop Shape Analysis
DSC	Differential Scanning Calorimetry
GTT	Gel Trapping Technique
HLB	hydrophile–lipophile balance
HPC	hydroxypropylcellulose
IPM	isopropyl myristate
OTFE	oligomer of tetrafluoroethylene
PDMS	polydimethylsiloxane
PEO	poly(ethylene oxide)
PIT	Phase Inversion Temperature
PLGA	poly(lactic-co-glycolic acid)
PLGA-COOH	poly(lactic-co-glycolic acid) modified with carboxylic groups
PLGA-NH ₂	poly(lactic-co-glycolic acid) modified with amidine groups
PTFE	polytetrafluoroethylene
SA	stearic acid
SEM	Scanning Electron Microscopy
TEM	Transmission Electron Microscopy
TFE	tetrafluoroethylene
UV	Ultraviolet
<i>cf.</i>	confer
<i>e.g.</i>	for example
<i>et al.</i>	and others
<i>i.e.</i>	in other words
§	section

CHAPTER 1 INTRODUCTION

1.1 Colloidal dispersions

A colloidal dispersion is defined as a two-phase system, where one phase (the dispersed phase) is dispersed in the second phase (the continuous phase).¹ The dispersed phase, usually in the size range 1 nm to 10 μm , may consist of spherical solid particles, liquid droplets or gas bubbles, as well as cube, plate or rod-like solid particles. The phases may be combinations of gases, liquids and solids, forming complex systems like aerosols, smoke, foams or emulsions.

Most colloidal dispersions are not thermodynamically stable, but as a consequence of the small size and large surface area of colloid, as well as the presence of a stabilising interfacial film on droplets, bubbles or particles, dispersions of these species can exhibit reasonable kinetic stability.² The large area-to-volume ratio of the dispersed phase characterising colloidal dispersions plays an important part in determining interactions within the system: the large interfacial area is associated with a large interfacial energy, which will often cause the dispersed phase to consolidate. Hence, the stability of colloidal systems is characterised by tendency to sediment (or cream) due to density difference, or their tendency to aggregate and coalesce/fuse. Encounters between species in a dispersion occur frequently (due to Brownian motion, sedimentation or stirring), and so dispersion stability depends upon how the species interact when this happens. In order to prevent aggregation, the repulsive energies between the colloids must be greater than the attractive ones. This interaction is quantitatively described by Derjaguin and Landau, and Verwey and Overbeek, known as DLVO theory.^{3,4}

1.1.1 DLVO forces

The DLVO theory takes into account the attractive van der Waals and the repulsive electrostatic energy between charged particles as they approach each other.^{3, 4} The theory includes estimations of the London-van der Waals energy as a function of interparticle distance and the energy due to the overlap of electric double layers, and their summation to give the total interaction energy.

The van der Waals attractive force is instigated by an uneven electron distribution around the atoms creating a dipole, and by extension an asymmetrical charge distribution on a particle surface. The total van der Waals interaction results from the sum of a dipole-dipole force (Keesom force), dipole-induced dipole force (Debye force) and dispersion forces (London force), with dispersion forces the main sources of attraction between colloidal particles.⁵ The early calculations, made by Hamaker and de Boer, involve summing the interaction of one atom in a particle with each atom in the adjacent particle and then summing that interaction over all the atoms in the first particle.⁶ The long-range interaction resulting from this calculation is directly proportional to the particle radius (r) and the composite Hamaker constant (A_H), and is inversely proportional to the particle separation (d). When the particle separation is small ($d \ll 2r$), the attractive potential energy is reduced to a simple form as in equation 1.1:

$$V_A = \frac{A_H}{d^2} \quad (1.1)$$

The Hamaker constant is a function of both the electronic polarisability and the density of the material: particles immersed in a medium experience a weakened attraction, due to their attraction with the medium. The composite Hamaker constant (A_H) used in equation 1.1 is estimated in equation 1.2 as the geometric mean of that of the particle (A_p) and that of the medium (A_m) with respect to their values in vacuum:

$$A_H = \sqrt{A_p} - \sqrt{A_m} \quad (1.2)$$

When the particles and the medium exhibit similar Hamaker constants, the composite Hamaker constant is small, leading to reduced attractive potential energy (V_A) and a more stable particle dispersion.

Electrical repulsion, due to the overlap of electric double layers of particles, is a key stabilising mechanism for particle dispersions in aqueous solutions or in liquids of moderate dielectric constant. The electrostatic repulsion can be explained with electrical double layer theory, which has been described by the Debye-Hückel approximation, and later by the Gouy-Chapman theory modified by Stern.¹ In a liquid, a surface can be charged either by surface group dissociation (*e.g.* SiOH for

silica) or by adsorption of charged molecules from the solution. As a result, the surface attracts oppositely charged ions (or counterions) forming the electrical double layer.

Figure 1.1. Schematic of the Electrical Double Layer of a positively charged surface. ϕ_0 is the potential at the surface, ϕ_s is the potential at the Stern layer and ζ is the potential at the slip plane.

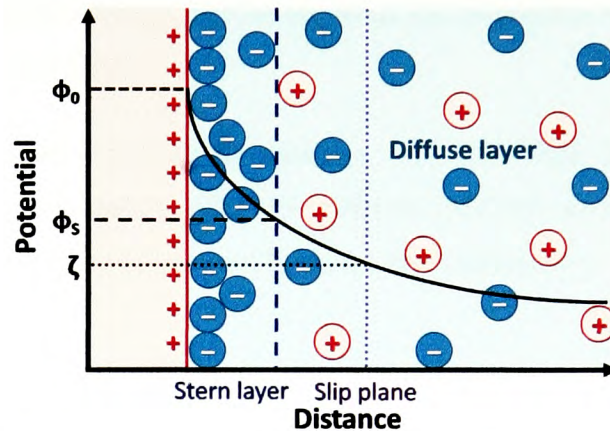


Figure 1.1 illustrates the electrical double layer for a positively charged surface: in solution the colloidal surface charge is balanced by an equal amount of oppositely charged ions gathered in a region of excess charge. Two regions constitute the electrical double layer: the Stern layer with ions strongly bound to the surface which has an electric potential decreasing with the distance from the particle surface, and the diffuse (or Gouy) layer which contains counterions distributed freely in the solution. The slip plane defines the region where the fluid moves together with the particles when an electrical field is applied in the solution; the potential at this plane is called the zeta potential (ζ). The electrical double layer with its counterion layer causes a screening of the particle charges; hence the zeta potential measured is always lower than the surface potential.

When two particles approach each other, their electrical double layers overlap and force the particles apart. The repulsive interaction energy between non-identical spheres under constant charge decreases exponentially with distance from the particle surface, and can be integrated with respect to distance:⁷

$$V_R = \frac{\epsilon r \Psi_0^2}{2} \ln 1 - \exp -\kappa d \quad (1.3)$$

where ϵ is the permittivity of free space, Ψ_0 is the particle surface potential and κ the reciprocal of the Debye length.

By combining the van der Waals interaction energy and the electrical double layer interactive energy, the total interaction between two particles or two surfaces in a liquid can be expressed by:

$$V = V_R + V_A \quad (1.4)$$

where the total interaction energy (V) results from the summation of the repulsive (V_R) and attractive (V_A) energies.

Figure 1.2. Total colloidal interaction energies, $V(1)$ and $V(2)$, obtained by the summation of an attractive energy, V_A , with different repulsive energies, $V_R(1)$ and $V_R(2)$ as a function of particle separation. Redrawn from reference 1.

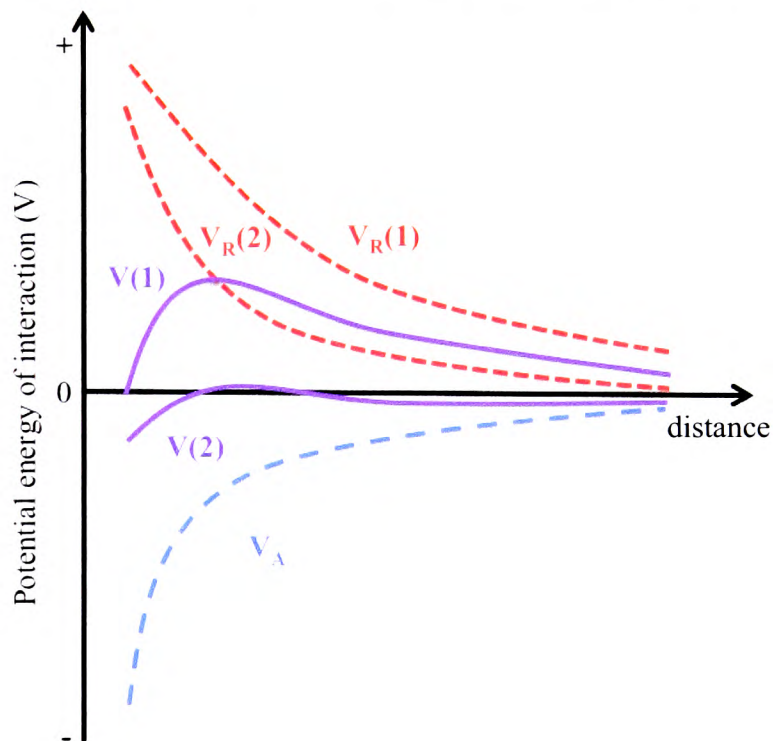


Figure 1.2 shows two general types of potential energy curve: the total interaction energy $V(1)$ exhibits a predominantly repulsive energy maximum, whereas that of $V(2)$ curve is attractive at almost all interparticle separations. For low electrolyte concentrations, electrical double-layer repulsion dominates ($V_R(1)$), so the particle dispersion is kinetically stable. As the electrolyte concentration is increased,

the electrical double layer repulsion is reduced ($V_R(2)$) and the inter-particle van der Waals attraction becomes more dominant causing an increase of the coagulation rate of the particles.

If the pH is brought close to the particle isoelectric point pH, the electrical double layer repulsion is also affected through a decrease in surface potential and the particle coagulation rate increases.

1.1.2 *Non-DLVO forces*

The DLVO theory neglects some interaction between particles because it treats the liquid in which particles are dispersed as a structureless continuum. At short separation, the medium has to be considered as a discrete structure, where the liquid molecules can order themselves and affect particle interaction. These short distance interactions have been called structural forces by Derjaguin, and are also known as solvation or hydration forces for aqueous dispersions.³ Hydration forces are short-range forces, which arise whenever water molecules strongly bind to a surface containing hydrophilic groups.⁸ For example, Binks and Lumsdon stated that silica is subjected to a repulsive force due to the polar surface inducing an ordering of the solvent.⁹ Consequently, they proposed a model based on the DLVO theory including a hydration-repulsion term (V_h) proportional to the solution electrolyte concentration, which better describes the behaviour of their silica particles in solution. On the other hand, attractive hydrophobic forces are longer range than hydration forces (up to 100 nm). They are mediated by structural changes in the thin water layer between hydrophobic surfaces.⁸

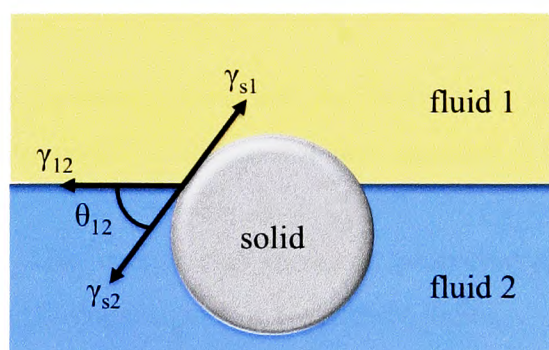
Two other major interparticle forces to consider are the steric force, which generally results from a surface layer of long chain organic molecules (like surfactants or polymers) overcoming the van der Waals attractive forces through unfavourable overlap of inter-particle surface layers, and the depletion force caused by a concentration gradient (of molecules or smaller particles) in the solution between the particles.¹⁰ The latter effect is attractive or repulsive depending on small particle volume fraction and interparticle separation producing either flocculation or stabilisation of the large particles.¹¹

1.2 Particles at fluid interfaces

1.2.1 Energy of particle detachment

Solid particles of colloidal dimension can adsorb at a fluid interface, air-liquid or liquid-liquid, which classifies them as surface-active. Their adsorption decreases the area of the fluid interface, with characteristic energy often higher than the thermal energy kT ; hence it is thermodynamically favourable.¹² Ramsden and Pickering were the first to realise that particles are surface-active while investigating the field of particles at liquid interfaces.^{13, 14} In 1903, Ramsden studied the spontaneous formation of solid layers on free surfaces (i.e. air-water) of protein solutions.¹⁴ Pickering, in 1907, published a paper which aimed at understanding the nature of emulsification and finding a new emulsifier for insecticidal purposes.¹³ This led to the discovery of a solid particulate emulsifier from copper sulphate that gave paraffin oil-in-water emulsions stable to creaming and coalescence. Their studies led to numerous works on emulsification with solid particles, especially on the effect of particle flocculation and on the wettability of solid surfaces.^{15, 16}

Figure 1.3. Schematic diagram of a spherical solid particle at a fluid-fluid interface showing the various interfacial energies and the three-phase contact angle measured into the fluid 2 phase.¹⁷



The particle wettability is a key parameter to understand particle behaviour at liquid interfaces. Therefore the three-phase contact angle θ needs to be measured. The contact angle is the angle at which a fluid-fluid interface meets the solid surface. Measured through the most polar of the two fluids, θ exists at each point of the three-

phase contact line where the solid and the two fluids meet. In a fluid 1-fluid 2 system, as shown in Figure 1.3, θ is measured through the fluid 2 phase, and depends on the surface free energies (or interfacial tensions) at the solid-fluid 2 (γ_{s2}), solid-fluid 1 (γ_{s1}) and fluid 1-fluid 2 (γ_{12}) interface according to Young's equation,¹⁸

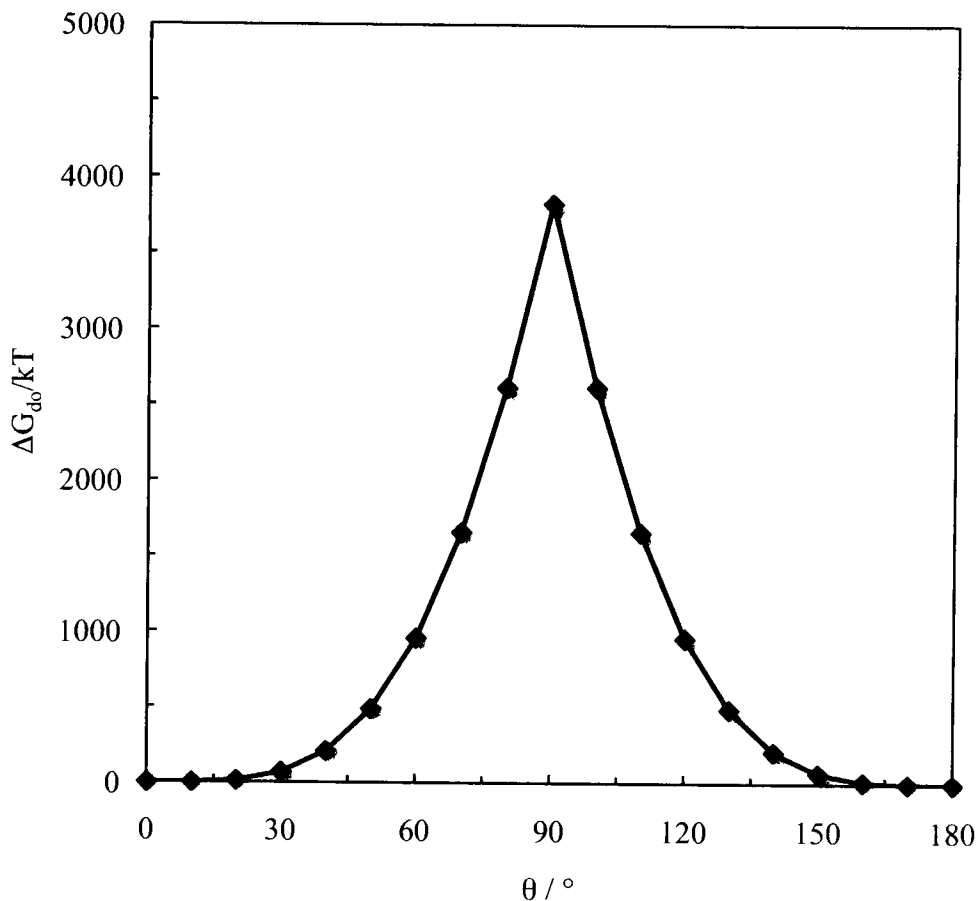
$$\cos\theta = \frac{\gamma_{s1} - \gamma_{s2}}{\gamma_{12}} \quad (1.5)$$

In an aqueous system, particles are either "hydrophilic" or "hydrophobic" depending on whether their contact angle through water is respectively smaller or larger than 90°. Particle wettability is also influenced by parameters such as surface roughness or particle shape. The equilibrium position of a solid particle at a horizontal fluid interface can be easily calculated for particles with simple shapes and smooth surfaces or sharp edges; this problem becomes difficult to solve in the case of complex shaped particles and inhomogeneous surfaces.¹⁹⁻²¹ For a spherical particle of radius r adsorbed at an oil-water interface at contact angle θ , the depth of immersion into water is $r(1 + \cos\theta)$. The energy needed to remove a particle from the oil-water interface is related not only to the wettability but also to the interfacial tension (γ_{ow}).¹⁷ The area of oil-water interface removed by the particle when it adsorbs is equal to $\pi r^2 \sin^2\theta$ (or $\pi r^2(1 - \cos^2\theta)$). Hence the energy required to remove the particle into the oil phase is

$$\Delta G_{do} = \pi r^2 \gamma_{ow} (1 - \cos\theta)^2 \quad (1.6)$$

For removing the same particle into the water phase, the sign before $\cos\theta$ in equation 1.6 becomes negative. Figure 1.4 and equation 1.6 make clear that the energy needed for removing a particle from the oil-water interface will be maximal when θ equals 90°. This energy also increases proportionally with the oil-water interfacial tension and with the square of the particle radius.

Figure 1.4. Variation in minimum energy of particle detachment *versus* contact angle in the case of a spherical particle of radius $r = 10$ nm at the planar dodecane-water interface of interfacial tension $\gamma_{ow} = 50$ mN m⁻¹ at 298 K.¹⁷



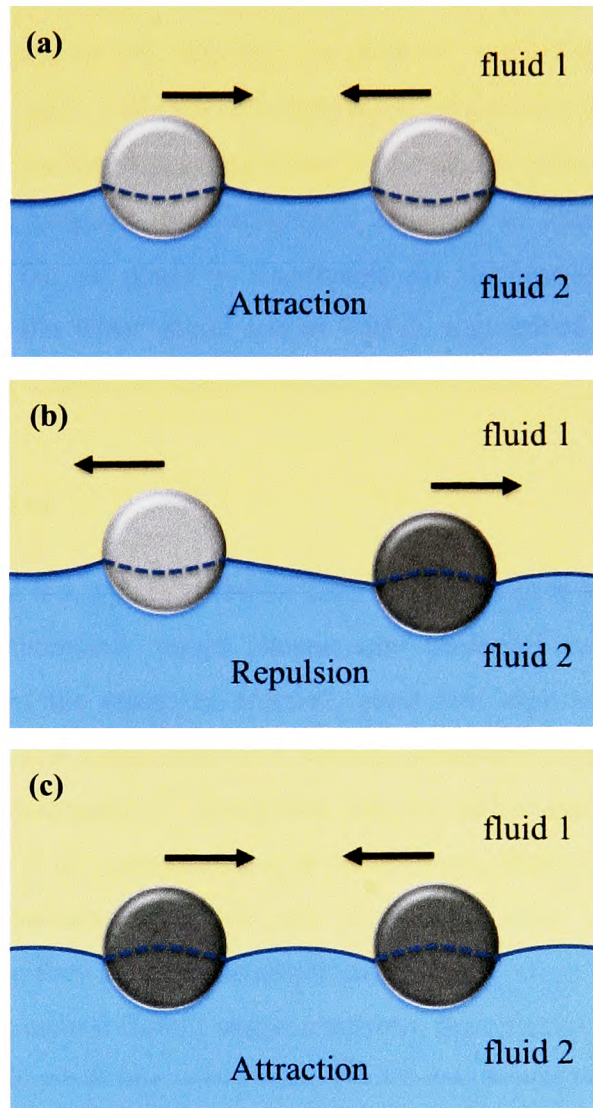
1.2.2 Forces between particles at fluid interfaces

At fluid interfaces, particles are affected by the same forces as those described in section 1.1 for bulk dispersions. However, some additional forces which have no analogy in bulk appear due to the presence of the second fluid creating an interface: capillary and long range repulsion interactions between the particles are introduced in addition to DLVO theory, the structural, steric and depletion forces. The DLVO expressions for the van der Waals and the electrical double layer energy have to be corrected:²² the presence of the interface reduces the degrees of freedom for particle movement, and in fluid-water systems particles are only partially in contact with the water phase, the main medium for carrying electrostatic repulsion. The van der

Waals energy, as seen in equation 1.1, varies with the Hamaker constant, which itself depends on the bulk phase. These forces will be different for the emergent parts and the immersed parts of the particles. When modelling these interactions Fernandez-Toledano *et al.* only considered the interaction between their emergent parts and between their immersed parts and neglected that between the emergent part of one particle and the immersed part of another.²²

Capillary interaction arises from the contact of particles with the fluid-fluid interface:²³ particle interactions differ with both phases, causing perturbation of the interface (depression or elevation) and forming the so-called meniscus around the particle. The overlap of the menisci of two approaching interfacial particles generates an interaction that can be either attractive or repulsive, enhancing or preventing particle surface flocculation. Two categories of capillary interaction exist: flotation and immersion capillary forces. Flotation capillary forces are due to gravitational effects: interfacial deformation depends on the particle weight and the buoyancy force. As shown in Figure 1.5, particles less dense than the lower fluid and those denser than it will create respectively positive and negative menisci. The overlap of same curvature menisci generates an attractive force between the particles, driven by a decrease in interfacial deformation. However, the overlap of opposite curvature menisci results in an increase in the interfacial deformation, causing the particles to experience a repulsive capillary force. These long-range interactions are negligible for particles of small size (radius below 5 μm), as they are unable to significantly deform the interface and the resulting interaction is negligible compared to that of the thermal energy. On the other hand, immersion capillary forces are caused by the wetting properties of the particle surface, *i.e.* to the position of the contact line and the magnitude of the contact angle, rather than to gravity. These interactions, which are also long-range, affect small colloidal particles trapped at liquid interfaces over a substrate or in a thin liquid film, causing their aggregation and ordering as observed in many experiments.²⁴ Recent studies have shown that immersion forces can also be caused by particle surface roughness, producing an irregular meniscus, or by electro-dipping, for which an external electric field pushes the particle into the more polar fluid.²⁵⁻³⁰

Figure 1.5. Capillary flotation interaction forces between two particles at a fluid-fluid interface: the resulting interaction force is attractive if the two particles are (a) less dense or (c) more dense than fluid 2, respectively. However the force is (b) repulsive between more and less dense particles. Redrawn from reference 5.



Aveyard *et al.* with polystyrene latex particles and Horozov *et al.* with silica particles have demonstrated the presence of a long-range repulsion by studying the structure and stability of particle monolayers at horizontal interfaces.^{31, 32} They have shown that the repulsion between hydrophilic particles ($\theta = 65^\circ$) at horizontal liquid interfaces is weak and mediated mainly through the water phase, resulting in disorder and loose flocculation of the particles. In contrast, monodispersed hydrophobic particles ($\theta = 152^\circ$) gave well-ordered monolayers of particles separated by several times the particle diameter, suggesting a very long-range repulsion mediated through the oil phase. It is believed that entrapment of traces of hydration water of the particle surface in the oil phase is responsible for the repulsion through oil, as addition of salt in the water phase led to further aggregation of the hydrophilic particles but did not change the state of the hydrophobic ones.

1.3 Emulsions

An emulsion is a type of colloidal dispersion, as seen in section 1.1, which is formed by two immiscible liquid phases, one dispersed as droplets within a continuous phase of the other. In practice, emulsions may contain droplets that exceed the classical size range limits of a colloid, sometimes ranging upwards to tens or hundreds of micrometres.³³ Emulsions can be either oil-in-water, when oil droplets are formed in an aqueous phase, or water-in-oil, when the dispersed phase is water. Complex emulsion types can also be formed when droplets themselves contain an emulsion; they are called multiple emulsions.

Pure liquids cannot form a stable emulsion. Specifically, the interfacial area between two liquids when one is dispersed as droplets in the other is larger than a single interface between the two bulk phases. Hence, the two liquids will separate to recover their minimum energy state. A third component called an emulsifier is needed to make the emulsion easier to form or to form a protective film, which will hinder the breaking of the emulsion: this is often a surfactant or solid particles.³⁴

Surfactants are amphiphilic compounds with one side that has an affinity for the nonpolar phase (the nonpolar hydrocarbon chain) and an other part that has an affinity for the polar phase, usually water (the polar group). At a fluid interface, it is

energetically more favourable for the surfactant molecules to orientate in such a way that each part of the molecule resides in the phase for which it has the greatest affinity. The nature of the surfactant will determine the dispersed and the continuous phase of an emulsion: Bancroft's rule, the oriented wedge theory, the hydrophile–lipophile balance (HLB) and the volume balance value were developed in order to predict the type of emulsion to be formed with a specific surfactant.^{35, 36} The HLB, which has been the most commonly used theory, relies on the hydrophilicity or lipophilicity of the surfactants: low HLB surfactants (lipophilic) usually stabilise water-in-oil emulsions, while high HLB surfactants (hydrophilic) would rather make an oil-in-water one.³⁷

Adsorption of surfactants at fluid interfaces is driven by the decrease of interfacial free energy (γ), which represents the amount of work required to expand the interface per unit area.³⁸ In the case of microemulsions, this decrease is sufficient to render the emulsification process spontaneous.³⁹ Macroemulsions however are generally considered thermodynamically unstable, due to the positive value of free energy of emulsion formation given by:³⁸

$$\Delta G = \gamma\Delta A - T\Delta S \quad (1.7)$$

where ΔG is the change in free energy of the system, γ the interfacial tension, ΔA the change in interfacial area, T the temperature and ΔS the change in entropy.

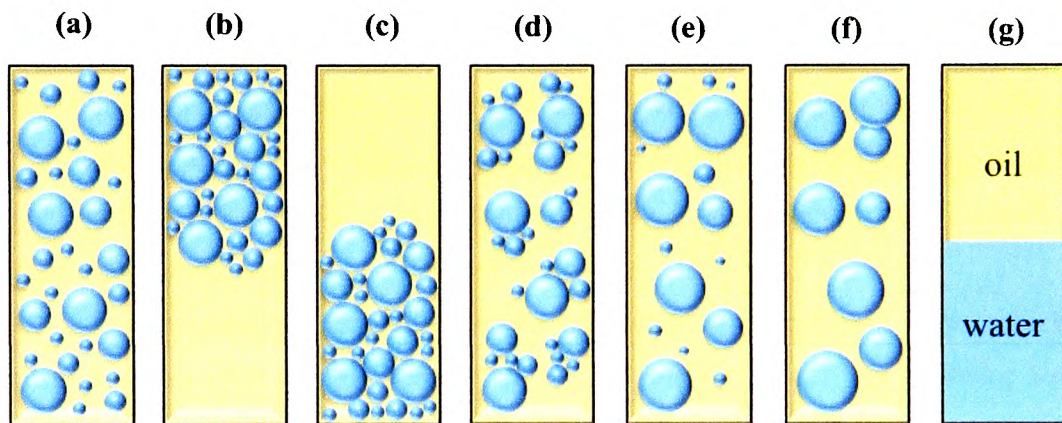
In macroemulsions, the energy required to expand the interface ($\gamma\Delta A$, with ΔA increase in interfacial area and γ is the interfacial tension) is large and positive and cannot be compensated by the small entropy of dispersion $T\Delta S$, which is also positive. This leads to a positive total free energy of formation of an emulsion, ΔG , meaning that the emulsion formation is non-spontaneous and that energy is required to produce the droplets.⁴⁰ Large droplets, requiring a low increase of interface, are fairly easy to form by breaking the two bulk phases with high-speed stirrers for example. In contrast, producing nanoemulsions necessitates a high energy or low interfacial tension.³⁷

As most emulsions are thermodynamically unstable, the kinetics of destabilisation determines whether emulsions have lives long enough to be useful.³³

1.3.1 Emulsion stability

The stability of an emulsion is defined as a resistance to physical changes over time. Flocculation, coalescence, sedimentation and creaming of the emulsion drops can affect this stability by occurring simultaneously or consecutively in the emulsion. Figure 1.6 illustrates these effects for a water-in-oil emulsion.⁴⁰

Figure 1.6. Processes affecting (a) water-in-oil emulsion stability: (b) creaming, (c) sedimentation, (d) flocculation, (e) Ostwald ripening and (f) coalescence, (g) resulting in complete phase separation.⁴⁰



Creaming and sedimentation are results of gravitation separations often indicated by the emergence of a distinct clearer phase less concentrated in droplets at the top or the bottom of the system. The term creaming comes from the familiar separation of cream from raw milk. The density difference between the dispersed and continuous phases causes a vertical concentration gradient in the system. Although the two separate layers produced have different dispersed phase concentrations, gravitation separation is not necessarily destabilisation of the emulsion as a gentle agitation of the system totally reverses the separation. However high levels of sedimentation or creaming can promote flocculation and coalescence.

Mathematical models applying Stokes' Law can be used to predict the rate at which an isolated drop (described as a rigid spherical particle) creams in an ideal liquid.³³

$$v_s = -\frac{2gr^2(\rho_2 - \rho_1)}{9\eta_1} \quad (1.8)$$

where v_s is the creaming velocity, r is the radius of the particle, g is the acceleration due to gravity, ρ_x is the density of fluid x , η_1 is the shear viscosity of fluid 1, and 1 and 2 refer to the continuous and dispersed fluid, respectively.

The sign of v_s establishes the movement of the drop in the surrounding fluid: the drop creams for positive values and sediments for negative values. Equation 1.8 highlights that gravitational separation can be retarded in an emulsion by reducing the density difference between the oil and water phases, decreasing the size of the droplets or increasing the viscosity of the continuous phase. A more accurate model would include other factors, like droplet fluidity, concentration, polydispersity, charge and interactions.⁴¹

Drop flocculation can be defined by the gathering of emulsion drops, which form aggregates with virtually no change in total surface area.³³ The tendency for droplets to flocculate depends mainly on the balance of attractive and repulsive forces between the drops: if attractive forces dominate (van der Waals, depletion and hydrophobic forces), the droplets will tend to aggregate, whereas they will be stable to aggregation if the repulsive forces dominate (electrostatic and steric forces), as described in section 1.1. The rate at which droplet flocculation occurs can be characterized in terms of the droplet-droplet *collision frequency* and *collision efficiency* defined by McClements.⁴¹ The collision frequency is the number of droplet collisions per unit volume of emulsion per unit time, which depends on Brownian motion, applied mechanical forces or gravity. The collision efficiency represents the fraction of droplet-droplet encounters that actually lead to flocculation, determined by the droplet interaction potential. Hence, flocculation in dilute emulsions causes an increase of creaming, resulting from the increase in mean particle size, whereas the creaming is retarded or prevented by formation of 3D networks of droplets in concentrated emulsions.⁴²

In contrast, drop coalescence affects the drop size: it occurs when two or more droplets fuse together to form a single larger unit, reducing the total surface area. It happens through a nucleation hole or bridge in the thin liquid film separating two droplets in close proximity: when the hole reaches a critical size, it grows and droplets coalesce in order to relax their shape under an interfacial tension effect, creating a new drop with reduced interfacial area.² If coalescence continues, the two phases separate totally, recovering the state of minimum energy. Coalescence causes an increase of the creaming or sedimentation rate of the droplets in the emulsion because of the increase in drop size. A change in the emulsion appearance often results from coalescence: large droplets scatter less light than small ones, so emulsions can appear less turbid and more intensely colored.⁴³ Coalescence proceeds either through a homogeneous or heterogeneous process:⁴⁴ for the homogeneous process, all the droplets grow at the same rate, so that a monomodal drop size distribution is formed, while the heterogeneous process cause the large droplet to increase quicker, in a similar way to Ostwald ripening.

Ostwald ripening is another way in which emulsions destabilise: large droplets grow at the expense of small ones because of mass transport of dispersed phase from one droplet to another through the continuous phase.⁴⁵⁻⁴⁷ This is due to the solubility differences of molecular species between dissimilar size drops, the solubility increasing as the size of the droplet decreases:^{45, 48}

$$S(r) = S(\infty) \exp\left(\frac{\alpha}{r}\right) \quad (1.9)$$

where $S(\infty)$ is the solubility of the solute in the continuous phase for a droplet with infinite curvature, $S(r)$ is the solubility of the solute when contained in a spherical droplet of radius r , $\alpha (= 2\gamma V / RT)$ is a characteristic length scale, with V the molar volume of the solute and γ the interfacial tension.

From the point of view of emulsion stability this process is almost always undesirable because the larger species will have greater rates of sedimentation or creaming. The rate of Ostwald ripening can be reduced by adsorbing surfactants and/or polymers at the interfaces, as they can hinder the rate of incorporation of new molecules into dispersed species, or by adding components that reduce the rate of diffusion of molecules within the continuous phase.⁴⁹

1.3.2 *Emulsions stabilised by solid particles*

Solid particles are present in many types of emulsions, but their use as sole emulsion stabiliser, or in addition to surfactants has been brought to attention only recently.¹² Solid-stabilised emulsions were named "Pickering emulsions" after Pickering, who conducted the first systematic study in 1907 on this subject and recognised the role of finely divided insoluble emulsifiers:¹³ he noted that particles more wetted by water than oil stabilised oil-in-water emulsions by residing at the interface. However, Ramsden was the first to actually report emulsions stabilised by fine solid particles four years earlier than Pickering in 1903.^{14, 50} Later, Finkle *et al.* considered that particles would preferentially reside in one of the liquids of the emulsion, which would become the continuous phase, similarly to Bancroft's rule in surfactant-stabilised emulsions.³⁵ This was better understood from the study by Schulman and Leja, which investigated the effect of particle wettability and interface contact angle in systems containing barium sulphate crystals and surfactant.¹⁶ Particles with contact angles slightly below 90° were found to produce oil-in-water emulsions, while those with contact angles slightly above 90° stabilised water-in-oil emulsions. However no stable emulsions were formed for extreme values of contact angles (close to 0 and 180°).

As described in section 1.2, particles can adsorb to fluid interfaces, and as such they stabilise droplets in emulsions (or bubbles in foams) by creating single or multiple particle layers. However, the wetting behaviour of solid particles is crucial in determining emulsion behaviour. Particles have to be wettable by both water and oil phases for emulsion stabilisation to be efficient.¹⁶ Like surfactants, the particle layer will curve such that the larger fraction of particles resides in the liquid which preferentially wets them.^{17, 51} Hence, hydrophilic particles with contact angle below 90° give oil-in-water emulsions, whereas hydrophobic ones with contact angle above 90° give water-in-oil. For particles with a contact angle of 90°, which means that they are equally wetted by both phases, emulsion type depends on the particle and solution properties.⁴⁰

It is believed that the main stabilisation mechanism for particle-stabilised emulsions happens through formation of a steric barrier, created by organisation of the particles in a close packed network at the interface.⁵²⁻⁵⁴ The particle layers

physically prevent coalescence of two colliding droplets. The formation of inter-droplet networks can also slow down or hinder the destabilisation of the emulsion by changing its rheological properties.⁵⁵ Another mechanism for emulsion stabilisation has been discussed by Horozov and Binks:⁵⁶ slightly hydrophobic particles were observed to “bridge” emulsion droplets, with an increase of particle density within the bridging film due to immersion capillary attraction (discussed in section 1.2.2). Vignati *et al.* witnessed stabilisation of droplets sparsely covered by domains of particles with formation of a single or double layer bridge at inter-droplet contact areas.⁵⁷ The stabilisation of drops sparsely coated with particles could also result from the formation of a 2-D network of particles on the drop surface.⁴⁰ Formation of a 3-D network of particles within the continuous phase has also been observed to increase emulsion stability.⁵⁸ Although particle layers are still present on the drop surface, the particle network extending through the continuous phase improves stability by preventing droplet-droplet contact and arresting drop movement.

A wide variety of particle types have been used as emulsion stabilisers to date: silica, latexes, metal oxides and sulphates, clays and carbon, waxes and microgels.^{9, 34, 59-65} Their effectiveness as emulsion stabiliser depends on their shape and size, their wettability and inter-particle interactions, as well as the emulsion medium.¹⁷ Some particles (like microgels) are able to invert the type of emulsion they are stabilising with change of pH or temperature.^{66, 67} Others, like paramagnetic particles, can also prevent as well as induce the destabilisation of an emulsion through application of external magnetic fields.⁶⁸

1.3.3 *Effect of particle concentration on emulsions*

Particle concentration in a system will significantly affect the characteristics and stability of emulsions they stabilise.^{69, 70} Apart from a few recent studies, which showed stable emulsions with low surface coverage of the droplets by particles, increasing the particle concentration will enhance the volume of most particle-stabilised emulsions and/or reduce the size of the drops.^{57, 60, 71} Emulsion drops with adsorbed particles usually coalesce until they reduce their interfacial area such that it is sufficiently covered with particles: this process is known as limited coalescence.^{69, 72} A linear relation between the inverse average droplet diameter and the

concentration of particles is generally established and assumes a constant adsorbed particle layer density.⁶⁹ This phenomenon has a limit however: Tambe and Sharma showed that above a limiting concentration corresponding to a full drop coverage by particles, any increase in concentration of particles would not result in smaller droplets or increased emulsion stability.⁷³ Excess particles have however been shown to increase emulsion stability by providing a 3-D network of particles surrounding droplets covered with particles.^{58, 74} To achieve high particle coverage of droplets a sufficient high particle concentration is needed in all systems. However high particle concentrations do not necessarily produce a densely packed monolayer, and many stable emulsions have been observed without this dense coverage.^{57, 60} Yan and Masliyah and Levine and Sanford observed the presence of particles in bulk emulsion phases when complete monolayer coverage of the emulsion droplets would require more particles than present in the system.^{75, 76} The diverse mechanisms for the stability of particle-stabilised emulsions, including steric hindrance or network formation, with both partial and complete particle coverage were reported in section 1.3.2.

1.3.4 *Transitional phase inversion*

Because it determines its wettability, the right particle surface chemical nature is essential in order to obtain emulsions with optimum stability. With a change in nature, pH or salt concentration some particles are able to invert the type of emulsions which they stabilise from oil-in-water to water-in-oil at fixed water-oil volume ratio; this is known as transitional phase inversion.^{77, 78}

In a traditional surfactant system, an emulsion inversion at fixed oil-water ratio requires affecting the surfactant HLB number, by changing the electrolyte concentration or the ratio of surfactants in a mixture.⁷⁹ For particulate emulsifiers, the equivalent of the HLB number is θ , the contact angle of the particle at the oil-water interface, which corresponds to the particle wettability. This can be varied by modifying the particle surface chemistry by adding a surfactant or chemically grafting different groups.^{73, 80} Tambe and Sharma showed how to control the wettability of several types of particles:⁸¹ by changing the concentration of stearic acid in the oil phase, they were able to induce phase inversion because the normally

water-wet particles became oil-wet. The stearic acid molecules were believed to contribute to the particle behaviour at the interface. Another way to control the particle wettability was found by Binks and Lumsdon, who varied the silanol content of silica particles, changing the particle surface with a covalently bound hydrophobising agent.⁵¹ The non-modified silica particles were hydrophilic due to the silanol groups on their surface, and so increasing levels of modification gave increasingly more hydrophobic particles of reduced silanol content. Toluene-water emulsions stabilised with the modified particles were shown to invert with the extent of particle modification: so that 79%SiOH particles stabilised oil-in-water emulsions and 50%SiOH particles stabilised water-in-oil. Binks and Lumsdon also demonstrated that transitional phase inversion can be achieved using silica particles hydrophobised to different extent and mixtures of different wettability particles.^{78, 82} It was observed that the stability to creaming and sedimentation of the emulsions was greatest around conditions of inversion, and that the average drop size displayed a distinct minimum. Several subsequent emulsion inversions have also been achieved for systems containing a nanoparticle-surfactant mixture of opposite charge.⁸³ The adsorption of surfactants on the particle surface increases particle hydrophobicity, causing oil-in-water to water-in-oil inversion, which subsequently turns back to oil-in-water upon deposition of a second surfactant layer, rendering the particles hydrophilic once more.

Another simple way of changing the particle wettability consists of varying the pH of the system.^{67, 84-89} This will affect the degree of charge on the particles if they have ionisable groups on their surface: increasing the charge will make them more hydrophilic, while removing it will increase their hydrophobicity. This approach has been investigated by Binks and Rodrigues, who varied the pH of polystyrene particles dispersed in water, and witnessed a water-in-oil to oil-in-water inversion.⁹⁰ Read *et al.* also observed transitional inversion on adjusting the solution pH of emulsions stabilised with polystyrene latex particles when oils of intermediate polarity (methyl myristate or cineole) were used.^{91, 92} On the contrary, non-polar oils (n-dodecane) and polar oils (1-undecanol) underwent demulsification on adjusting the solution pH. Likewise, Gautier *et al.* and Li and Stöver did not observe any

emulsion inversion but an effect of pH on the emulsion stability, and on final drop diameter, which disappeared when salt was added.^{87, 93}

Another type of emulsion inversion consists in varying the oil-water volume ratio in the system. The resulting inversion is called “catastrophic”.⁹⁴ For particles of intermediate hydrophobicity, catastrophic inversion of emulsions occurs upon increasing the volume fraction of water, and emulsion stability to sedimentation or creaming increases approaching inversion. This inversion seems to occur through multiple emulsion formation, where some of the continuous phase is enclosed in the dispersed one. Ultimately the continuous phase becomes entirely enveloped within the disperse droplets and hence phase inversion occurs.⁸⁰ Emulsion inversion can also be affected by changing the initial location of particles or increasing the homogenisation time.⁷²

1.3.5 *Effect of oil type on emulsions*

Although the particle wettability determines the type of emulsion to be formed, the oil type affects the stability of this emulsion.^{34, 70, 72} This can be understood from equations 1.5 and 1.6, which show that the particle contact angle (θ) and the energy of particle detachment both depend on the tension between the oil and water or the particle surface.

Binks and Clint have developed a theoretical treatment for the wetting of a solid particle at oil-water interfaces.⁷⁷ Particle oil-water contact angles, calculated in terms of the components of the surface energies of the three phases (equation 1.5), agree with experimental data for a range of oils of different polarity. Systems with non-polar oils tend to produce oil-in-water emulsions whereas water-in-oil emulsions are preferred for systems with polar oils. Binks *et al.* reported the measured and calculated oil-ionic liquid, water-ionic liquid and oil-water contact angles on silica surfaces hydrophobised to different extents.⁹⁵ Binks *et al.* also correlated the contact angle data with the phase inversion points and stabilities of the corresponding particle-stabilised emulsions for a large variety of oils.⁹⁶

1.3.6 Mixture of particles and surfactant in emulsions

Mixtures of particles and surfactant have been investigated in several studies in order to understand how they interact. Yan and Masliyah showed that addition of anionic palmitic acid and cationic dodecyl amine to emulsions stabilised by negatively-charged kaolinite clay particles caused a drop in interfacial tension, thought to be due to attraction between particles and oppositely charged surfactant.⁷⁶ A similar observation was made by Tambe and Sharma, who found that stearic acid addition to particle mixtures led to emulsion stability or inversion, as the surfactant had the ability to increase the particle contact angle.⁷³ A clear synergy was also observed in the case of silica and both poly(ethylene oxide) (PEO) and hydroxypropylcellulose (HPC) surfactants.^{60, 97} stabilisation initially increasing and then decreasing, at surfactant concentration high enough to compete for the oil-water interface. Increase in flocculation of silica with surfactant addition and increase in particle contact angle were monitored. Similar synergistic mechanisms between particles and surfactant were evidenced by Binks *et al.*⁹⁸ For stable systems of nanosilica and non-ionic PEO type surfactants, small aggregate formation and increased viscosity were observed. Addition of particles caused an increase in surface tension, which was balanced by a change of particle contact angle, and led to a net increase in the theoretical detachment energy. In summary, surfactant-particle mixtures may increase interfacial elasticity, affect the interfacial viscosities, decrease the interfacial tension, change particle contact angle and promote partial particle flocculation.

1.4 Heteroaggregation in emulsions

The mechanism of aggregation of emulsion drops can be understood through studying that of solid particles, in which the emulsion drops have to be considered rigid. In colloidal particle dispersions, aggregation can take place between the same type of particles (homoaggregation) or unlike particles (heteroaggregation).^{99, 100} Particles can be different in size, charge, shape, charge density or composition. Aggregation is usually caused by an attraction resulting from oppositely charged electrical double layers, causing bridging and charge neutralisation mechanisms. The

relative amount and size of the particles will determine the morphology of the aggregates:¹⁰¹ if there is a significant difference in size, more numerous small particles will adsorb on the big, if they are of similar size, they will organise themselves into fractal clusters.

The maximum number of particles able to adsorb onto another particle surface assuming hexagonal packing was derived by Jones and Pilpel:¹⁰²

$$N_{hex} = \frac{2\pi}{\sqrt{3}} \left(\frac{D}{d} - 1 \right)^2 \quad (1.10)$$

where N_{hex} is the maximum number of particles on the surface, D the large particle diameter and d the small particle diameter.

Furusawa and Anzai found that this maximum theoretical coverage was not reached for size ratio greater than 0.15 with latex and silica particles.¹⁰¹ They also observed that the aggregate architecture varied with size ratio: when $d/D=0.33$, aggregates are discrete heterocoagulates, above this value they form large irregular structures. Onoda and Liniger and later Johnson and Lenhoff reckoned that hexagonal close packing is unlikely to occur in reality:^{103, 104} the random adsorption of colloidal particles onto a flat surface produces areas of unoccupied space, most likely due to charge repulsion. Luckham *et al.* noticed that varying the salt concentration could improve the maximum surface coverage by screening the repulsion between like charged particles.¹⁰⁵

Rasa *et al.*, studying mixtures of positively and negatively charged Ludox particles, monitored a non-linear decrease in conductivity (and mobility) with the concentration of negative particles in the dispersion.¹⁰⁶ Heteroaggregation was observed for mixtures with a low content of positive particles only, and for these aggregates an average of zero mobility was measured. It was concluded that the outer shell of the aggregates consisted of both positive and negative particles, leading to a neutral surface. Later on, Yates *et al.* added silica particles to alumina dispersions, and found that they did adsorb onto the alumina surface due to their opposite charges.¹⁰⁰ They noted that when the particle size ratio increases, the number of particles required for forming optimum aggregates with alumina decreases although the total amount of silica increases.

Weakly flocculated dispersions of particles are reported to be more efficient for stabilising emulsions than discrete particles or highly aggregated ones.^{83, 107} For mixtures of silica nanoparticles and pure cationic surfactants, the more stable emulsions are formed when particles are flocculated. Both emulsifiers alone stabilise oil-in-water emulsions, but at high pH particles alone are ineffective. A synergistic effect is observed when surfactants are added to particle dispersions: particle flocculation occurs, due to formation of surfactant monolayers around the particles increasing their hydrophobicity, and the aggregates adsorb at the oil-water interface leading to a stable emulsion. However, it is interesting to note that further addition of surfactants is followed by a re-dispersion of particles, with a concomitant decrease in emulsion stability. A similar study was made with positively charged alumina-coated silica particles and negatively charged surfactant, which also witnessed the maximum emulsion stability for the least stable dispersions.¹⁰⁸

Binks *et al.* also investigated systems containing only particles, positively and negatively charged.¹⁰⁹ Alone these particles did not stabilise any emulsion, because they were too hydrophilic to adsorb at the oil-water interface. Mixing the negatively charged particles with the positively charged ones reduced the net charge of the aqueous dispersion, and so increased the particle wettability. The optimum particle ratio was found to be 2:1 negative/positive particles, due to the asymmetry of the pH dependence of the zeta potentials of the two particles. This gave a maximum particle sediment height in the dispersion, indicating the greatest particle flocculation and hence the best stability for the corresponding emulsion.

Aggregation of emulsion drops has been observed in several systems: water in a continuous oil phase depends on the droplet size, the surfactant concentration, the oil type and the temperature.¹¹⁰ In particle-stabilised emulsions, aggregation between the emulsion drops can occur due to the formation of 3-D network of particles, due to particle bridging (as seen in section 1.3.2) or weak electrostatic repulsion.⁵⁸

A rare study exists investigating the heteroaggregation of drops within emulsion systems. Gu *et al.* described the formation of colloidosomes from large anionic droplets with small cationic droplets adsorbed on their surface.¹¹¹ The charged droplets were obtained by stabilising oil-in-water emulsions with positively

charged proteins, before coating half with pectin to reverse the charge on those drops. Mixed at a specific ratio, the small droplets coat the surface of the large droplet, causing a zeta potential inversion of the drop. The emulsion mixture aggregation observed at intermediate and high concentrations of small droplets was attributed to either bridging or depletion flocculation of the drops.

1.5 Foams

Like emulsions, foams are commonly found in consumer and industrial products like foods, pharmaceutical and personal care products, fire-fighting foam, and detergents.¹¹²⁻¹¹⁷ The properties of foams are greatly affected by the surfactants or other stabilisers used as they can reduce the interfacial tension and the viscosity of the liquids:³⁷ soluble proteins, for example can stabilise foam by forming a rigid layer at the liquid-gas interface.¹¹⁸ Foams can also be found in the form of froths in mineral-separation processes and in the petroleum industry.² Micro-foams are a subtype of foams, where a dispersion of aggregates of very small foam bubbles is created by injection of gas into surfactant solution with very high shear. While the bubble diameters in foams are typically in the range 50–300 μm , they are a up to 100 times smaller in micro-foam, conferring to them a higher stability.¹¹⁹

Foams other than in flotation froth processes are generally unwanted in industrial processes, as they can increase wear and block throughout.² Hence some agents, like high molecular mass alcohols, were developed to reduce the foam stability or to prevent foam formation by changing the nature of the gas-liquid interface (increase of surface tension, decrease of surface elasticity, decrease of surface viscosity or decrease of surface potential).^{119, 120}

1.5.1 *Foam formation and stability*

A foam is defined as a colloidal dispersion of a gas in a continuous liquid phase.² Like for emulsions, pure liquids do not foam, foam formation requires adsorption of a foam stabiliser. Two structural situations exist: wet foams (also called transient, dilute or Kugelschaum), made from slightly surface-active stabilisers, consist of spherical bubbles separated by thick liquid films, while dry

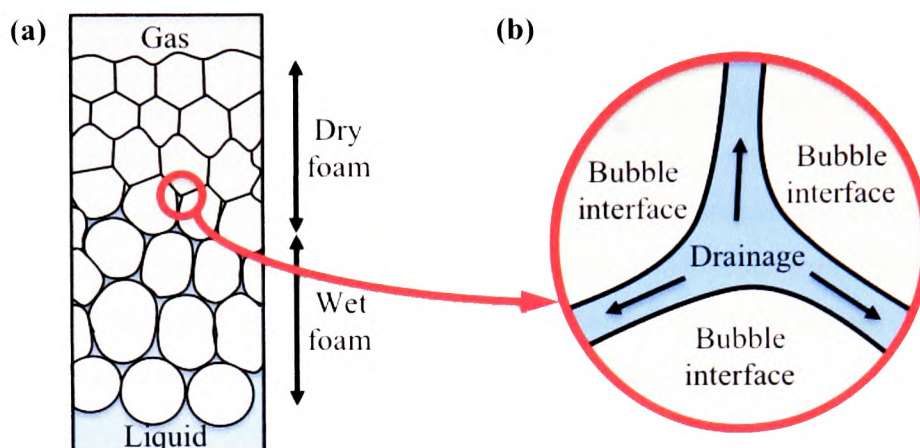
foams (persistent or concentrated) are large polyhedral gas cells separated by thin liquid films stabilised with components of strong surface-activity. The gas bubble geometry depends on the gas volume fractions (ϕ_{al}) within the system:² in wet foams, ϕ_{al} can have a value of up to 0.74, which represents the maximum volume fraction possible for an internal phase made up of uniform and incompressible spheres, but with an increase of ϕ_{al} in drier foams the foam bubbles start to distort, taking on a variety of polyhedral shapes. The most stable polyhedra model shape is the Kelvin tetrakaidecahedron, which minimises surface free energy with eight non-planar hexagon faces and six planar quadrilateral faces.¹²¹

In a persistent foam, the polyhedral bubbles are separated by almost flat liquid films, which come together in 2-D at equal angles of 120° (Steiner angle). These angles result from the equalisation in the Plateau border of the surface tension vectors along the liquid films (Figure 1.7). Such foams are referred to as dry foams, or Polyederschaum. In 3-D, four liquid films meet with a tetrahedral angle ($\sim 109^\circ$), however whenever more than 4 foam films meet an immediate rearrangement happens restoring the three films junction.

Foam stability involves two different processes: film thinning and bubble coalescence. Although there might be an optimum size for a foam type, foam stability does not necessarily depend on bubble size. However the bubble size distribution causes pressure gradients between bubbles of different size, which promotes gas diffusion between them. Like Ostwald ripening in emulsions (section 1.3.1), disproportionation in foams defines the process of larger bubbles growing at the expense of smaller bubbles.² Foam drainage as represented in Figure 1.7, which is driven by capillary pressure, will determine the film thinning: a typical foam has a half-life drainage of the order of tens of minutes, but some surfactant-stabilised foams can be stable for years.¹²² Film thinning does not cause foam degeneration, as no change in total surface area occurs, but it can enhance the coalescence mechanism. The rupture of the thin liquid film between bubbles causes coalescence of the bubbles, which fuse together forming a single larger bubble.



Figure 1.7. Schematic presentation of (a) a foam column (wet at the bottom and dry at the top) and (b) the Plateau border where 3 bubbles meet in 2D creating a capillary pressure, which causes drainage.



Foaming capability or foamability relates to both foam formation and foam persistence. Enhancement of foamability can be done through surface tension lowering, surface elasticity increase and surface viscosity increase.¹²³ It is the surface-active compounds used to stabilise the foam which determine stability and foamability: mildly surface-active compounds will weakly stabilise transient foams, whereas more strongly surface-active compounds can stabilise quite strong, metastable foams.¹²⁴

1.5.2 *Foams stabilised with solid particles*

Although the interest of particles as aqueous foams stabiliser has increased lately, solid particles are mainly known for their role in foam destruction.¹²⁵ However hydrophilic particles with the right wettability can actually enhance the stability of surfactant-stabilised aqueous foams, by collecting in the Plateau borders of the foam and retarding film drainage.¹²⁶ Hydrophobic particles do not benefit surfactant-stabilised foams, as foams will break from the strong opposite bending energies between the particles and the liquid films (bridging drainage) resulting in their use as foam breakers.^{127, 128} The deformability and the ‘delicate’ nature of foams render them susceptible to destruction by particle piercing.

Although the interest in particles as the sole stabiliser of foams is recent, it

has long been known that finely dispersed particles play an important role in the stabilisation of many different types of foams: foaming in rivers, waste treatment, the oil industry, paper industry, production of metal foams and the preparation of foods.¹²⁹⁻¹³¹ Hoffmann was the first to suggest that finely divided particles played a role in stabilisation of foams or froth, in his study of mineral frothers and ore flotation.¹³² Later, other studies shows that partially hydrophobic particles could enhance or completely stabilise froths, whereas entirely wetted particles had no effect on the stability.¹³³⁻¹³⁵ More recently, Tang *et al.* showed that the addition of fine silica particles enhanced the stability of sodium dodecyl sulfate (SDS)-stabilised foam, and that like in emulsion systems, stability was proportional to particle concentration and inversely proportional to particle size.¹³⁶

The stability provided by the particles to the foam is likely to be mainly due to creation of a steric barrier to coalescence and as with emulsions, smaller particles in high concentrations give the most effective barrier.¹³⁷ However the use of particles is more complicated in foams than in emulsions: particles can cause retardation of drainage and increase maximum capillary pressure, but also bridge bubbles which can have a positive or a negative effect on the foam stability depending on the particle. Hydrophobic particles are recognised for their antifoam action caused by a heightened capillary de-wetting action:¹³⁸ particles bridge between bubble films, with the receding particle contact angle causing film drainage, which is also caused by a positive Laplace pressure in the film adjacent to the particle.¹³⁹ The de-wetting will accelerate until the inter-film is completely drained. On the contrary for hydrophilic particles, drainage stops as the Laplace pressure difference reduces to zero and the film becomes essentially planar. A further drainage of the film would even cause the Laplace pressure to draw liquid back into the particle film, creating a stable bridging mechanism. Pugh and Johansson observed this phenomenon with hydrophilic quartz particles of small contact angle, which did not affect froth stability, whereas particles with contact angle around 65° gave optimum froth stability, and more hydrophobic particles led to collapse of the froth.¹⁴⁰ Similar contact angle values giving optimum foam stability were found by other groups.¹⁴¹⁻¹⁴³ The work of Aveyard *et al.* concluded that particles can stabilise foams within a small range of contact angles, and outside this range they behave as efficient de-stabilisers.¹⁴⁴ Although the wetting

mechanisms imply that all hydrophilic particles should act as foam stabilisers, it is known now that the effects of meniscus formation and surface roughness can cause hydrophilic particles to be efficient de-foamers.²⁹

Studying the general forces governing stability in particle-stabilised foams, Kaptay found that particles could stabilise foams under different conditions:¹⁴⁵ they could form a network and loose monolayers or packed multilayers on bubble surfaces. His observations showed that particle size affects strongly foam more than emulsion systems: large particles will tend to pierce and break the foam film, whereas they will stabilise larger drops in emulsions. The unpublished work of Wilson with latex particles confirmed that most stable froths were produced from conditions close to bulk particle coagulation (produced by change of pH, addition of salt or surfactant).¹⁴⁶ Similarly, Dickinson, Binks and co-workers observed that nano-particle of silica should be partially coagulated to stabilise bubbles and foams.¹⁴⁷⁻¹⁴⁹ Armes *et al.* continuing Wilson's study found that in foam solely stabilised by latex particles, the foam stability increased with a decrease in particle size only to a point, as particles smaller than 260 nm were not able to stabilise a foam.¹⁵⁰ However they noted that the decrease in stability was due to the incapacity of the small particles to form homogenous intrinsically strong networks, as they were highly polydisperse.¹⁵¹ Another important factor is the shape of particles: Dippenaar established that flat type particles generally result in more stable froths, while rounded or spherical particles enhance thinning of liquid films, and sharp-edged particles ruptured the liquid film really quickly.¹²⁸

1.5.3 *Non-aqueous foams*

Like seen previously, foam formation requires a thermodynamically favourable adsorption of a stabiliser, which will lower the gas-liquid interfacial tension.¹⁵² As the water-air surface tension is relatively high (72 mN m^{-1}), strong adsorption at the air-aqueous solution surface is favourable for many species, and renders aqueous foams more common than non-aqueous. The pure oil-air surface tension is typically around $25\text{-}30 \text{ mN m}^{-1}$, too low to drive adsorption of most solute species. However, fluorocarbons have surface energies lower than hydrocarbons, hence fluorosurfactants adsorb relatively strongly at hydrocarbon liquid-air surfaces,

producing stable foams of hydrocarbon liquids.¹⁵³ Ross *et al.* showed that specific conditions of solute concentration and temperature have to be fulfilled for the foam to be stable:¹⁵⁴⁻¹⁵⁶ the system should be close to a phase separation boundary, as the tendency of solute to adsorb is enhanced when solvent and solute have a low affinity. Binks *et al.*, investigating the foaming properties of a hydrocarbon oil solvent with additives, noted a similar behaviour.¹⁵⁷ An analogous observation has been made by Friberg *et al.* and Shrestha *et al.* that surfactant solutions in hydrocarbon solvents show foaming for compositions close to phase separation of a lyotropic liquid crystalline phase, where foam bubbles are coated with a film of highly viscous liquid crystal.¹⁵⁸⁻¹⁶⁰

1.5.4 Dry water

In emulsion systems, the change of particle contact angle can cause inversion of the type of emulsion, as seen in section 1.3.4.¹⁶¹⁻¹⁶³ In a similar manner, it has been shown by Binks and Murakami that aqueous foams stabilised solely by particles can phase invert into a free flowing powdered material, that they called ‘dry water’.¹⁶² In a similar way to that was used on emulsions systems, the wettability of the silica nanoparticles was varied by coating the particles to different extent with a silane reagent, resulting in production of a range of particle wettabilities.⁵¹ The relatively hydrophilic particles stabilised bubbles producing air-in-water foams, whereas the very hydrophobic particles made a water-in-air powder. The change of particle wettability caused inversion of the curvature of the fluid interface, which can be compared to transitional emulsion inversion.⁵¹ Catastrophic phase inversion, which is caused by varying the fluid:fluid ratio, was also observed for the foam-dry water systems: keeping a fixed particle wettability and increasing the air: water ratio, inversion from foam to dry powder occurred.¹⁶² Investigation of the charge properties of the silica particles by affecting pH and salt concentration was also made:¹⁶⁴ low pH or high salt concentration favoured the formation of ‘dry water’, by rendering the particle hydrophobic, while a high pH or low salt concentration promoted formation of foam, as the particles were charged and partially hydrophilic. In a later study, Binks *et al.* demonstrated that hydrophobic silica particles can be

rendered hydrophilic via surfactant adsorption, providing an alternative way of converting the 'dry water' material to aqueous foam.¹⁶⁵

1.6 Presentation of thesis

The general aim of this thesis was to produce new materials using novel particles, possessing interesting stimuli responsive properties. For that purpose, stimuli responsive emulsions were made, stabilised with different solid particles (Chapters 3 to 6 and 8), as well as oil foams stabilised with tetrafluoroethylene particles (Chapter 7) and an emulsion encapsulated within a solid powder (Chapter 8). It is believed that these new materials can find applications and enhance understanding in the food, pharmaceutical, cosmetic or automobile industries.

Emulsions stabilised solely with micro-wax particles were produced in Chapter 3, and it was shown that the effect of particle concentration on the emulsion stability depended on the type of particles and whether they formed a network or not. The main investigation was on the effect of temperature on these wax-stabilised emulsions. It was highlighted that the emulsions broke with an increase of temperature when produced at room temperature, as the particles could not provide steric hindrance to coalescence when they melted. However, when produced at elevated temperature, emulsions displayed a higher stability.

Similarly, emulsions stabilised by biodegradable poly(lactic-co-glycolic) acid (PLGA) particles were observed to break with time, as the degrading particles could not stabilise the oil-water interface. Chapter 4 presents the study of emulsions stabilised with modified and unmodified PLGA particles, and demonstrates that the pH affects emulsions stabilised with unmodified particles, whereas modified ones seemed to delay or stop the destabilisation of the emulsions at all pH values.

In Chapter 5, the possibility of designing emulsion heteroaggregates with controlled architecture was examined. Emulsions stabilised with oppositely charged colloidal particles were formed separately and mixed in order to organise positively charged droplets around negative ones, or *vice versa*. The effects of oil type used as the dispersed phase, pH of the water phase and initial oil fraction were studied to form the parent-emulsions. Then the mixing protocol, the excess particle

concentration, drop size and drop size ratio were varied to find the optimum parameters in order to observe drop heteroaggregation.

Like the wax, PLGA and silica particles, natural sporopollenin particles were found to stabilise emulsions in Chapter 6. A decrease of pH was observed to enable emulsion inversion from oil-in-water to water-in-oil, demonstrating that the sporopollenin particles are efficient emulsifiers for both types of emulsions due to the change of charge on the particle surface. Interestingly, specific orientation of the non-spherical particles at the fluid interface was observed exclusively in water-in-oil emulsions. Sporopollenin particles were also able to strongly stabilise liquid marbles, whose formation was not affected by the pH or salt concentration of the encapsulated water, due to contact angle hysteresis.

Chapter 7 shows that PTFE particles can stabilise liquid marbles, with the internal phase being either water or oil. However, the main interest of this chapter was to reveal that TFE particles efficiently stabilise non-aqueous foams for a wide range of liquid surface tensions. Different methods were used to produce these foams, and the liquid and particle types were shown to affect the stability and foaming capability of the systems. Dry powders were produced with liquids of higher surface tension, like water and glycerol.

Following the liquid marble production in Chapter 6 and the dry powder in Chapter 7, Chapter 8 aimed at developing a protocol for dry encapsulation of oil in the form of emulsions. The principle of dry water formation is exploited here: silica-stabilised oil-in-water emulsions were produced then diluted to different extents before being blended with hydrophobic silica particles, as in the production of dry water. The system was observed to be sensitive to particle hydrophobicity and oil volume fraction of the emulsion to encapsulate, and it was demonstrated that the blending time was a key parameter to achieve formation of powdered emulsions.

Finally, a summary of conclusions, future work suggestions and an Appendix with experimental values are described at the end of this thesis.

1.7 References

1. T. Cosgrove, *Colloid Science: Principles, Methods and Applications*, Blackwell Publishing, Bristol, 2005.
2. L. L. Schramm, *Emulsions, Foams, and Suspensions: Fundamental and Applications*, Wiley-vch, Weinheim, 2005.
3. B. V. Derjaguin and L. Landau, *Acta Physico chemica URSS*, **14**, 633 (1941).
4. E. J. W. Verwey and J. T. G. Overbeek, *Theory of the stability of lyophobic colloids*, Elsevier, 1948.
5. H.-J. Butt and M. Kappl, *Surface and Interfacial Forces*, Wiley-vch, Weinheim, 2010.
6. H. C. Hamaker, *Physica*, **4**, 1058 (1937).
7. R. Hogg, T. W. Healey and D. W. Fuerstenau, *Trans. Faraday Soc.*, **62**, 1638 (1966).
8. K. S. Birdi, *Handbook of Surface and Colloid Chemistry*, CRC Press, 2008.
9. B. P. Binks and S. O. Lumsdon, *Phys. Chem. Chem. Phys.*, **1**, 3007 (1999).
10. H. J. Butt, M. Kappl, H. Mueller, R. Raiteri, W. Meyer and J. Ruhe, *Langmuir*, **15**, 2559 (1999).
11. C. Cowell, R. Lin-in-on and B. Vincent, *J. Chem. Soc.*, **74**, 337 (1978).
12. B. P. Binks and T. S. Horozov, *Colloidal particles at liquid interfaces*, University Press, Cambridge, 2006.
13. S. U. Pickering, *J. Chem. Soc.*, **91**, 2001 (1907).
14. W. Ramsden, *Proc. Roy. Soc.*, **72**, 156 (1903).
15. P. Finkle, H. D. Draper and J. H. Hildebrand, *J. Am. Chem. Soc.*, **45**, 2780 (1923).
16. J. H. Schulman and J. Leja, *Trans. Faraday Soc.*, **50**, 598 (1954).
17. B. P. Binks and T. S. Horozov, Colloidal Particles at Liquid Interfaces: An Introduction, in *Colloidal particles at liquid interfaces*; Binks, B. P.; Horozov, T. S. ed., Cambridge University Press, Cambridge, 2006.
18. T. Young, *Phil. Trans.*, **95**, 84 (1805).
19. I. B. Ivanov, P. A. Kralchevsky and A. D. Nikolov, *J. Colloid Interface Sci.*, **112**, 97 (1986).

20. A. V. Rapacchietta, A. W. Neumann and S. N. Omenyi, *J. Colloid Interface Sci.*, **59**, 541 (1977).
21. A. W. Neumann and J. K. Spelt, *Applied Surface Thermodynamics*, Marcel Dekker, New York, 1996.
22. J. C. Fernández-Toledano, A. Moncho-Jordá, F. Martínez-López and R. Hidalgo-Álvarez, Theory for Interactions between Particles in Monolayers, in *Colloidal particles at liquid interfaces*; Binks, B. P.; Horozov, T. S. ed., Cambridge University Press, Cambridge, 2006.
23. P. A. Kralchevsky and K. D. Danov, Interactions between Particles at a Fluid Interface, in *Nanoscience: Colloidal and Interfacial Aspects*; Starov, V. M. ed., CRC Press, New York, 2010.
24. K. P. Velikov and O. D. Velev, Novel Materials Derived from Particles Assembled on Liquid Surfaces, in *Colloidal particles at liquid interfaces*; Binks, B. P.; Horozov, T. S. ed., Cambridge University Press, Cambridge, 2006.
25. M. Oettel, A. Domínguez and S. Dietrich, *Phys. Rev. E*, **71**, 051401 (2005).
26. K. D. Danov, P. A. Kralchevsky and M. P. Boneva, *Langmuir*, **20**, 6139 (2004).
27. M. Megens and J. Aizenberg, *Nature*, **424**, 1014 (2003).
28. M. G. Nikolaides, A. R. Bausch, M. F. Hsu, A. D. Dinsmore, M. P. Brenner, C. Gay and D. A. Weitz, *Nature*, **420**, 299 (2002).
29. P. A. Kralchevsky, N. D. Denkov and K. D. Danov, *Langmuir*, **17**, 7694 (2001).
30. D. Stamou, C. Duschl and D. Johannsmann, *Phys. Rev. E*, **62**, 5263 (2000).
31. R. Aveyard, J. H. Clint, D. Nees and V. N. Paunov, *Langmuir*, **16**, 1969 (2000).
32. T. S. Horozov, R. Aveyard, J. H. Clint and B. P. Binks, *Langmuir*, **19**, 2822 (2003).
33. D. J. McClements, *Critical Reviews in Food Science and Nutrition*, **47**, 611 (2007).
34. B. P. Binks, *Curr. Opin. Colloid Interface Sci.*, **7**, 21 (2002).
35. P. Becher and M. J. Schick, *Nonionic Surfactants*, Marcel Dekker, New York, 1987.

36. W. C. Griffin, *J. Cosmet. Chem.*, **1**, 311 (1954).
37. T. F. Tadros, *Applied Surfactants: Principles and Applications*, Wiley-vch, Weinheim, 2005.
38. D. J. McClements, *Food Emulsions: Principles, Practice and Techniques*, 1 ed., CRC Press, Boca Raton, 1999.
39. R. J. Hunter, *Foundations of Colloid Science*, Oxford University Press, Oxford, 1989.
40. R. J. G. Lopetinsky, J. H. Masliyah and Z. Xu, Solids-Stabilized Emulsions: A Review, in *Colloidal particles at liquid interfaces*; Binks, B. P.; Horozov, T. S. ed., Cambridge University Press, Cambridge, 2006.
41. D. J. McClements, *Food Emulsions: Principles, Practice and Techniques*, 2 ed., CRC Press, Boca Raton, 2005.
42. R. Chanamai and D. J. McClements, *J. Colloid Interf. Sci.*, **225**, 214 (2000).
43. D. J. McClements, *Curr. Opin. Colloid Interface Sci.*, **7**, 451 (2002).
44. B. Deminiere, A. Colin, F. L. Calderon and J. Bibette, Lifetime and destruction of concentrated emulsions undergoing coalescence, in *Modern Aspects of Emulsion Science*; Binks, B. P. ed., Royal Society of Chemistry, Cambridge, 1998.
45. A. Kabalnov, *J. Dispersion Sci. Technol.*, **22**, 1 (2001).
46. A. Kabalnov and J. Weers, *Langmuir*, **12**, 3442 (1996).
47. A. S. Kabalnov, L. D. Gervits and K. N. Makarov, *Colloid Journal of the USSR*, **52**, 915 (1990).
48. J. G. Weers, Ostwald ripening in emulsions, in *Modern Aspects of Emulsion Science*; Binks, B. P. ed., Royal Society of Chemistry, Cambridge, 1998.
49. E. Dickinson, *Food Hydrocolloids*, **23**, 1473 (2009).
50. T. R. Briggs, *J. Ind. Eng. Chem.*, **13**, 1008 (1921).
51. B. P. Binks and S. O. Lumsdon, *Langmuir*, **16**, 8622 (2000).
52. B. S. Murray and R. Ettelaie, *Curr. Opin. Colloid Interface Sci.*, **9**, 314 (2004).
53. A. Prakash, M. Joseph and M. E. Mangino, *Food Hydrocolloids*, **4**, 177 (1990).
54. E. Dickinson, *J. Dairy Sci.*, **80**, 2607 (1997).

55. T. N. Hunter, R. J. Pugh, G. V. Franks and G. J. Jameson, *Adv. Colloid Interface Sci.*, **137**, 57 (2008).
56. T. S. Horozov and B. P. Binks, *Angew. Chem. Int. Ed.*, **118**, 787 (2006).
57. E. Vignati, R. Piazza and T. P. Lockhart, *Langmuir*, **19**, 6650 (2003).
58. J. Thieme, S. Abend and G. Lagaly, *Colloid Polym. Sci.*, **277**, 257 (1999).
59. S. Abend, N. Bonnke, U. Gutschner and G. Lagaly, *Colloid Polym. Sci.*, **276**, 730 (1998).
60. B. R. Midmore, *Colloids Surf. A*, **132**, 257 (1998).
61. N. P. Ashby and B. P. Binks, *Phys. Chem. Chem. Phys.*, **2**, 5640 (2000).
62. B. P. Binks and S. O. Lumsdon, *Langmuir*, **17**, 4540 (2001).
63. N. X. Yan, M. R. Gray and J. H. Masliyah, *Colloids Surf. A*, **193**, 97 (2001).
64. S. Fujii, E. S. Read, B. P. Binks and S. P. Armes, *Adv. Mater.*, **17**, 1014 (2005).
65. B. P. Binks and A. Rocher, *J. Colloid Interf. Sci.*, **335**, 94 (2009).
66. B. P. Binks, R. Murakami, S. P. Armes and S. Fujii, *Angew. Chem. Int. Ed.*, **44**, 4795 (2005).
67. B. P. Binks, R. Murakami, S. P. Armes and S. Fujii, *Langmuir*, **22**, 2050 (2006).
68. S. Melle, M. Lask and G. G. Fuller, *Langmuir*, **21**, 2158 (2005).
69. S. Arditty, C. P. Whitby, B. P. Binks, V. Schmitt and F. Leal-Calderon, *Eur. Phys. J. E Soft Matter*, **11**, 273 (2003).
70. B. P. Binks and S. O. Lumsdon, *Phys. Chem. Chem. Phys.*, **2**, 2959 (2000).
71. B. P. Binks, J. H. Clint, G. Mackenzie, C. Simcock and C. P. Whitby, *Langmuir*, **21**, 8161 (2005).
72. B. P. Binks and C. P. Whitby, *Langmuir*, **20**, 1130 (2004).
73. D. E. Tambe and M. M. Sharma, *Adv. Colloid Interface Sci.*, **52**, 1 (1994).
74. S. Abend and G. Lagaly, *Clay Min.*, **36**, 557 (2001).
75. S. Levine and E. Sanford, *Can. J. Chem. Eng.*, **63**, 258 (1985).
76. Y. Yan and J. H. Masliyah, *Colloids Surf. A*, **75**, 123 (1993).
77. B. P. Binks and J. H. Clint, *Langmuir*, **18**, 1270 (2002).
78. B. P. Binks and S. O. Lumsdon, *Langmuir*, **16**, 3748 (2000).

79. B. P. Binks, *Modern Aspects of Emulsion Science*, The Royal Society of Chemistry; Cambridge, 1998;
80. B. P. Binks and J. A. Rodrigues, *Langmuir*, **19**, 4905 (2003).
81. D. E. Tambe and M. M. Sharma, *J. Colloid Interf. Sci.*, **157**, 244 (1993).
82. B. P. Binks and S. O. Lumsdon, *Abstr. Paper. Am. Chem. Soc.*, **223**, 296 (2002).
83. B. P. Binks and J. A. Rodrigues, *Angew. Chem.*, **46**, 5389 (2007).
84. S. Fujii, D. P. Randall and S. P. Armes, *Langmuir*, **20**, 11329 (2004).
85. S. Fujii, Y. L. Cai, J. V. M. Weaver and S. P. Armes, *J. Am. Chem. Soc.*, **127**, 7304 (2005).
86. S. Fujii, S. P. Armes, B. P. Binks and R. Murakami, *Langmuir*, **22**, 6818 (2006).
87. F. Gautier, M. Destribats, R. Perrier-Cornet, J. F. Dechezelles, J. Giermanska, V. Heroguez, S. Ravaine, F. Leal-Calderon and V. Schmitt, *Phys. Chem. Chem. Phys.*, **9**, 6455 (2007).
88. T. Ngai, S. H. Behrens and H. Auweter, *Chem. Commun.*, **3**, 331 (2005).
89. T. Ngai, H. Auweter and S. H. Behrens, *Macromol.*, **39**, 8171 (2006).
90. B. P. Binks and J. A. Rodrigues, *Angew. Chem. Int. Ed.*, **44**, 441 (2005).
91. E. S. Read, S. Fujii, J. I. Amalvy, D. P. Randall and S. P. Armes, *Langmuir*, **20**, 7422 (2004).
92. E. S. Read, S. Fujii, J. I. Amalvy, D. P. Randall and S. P. Armes, *Langmuir*, **21**, 1662 (2005).
93. J. Li and H. D. H. Stover, *Langmuir*, **24**, 13237 (2008).
94. B. P. Binks and S. O. Lumsdon, *Langmuir*, **16**, 2539 (2000).
95. B. P. Binks, A. K. F. Dyab and P. D. I. Fletcher, *Phys. Chem. Chem. Phys.*, **9**, 6391 (2007).
96. B. P. Binks, P. D. I. Fletcher, B. L. Holt, P. Beaussoubre and K. Wong, *Phys. Chem. Chem. Phys.*, **12**, 11954 (2010).
97. B. R. Midmore, *J. Colloid Interf. Sci.*, **213**, 352 (1999).
98. B. P. Binks, A. Desforges and D. G. Duff, *Langmuir*, **23**, 1098 (2007).
99. J. M. Lopez-Lopez, A. Schmitt, A. Moncho-Jorda and R. Hidalgo-Alvarez, *Adv. Colloid Interface Sci.*, **147-48**, 186 (2009).

100. P. D. Yates, G. V. Franks, S. Biggs and G. J. Jameson, *Colloids Surf. A*, **255**, 85 (2005).
101. K. Furusawa and C. Anzai, in *Heterocoagulation Behavior of Polymer Lattices with Spherical Silica*, Ralph K Iler Memorial Symp. on Colloid Chemistry of Silica, 200th National Meeting of the American Chem. Soc., Washington DC, 103, 1990.
102. T. M. Jones and N. Pilpel, *J. Pharm. Pharmacol.*, **17**, 440 (1965).
103. C. A. Johnson and A. M. Lenhoff, *J. Colloid Interf. Sci.*, **179**, 587 (1996).
104. G. Y. Onoda and E. G. Liniger, *Phys. Rev. A*, **33**, 715 (1986).
105. P. Luckham, B. Vincent, C. A. Hart and T. F. Tadros, *Colloids and Surfaces*, **1**, 281 (1980).
106. M. Rasa, A. P. Philipse and J. D. Meeldijk, *J. Colloid Interf. Sci.*, **278**, 115 (2004).
107. B. P. Binks, J. A. Rodrigues and W. J. Frith, *Langmuir*, **23**, 3626 (2007).
108. B. P. Binks and J. A. Rodrigues, *Langmuir*, **23**, 7436 (2007).
109. B. P. Binks, W. Liu and J. A. Rodrigues, *Langmuir*, **24**, 4443 (2008).
110. F. Leal-Calderon, B. Gerhardi, A. Espert, F. Brossard, V. Alard, J. F. Tranchant, T. Stora and J. Bibette, *Langmuir*, **12**, 872 (1996).
111. Y. S. Gu, E. A. Decker and D. J. McClements, *Food Hydrocolloids*, **21**, 516 (2007).
112. P. C. Vandevivere, R. Bianchi and W. Verstraete, *J. Chem. Technol. Biotechnol.*, **72**, 289 (1998).
113. C. A. Moody and J. A. Field, *Env. Sci. Technol.*, **34**, 3864 (2000).
114. Y. J. Zhao, S. A. Jones and M. B. Brown, *J. Pharm. Pharmacol.*, **62**, 678 (2010).
115. A. Arzhavitina and H. Steckel, *Int. J. Pharm.*, **394**, 1 (2010).
116. H. D. Goff, *International Dairy Journal*, **7**, 363 (1997).
117. C. W. Bamforth, *J. Inst. Brewing*, **91**, 370 (1985).
118. H.-D. Belitz, W. Grosch and P. Schieberle, *Food Chemistry*, 4 ed., Springer, Berlin, 2009.
119. F. Sebba, *Foams and Biliquid Foams - Aphrons*, Wiley, NewYork, 1987.

120. A. A. Zotto, Antifoams and Release Agents, in *Food Additive User's Handbook*; Smith, J. ed., Blackie, Glasgow, 1991.
121. A. V. Nguyen, R. J. Pugh and G. J. Jameson, Collection and Attachment of Particles by Air Bubbles in Froth Flotation, in *Colloidal particles at liquid interfaces*; Binks, B. P.; Horozov, T. S. ed., University Press, Cambridge, 2006.
122. C. Isenberg, *The Science of Soap Films and Soap Bubbles*, Tieto, Clevedon, 1978.
123. L. L. Schramm and F. Wassmuth, Foams: Basic Principles, in *Foams, Fundamentals and Applications in the Petroleum Industry*; Schramm, L. L. ed., American Chemical Society, Washington DC, 1994.
124. D. J. Shaw, *Introduction to Colloid and Surface Chemistry*, Fourth Edition ed., Butterworth-Heinemann, Oxford, 1992.
125. N. D. Denkov and K. G. Marinova, Antifoam Effects of Solid Particles, Oil Drops and Oil–Solid Compounds in Aqueous Foams, in *Colloidal particles at liquid interfaces*; Binks, B. P.; Horozov, T. S. ed., Cambridge University Press, Cambridge, 2006.
126. T. Wuebben and S. Odenbach, *Colloids Surf. A*, **266**, 207 (2005).
127. A. Dippenaar, *Int. J. Miner. Process.*, **9**, 15 (1982).
128. A. Dippenaar, *Int. J. Miner. Process.*, **9**, 1 (1982).
129. E. Dickinson, *An Introduction to Food Colloids.*, Oxford University Press, Oxford, 1992.
130. J. G. Speight, *The Chemistry and Technology of Petroleum*, Marcel Dekker, New York, 1991.
131. P. M. Spiecker and P. K. Kilpatrick, *Langmuir*, **20**, 4022 (2004).
132. Z. Hoffman, *Chem. Phys.*, **83**, 385 (1913).
133. R. H. Ottewill, D. L. Segal and R. C. Watkins, *Chemistry & Industry*, London, 1981.
134. D. M. Hausen, *Can. Metall. Q.*, **13**, 659 (1974).
135. O. Bartsch, *Kolloidchemische Beihefte*, **20**, 50 (1924).
136. F. Tang, Z. Xiao, J. Tang and L. Jiang, *J. Colloid Interf. Sci.*, **131**, 498 (1989).
137. S. W. Ip, Y. Wang and J. M. Toguri, *Can. Metall. Q.*, **38**, 81 (1999).

138. S. Simovic and C. A. Prestidge, *Langmuir*, **20**, 8357 (2004).
139. R. J. Pugh, *Adv. Colloid Interface Sci.*, **64**, 67 (1996).
140. G. Johansson and R. J. Pugh, *Int. J. Miner. Process.*, **34**, 1 (1992).
141. S. Ata, N. Ahmed and G. Jameson, *J. Min. Eng.*, **17**, 897 (2004).
142. S. Ata, N. Ahmed and G. J. Jameson, *Int. J. Min. Process.*, **64**, 101 (2002).
143. S. Schwarz and S. Grano, *Colloids Surf. A*, **256**, 157 (2005).
144. R. Aveyard, B. P. Binks, P. D. I. Fletcher, T. G. Peck and C. E. Rutherford, *Adv. Colloid Interface Sci.*, **48**, 93 (1994).
145. G. Kaptay, *Colloids Surf. A*, **230**, 67 (2003).
146. J. Wilson, A Study of Particulate Foams. Ph.D., University of Bristol, 1980.
147. Z. P. Du, M. P. Bilbao-Montoya, B. P. Binks, E. Dickinson, R. Ettelaie and B. S. Murray, *Langmuir*, **19**, 3106 (2003).
148. E. Dickinson, R. Ettelaie, T. Kostakis and B. S. Murray, *Langmuir*, **20**, 8517 (2004).
149. B. P. Binks and T. S. Horozov, *Angew. Chem. Int. Ed.*, **44**, 3722 (2005).
150. S. Fujii, P. D. Iddon, A. J. Ryan and S. P. Armes, *Langmuir*, **22**, 7512 (2006).
151. S. K. Bindal, G. Sethumadhavan, A. D. Nikolov and D. T. Wasan, *AIChEJ*, **48**, 2307 (2002).
152. P. D. I. Fletcher, in *Specialist Surfactants*; Robb, I. D. ed., Blackie, London, 1997.
153. V. Bergeron, J. E. Hanssen and F. N. Shoghl, *Colloids Surf. A*, **123–124**, 609 (1997).
154. G. M. Nishioka, L. L. Lacy and B. R. Facemire, *J. Colloid Interf. Sci.*, **80**, 197 (1981).
155. S. Ross and G. Nishioka, *Colloid Polym. Sci.*, **255**, 560 (1977).
156. S. Ross and G. Nishioka, *J. Phys. Chem.*, **79**, 1561 (1975).
157. B. P. Binks, C. A. Davies, P. D. I. Fletcher and E. L. Sharp, *Colloids Surf. A*, **360**, 198 (2010).
158. L. K. Shrestha, R. G. Shrestha, C. Solans and K. Aramaki, *Langmuir*, **23**, 6918 (2007).
159. L. K. Shrestha, K. Aramaki, H. Kato, Y. Takase and H. Kunieda, *Langmuir*, **22**, 8337 (2006).

160. S. E. Friberg, I. Blute, H. Kunieda and P. Stenius, *Langmuir*, **2**, 659 (1986).
161. S. Hasenzahl, A. Gray and A. Braunagel, *SOEFW J.*, **131**, 8 (2005).
162. B. P. Binks and R. Murakami, *Nature Mater.*, **5**, 865 (2006).
163. L. Forny, I. Pezron, K. Saleh, P. Guigon and L. Komunjer, *Powder Technol.*, **171**, 15 (2007).
164. B. P. Binks, B. Duncumb and R. Murakami, *Langmuir*, **23**, 9143 (2007).
165. B. P. Binks, A. J. Johnson and J. A. Rodrigues, *Soft Matter*, **6**, 126 (2010).

CHAPTER 2 EXPERIMENTAL

2.1 Materials

2.1.1 Water

Water was purified through an Elgastat Prima reverse osmosis unit followed by a Millipore Milli-Q reagent water system. Measurements of the resulting surface tension using the plate method were typically 73.0 mN m^{-1} at 25°C , in good agreement with the accepted literature value.¹ The resistivity of the Milli-Q water was consistently around $18 \text{ M}\Omega \text{ cm}$.

2.1.2 Oils and other liquids

Table 2.1 summarises the oils used in this work with their suppliers and purities.

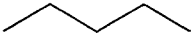
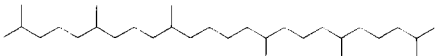
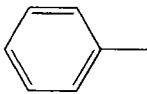
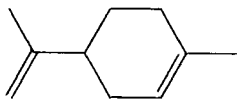
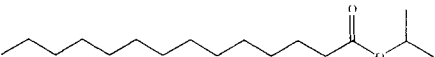
Table 2.1. Supplier and purity of the oils used.

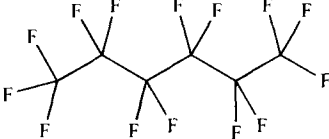
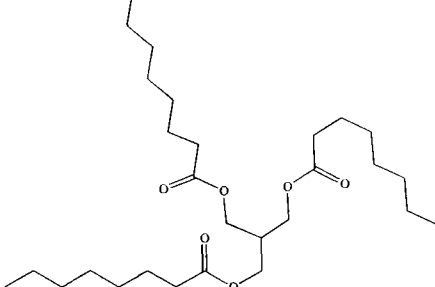
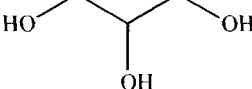
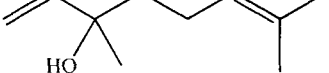
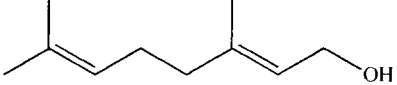
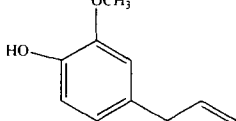
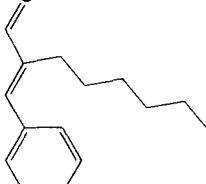
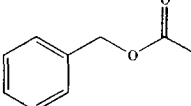
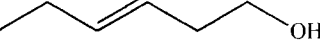
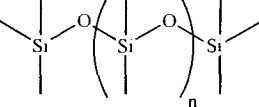
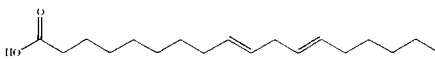
Liquid	Supplier	Purity/ %
<i>Pentane</i>	Fisher	> 99
<i>Hexane</i>	Fisher	95
<i>Heptane</i>	Fisher	99
<i>Dodecane</i>	Fisher	99
<i>Tetradecane</i>	Fisher	99
<i>Hexadecane</i>	Fisher	98
<i>Squalane</i>	Aldrich	99
<i>Cyclohexane</i>	Fisher	> 99
<i>Toluene</i>	Fisher	99
<i>Limonene</i>	Aldrich	97

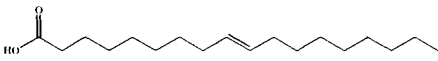
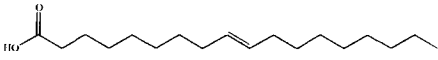
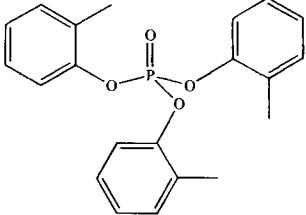
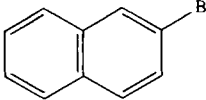
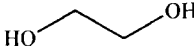
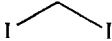
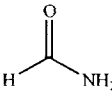
Liquid	Supplier	Purity / %
<i>Benzene</i>	Aldrich	> 99
<i>Isopropyl myristate</i>	Aldrich	> 98
<i>Tricaprylin</i>	Aldrich	> 99
<i>Perfluorohexane</i>	Aldrich	99
<i>Miglyol 812N</i>	Sasol	-
<i>Glycerol</i>	Aldrich	99
<i>Linalool</i>	Aldrich	> 97
<i>Geraniol</i>	Aldrich	> 97
<i>Eugenol</i>	Aldrich	> 98
<i>α-hexylcinnamaldehyde</i>	Aldrich	> 95
<i>Benzyl Acetate</i>	Aldrich	> 99
<i>cis-3-hexenol</i>	Aldrich	> 98
<i>PDMS 0.65 cS</i>	Dow Corning	100
<i>PDMS 10 cS</i>	Dow Corning	-
<i>PDMS 100 cS</i>	Dow Corning	-
<i>PDMS 500 cS</i>	Dow Corning	-
<i>Sunflower oil</i>	Co-op	-
<i>Rapeseed oil</i>	Tesco	-
<i>Peanut oil</i>	EULIP	-
<i>Tricresyl Phosphate</i>	Aldrich	> 99
<i>α-bromonaphthalene</i>	Aldrich	97
<i>Ethylene glycol</i>	Aldrich	> 99
<i>Diiodomethane</i>	Aldrich	99
<i>Formamide</i>	Aldrich	> 99

Prior to their use, all of the oils were purified by column chromatography by passing them 3 times through activated neutral alumina oxide in order to remove the more polar surface-active impurities. The structures of the oils as well as their densities are given in Table 2.2.

Table 2.2. Structure and density of the liquids used in this study.

Name	Structure	Density / g cm ⁻³ at 20°C
<i>Pentane</i>		0.63
<i>Hexane</i>		0.66
<i>Heptane</i>		0.68
<i>Dodecane</i>		0.75
<i>Tetradecane</i>		0.76
<i>Hexadecane</i>		0.77
<i>Squalane</i>		0.81
<i>Cyclohexane</i>		0.78
<i>Toluene</i>		0.87
<i>Benzene</i>		0.88
<i>Limonene</i>		0.84
<i>Isopropyl myristate</i>		0.85

Name	Structure	Density/ g cm ⁻³ at 20°C
<i>Perfluorohexane</i>		1.71
<i>Tricaprylin</i>		0.95
<i>Glycerol</i>		1.26
<i>Linalool</i>		0.87
<i>Geraniol</i>		0.88
<i>Eugenol</i>		1.07
<i>α-hexyl cinnamaldehyde</i>		0.95
<i>Benzyl Acetate</i>		1.05
<i>cis-3-hexenol</i>		0.85
<i>PDMS 0.65 cS</i> <i>PDMS 10 cS</i> <i>PDMS 100 cS</i> <i>PDMS 500 cS</i>		0.76 0.93 0.96 0.97
<i>Sunflower oil</i> (>50% linoleic acid)		0.92

Name	Structure	Density/ g cm ⁻³ at 20°C
<i>Rapeseed oil</i> (>60% oleic acid)		0.92
<i>Peanut oil</i> (>50% oleic acid)		0.91
<i>Tricresyl Phosphate</i>		1.16
<i>α-bromonaphthalene</i>		1.48
<i>Ethylene glycol</i>		1.11
<i>Diiodomethane</i>		3.33
<i>Formamide</i>		1.13

2.1.3 Particles

A wide range of particles, either kindly provided by the suppliers (Florabeads, Floraspheres, Aquawax 114, Microklear 418, Ultraflon MP-8T, Ultraflon UF-8TA and OTFE) or bought, was used in this study.

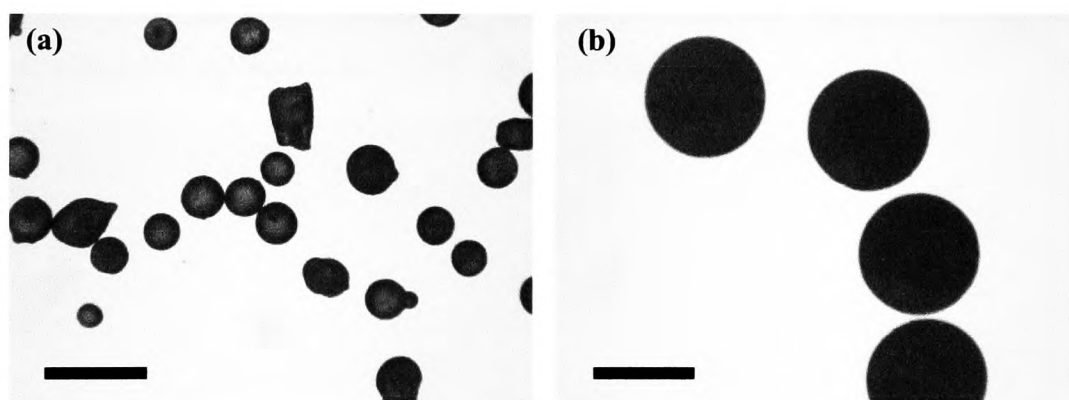
Table 2.3. Names, supplier and size of particles used in this study.

Particle	Supplier	Diameter / μm
Florabeads	Chesham Specialty Ingredients	$200 \pm 50 \mu\text{m}$
Floraspheres		$500 \pm 200 \mu\text{m}$
Glyceryl tripalmitate	Fluka (> 99 %)	$150 \pm 50 \mu\text{m}$
Aquawax 114	Micro Powder	$8 \pm 2 \mu\text{m}$
Microklear 418		$11 \pm 2 \mu\text{m}$
PLGA (50:50)	micromod	$250 \pm 60 \text{ nm}$
PLGA-COOH		$250 \pm 60 \text{ nm}$
PLGA-NH ₂		$250 \pm 60 \text{ nm}$
PLGA (65:35)		$250 \pm 60 \text{ nm}$
PLGA (75:25)		$250 \pm 60 \text{ nm}$
Ludox HS-30	Aldrich	$15 \pm 2 \text{ nm}$
Ludox CL		$15 \pm 2 \text{ nm}$
Sporopollenin	Tibrewala Int., Nepal	$30 \pm 5 \mu\text{m}$
PTFE Zonyl MP1100	E&E Ltd, UK	$0.3 \mu\text{m}$
PTFE Zonyl MP1400		$10 \mu\text{m}$
PTFE Ultraflon MP-8T	Laurel Products, UK	$2.5 \mu\text{m}$
PTFE Ultraflon UF-8TA		$0.3 \mu\text{m}$
OTFE	Central Glass Co. Ltd, Japan	$1.3 \mu\text{m}$
Fumed silica (80, 71, 20 and 14% SiOH content)	Wacker	$20 \pm 2 \text{ nm}$

2.1.3.1 Waxes and fat

The two different Flora particles are shown in Figure 2.1. Florabeads are smooth spherical particles of $200 \pm 50 \mu\text{m}$ average diameter with a melting point of $68 \pm 2^\circ\text{C}$. Floraspheres are also spherical particles, but with a larger average diameter ($500 \pm 200 \mu\text{m}$) and a lower melting point of $52 \pm 7^\circ\text{C}$. Both particles are composed of jojoba ester extracted from the *Simmondsia chinensis* oil and are insoluble in water; the structure of an ester of jojoba wax is shown in Figure 2.2 and composed mainly of C_{38} to C_{44} alkyl chains.^{2,3}

Figure 2.1. Optical microscopy of dry (a) Florabeads and (b) Florapheres. Scale bars represent $400 \mu\text{m}$.



The triglyceride glyceryl tripalmitate is a solid crystallisable fat, found abundantly in animal and vegetal (particularly palm oil). Glyceryl tripalmitate powder was purchased from Fluka as long crystals ($150 \pm 50 \mu\text{m}$) in a powder form with a low melting point of $67 \pm 1^\circ\text{C}$. The molecule, represented in Figure 2.2, has the structure of a triester made with three palmitic acids (C_{16}). Glyceryl tripalmitate crystals were re-crystallised in acetone by heating them to 70°C in an oil bath and cooling them rapidly by handshaking for 5 minutes in an ice bath, before evaporating the acetone with a Heidolph Laborota 4000 eco rotary-evaporator. The crystals, before and after recrystallisation, are shown in Figure 2.3.

Figure 2.2. Structure of (a) jojoba wax ester and (b) glyceryl tripalmitate.

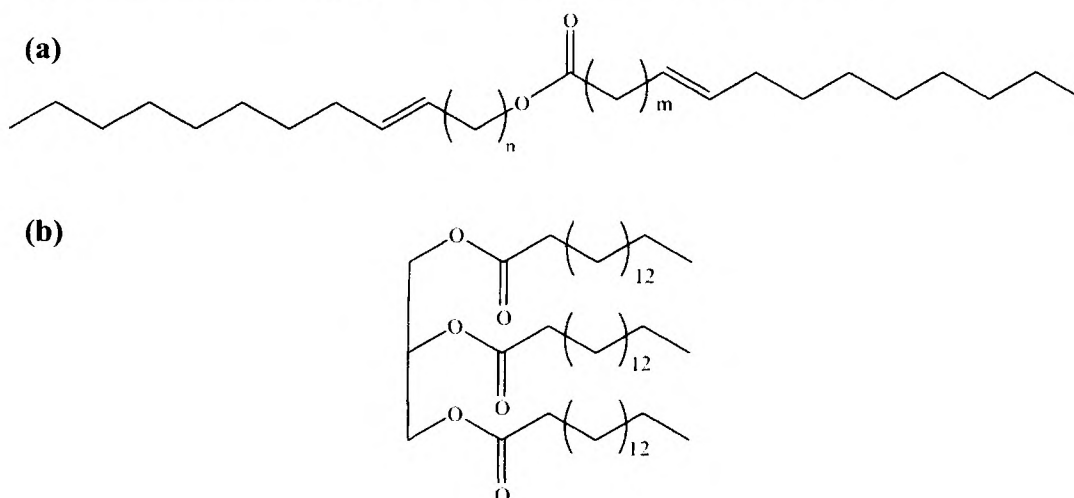
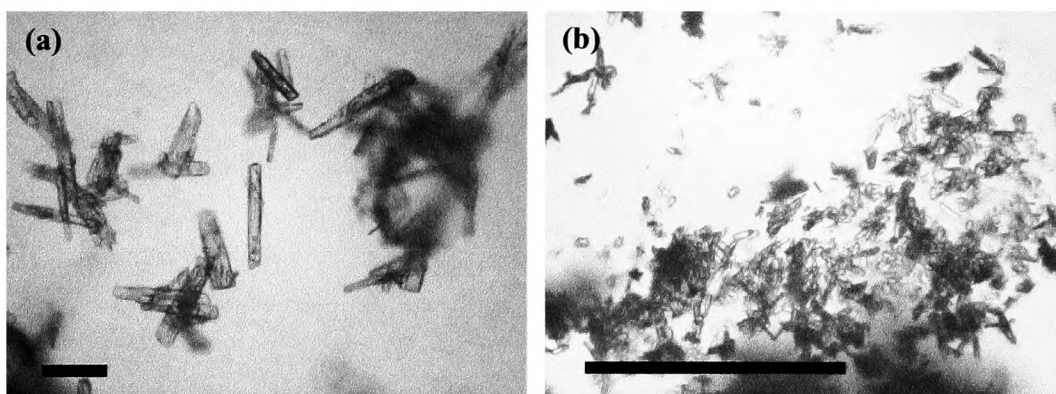


Figure 2.3. Optical micrographs of dry glyceryl tripalmitate crystal before (a) and after (b) re-crystallisation. Scale bars represent 100 μm .



Aquawax 114 and Microklear 418 waxes were provided by Micro Powder. Both of them are irregularly shaped particles, as displayed in Figure 2.4, and have a density close to that of water being 0.94 g cm^{-3} for Aquawax 114 and 0.99 g cm^{-3} for Microklear 418 at $25 \text{ }^\circ\text{C}$. Their melting points, measured with a capillary melting point apparatus, were of $108 \pm 1 \text{ }^\circ\text{C}$ for Aquawax 114 and $83 \pm 1 \text{ }^\circ\text{C}$ for Microklear 418. The Aquawax 114 is a synthetic wax, which, according to the manufacturer, is composed of saturated straight chain hydrocarbon molecules. Microklear 418 comes from the natural yellow carnauba wax, peeled off *Copernicia prunifera* leaves, and is composed of a mixture of cinnamic ester, fatty acid (Figure 2.5) and fatty alcohol.^{4,5}

Figure 2.4. SEM microscopy of dry (a) Aquawax 114 and (b) Microklear 418. Scale bars represent 10 μm .

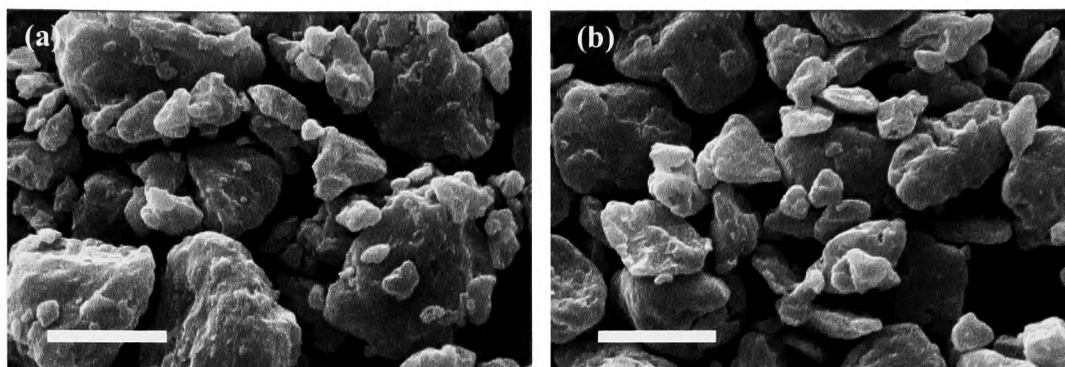
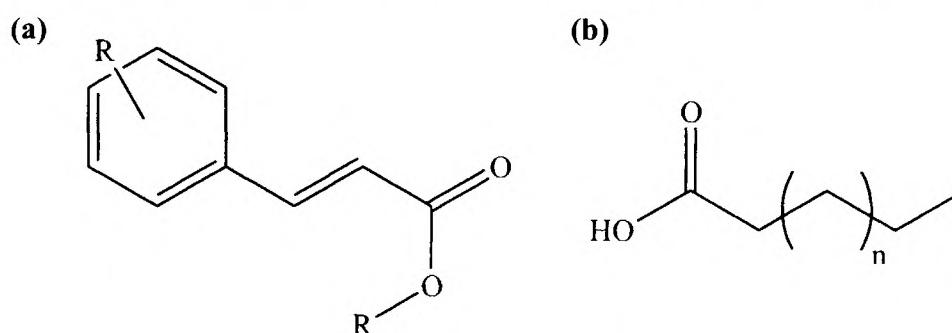


Figure 2.5. Structure of (a) cinnamic ester and (b) saturated fatty acid.



2.1.3.2 Poly(lactic-co-glycolic) acid

The biodegradable poly(lactic-co-glycolic) acid (PLGA) nanoparticles were purchased from micromod (Germany). The unmodified PLGA particles are composed of a 50:50 lactic:glycolic (L:G) acid monomer ratio, as represented in Figure 2.6. PLGA particles degrade at room temperature, hence they were stored at 5°C prior to use.⁶ They were functionalised with COOH and NH₂ groups especially for this study in order to obtain negatively and positively charged particles for a specific range of pH. Two more PLGA particle types were manufactured for this study: the L:G ratio was changed to 65:35 and 75:25. PLGA (all ratio), PLGA-COOH and PLGA-NH₂ particles were observed by TEM microscopy in Figure 2.7, which revealed that they are spherical and around 250 nm in diameter.

Figure 2.6. Structure of poly(lactic-co-glycolic) acid.

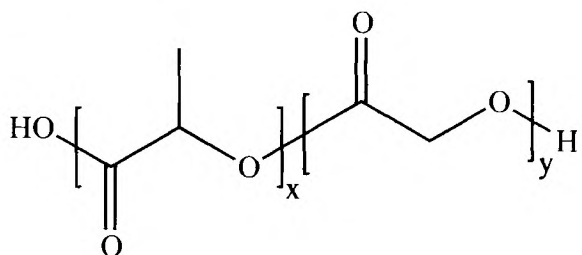
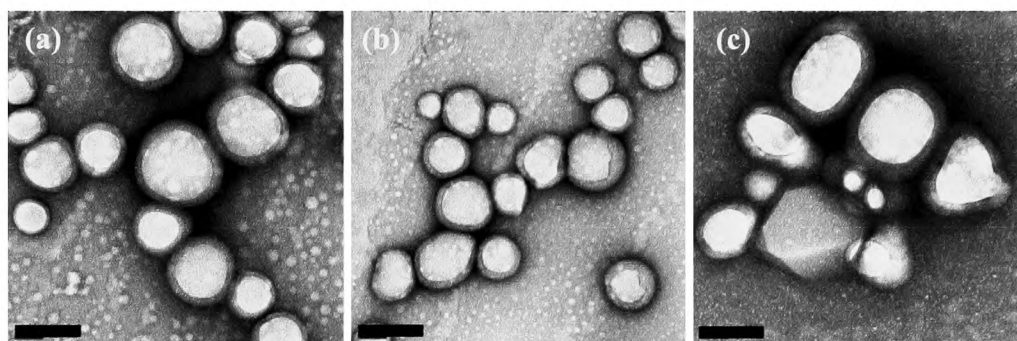


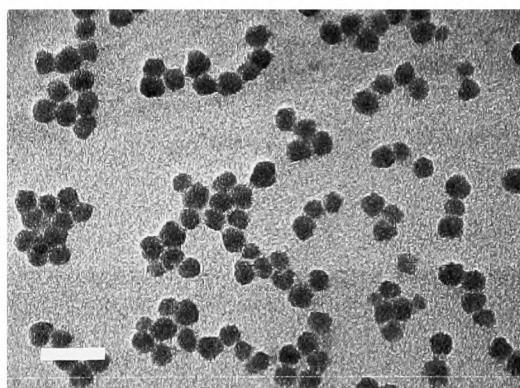
Figure 2.7. TEM image of 0.001 wt.% aqueous dispersion of (a) PLGA (50:50), (b) PLGA-COOH and (c) PLGA-NH₂ particles. Scale bars represent 200 nm.



2.1.3.3 Ludox HS-30 and Ludox CL

Ludox HS-30 and Ludox CL bought from Aldrich were received as a 30 wt.% aqueous dispersion at pH 9.8 and 3.5, respectively. These particles are spherical and relatively monodisperse, as can be seen in Figure 2.8, with an average diameter of 15 ± 2 nm.⁷ They were chosen for their opposite charge within a range of pH: Ludox HS-30 are negatively charged silica particles above pH 2, and Ludox CL are positively charged alumina-coated silica particles below pH 8.

Figure 2.8. TEM image of 0.1 wt.% aqueous dispersion of Ludox HS-30 particles at pH 9.5, taken from ref. 7. Scale bar represents 50 nm.

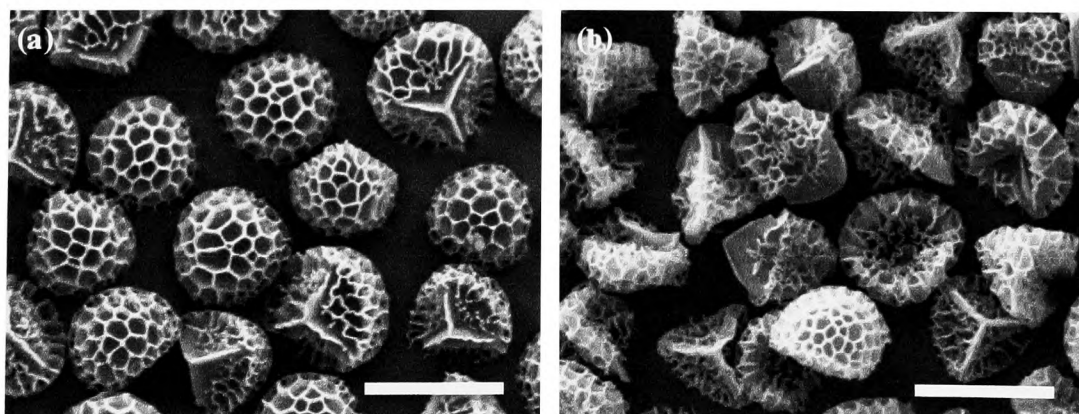


2.1.3.4 Sporopollenin

Lycopodium clavatum spores were obtained from Tibrewala International (Nepal).⁸ The sporopollenin particles were extracted from *Lycopodium clavatum* spores with the following organic solvent washings, plus alkaline and acidic treatments. 100 g of *Lycopodium clavatum* spores were boiled in 500 mL of acetone under reflux for 4 hours. The suspension was dried with phosphorus pentoxide for 2 days before being refluxed with 500 mL of 6% potassium hydroxide for 6 hours. The particles were then filtered and washed with 1.5 L of water and the KOH treatment was repeated a second time before drying them for several hours. They were then refluxed with 300 mL of 85% ortho-phosphoric acid for 5 days, washed consecutively with hot water, 2 M NaOH solution, and ethanol several times. These processes enable the elimination of the outside lipid layer of the spores, as well as the degradation and removal of the internal genetic material. The sporopollenins resulting from this are composed of the strongest part of the spore, although they originally contributed to only 25% of the spore total weight. They are edible and non-allergenic, so can be used for a variety of applications in the cosmetic or food industries.

The resulting particles are approximately 30 μm in diameter and seem reasonably monodisperse. They have a rough surface, and present a spherical cap with a 3-fold marking (Y-shape). A comparison of the spores and the sporopollenins of *Lycopodium clavatum* is displayed in Figure 2.9. The sporopollenins appear collapsed on themselves demonstrating the success of the intine removal process.

Figure 2.9. SEM microscopy of (a) spores taken from ref. 8 and (b) sporopollenins of *Lycopodium clavatum*. Scale bars represent 25 μm .



2.1.3.5 Tetrafluoroethylene

Four types of polytetrafluoroethylene (PTFE) and an oligomeric tetrafluoroethylene (OTFE) particles were used in this study. The structure of TFE and scanning electron microscope (SEM) images of the particles are given in Figure 2.10 and 2.11, respectively. These particles range from 0.3 to 10 μm (mean diameter). Zonyl MP1100 and MP1400 particles were made by DuPont and supplied by E&E Ltd, UK. Ultraflon MP-8T and UF-8TA were obtained from Laurel Products, UK. OTFE particles were supplied by Central Glass Co. Ltd, Japan. A distinction can be made between the PTFE particles, as can be seen in Figures 2.11 (a) to (d): Zonyl MP1100 and Ultraflon UF-8TA particles, measuring approximately 0.3 μm in diameter, have smooth surfaces and rounded shape and are fairly monodisperse, whereas Zonyl MP1400 and Ultraflon MP-8TA, of respectively 10 and 2.5 μm in diameter, are rough-surfaced and irregularly shaped polydispersed particles. OTFE particles are similar to Zonyl MP1100, but their diameter is larger ($\sim 1.3 \mu\text{m}$) and their shape almost spherical.

Figure 2.10. Structure of tetrafluoroethylene (TFE).

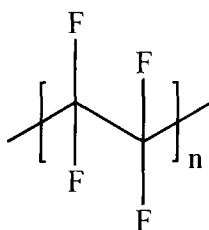
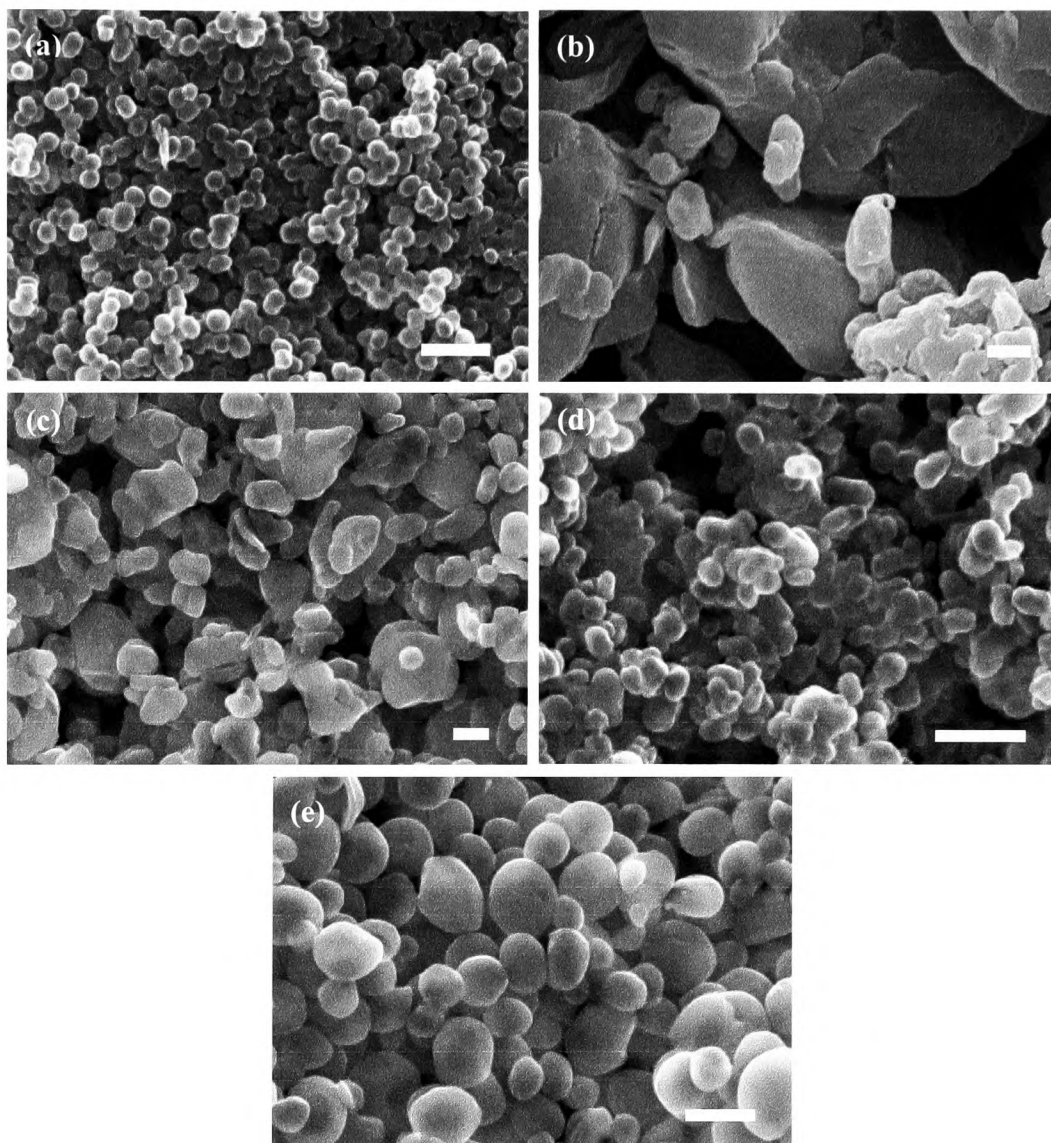


Figure 2.11. SEM images of dry (a) Zonyl MP1100, (b) Zonyl MP1400, (c) Ultraflon MP-8T, (d) Ultraflon UF-8TA and (e) OTFE particles. Scale bars represent 1 μm .

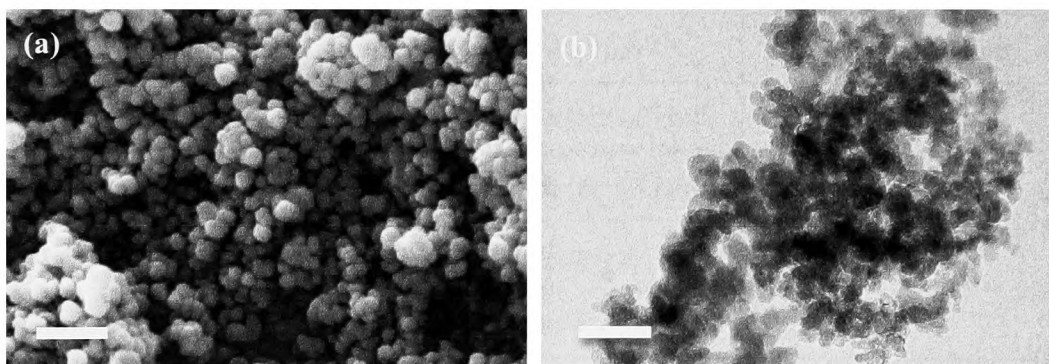


2.1.3.6 Fumed silica

Amorphous fumed silica particles were a gift from Wacker-Chemie (Munich). They are approximately spherical with an average primary diameter between 5 and 30 nm, as can be seen in Figure 2.12. The primary particles can aggregate into larger units of about 100 nm in diameter. Hydrophilic silica particles were silanated to various extents by reaction with dimethyldichlorosilane in the presence of water followed by drying at 300°C for 2 h, leaving the particle surfaces containing silanol (SiOH) and dimethylsilane (SiOSi(CH₃)₂) groups.⁹

The resulting particles ranged from completely hydrophilic, N20, with a relative surface silanol (SiOH) content of 100%, to partially hydrophobic, H30 (50% SiOH), to completely hydrophobic, H18 (20% SiOH).¹⁰

Figure 2.12. (a) SEM image of powdered hydrophobic fumed silica H18 and (b) TEM image of a dried ethanolic dispersion of the same, taken from ref. 11. Scale bars represent 50 nm.



2.1.4 Other chemicals

Within the specific sections of this work, materials other than those already detailed have been used. These materials along with their supplier and purity are listed in Table 2.4. All these chemicals were used as received.

Table 2.4 Supplier and purity of the other chemicals used in this study.

Chemical	Supplier	Purity / %
Sodium hydroxide	VWR International	> 99
Potassium hydroxide	VWR International	> 99
Aqueous hydrochloric acid	Fluka	37 wt., analytical grade
Sodium bis(2-ethylhexyl) sulfosuccinate (AOT)	Fluka	> 99
Stearic acid	Fisher Chemicals	> 99
Nile red dye	Aldrich	Technical grade
Ethanol	University of Hull	Analytical grade
Acetone	University of Hull	Analytical grade
Isopropyl alcohol	Aldrich	99.9
PDMS Sylgard 184 elastomer	Dow Corning	unkown

2.2 Methods

2.2.1 *Surface tension of oils*

A Krüss K12 digital tensiometer using the Wilhelmy plate method was used at 25°C to determine the surface tension of a few liquids used in Chapter 7. The balance was checked before use, as was the plate by measurement of the dodecane surface tension. The cleaning procedure consisted in rinsing the glass vessel in alcoholic KOH solution and Milli-Q water before letting it dry an hour in an oven at 60°C. The plate was rinsed with ethanol and then heated to glowing in a blue Bunsen flame.

2.2.2 *Characterisation of particles*

2.2.2.1 Microscopy: optical, SEM and TEM

Optical microscopy, Scanning Electron Microscopy (SEM) and Transmission Electron Microscopy (TEM) were used to visualise some of the particles.

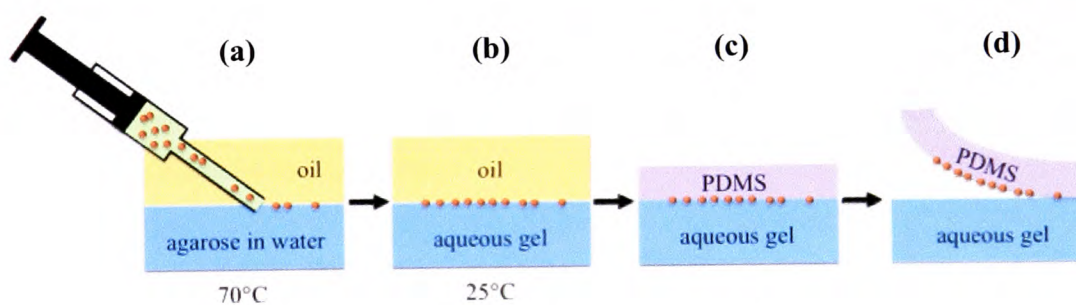
The large Floraspheres, Florabeads, glyceryl tripalmitate crystals and sporopollenin particles were observed with a Nikon Labophot Optical Transmission microscope with 4, 10, 40 and 100 x plan objectives and fitted with a QICAM Fast 1394 camera from QImaging. Images were recorded using Image-Pro Plus software (Media Cybernetics, Silver Springs, MD). The dry particles were spread on a glass slide for microscopy.

Aquawax 114, Microklear 418, sporopollenin, Zonyl MP1100, Zonyl MP1400, Ultraflon MP-8T, Ultraflon UF-8TA and OTFE particles were observed by SEM with a Zeiss EVO 60 SEM instrument with a voltage of 22 kV, a resolution of 3 nm and a probe current of 20 pA. Samples of dry particles were coated with an Au/Pd (mass ratio 82:18) film of 1.5 nm thickness with the Polaron SC7640 Sputter Coater fitted with a FT7690 Thickness Monitor.

Sporopollenin particles were also observed using the Gel Trapping Technique (GTT) in order to study their orientation at the air-water and oil-water interfaces.¹² This method aims at locking the particles in their original position at a fluid interface so that they may be observed by SEM. Agarose was dissolved in water (pH 6.5) at

70°C, and then centrifuged to remove the bubbles, before being poured onto a plastic Petri dish. For the air-water interface, dry sporopollenin particles were spread on the agarose solution by blowing them from a glass slide onto the agarose (Figure 2.13 (a)). For the oil-water interface, the 70°C oil was poured on top of the agarose, and a 0.01 wt.% dispersion of sporopollenin particles in isopropyl alcohol was injected at the agarose-oil interface. The agarose was left an hour to settle, and in the oil-water case, the oil was removed (Figure 2.13 (b)). PDMS Sylgard 184 elastomer was poured on top of the gelled agarose (Figure 2.13 (c)). After 48h of curing, the polymer was peeled off, and then washed in boiling water (Figure 2.13 (d)). The sample was checked by optical microscopy, before being submitted for SEM imaging. Samples for SEM were coated with an Au/Pd (mass ratio 82:18) film of 1.5 nm thickness.

Figure 2.13 Schematic representation of the Gel Trapping Technique performed at the oil-water interface.



PLGA particles (plain, NH₂ and COOH coated) were observed by TEM with a JEOL JEM 2011 TEM operated at an accelerating voltage of 120 kV. The 0.001 wt.% aqueous dispersions were dropped onto a carbon-coated copper grid then stained with uranyl acetate (1 wt.%) prior to characterisation.

2.2.2.2 Light scattering

A Malvern Zetasizer HS 3000 instrument was used to determine both the size and/or zeta potential distributions of particles at 20°C. For zeta potential measurements, the dispersions were contained within an electrophoretic cell and a known electrical field was applied across the electrodes. The velocity of the particles

was measured by light scattering from crossed focused lasers, and then converted to zeta potential using the computational software *via* the Smoluchowski approximation.

PLGA particle dispersions, of modified and unmodified particles, were diluted in Milli-Q water to 0.002 wt.%, before being placed within a quartz cell in the apparatus for size measurements.

Dispersions of 0.02 wt.% of PLGA, Ludox and sporopollenin particles were subject to zeta potential measurements: the solutions were poured in the quartz cell and the palladium electrodes were placed into the cell. Zeta potentials were measured as a function of solution pH, varying the pH by addition of small volumes (< 20 μ L) of NaOH or HCl (1M) to the natural dispersion in Milli-Q water.

A Malvern Mastersizer 2000 was used for measuring the size distribution of the four types of PTFE particles and the OTFE particles. TFE particles were dispersed in methanol at 0.2 wt.% using the ultrasonic processor Vibra-cell (Sonics & Materials). The processor was operated with a probe tip of diameter 3 mm at 20 kHz, and up to 10 W for 1 minutes. The vessel was kept cool in an ice bath during the process. A drop of the dispersion was then diluted 100 times in methanol with the dispersion unit before being measured by inputting the refractive indices of the TFE (1.345) and the methanol (1.329).

2.2.2.3 Differential scanning calorimetry

The determination of the melting point of wax particles by standard capillary tube measurements only partially describes the wax thermal properties, so Differential Scanning Calorimetry (DSC) was used for the two micro-waxes.¹³ DSC measurements enable precise determination of the melting temperature range of a material, as well as the amount of energy associated with the melting transition. A Mettler Toledo DSC-822e instrument was used for the wax thermal analyses; it was calibrated with an indium standard, and used dry nitrogen as the purge gas. Sealed aluminium pans containing the powdered wax samples (~ 5 mg) were run alongside an empty pan. First, the samples were held for 10 min at 25 °C, then heated at a particular rate (2 or 10 °C/min) to a temperature of either 100 or 120 °C, and finally cooled at the same rate. A second heating–cooling cycle was performed

subsequently. The plotted results (heat flow as a function of temperature) were used to obtain the onset, major peak and end of the melting/solidification transitions, while the software determined the associated heats by standard methods.

2.2.2.4 Attenuated Total Reflection Fourier Transform Infrared Spectroscopy

Attenuated Total Reflection Fourier Transform Infrared Spectroscopy (ATR-FTIR) was used to analyse the Aquawax 114 and Microklear 418 composition. Infrared spectra ($400\text{-}4000\text{ cm}^{-1}$) of a small amount of dry wax powder ($\sim 1\text{ mg}$) were recorded with a Nicolet 380 FTIR equipped with a Smart Orbit diamond ATR crystal.

2.2.2.5 Contact angles

A thermostated Krüss DSA10 instrument was used for the contact angle measurements on wax and PLGA coated layers and on PTFE compressed powder as described herein.

Contact angles of sessile water drops on Aquawax 114 and Microklear 418 layers under squalane were measured at different temperatures. Hydrophilic microscope glass slides were cleaned with aqueous KOH solution and Milli-Q water, before being oven dried. The wax coating was made by pouring powdered wax onto the heated slides, melting the powder on further heating, and flattening the wax layer with a second slide to obtain a coating of uniform thickness on cooling. Advancing contact angles of sessile water drops ($20\text{ }\mu\text{L}$, $\text{pH} = 5.8$) under squalane, where oil contacted the solid first, were measured in a 20 mm cubical glass cell. The average value of three drops was taken and the temperature of the cell was increased progressively with a water drop in place.

Contact angles of sessile water drops on a PLGA layer, with L:G ratios of 50:50 and 65:35, were measured in air and under dodecane. Hydrophilic microscope glass slides were cleaned with aqueous KOH solution and purified water, before being oven dried. PLGA 50:50 and 65:35 polymers were spin coated onto the slides using solutions of PLGA in chloroform (50 wt.%), forming a thin uniform coating.

Advancing contact angles of sessile water drops (20 μL , $\text{pH} = 5.8$) in air and under dodecane were measured both with water contacting the substrate first and dodecane contacting the substrate first. The average value of three drops was taken at room temperature ($20 \pm 1^\circ\text{C}$).

Contact angles of sessile drops of different liquids were measured in air onto a solid pellet of Zonyl MP1100 particles. The pellet was made by compressing 0.2 g of dry particles into a 1.2 cm diameter die with a hydraulic press under 10 Tons pressure. Advancing and receding contact angles of a 50 μL drop of different liquids were measured. The average value of four drops was taken at room temperature ($20 \pm 1^\circ\text{C}$).

2.2.2.6 Powder wetting

Static and dynamic wettability tests were carried out on the different TFE particles. Static wettability was estimated by placing 50 mg of each particle powder on the surface of 1 cm^3 of a given liquid contained in a tube of diameter 8 mm at room temperature, and monitoring if particles immersed or not over 24h. The dynamic wettability test consisted in handshaking the vessel gently 10 times after the static wettability test was performed, and recording if the powder entered the liquid. The static stability results were recorded in terms of “wetted” when the particle layer entered the liquid completely, “partially wetted” when some particles only entered or “non-wetted” when the particles remained completely on top of the liquid. The dynamic wettabilities were classified as “dispersed”, “few bubbles”, “bubbles” and “dry material”, depending on the observation made after handshaking the mixtures.

2.2.2.7 pH titration

Sporopollenin particle dispersions were titrated with NaOH to investigate the charging of their surface groups. An initial 0.5 wt.% dispersion of dry sporopollenin particles at pH 3.7 was titrated with addition of a 0.01 M solution of NaOH. The pH of the particle dispersion was measured using a FisherBrand Hydrus 400 meter fitted with a glass electrode. The titration enabled the determination of the pK_a of the particles.

2.2.3 *Preparation of particle dispersions*

2.2.3.1 Wax particle dispersions

Dispersions of Flora particles (section 3.3.1.1) were prepared in squalane oil or Milli-Q water by two different methods: with magnetic bar agitation using a MP3001 Hot Plate Stirrer (Heidolph) or with a High Intensity Ultrasonic Processor Vibra-cell VC100 with a 20 kV CV18 Ultrasonic probe of 3 mm diameter (Sonic & Materials). A known amount of particles was dispersed in the oil either by operating the stirrer for 1 minute at 1000 rpm or by operating the ultrasonic apparatus at 10 W during 2 minutes while immersing the vessel in an ice bath. The dispersion was processed at room temperature ($21 \pm 1^\circ\text{C}$).

A known amount of glyceryl tripalmitate crystals (section 3.3.2.1) was dispersed in squalane for 10 minutes using a FS3006 Decon Ultrasonic bath at room temperature ($21 \pm 1^\circ\text{C}$).

Dispersions of Aquawax 114 and Microklear 418 particles (section 3.3.3.1) in squalane oil were prepared with a VXR Vibrax basic shaker (IKA) at 500 rpm during 1 minute at room temperature.

Other particle dispersions were prepared by handshaking strongly a known amount of particles for 10 seconds at room temperature.

2.2.3.2 Fumed silica particle dispersions

Dispersions of fumed silica particles (section 8.2) were prepared using the High Intensity Ultrasonic Processor Vibra-cell VC100 with a 20 kV CV18 Ultrasonic probe of 3 mm diameter (Sonic & Materials). A known amount of particles was dispersed in water by operating the processor up to 10 W for 2 minutes, while keeping the vessel immersed in an ice bath.

2.2.3.3 Other particle dispersions

A known amount of Zonyl MP1400 particles (section 7.3.1.4) were dispersed in oil for 10 minutes using a FS3006 Decon Ultrasonic bath at room temperature (21 ± 1 °C). Sporopollenin particles (section 6.2.2) were dispersed in water by homogenisation with an IKA Ultra Turrax model T25 operated at 11000 rpm for 1 minute in Milli-Q water. Other particle dispersions were prepared by 10 seconds strong handshaking. A known amount of PLGA (section 4.2.1), Ludox (section 5.2) or sporopollenin (section 6.2.2) particles were dispersed in Milli-Q water or oil at room temperature (21 ± 1 °C).

2.2.4 *Preparation of emulsions*

A 10 mL mixture of oil, water and particles was emulsified for all emulsion systems. In some cases, Nile red dye was dissolved in the oil phase at 0.005 wt.%. Emulsification was achieved either with an Ultra Turrax apparatus, by handshaking or by magnetic stirring, depending on the system.

2.2.4.1 Ultra Turrax homogenisation

An Ultra Turrax T25 basic homogeniser (IKA) was used to prepare emulsions with wax, PLGA and silica particles (Chapters 3, 4, 5 and 8) at 11 000 or 13 000 rpm up to 2 minutes. The rotor-stator mixing head was immersed in the mixture to create shearing, which breaks down the separated liquid phases into drops.

2.2.4.2 Handshaking

The handshaking homogenisation, used for the wax and sporopollenin-stabilised emulsions (Chapters 3 and 6), consisted of a vigorous handshaking of the sealed vessel containing the oil-water-particle mixtures up to 2 minutes. The strong and rapid displacement of the two liquid phases against the walls of the vessel creates a large turbulence within the bulk of the fluid and eventually disperses one phase as drops in the other.

2.2.4.3 Magnetic stirring

A Heidolph MP3001 Hot Plate Stirrer was used for the magnetic stirring emulsification with a magnetic bar (101.6 x 15.9 mm), which was added to the mixture. The stirring was for 2 minutes at 2000 rpm at room temperature ($21 \pm 1^\circ\text{C}$). The stirring creates a vortex in the mixture and breaks the bulk phases into emulsion drops.

2.2.4.4 Temperature studies

Temperature studies were carried out with wax-stabilised emulsions (section 3.4), where the emulsification was either performed at room temperature or at elevated temperatures.

2.2.4.4.1 Emulsions made at room temperature

10 wt.% Aquawax 114 and Microklear 418-stabilised emulsions were made at room temperature ($21 \pm 1^\circ\text{C}$) either with the Ultra Turrax or by handshaking, as described in sections 2.2.4.1 and 2.2.4.2. Emulsions were then placed in a water bath, with the temperature controlled with a GD120K Grant thermostat. The bath temperature was increased to 30°C and the emulsions were gently shaken to re-disperse any cream in their continuous phase. The process was repeated by increasing the temperature further to 40, 50, 60, 70, 80 and 90°C . Emulsion stability was recorded for each temperature change. Finally, the emulsion was removed from the bath and stored at room temperature ($21 \pm 1^\circ\text{C}$).

2.2.4.4.2 Emulsions made at different temperatures

10 wt.% Aquawax 114 and Microklear 418, and 3 wt.% glyceryl tripalmitate-stabilised emulsions were made at room temperature ($21 \pm 1^\circ\text{C}$) with the Ultra Turrax or by handshaking at elevated temperatures. The particles dispersed in oil and the water were heated up to each of these temperatures, then mixed together and homogenised. Emulsification took place in a water jacket filled with water with the temperature controlled with a GD120K Grant thermostat. It consisted in either Ultra Turrax homogenisation or in handshaking in the water enabled by attaching the

sealed vessel to a wooden tong. Emulsions were left in the water bath for 5 minutes after emulsification, then they were removed and stored at room temperature (21 ± 1 °C), before recording their stability.

2.2.5 *Characterisation of emulsions*

2.2.5.1 Drop test

The type of emulsion was determined by observing the behaviour of an emulsion drop added to Milli-Q water or pure oil. The emulsion drop will disperse in the phase which is its continuous phase, whereas it will remain as a drop in its dispersed phase.¹⁴ Therefore, a water-in-oil emulsion will disperse in an oil phase but stay as a drop on the surface of a water phase. However an oil-in-water emulsion will disperse in water and sediment as a drop in an oil phase.

2.2.5.2 Conductivity

Emulsion conductivities were measured immediately after emulsification with a Jenway 4510 Conductivity/TDS Meter fitted with Pt/Pt black electrodes. Low conductivity values were attributed to oil continuous emulsions, whereas relatively high values were related to water continuous emulsions.¹⁵ The conductivities of the pure liquids are: $\kappa_{\text{Milli-Q water}} = 2.30 \mu\text{S cm}^{-1}$, $\kappa_{\text{squalane}} = 0.01 \mu\text{S cm}^{-1}$, $\kappa_{\text{dodecane}} = 0.06 \mu\text{S cm}^{-1}$ and $\kappa_{\text{isopropyl myristate}} = 0.03 \mu\text{S cm}^{-1}$.

2.2.5.3 Stability

As described in section 1.3.1, the stability of an emulsion is a kinetic concept: an emulsion is stable if it is resistant over time to physical changes such as creaming and sedimentation.¹⁶ Emulsions were stored at room temperature in the glass vessels used during homogenisation. These were stoppered with foil-lined screw caps. The glass vessels were of inner diameter 15 mm and height 90 mm.

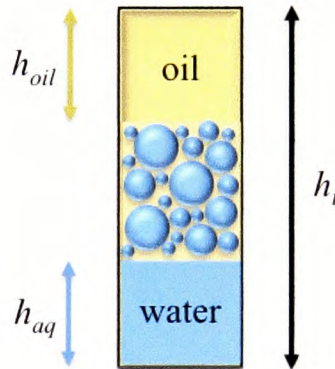
Emulsion stability was recorded in terms of the fraction of water (f_{aq}) or oil (f_{oil}) resolved compared to the amount of water and oil introduced in the system initially (Figure 2.14).

f_{aq} and f_{oil} were calculated from the height of water resolved (h_{aq}), the height of oil resolved (h_{oil}) and the total height of the liquid (h_t), knowing that the initial fraction of water was always $\phi_w = 0.5$:

$$f_{aq} = \frac{h_{aq}}{0.5h_t} \text{ and } f_{oil} = \frac{h_{oil}}{0.5h_t}$$

Thereby, for a water-in-oil emulsion, f_{aq} will indicate the stability to coalescence, f_{oil} the stability to sedimentation, and *vice-versa* for an oil-in-water emulsion. For stable emulsions, f_{aq} or f_{oil} values would be equal to 0; when the phases are totally separated these values would be equal to 1.

Figure 2.14. Representation of the determination of water and oil fraction resolved in an emulsion.



2.2.5.4 Optical microscopy

Optical micrographs were recorded using a Nikon Labophot Optical Transmission microscope with 4, 10, 40 and 100 x plan objectives and fitted with a QICAM Fast 1394 camera from QImaging. The emulsions were observed pure or diluted in their continuous phase, on a single cavity glass slide. Depending on the drop size, samples were covered or not with a coverslip, as the larger drops (>1 mm diameter) coalesced due to the pressure applied by the coverslip. Digital micrographs of each emulsion were recorded using Image-Pro Plus software within 5 minutes after emulsification, and the average diameter of the drops was calculated by

measuring the diameter of every drop on these micrographs. Digital micrographs were edited with Adobe Photoshop Elements 2.0 and scale bars were added to them.

Optical and fluorescence microscopy was employed when observing emulsion mixtures (Chapter 5) and powdered emulsions (Chapter 8), using an Olympus BX-51 fluorescence microscope. Excitation of the dissolved Nile red dye occurred with light from an Hg-arc lamp housed in an Olympus U-RFL-T power supply, which was filtered through an Olympus model UMF2 filter set, providing excitation at wavelengths between 451 and 490 nm light while transmitting fluorescence light to the camera between 491 and 540 nm. Digital micrographs were taken with an Olympus DP70 camera and analysed with Image-Pro Plus software.

2.2.5.5 Zeta potential

The zeta potential of isopropyl myristate-in-water emulsions stabilised by Ludox HS-30 or CL particles was measured with a ZetaSizer HS3000 instrument (Malvern) at 20°C. The emulsions were washed with Milli-Q water at pH 7.5 three times, to remove excess particles in the continuous phase, before being sampled and diluted. The Ludox CL emulsion was diluted 10 times, while the Ludox HS-30 was diluted 100 times in Milli-Q water, before proceeding to measurement described in section 2.2.2.2.

2.2.6 *Preparation of emulsion mixtures*

Mixtures of Ludox HS-30-stabilised emulsion and Ludox CL-stabilised emulsion were mixed by adding one emulsion dropwise to the other. The volume ratio of emulsions was either 1:1 or calculated in order to increase the ratio of large:small drops. The mixing proceeded either by gentle handshaking of the mixture between each addition or by mechanical stirring at low speed (100 rpm) during the addition process.

2.2.7 *Characterisation of emulsion mixtures*

Emulsion mixtures were left to rest 5 minutes before sampling from the middle of the mixture, and observing them by optical and fluorescence microscopy. The stability of the mixture was recorded in terms of the fraction of water and oil resolved, and compared to the stability of a sample from the parent emulsions.

2.2.8 *Preparation of liquid marbles*

Liquid marbles are obtained by making a small amount of liquid (typically 20 μL) roll on top of a bed of particles contained on a watch glass.¹⁷ Sporopollenin, PTFE and fumed silica particles were used for this purpose. The particles spontaneously coat the drop, which can eventually be transferred onto other substrates.

2.2.9 *Characterisation of liquid marbles*

2.2.9.1 Static and dynamic stability

The liquid marble stability was judged from the ability to form the liquid marble, *i.e.* without the marble collapsing. Static stability refers to the stability of the liquid marble when left to stand on the glass substrate after formation. The ability of the marbles to stay stable when rolled onto a glass substrate without breaking was termed “dynamic stability”. Both types of stability were estimated in terms of “stable” or “not stable”.

2.2.9.2 Evaporation and buckling

Liquid marbles were left to evaporate in the open atmosphere on the watch glass. Their development was followed either by taking photographs with a Lumix DMC-L10 camera (Panasonic), or by capturing their profile images with a Krüss DSA10 instrument every 5 minutes while recording the temperature and humidity with a thermometer and humidity meter DT-615 (CEM). For replicate experiments, the temperature and humidity were kept constant by keeping the liquid marbles in a thermostated cell.

2.2.10 Preparation of foams

Foams made from a mixture of oil and 5 wt.% of PTFE or OTFE particles were prepared in foil-lined screw capped glass vessels either by homogenisation in a glass jug blender, or using an Ultra Turrax, or by handshaking or by aeration with a diffuser.

The protocol to form dry water from the paper by Binks and Murakami was followed.¹⁸ Water was replaced with 95g of non-aqueous liquid and 5g of Zonyl MP1400 particles were added. The powder was placed on top of the oil in the blender jug (Braun, Glass Jug Power-Blend MX2050, 1.7 L with lid), before operating the blender at its maximum speed (25 000 rpm) for 30 seconds.

The material quantities were reduced for the production of foam with the Ultra Turrax. 5 wt.% of particle was placed on top of 10 mL of liquid in a glass sample tube, before operating the mixing head immersed in the liquid at 13000 rpm for 1 minute.

The handshaking method used the same quantity of material as the Ultra Turrax one. 5 wt.% of particle powder was placed on top of 10 mL of liquid in the sample tube, before handshaking for 30 seconds.

The diffuser aeration method employed larger quantities of materials and followed the method described by Binks *et al.*¹⁹ A range of particle concentrations from 0.1 to 5 wt.% were dispersed in 100 mL of oil. Compressed air was passed through a purification column filled with activated charcoal, a drying tube filled with silica gel and a flow meter (Platon) at a flow rate of $94 \text{ cm}^3 \text{ min}^{-1}$ into a Mott diffuser. A Stanhope Seta Mott diffuser with a mean pore diameter of $22 \text{ }\mu\text{m}$ and a permeability of $5100 \text{ mL air min}^{-1}$ at a pressure drop of 2.45 kPa was situated at the bottom of the liquid sample contained within a 1 L graduated measuring cylinder. Aeration *via* the Mott diffuser was carried out for 5 min.

2.2.11 Characterisation of foams

Immediately after homogenisation with the blender, Ultra Turrax or by handshaking, the volumes of foam (v_f), liquid (v_l) and total volume (v_t) were recorded to provide a measure of the foamability and foam stability as a function of time.

Photographs of the vessels containing samples were taken with a Lumix DMC-L10 camera (Panasonic). Small samples of the foam were placed in a single cavity cell (Fisher) and observed with an Olympus BX-51 microscope fitted with a DP50 CCD camera, using Image-Pro Plus 5.1 software (Media Cybernetics). Freeze-fracture SEM measurements were also carried out at Unilever Colworth on selected foam samples. A small volume of fresh sample was mounted onto a 0.1 cm diameter Al stub and plunged into nitrogen slush at -196°C . The frozen sample was transferred to a Gatan Alto 2500 cryo-preparation chamber and fractured with a scalpel blade at -175°C under high vacuum. It was then etched at -98°C and coated at -110°C with an Au/Pd sputter at low vacuum after which it was transferred to the chamber of a JEOL JSM-6301F SEM at -150°C . Image acquisition was obtained using the software Scandium (Soft Imaging System).

For the foam production by diffuser aeration, the foam and liquid volumes were recorded to provide a measure of the foamability and initial bubble volume fraction in the foam following cessation of the airflow. After the airflow was halted, the evolution of the foam and liquid volumes were recorded as a function of time to determine the foam stability.

2.2.12 *Preparation and characterisation of powdered emulsions*

Powdered emulsions, which can also be called oil-in-water-in-air systems, were prepared in two steps. An oil-in-water emulsion stabilised with hydrophilic silica particles was produced. This emulsion was encapsulated within hydrophobic silica particles into a powdered emulsion form.

Emulsions with a range of initial oil volume fractions were produced following the protocol described in section 2.2.4.1. Then they were diluted in Milli-Q water to different extents before being blended. The protocol to form dry water from the Binks and Murakami paper was followed with 95g of water (Milli-Q at pH 5.8) and 5g of Zonyl (PTFE) particles supplied by E&E (UK).¹⁸ The powder was placed on top of the diluted emulsion in the blender jug (Braun, Glass Jug Power-Blend MX2050, 1.7 L with lid), then the blender was operated at its maximum speed (25000 rpm) up to 30 seconds.

The initial emulsion was characterised as described in section 2.2.5, and the powdered emulsions were observed by optical and fluorescence microscopy as described previously for the emulsions. The continuous phase of the material formed was determined using a drop test into water: dry powders remained on the surface of water, while the other materials dispersed slightly. Immediately after preparation, the samples were transferred into plastic vessels to prevent destabilisation of the dry powders on contact with glass and observations about their appearance were noted over time. Photographs of vessels were taken using a Lumix DMC-L10 camera (Panasonic).

2.3 References

1. D. R. Lide, *CRC Handbook of Chemistry and Physics*, 89th ed., CRC Press, Boca Raton, 2008.
2. J. F. McLellan, R. M. Mortier, S. T. Orszulik and R. M. Paton, *J. Am. Oil Chem. Soc.*, **71**, 231 (1994).
3. H. J. Nieschlag, G. F. Spencer, R. V. Madrigal and J. A. Rothfus, *Ind. Eng. Chem. Prod. Res. Dev.*, **16**, 202 (1977).
4. A. Asperger, W. Engewald and G. Fabian, *J. Anal. Appl. Pyrolysis*, **50**, 103 (1999).
5. L. L. Wang, S. Ando, Y. Ishida, H. Ohtani, S. Tsuge and T. Nakayama, Quantitative and discriminative analysis of carnauba waxes by reactive pyrolysis-GC in the presence of organic alkali using a vertical microfurnace pyrolyzer. In *14th International Symposium on Analytical and Applied Pyrolysis*, Elsevier: Seville, 2000; pp 525.
6. S. J. De and D. H. Robinson, *AAPS PharmSciTech*, **5**, 7 (2004).
7. B. P. Binks, J. A. Rodrigues and W. J. Frith, *Langmuir*, **23**, 3626 (2007).
8. B. P. Binks, J. H. Clint, G. Mackenzie, C. Simcock and C. P. Whitby, *Langmuir*, **21**, 8161 (2005).
9. H. Balard, E. Papirer, A. Khalfi and H. Barthel, *Compos. Interfaces*, **6**, 19 (1999).
10. B. P. Binks and S. O. Lumsdon, *Langmuir*, **16**, 8622 (2000).
11. B. P. Binks, A. J. Johnson and J. A. Rodrigues, *Soft Matter*, **6**, 126 (2010).
12. V. N. Paunov, *Langmuir*, **19**, 7970 (2003).
13. R. Buchwald, M. D. Breed and A. R. Greenberg, *J. Exp. Biol.*, **211**, 121 (2008).
14. B. P. Binks and T. S. Horozov, Colloidal Particles at Liquid Interfaces: An Introduction. In *Colloidal particles at liquid interfaces*; Cambridge University Press, Cambridge, 2006.
15. I. D. Morrison and S. Ross, *Colloidal Dispersion: Suspensions, Emulsions and Foams*, Wiley-Interscience, New York, 2002.

16. B. P. Binks and T. S. Horozov, *Colloidal particles at liquid interfaces*, Cambridge University Press: Cambridge, 2006;
17. P. McEleney, G. M. Walker, I. A. Larmour and S. E. J. Bell, *Chem. Eng. J.*, **147**, 373 (2009).
18. B. P. Binks and R. Murakami, *Nature Mater.*, **5**, 865 (2006).
19. B. P. Binks, C. A. Davies, P. D. I. Fletcher and E. L. Sharp, *Colloids Surf. A*, **360**, 198 (2010).

CHAPTER 3 EFFECT OF TEMPERATURE ON EMULSIONS STABILISED SOLELY BY WAX PARTICLES

3.1 Introduction

The stability of Pickering emulsions mainly depends on the particle position at the oil-water interface. The wettability of the particle determines both its position and strength of adsorption at the interface, and consequently the type of emulsion formed and its stability. Hydrophilic particles with contact angle smaller than 90° stabilise oil-in-water emulsions, while hydrophobic ones with contact angle larger than 90° are more likely to stabilise water-in-oil.¹

By modifying the contact angle of the particle at the fluid interface, it is possible to induce emulsion inversion, drop coalescence or phase separation.² Several methods for varying the wettability of particles used for emulsion stabilisation have been applied previously, *e.g.* altering the pH or the salt concentration of the aqueous phase, adding surfactants or modifying the surface of the particles themselves.²⁻⁵ Changing the temperature has also been observed by Binks and Lumsdon to affect high viscosity water-in-undecanol emulsions stabilised with nano-particles, which broke down completely into the separate phases over time.⁶ The stability of the emulsion to sedimentation was also witnessed to pass through a maximum as a function of temperature. In a further study, they concluded that the undecanol formed a solid-like layer at the undecanol-water interface at temperatures up to 10°C above the melting point of the alcohol.⁷ Crystals of the alcohol enhanced coalescence by bridging the thin films formed between drops at close separations, but addition of solid particles could prevent the close approach of the drops, and reduced the extent of coalescence. Inversion of emulsions has been achieved by Binks *et al.*, by modulating the temperature of sterically stabilized polystyrene latex particles used as sole emulsifiers.⁸ The particle, a diblock copolymer with one thermo-responsive block, exhibits inverse temperature solubility behavior: it becomes less water-soluble at higher temperature. This caused inversion from o/w to w/o to occur in batch emulsions with increasing temperature; the

emulsions were temperature-dependent but not temperature-responsive. Tsuji and Kawaguchi also showed that Poly(*N*-isopropylacrylamide)-carrying particles, which are thermosensitive, formed oil-in-water emulsions stable for months at room temperature, but exhibited phase separation at 40°C when the particles partitioned more in the water phase.⁹

Wax is used in a wide variety of industries as a coating and polishing ingredient for paper, fabric, paint, cosmetics and food. Waxes can be from animal, vegetal or mineral natural origin, like bees-wax, carnauba wax and paraffin respectively. But they can also be synthesised such as the polyethylene-based ones. Natural waxes contain a wide variety of long chain alkanes, esters, polyesters and hydroxyl esters of long chain alcohols and fatty acids. This composition makes them insoluble in water and very hydrophobic, rendering them able to waterproof fabrics. Paraffin waxes also present a major problem in the oil industry, as they deposit in the production reservoir of the crude oil due to their low temperatures of precipitation.¹⁰

¹¹ Wax particles can adsorb to the crude oil-water interface, and provide a steric barrier to emulsion drop coalescence, rendering water-in-crude oil emulsions formed in the pipelines highly stable to coalescence.¹¹⁻¹³ However, the presence of other surface-active materials (surfactants, resins and asphaltenes) makes it difficult to determine their precise role in the stabilisation process.^{10,11}

Several studies on the influence of wax particles on the properties of surfactant-stabilised emulsions have been done.¹⁴⁻¹⁶ Rousseau and Hodge observed that paraffin wax crystals can aid in the stabilisation of water-in-oil emulsions stabilised primarily by an oil-soluble surfactant. They found that the water drop flocculation and coalescence were dependent on wax crystals: these latter were either present in the continuous oil phase prior to emulsification at room temperature, or they were formed *in situ* by emulsification at high temperature followed by quench-cooling.¹⁶ When emulsions were made with post-crystallised waxes, they showed a higher stability and the wax crystals formed were smaller than when emulsions were made with the pre-crystallised waxes. In both cases, the wax crystals prevented sedimentation by associating with the drop interfaces and forming networks in the continuous phase, which immobilised the drops.

To date, no studies have been found on the use of wax particles as the sole

emulsifier of an oil-water system, but a recent paper has shown that Shellac wax particles are good stabilisers of aqueous foams.¹⁷ On the other hand, emulsions partly stabilised by triglyceride or fat particles have been studied, and one can consider it interesting to compare these systems to wax systems as those particles are also classified as lipids.¹⁸⁻²⁰

Wax particles have also been examined for their antifoam properties at liquid surfaces in surfactant-stabilised aqueous foams. Aronson's study demonstrates that wax particles' effectiveness as antifoams was determined by their physical state, *e.g.* paraffin wax antifoaming properties were high below the melting point of the particles but decreased substantially at and above it.²¹ It was believed to be caused by the larger roughness of solid particles compared with liquid drops: the asperities on solid particles are capable of puncturing the aqueous foam films, while liquid drops are deformable.

In our study, the results of the investigation of the ability of wax particles to act as the sole emulsifier of oil-water mixtures is presented. The influence of temperature on these systems in relation to the melting of the particles is described in detail, in order to provide a means to control the coalescence tendency of such emulsions.

3.2 Wax particle characterisation

3.2.1 DSC measurements

The DSC traces for Microklear 418 and Aquawax 114 particles (~10 µm) are given in Figures 3.1 and 3.2, and show the heat flow plotted against temperature, with two heating and cooling cycles for each. The DSC cycles were determined at a high (10°C/min) and low (2°C/min) rate of temperature change, and little difference between the two rates is observed. Only the low rate is plotted since it corresponds to the rate of temperature rise set in the following emulsion studies.

In Figure 3.1, Microklear 418, which melts visually at 83°C (capillary measurements), shows reproducible heating and cooling curves with a small degree of hysteresis in the heating/cooling cycles. It can be seen that the melting is occurring gradually from 72 to 85°C, with only two peaks appearing at 77 and 82°C. On

cooling, the wax solidifies from 81 until 65°C. The average enthalpy change on melting is $+173 \pm 7 \text{ J g}^{-1}$, while that on solidification is $-146 \pm 5 \text{ J g}^{-1}$. These values are comparable with that of the aliphatic hydrocarbon hexacosane (C_{26}) of $\pm 143 \text{ J g}^{-1}$.²²

By contrast, Figure 3.2 for Aquawax 114, which was previously found to melt visually at 108°C, shows the non-reproducibility of the heating/cooling curves. The melting happens over a very large range of temperature (60°C), from 55 to 115°C. The wax solidifies between 102 and 50°C and exhibits a number of peaks. The corresponding enthalpy changes are $+170 \pm 10 \text{ J g}^{-1}$ on melting and $-178 \pm 8 \text{ J g}^{-1}$ on solidification.

The temperature range over which the melting occurs is due to the large variety of compounds in each wax, each of them having a different melting temperature.

Figure 3.1. DSC trace for the melting and solidification of Microklear 418 (~ 4.82 mg). The two heating/cooling cycles were performed from 25 to 100°C at a rate of 2°C min⁻¹.

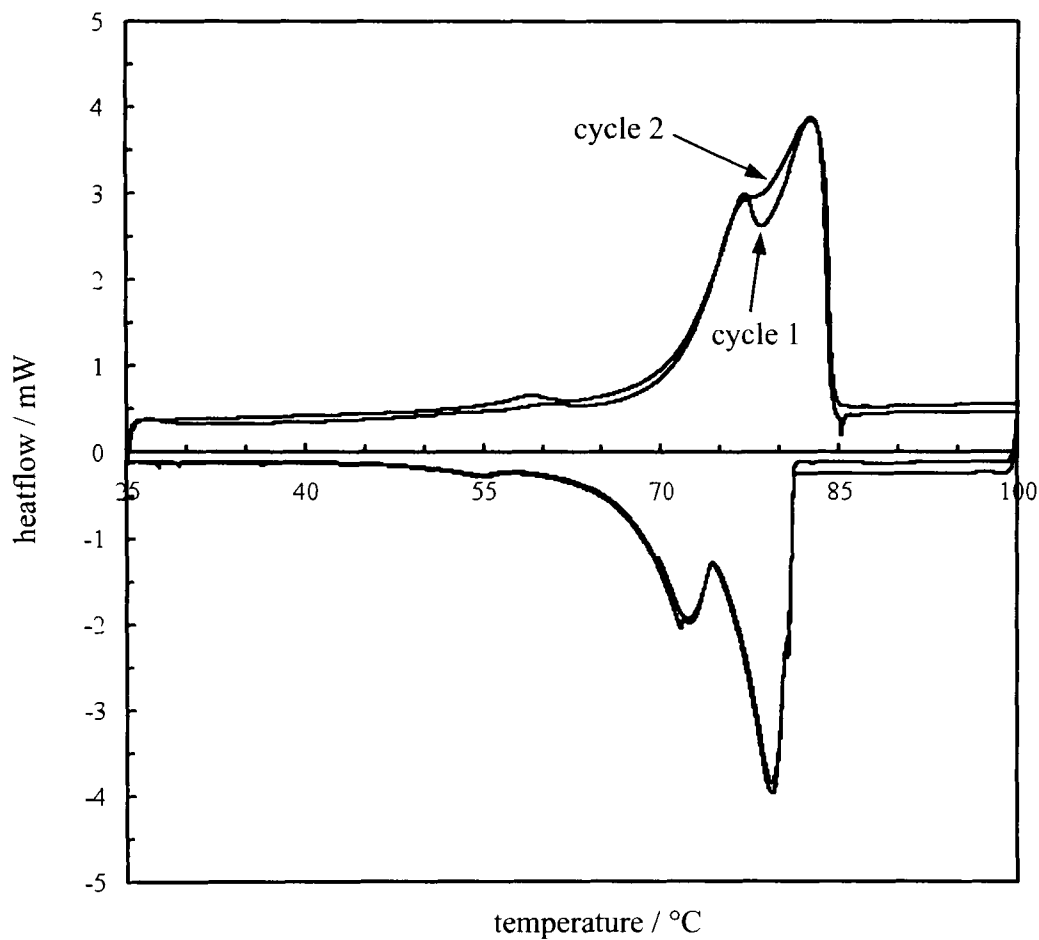
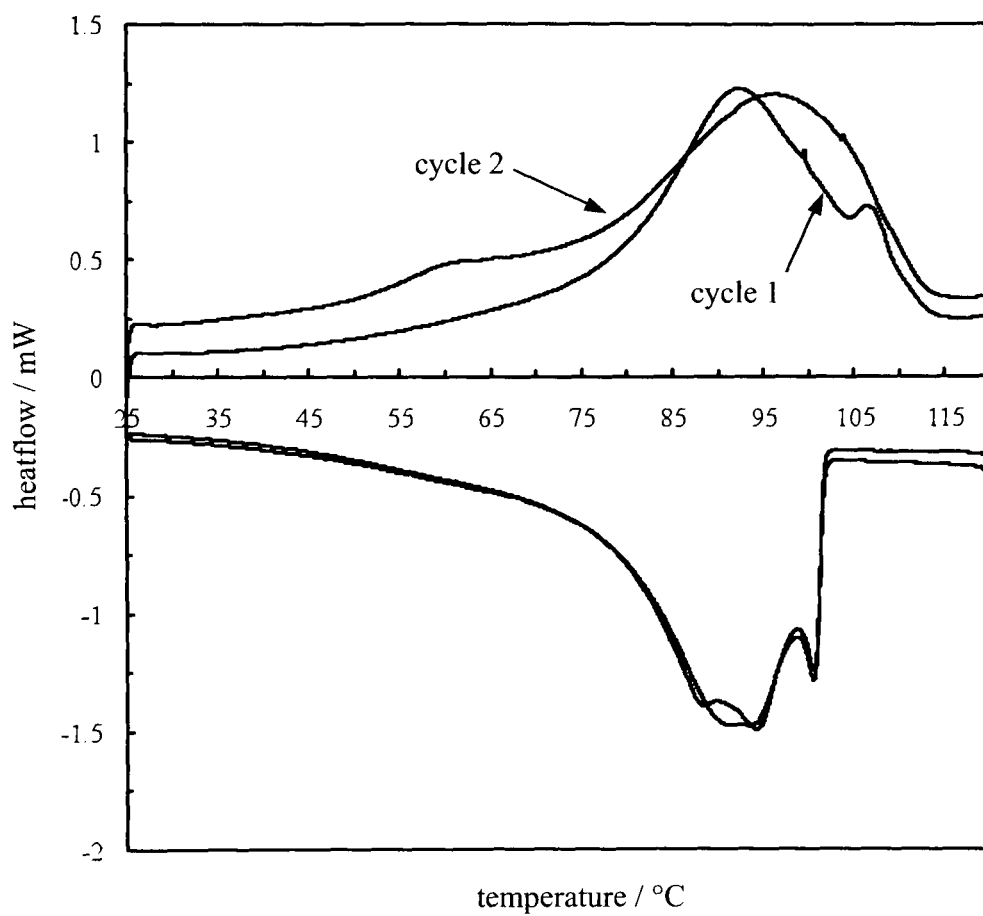


Figure 3.2. DSC trace for the melting and solidification of Aquawax 114 (~ 5.3 mg). The two heating/cooling cycles were performed from 25 to 120°C at a rate of 2°C min⁻¹.



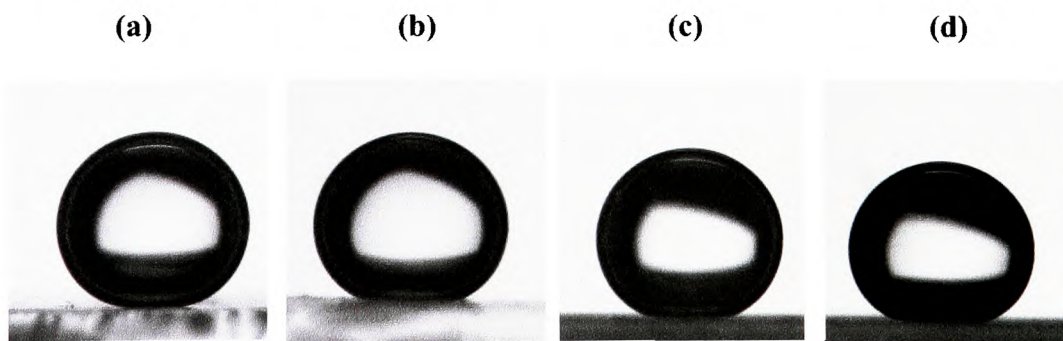
3.2.2 Contact angle measurements

The wettability of particles at the oil–water interface is critical to determine which emulsion type will be preferentially formed, and if the emulsion will be stable.² Temperature changes, by either affecting the fluid phase or the particles, can induce a modification of the particle position at the interface.

It is interesting to note that the same particles exhibit a different contact angle at the oil-water interface depending on whether they are initially dispersed in the oil or in the water; this phenomenon is known as “contact angle hysteresis”.²³ If the particles are originally in water, they will move into the oil to position themselves at the interface. This corresponds to the measurement of the receding contact angle of water on a particle surface, because the water recedes over the particle surface. By contrast, if the particles are in the oil originally, the corresponding contact angle is the advancing one. Microklear and Aquawax will be initially dispersed in the oil phase prior to emulsification, so the advancing contact angle is more relevant here.

For glass slides coated with Microklear 418, the advancing contact angle through water under squalane was $171 \pm 2^\circ$ between 20 and 50°C (Figure 3.3). For Aquawax 114 it was equal to $165 \pm 2^\circ$ over the same temperature range. The measurements were unreliable above 50°C, because the water drop began to enter the softer, partially melted substrate, and the wax layer started to peel from the glass slide. However, our findings agree with literature measurements of the contact angle of a water drop on wax-coated surfaces under non-polar oils, which have been found in the range of 135 to 145°, depending on the wax type.²⁴ From these measurements, it is expected that wax particles will stabilise water-in-oil emulsions up to 50°C.²⁵

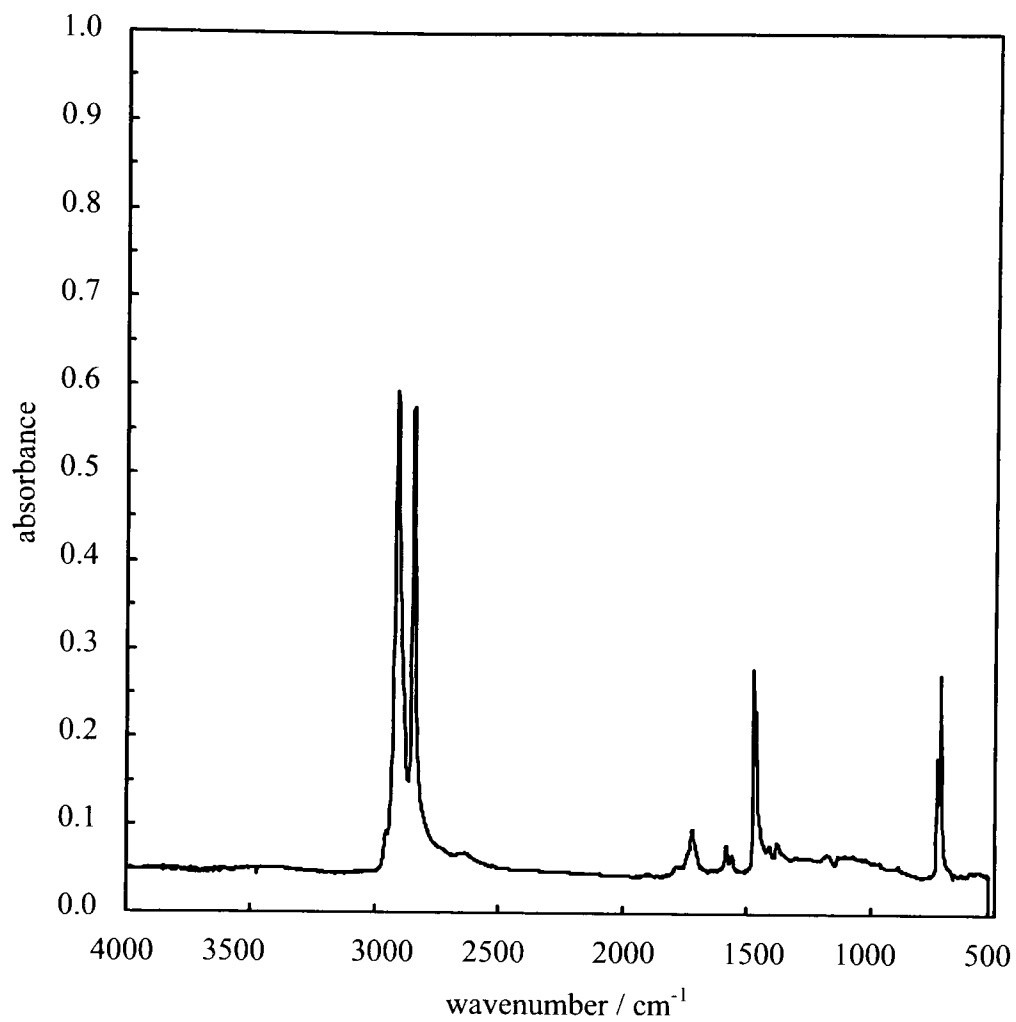
Figure 3.3. DSA micrographs of water drops on Microklear 418 (a, b) or Aquawax 114 (c, d) -modified glass slide under squalane at 20 (a, c) and 50°C (b, d).



3.2.3 *ATR-FTIR measurements*

ATR-FTIR spectra of a small sample of Aquawax 114, displayed in Figure 3.4, reveals a band of significant peak intensity corresponding to a -C=O stretch (at 1722 cm^{-1}). This band can be attributed either to an ester or to a carboxylic acid group. An identical band has been detected in the Microklear 418 ATR-FTIR spectrum. Hence, contrary to the manufacturer description, Aquawax 114 contains not only long chain hydrocarbons but also polar molecules, which should be capable of adsorbing to the oil–water interface when released in the system by the melting of the particles.

Figure 3.4. ATR-FTIR profile of Aquawax 114 powder.



3.3 Effect of particle type

Three main types of particles were studied in this work: large spherical wax particles (Florabeads and Floraspheres), triglyceride crystals and non-spherical wax particles (Microklear 418 and Aquawax 114). These particles are all hydrophobic, but their composition and shape are different. Several studies have investigated the influence of particle size and shape on emulsion stability. Tambe and Sharma observed that a decrease in particle size is associated with an increase in emulsion stability and a decrease in drop average diameter, until the particles reach a critical size.²⁶ It has also been noticed by Binks and Lumsdon that larger particles produced less stable emulsions.²⁷ Yan *et al.* showed that non-spherical particles, like fine clay and fumed silica, could stabilise emulsions.²⁸ However, the roughness of the particles determined the emulsion stability. Vignati *et al.* demonstrated that small particles with rough surfaces gave emulsions of lower stability than larger smooth spherical particles.²⁹ They also observed a differential surface coverage of the drops by the particles: the rough particles were randomly distributed on a sparsely covered surface, while the spherical ones formed a high-density even coverage. The roughness might be responsible for lowering the particle-interface contact, decreasing the particle energy of adsorption.

In this part, the effects of dispersion and emulsification methods on emulsion stability were compared, in order to determine the system most suitable to temperature study.

3.3.1 *Large spherical wax*

The effect of the particle size can be investigated with the Florabeads and Floraspheres, which are spherical particles of Jojoba wax of different sizes: the Florabead particles measure around 200 μm , whereas the Floraspheres measure 500 μm .

3.3.1.1 Dispersion

The state of a particle dispersion before emulsification can influence the type of emulsion formed and its stability. Previous investigations of particle-stabilised emulsions observed differences in emulsion type and stability, due to a change of dispersing phase or the state of aggregation/dispersion of the particles. Four different methods of dispersing in oil and water were compared to evaluate which gave the best particle dispersion: sonication, stirring, handshaking or Ultra Turrax homogenisation. Dispersion by ultrasound or sonication is a consequence of micro-turbulences caused by fluctuation of pressure and cavitation. It has previously been found efficient for nano-size silica particles prior to emulsification.⁶ Magnetic stirring and handshaking use low mechanical energy to disperse particles relative to the Ultra Turrax, which applies a strong shear to the system.

The high hydrophobicity of the Floraparticles was found to prevent their dispersion in water. No particles were dispersed into the water phase, and some spread onto the glass wall of the vessel carried by the water, reducing water contact to avoid particle immersion energetically unfavourable. A similar observation has been previously described by Binks *et al.*³⁰

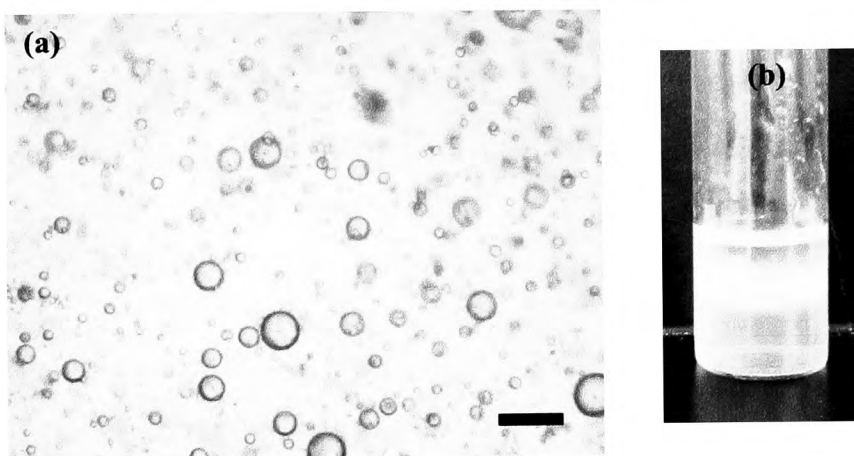
In the oil phase, sonication was witnessed to induce melting of the particles with a low melting point of $68 \pm 2^\circ\text{C}$. The agitation created by the ultrasound disperses few particles, but localises heat near the probe, which melts some wax particles. Ultra Turrax shearing for 1 min. at 13000 rpm on particles in oil produces broken pieces of particles of the Florabeads, or 20 μm long fibers of the Floraspheres. Magnetic stirring and handshaking were able to disperse the particles, but they were observed to sediment to the bottom of the sample in less than a minute. Handshaking dispersion in oil was chosen as the simplest method to disperse the Flora particles without modifying their characteristics.

3.3.1.2 Emulsification

Three different methods of emulsification were investigated on oil dispersions containing 2 wt.% of Flora particles and the same volume of water: handshaking, magnetic stirring and homogenisation with the Ultra Turrax. When strong

handshaking or 2000 rpm magnetic stirring was applied for 2 minutes, oil and water separated in less than 10 seconds after mixing, the particles remaining in oil at the planar oil-water interface. When Ultra Turrax homogenisation of 1 minute at 11 000 rpm of the Florasphere oil dispersion was done, a water-in-oil emulsion is stabilised for a short period of time by the wax fibres (Figure 3.5). Although the oil and the water phases are totally separated after 2 minutes, a mean diameter of $40 \pm 10 \mu\text{m}$ was measured initially for the water drops. We can conclude from this observation that these wax particles would prefer to stabilise w/o emulsions but, due to their large size ($\sim 500 \mu\text{m}$), cannot remain at the interface around drops.

Figure 3.5. Micrograph of (a) a water-in-squalane emulsion stabilised by 2 wt.% Floraspheres after 1 minute at 11000 rpm Ultra-Turrax homogenisation. Scale bar represents 100 μm . (b) Same emulsion 1 minute after emulsification; the white phase is the emulsion, the upper phase is the squalane oil resolved and the bottom phase is the water resolved.



A complete analysis of the forces acting on particles held at liquid interfaces is very complex, due partly to the deformation of the surface caused by the presence of the particle.¹³ As the equilibrium of a particle at a fluid interface depends on its weight, the vertical capillary force and the vertical resultant of the hydrostatic pressure, a rough approximation for a spherical particle can be done. It shows that the buoyancy force counteracts the interfacial tension force; the former is proportional to the cube of the particle radius and the latter with the radius to the power unity. For large particles with densities between 1000 and several thousand kg

m^{-3} at alkane-water interfaces, the buoyancy term exceeds the tension term. This means that millimeter size particles are pushed away from the interface, hence will not be able to stabilise it. However, when fragmented into smaller rod-like particles, the driving energy of attachment increases due both to the change of shape and size of the particles.

3.3.1.3 Addition of surfactant

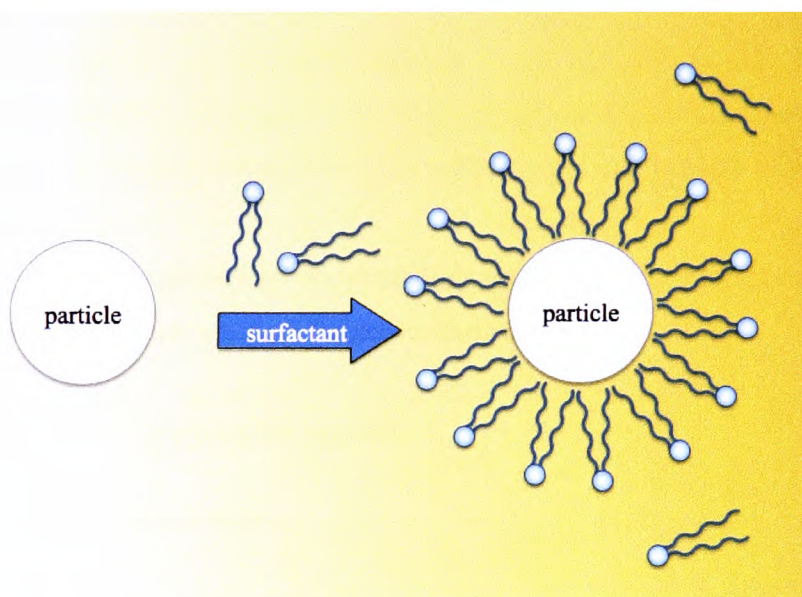
Mixtures of surfactant and particles have been extensively studied these past few years, and it is known that the addition of surfactant to a particle-stabilised system can change the resulting emulsions. Binks *et al.* have shown that, for mixtures of negatively charged silica nanoparticles and cationic surfactant, oil-in-water emulsions are most stable to creaming and coalescence at conditions of maximum flocculation of particles by surfactant in aqueous dispersions alone.³¹ The study was extended to the use of positively charged silica particles in mixtures with anionic surfactant.³² Binks and Rodrigues found that very hydrophilic particles, which are poor emulsifiers alone, exhibited improvement in stabilising emulsions due to the adsorption of surfactant on particle surfaces through their hydrophilic head groups. This was believed to be caused by the formation of a surfactant monolayer on particle surfaces leaving the chains of the surfactant exposed to water and thus increasing the hydrophobicity of the particles. By choosing a di-chain cationic surfactant in mixtures with negatively charged silica nanoparticles, Binks and Rodrigues demonstrated the possibility of effecting two emulsion inversions induced by increasing surfactant concentration alone.³³ The addition of charged surfactant to mixtures of air, water and hydrophobic silica nanoparticles has also been observed to induce transitional phase inversion from a water-in-air powder to an air-in-water foam under high shear.³⁴

The Flora particles alone are not able to stabilise any emulsion because the gravitational force is greater than the surface tension, but they might be able to stabilise an emulsion in the presence of surfactant molecules. The addition of surfactant to the oil particle dispersion could modify the particle wettability, as illustrated in Figure 3.6. Theoretically, the surfactants should be able to coat the Flora particles, with their hydrophobic tails interacting with the hydrophobic surface

of the particles. Their negatively charged head, exposed toward the liquid medium, will make the Flora particles more hydrophilic, and able to adsorb more strongly at the oil-water interface.

Two different surfactants were added to the particle dispersion in oil: sodium di(2-ethylhexyl) sulfosuccinate (Aerosol-OT or AOT) and stearic acid (SA).

Figure 3.6. Schematic representation of surfactant interaction with hydrophobic particles in oil.



Emulsions with 10^{-6} to 10^{-4} M in oil of AOT or SA only were made by handshaking equal volumes of Milli-Q water and squalane, and were found to always give oil-in-water emulsions, with the stability increasing with increasing surfactant concentration. When Flora particles were added to the systems at 2 wt.%, they were observed to modify the stability of the emulsions. The small Florabeads decreased the stability to coalescence, whereas the Floraspheres increased slightly one of the squalane-in-water emulsions. As the two particles have the same chemical composition, this opposite behaviour is surprising. Their interaction with the surfactant differs although it should be similar if they have identical groups on their surface.

The decrease in stability induced by the Florabeads might be due to antagonistic behaviour with the surfactants. The hydrophobic particles, wetted more

by the oil phase, would tend to stabilise water-in-oil drops whereas the surfactants stabilise oil-in-water. The oil-in-water emulsion observed confirms that the surfactant dominates the emulsion stabilisation, however it is possible that particles adsorb at the oil-water interface and bridge the oil drops. It is known that for particles, which are preferentially wet by the dispersed phase, bridging of two drops will facilitate coalescence.³⁵

Floraspheres, larger than the Florabeads, are expected to stabilise water-in-squalane emulsions (*cf.* § 3.1.4.2). The fact that they enhance the oil-in-water emulsion stability is rather surprising. All Florasphere particles are observed to rest in the oil phase close to the oil-water interface. It is believed that the increased stability is mainly due to small fragments of the Florasphere (nanometre size), whose wettability may have been modified enough to stabilise a small volume of squalane-in-water emulsion.

Due to the poor stability of the emulsions made with the Floraparticles, the large spherical wax particles were no longer investigated.

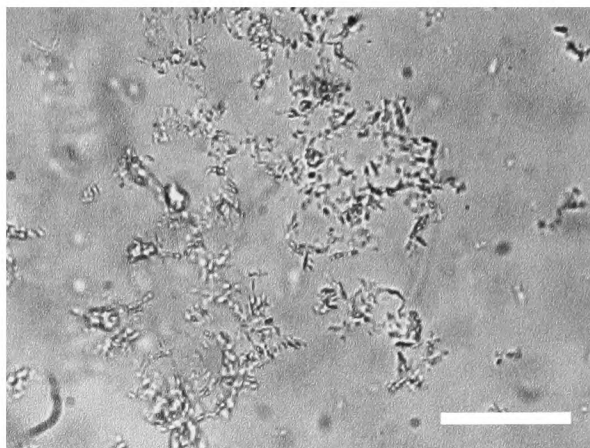
3.3.2 *Triglyceride crystals*

3.3.2.1 Dispersion

Recrystallised glyceryl tripalmitate particles, of 10 ± 1 μm length, were dispersed in oil either by 10 s handshaking or by 10 min low power sonication to break the particle aggregates. Both methods were observed to give equivalent dispersions, where no sedimentation was witnessed up to 1 day after preparation.

After handshaking 3 wt.% of the glyceryl tripalmitate particles in oil, a crystal network was observed by optical microscopy as displayed in Figure 3.7. This observation agrees with the study by Lucassen-Reynders and van den Temple, which states that the triglyceride crystals form a 3-D network in the oil phase with strong interparticle bonds.¹⁹

Figure 3.7. Optical micrograph of 3 wt.% glyceryl tripalmitate crystals dispersed in squalane by handshaking. Scale bar represents 50 μm .



3.3.2.2 Emulsification

Only handshaking emulsification was used in the case of the triglyceride crystals, as it was found to give an emulsion with little coalescence. More details about the emulsions obtained with the triglyceride crystals are given in the following sections 3.4 and 3.5. The use of Ultra Turrax was rejected, due to the high shear involved which could have broken or melted the crystals.

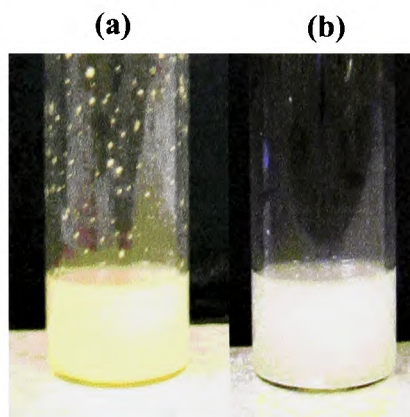
3.3.3 *Non-spherical wax particles*

3.3.3.1 Dispersion

As the wax particles are hydrophobic (*cf* § 3.1.1), they were always dispersed in the oil phase. Two methods of dispersion were investigated with Aquawax 114 and Microklear 418: 10 s. handshaking and 1 min shaking with a VXR Vibrax basic shaker (IKA) at 500 rpm. The two methods gave good dispersion; breaking the initial aggregates occurred in the case of Microklear 418. Particle sedimentation was however still observed 2 hours after shaking.

The Aquawax 114 and Microklear 418 oil dispersions, displayed in Figure 3.8, present a different appearance: the Aquawax dispersion is white, whereas the Microklear 418 one appears yellow in squalane.

Figure 3.8. Photographs of 2 wt.% (a) Microklear 418 or (b) Aquawax 114 dispersions in squalane 30 sec. after handshaking.

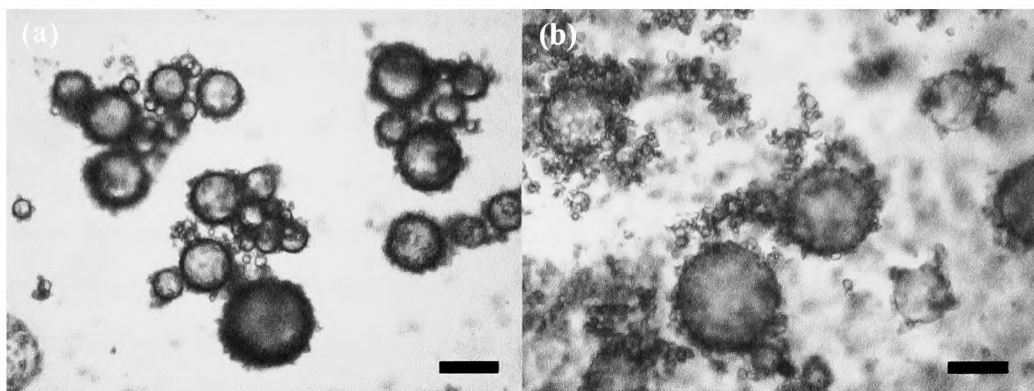


3.3.3.2 Emulsification

Two emulsification methods were employed and compared with systems containing 2 wt.% of Aquawax 114 and Microklear 418 particles in squalane: 2 minutes strong handshaking and 1 minute Ultra Turrax homogenisation at 11000 rpm. All emulsions formed were determined as water-in-squalane, with varying stability observed. Emulsions made with the Ultra Turrax displayed little resolved water (which indicates coalescence) compared to those made by handshaking. The Ultra Turrax homogenisation may emulsify the system more efficiently by introducing more energy than handshaking. It is also possible that the high shear of the Ultra Turrax generates breaking or melting of the wax particles. An increasing number of particles would be able to stabilise more oil-water interfacial area, so lead to better stability. The heat localised close to the mixing head of the Ultra Turrax could melt the wax particles, which would release their polar component increasing the emulsion stability (*cf.* § 3.1.3). However, a system solely stabilised by such surfactant-like molecules is refuted by the microscopic observation of the water-in-squalane emulsions. Figure 3.9 shows the water drops coated by wax particles, giving them a rough appearance on their surface.

Both emulsification methods were used in the following study in order to compare the relatively inert handshaking to the efficient Ultra Turrax homogenisation.

Figure 3.9. Micrographs of water-in-squalane emulsions stabilised by 2 wt.% (a) Microklear 418 or (b) Aquawax 114 particles homogenised with an Ultra Turrax for 1 minute at 11000 rpm. Scale bars represent 100 μm .



3.4 Effect of particle concentration

In Pickering emulsions, it is a common observation to see increasing emulsion stability when particle concentration is increased.¹³ The more particles there are available to adsorb at the oil-water interface, the bigger the area they can stabilise, *i.e.* the smaller emulsion drops.

This part of the study is aimed at determining the stability plateau of the emulsions: the emulsion stability increases with particle concentration, until it reaches a maximum, where further increase in particle quantity in the system does not change the stability to coalescence anymore. This will enable choosing the most stable emulsion containing the lowest particle concentration.

3.4.1 Triglyceride crystals

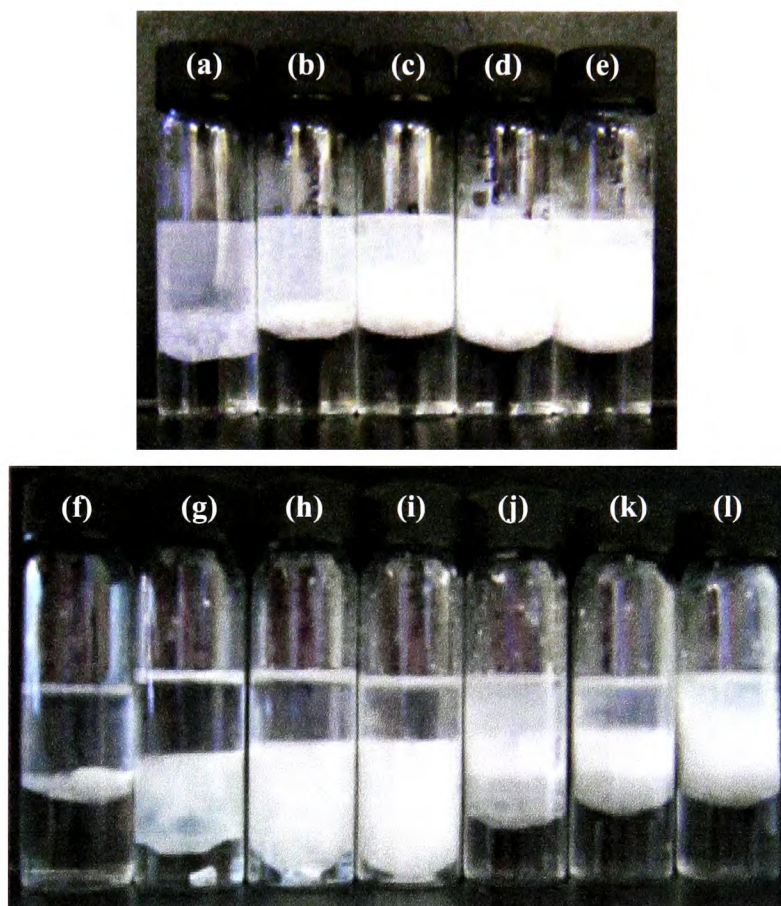
For the triglyceride particles, the effect of concentration was studied in parallel with the effect of particle dispersion. Two series of emulsions were produced, enabling comparison between the handshaking and the sonication dispersion methods used previously.

When the glyceryl tripalmitate particles dispersed by sonication are emulsified, the water-in-squalane emulsions formed show an increasing stability to

sedimentation and coalescence with increasing particle concentration from 1 to 4 wt.% (Figure 3.10). Increasing stability with particle concentration, apart for the surprising decrease between 0.5 and 1 wt.%, is expected; similar observations have been commonly made in the literature.¹³ Still in agreement with the literature, the average drop diameter, estimated by eye, decreases from around 2 to 0.5 mm.

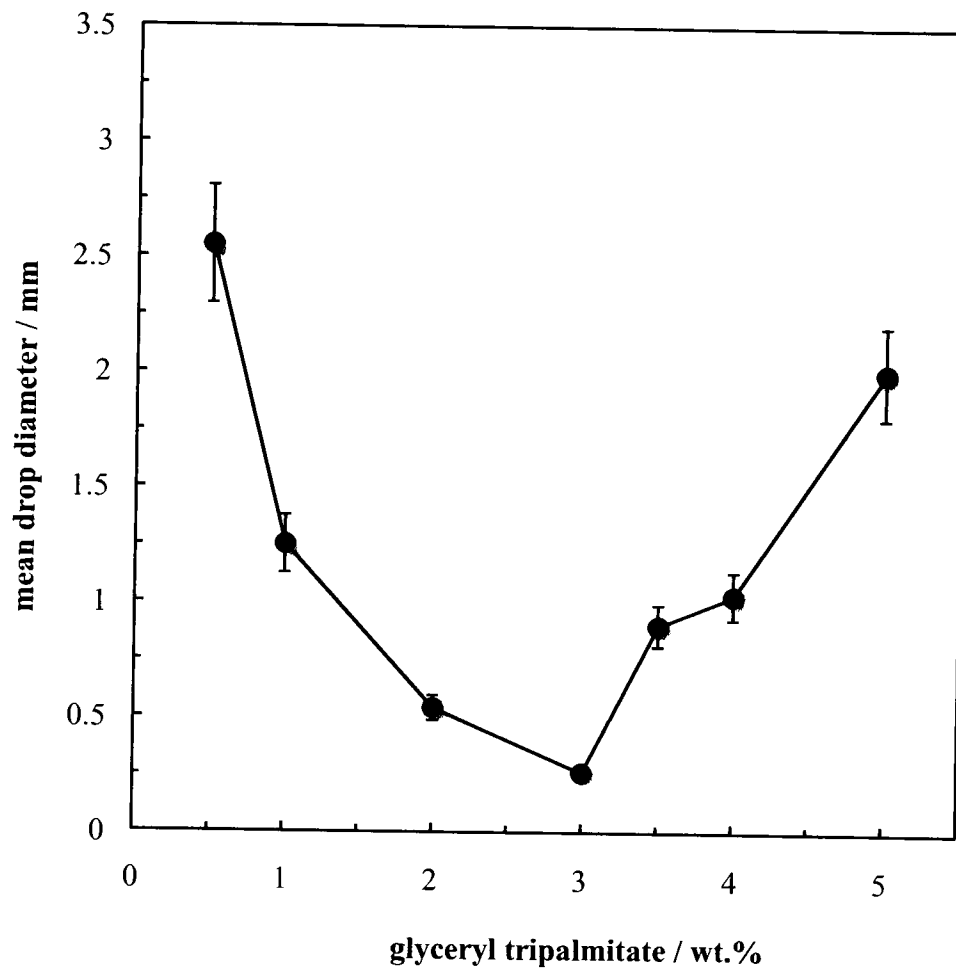
However, when the particles dispersed by handshaking are emulsified, a maximum in stability for the squalane-in-water emulsion series is observed at 3 wt.%, followed by a sharp drop in stability to coalescence from 3.5 to 5 wt.%. The water-in-squalane emulsions formed with the handshaking dispersion appear more stable than those formed with the sonication dispersion. The average drop diameter is estimated by eye *in situ*, and found to decrease when the stability increases and to increase with decreasing stability, as Figure 3.11 displays.

Figure 3.10. Photographs of water-in-squalane emulsions stabilised with (a,f) 0.5, (b,g) 1, (c,h) 2, (d,i) 3, (j) 3.5, (e,k) 4 and (l) 5 wt.% glyceryl tripalmitate particles dispersed in squalane either by 10 minutes low power sonication (a-e) or by 10 seconds handshaking (f-l). Emulsions were made by 2 minutes handshaking, and the pictures refer to 2 weeks after emulsification.



The differences observed for the two dispersion types can be explained by an alteration of the aggregation state of the particles. Lucassen-Reynders and van den Temple were the first to formulate the idea that the triglyceride crystals formed a 3-D network in the oil phase responsible for a completely flocculated system.¹⁹ Emulsions can be formed with partially flocculated particles, or when moderate attraction between particles occur, but no emulsion can be formed in a highly flocculated system. In the handshaking particle series, the destabilisation of the emulsion above 3 wt.% of particles could be due to the formation of a crystal network too strong to be broken by the handshaking emulsification, hence the system would be unable to stabilise drops. At low particle concentration, or when particle flocculation has been reduced by sonication, the system can form emulsions with stability increasing with particle concentration. This argument can also be supported by the better stability observed in the case of emulsions stabilised with handshaken particles: the low strength particle network helps to stabilise water drops, whereas this network has been reduced during the sonication process, resulting in less stable emulsions.

Figure 3.11. Water-in-squalane emulsion mean drop diameter measured with a ruler 2 minutes after emulsification as a function of the quantity of glyceryl tripalmitate particles dispersed by 10 seconds handshaking before emulsification. Emulsions are made by 2 minutes handshaking.

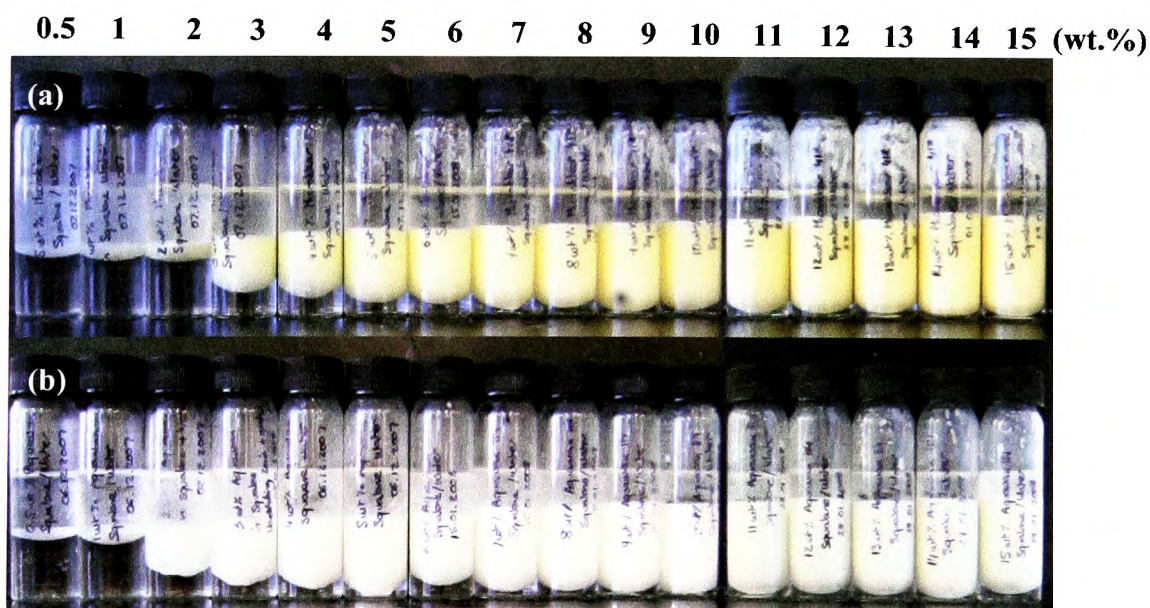


3.4.2 Wax particles

The effect of particle concentration when using non-spherical wax particles was investigated by making two series of emulsions stabilised with an increasing concentration of either Microklear 418 or Aquawax 114 particles. Wax particles were both dispersed by 10 seconds handshaking in oil before adding an equal volume of water and handshaking strongly during 2 minutes at room temperature. The vessels were stored at this temperature after emulsification, and their appearance 1 month after is shown in Figure 3.12 for both Microklear 418 (a) and Aquawax 114 (b) systems.

For both series, emulsions are water-in-squalane as expected from the contact angle measurements (*cf.* § 3.1.2) and the previous emulsifications (*cf.* § 3.1.2.2). Their stability to coalescence was observed to increase initially with particle concentration and to reach a limit around 10 wt.% particles.

Figure 3.12. Photographs of the vessels containing water-in-squalane emulsions stabilised by (a) Microklear 418 and (b) Aquawax 114 wax particles as a function of initial particle concentration in oil (given in wt.%) 1 month after emulsification. Emulsions were prepared and stored at room temperature by hand shaking.



Emulsion stability is quantified in terms of f_{aq} or f_{oil} (defined in § 2), which are plotted as a function of particle concentration in Figures 3.13 and 3.14. For both the Microklear 418 and Aquawax 114 series, complete phase separation occurs rapidly at and below 1 wt.% of particles, and stability to sedimentation and coalescence increases progressively above this. By 10 wt.% of particles, water-in-oil emulsions exhibiting a small amount of coalescence can be formed both with Microklear 418 and Aquawax 114.

For both series, f_{oil} is always observed to be larger than f_{aq} , and to continue decreasing when f_{aq} reaches a plateau. This might be due either to the added particles rendering the oil more viscous so reducing the water drop sedimentation, or the free particles form a sedimented layer difficult to distinguish from the emulsion.

For the same particle concentration, the Microklear 418 series displays more coalescence than the Aquawax 114 one. For example, at 2 wt.% particles, the emulsion made with Microklear particles shows about 0.9 fraction of water resolved, while the Aquawax shows only about 0.3. This difference can be rationalised by studying the drop diameter of these emulsions.

The variation of the average water drop sizes and size distributions with particle concentration is shown in Figures 3.15 and 3.16. Below 1 wt.% of particles, only small drops exist initially, which coalesce rapidly yielding bulk oil. At 2 wt.% the Microklear 418 emulsion contains only really small drops, whereas the Aquawax emulsion is also composed of large water drops, which contribute to the decrease in water resolved observed when Figures 3.13 and 3.14 are compared.

Figure 3.13. Water-in-squalane emulsion stability for the systems in Figure 3.12(a) for Microklear 418 particles. Filled points refer to f_{oil} (sedimentation), open points to f_{aq} (coalescence) after 1 day.

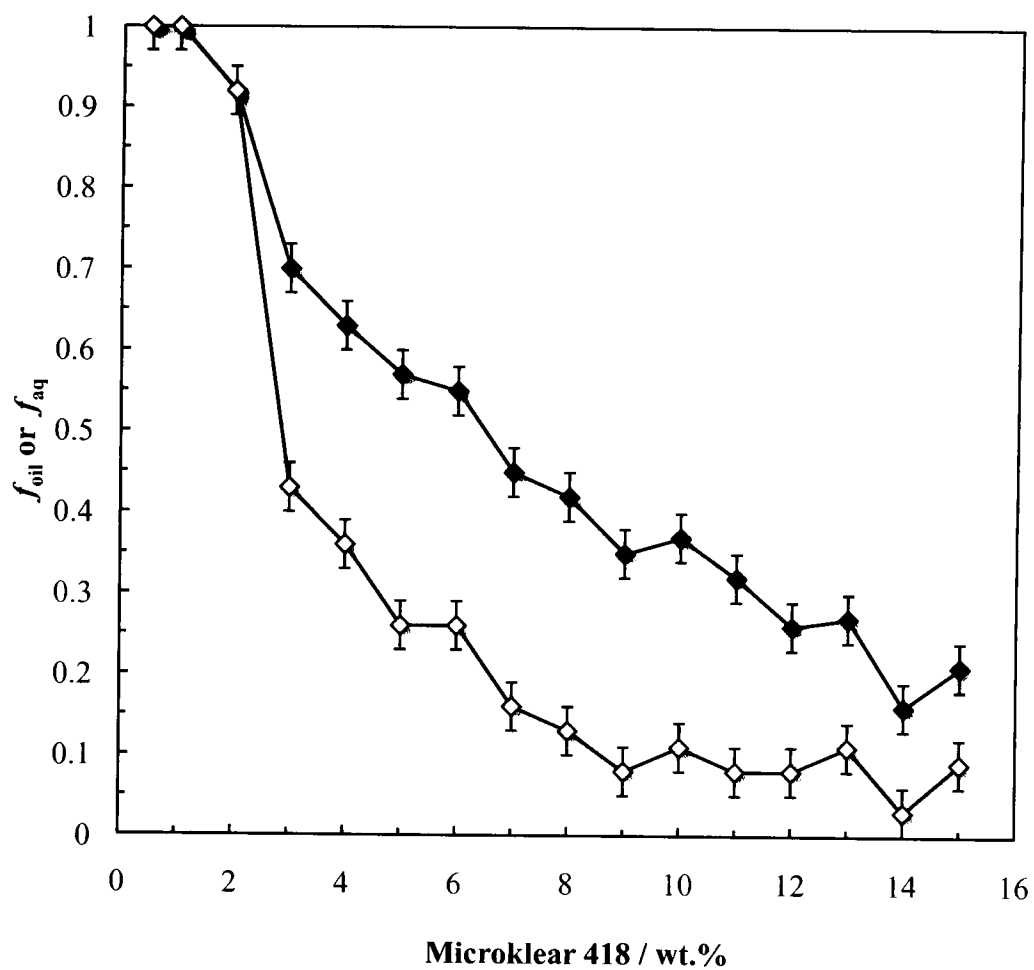
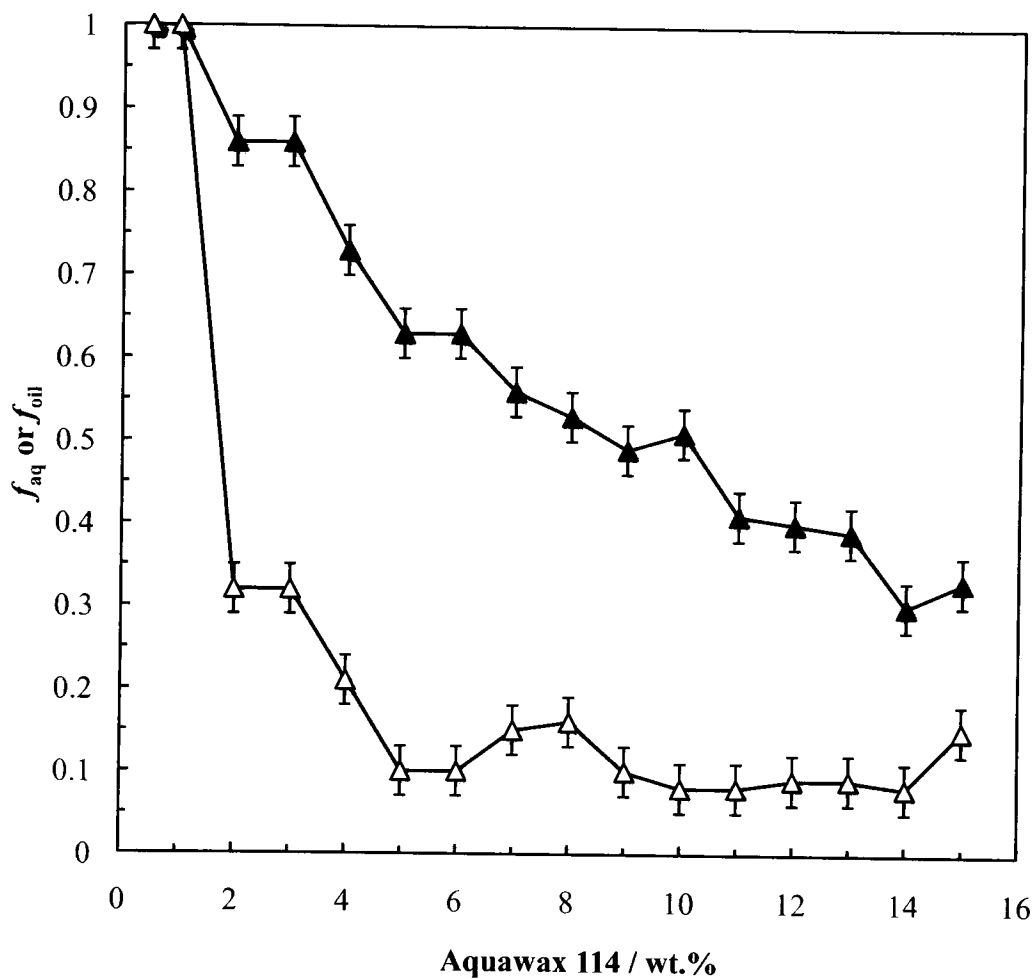


Figure 3.14. Water-in-squalane emulsion stability for the systems in Figure 3.12(b) for Aquawax 114 particles. Filled points refer to f_{oil} (sedimentation), open points to f_{aq} (coalescence) after 1 day.



At intermediate concentrations, emulsion drops display a bimodal distribution in size: a population of small drops tens of μm measured microscopically, and one of much larger drops, which are measured with a ruler because of their millimeter-size, are both present. It has been observed previously for latex particle-stabilised drops that the smaller drops are stabilised by the smaller size fraction of the particles and the opposite for the larger drops.²⁷ The polydispersity in the size of the wax particles may lead to the same consequences, and could offer a new mean for separation of different sizes of the same type of particles. This could be done by preparing particle-stabilised emulsions and separating the different drop populations by centrifugation.

At higher concentrations, a single small drop population exists again. All the drops are spherical and a coating of wax particles on their surfaces can be observed by optical microscopy in Figure 3.17. Excess wax particles are also visible in the continuous oil phase at higher concentrations.

Above a particular concentration, the average drop size and width of the distribution decrease with concentration. The microscopy images also show that the Microklear 418 water drops are more polydisperse and smaller in size than the Aquawax 114 drops. At about 10 wt.% of particles, the emulsion drop diameters reach a plateau value of around 100 μm for Microklear 418 and 500 μm for Aquawax 114 systems. These observations are in line with the changes in emulsion stability: Microklear 418 particles appear to give more stable emulsions than the equivalent concentration of Aquawax 114 particles at room temperature.

Figure 3.15. Variation of the mean water drop diameter and size distribution at 5 min. after emulsification with particle concentration for w/o emulsions stabilised by Microklear 418 particles prepared and stored as in Figure 3.12(a). The very small drops at the lowest concentrations rapidly grow by coalescence.

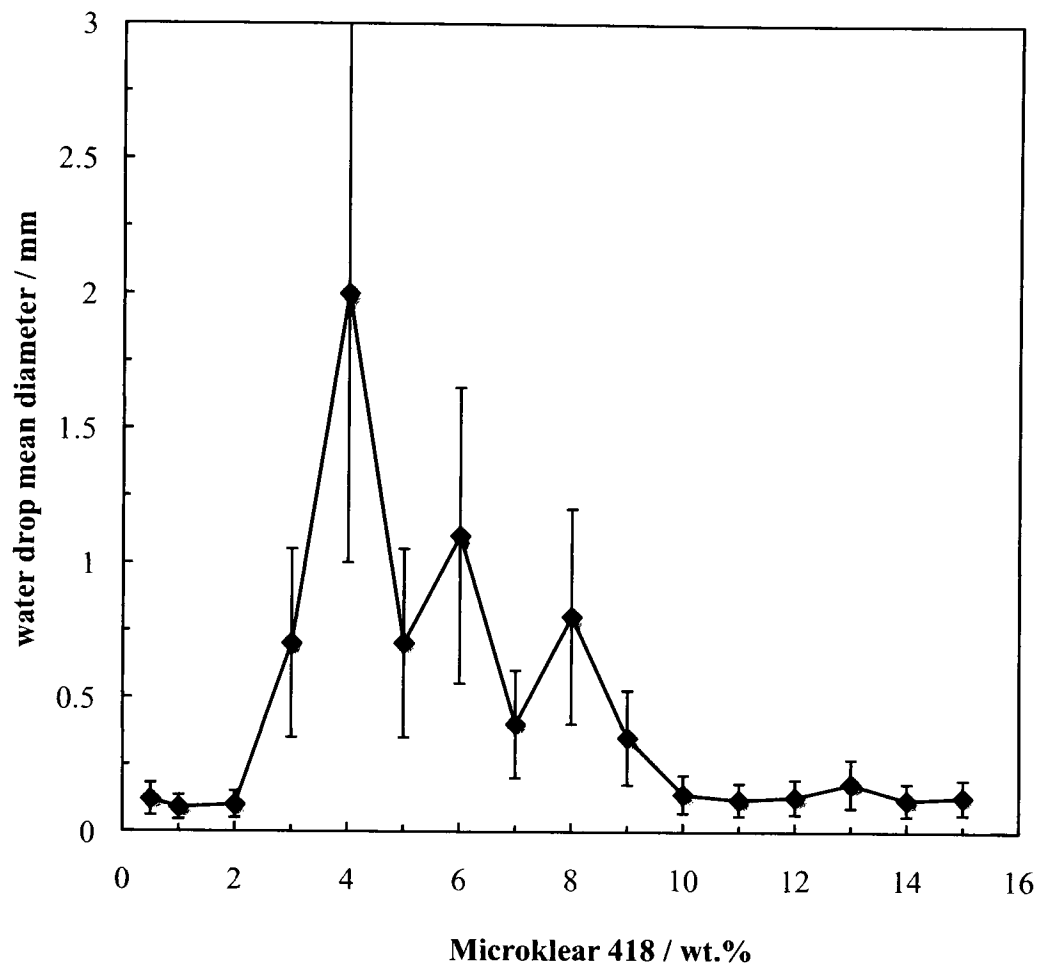


Figure 3.16. Variation of the mean water drop diameter and size distribution at 5 min. after emulsification with particle concentration for w/o emulsions stabilised by Aquawax 114 particles prepared and stored as in Figure 3.12(b). The very small drops at the lowest concentrations rapidly grow by coalescence.

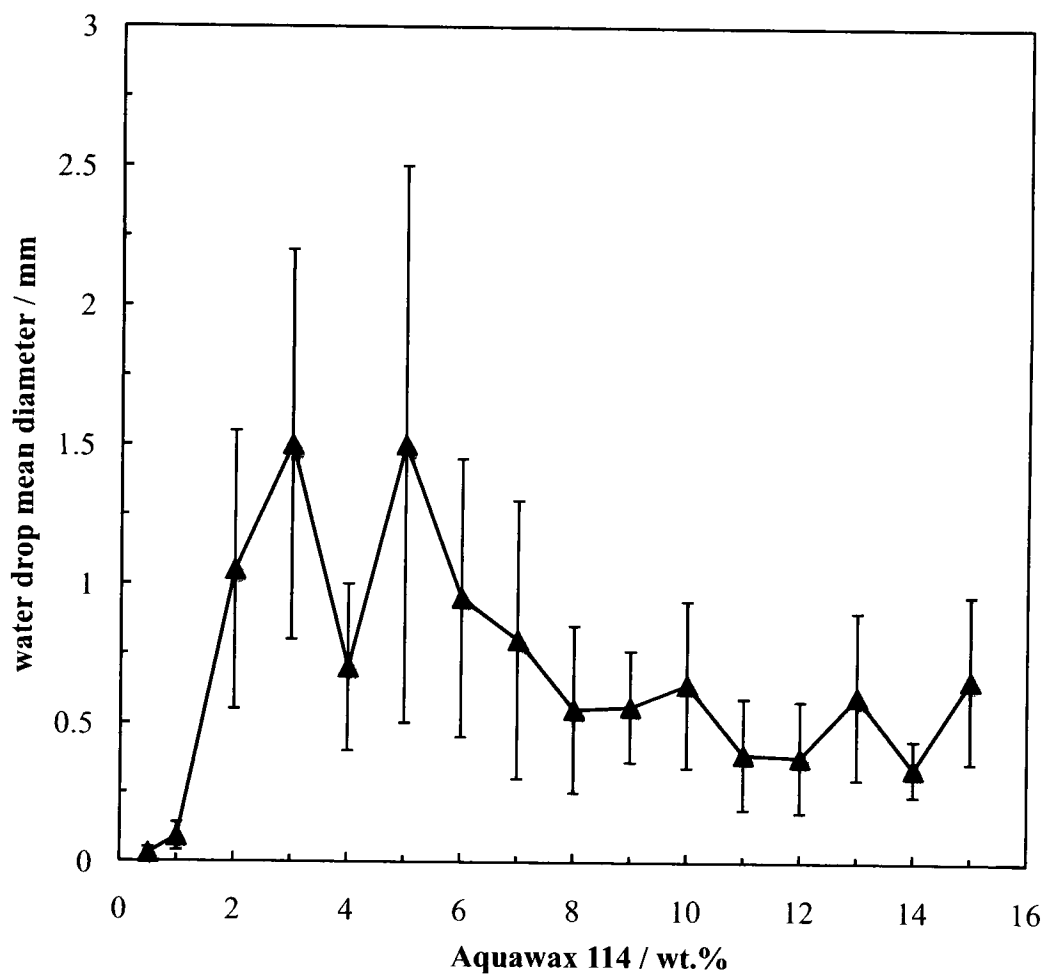
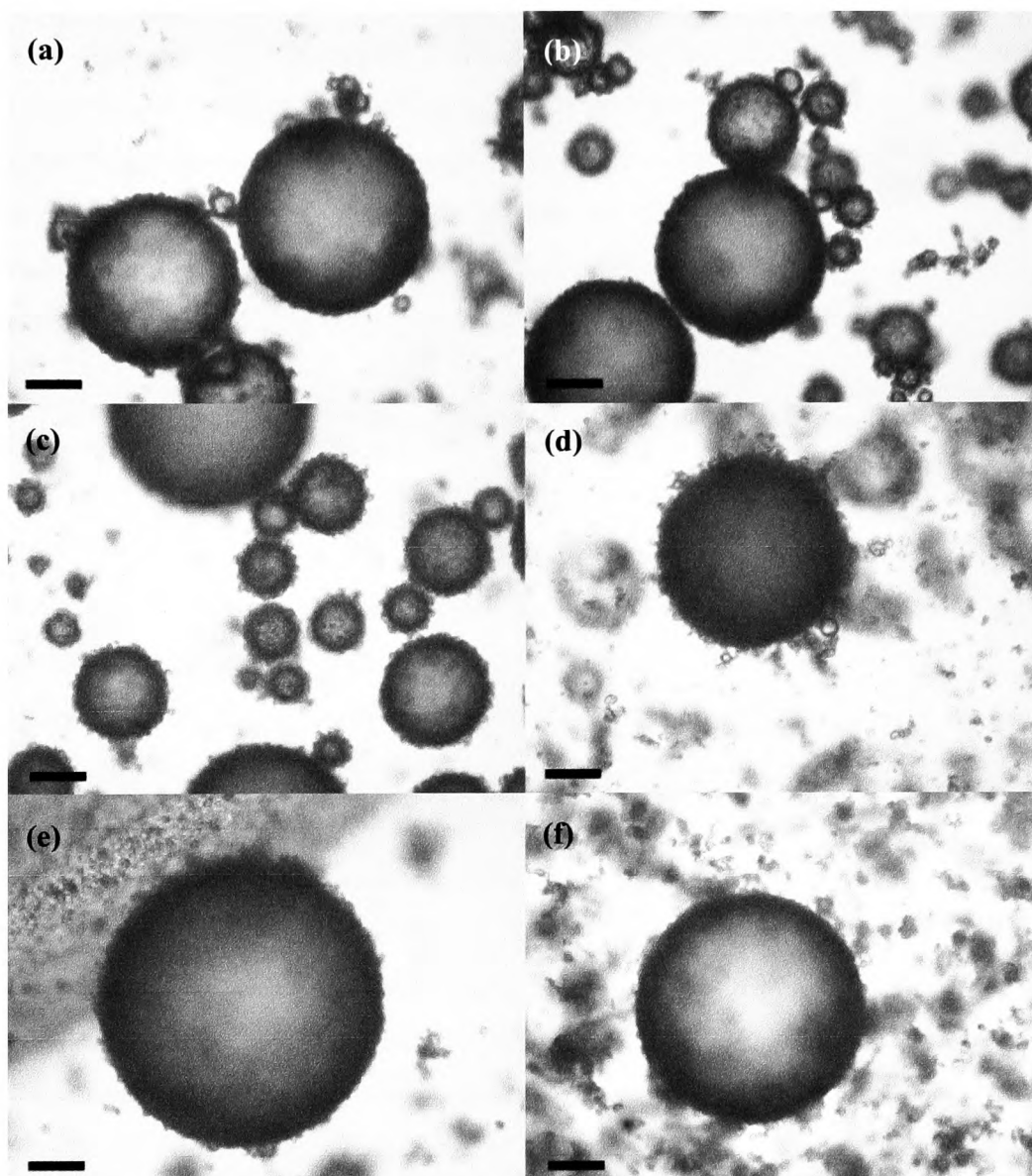


Figure 3.17. Optical microscopy images of w/o emulsions (as in Figure 3.12) stabilised by Microklear 418 particles at (a) 2, (b) 7 and (c) 15 wt.% and by Aquawax 114 particles at (d) 1, (e) 5 and (f) 13 wt.%. Scale bars represent 100 μm .



3.5 Effect of temperature

The effect of temperature on particle-stabilised emulsions has previously been investigated, and an emulsion type and stability dependence were observed.⁶⁻⁹ In our study, the way the temperature is changed, whether increasing the temperature of a preformed emulsion or emulsifying at different temperatures, was found decisive for the results obtained. Particles already adsorbed at the oil-water interface at room temperature will be modified by the temperature change. Particles dispersed in the pre-heated oil phase are already modified (composition, shape or state of matter) and will then adsorb at the oil-water interface.

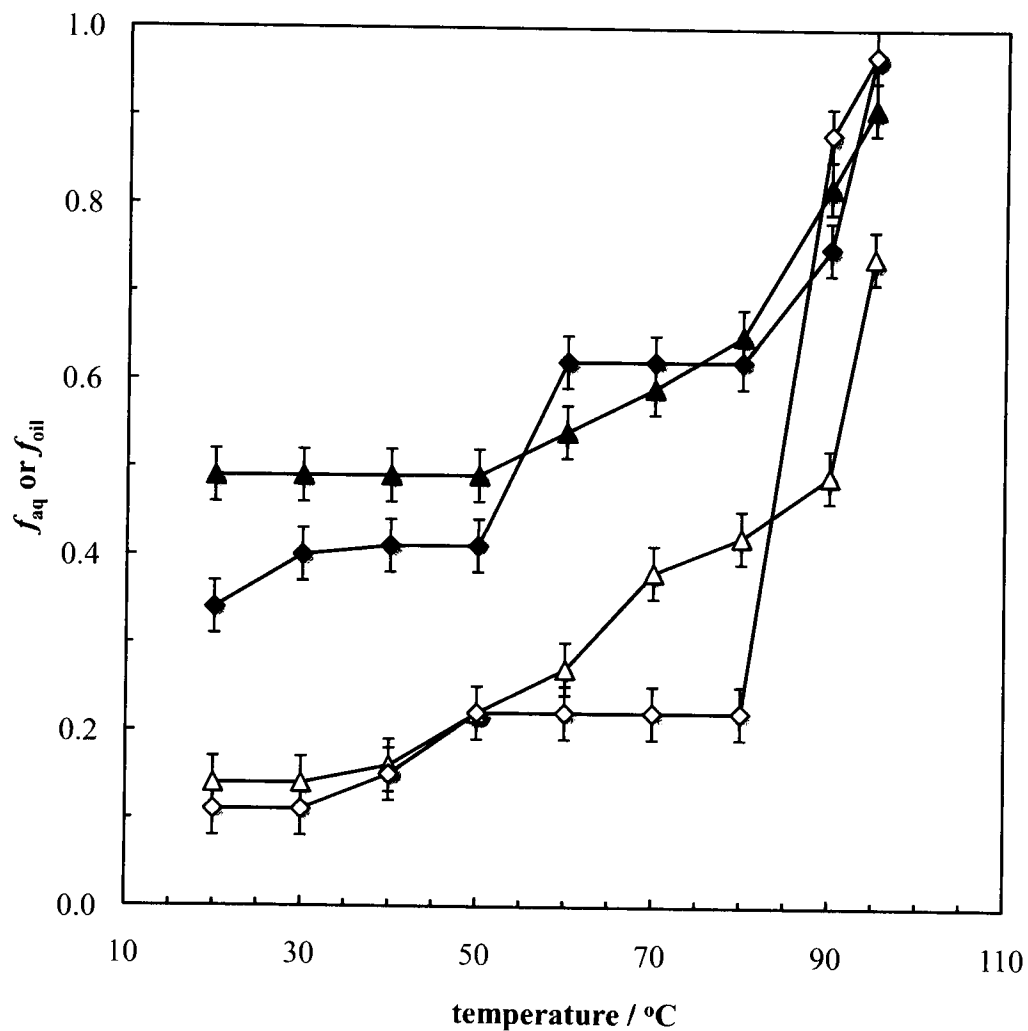
3.5.1 *Effect of temperature increase after emulsification*

3.5.1.1 Handshaking

Based on the results obtained by studying the particle concentration effect, a particle concentration, which yields stable emulsions at room temperature was chosen. The stability of these emulsions to coalescence upon gradually increasing the temperature was investigated, in order to determine if it was sensitive to the physical state of the adsorbed particles below and above the melting point range.

In the same way as in section 3.2.2, two emulsions were prepared from a 10 wt.% dispersion of Microklear 418 or Aquawax 114 particles in squalane and an equal volume of water by handshaking for 2 min. at room temperature. These emulsions were heated using a water bath, in which the temperature was increased in 10°C steps to 95°C. Between each temperature, the rate of temperature increase was close to 2°C/min, comparable to that in the DSC studies. The vessels were gently agitated every 10°C, to re-disperse all the emulsion in its continuous phase and then held for 1 h. at each temperature. After 95°C was reached and the samples held at this temperature for an hour, the samples were removed from the bath and stored at room temperature.

Figure 3.18. Stability after 1 h of water-in-squalane emulsions prepared at room temperature and stabilised by 10 wt.% (◆) Microklear 418 or (▲) Aquawax 114 particles as a function of temperature after preparation. Filled points refer to f_{oil} (sedimentation), open points to f_{aq} (coalescence).



The evolution of the emulsion stabilities is plotted versus temperature in Figure 3.18 for both wax-stabilised systems. With increasing temperature, the overall trend observed in both systems is that the sedimentation (f_{oil}) and coalescence (f_{aq}) extents increase. Particles, transformed from solid to liquid, desorb from the oil-water interface and dissolve in the oil phase. This results in the water drops losing their protective armour and fusion between them can proceed. Figure 3.18 shows that significant coalescence occurs in a narrow temperature range above 80°C for Microklear 418 emulsions, whereas it is more gradual between 50 and 95°C for Aquawax 114 emulsions. This difference is related to the melting point range determined earlier (*cf.* § 3.1.1): for Microklear 418 the melting occurs over a relatively narrow range of temperature, whereas Aquawax 114 was seen to melt over a much wider range. This suggests that the dominant influence of temperature in the emulsions is governed by the properties of the wax particles themselves. The increase in sedimentation may be due in part to the increase in coalescence as drops become more concentrated, but also to the decrease in the viscosity of the continuous oil phase with temperature. The latter has been observed to fall by over a factor of three when the temperature of squalane is increased from 20 and 60°C.³⁶

Photographs of the vessels are displayed in Figure 3.19, and it can be observed that neither of the two emulsions are totally separated when 95°C is attained. Phase separation is nearly complete for Microklear 418 emulsions, as this temperature is well above its melting range. However, as the Aquawax 114 finishes melting above 110°C, the emulsion separation is incomplete at 95°C. When the samples are cooled to room temperature, some 0.5 to 1 mm diameter water drops were observed, trapped in the oil solidified by the dissolved wax.

Figure 3.19. Vessels of water-in-squalane emulsions initially prepared at room temperature and stabilised by 10 wt.% (a) Microklear 418 and (b) Aquawax 114, after heating to 95°C.

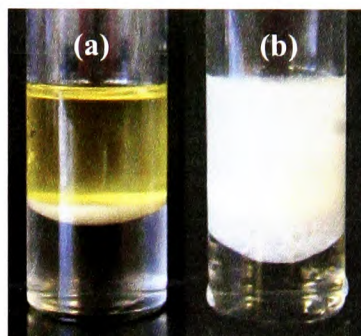
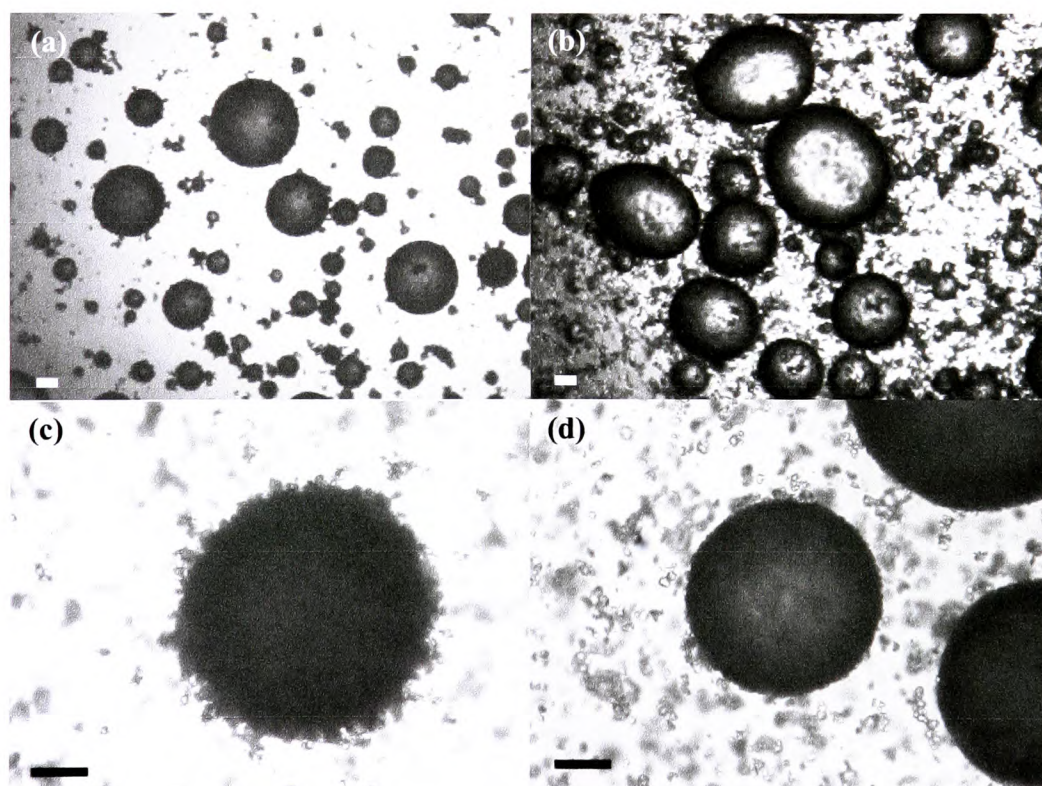


Figure 3.20. Optical microscopy images of some of the emulsions treated as in Figure 3.18. Microklear 418 systems at (a) 20 and (b) 60°C, Aquawax systems at (c) 30 and (d) 70°C. Scale bars represent 400 μm .

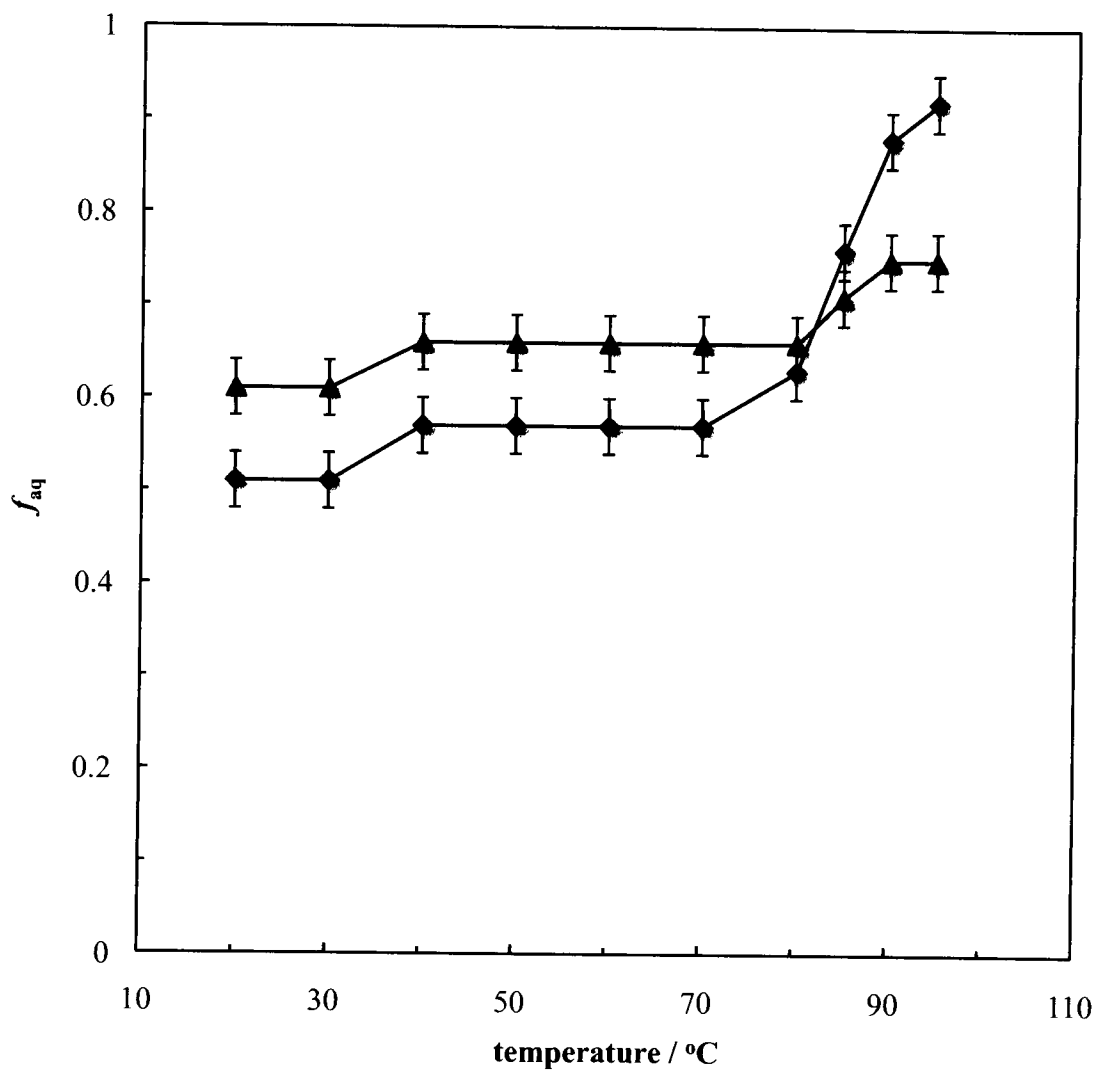


In order to demonstrate the changes in water drop appearance throughout the temperature increase, a few selected microscope images of emulsions are given in Figure 3.20. On increasing the temperature of the Microklear 418 emulsion from 20 to 60°C, Figures 3.20 (a) and (b), some of the drops appear to become non-spherical. This is a characteristic of particle-stabilised emulsions subjected to coalescence and is linked to the irreversible nature of particle adsorption.³⁷ The Aquawax 114 emulsion, which presents larger drops than the Microklear 418 (Figures 3.20 (c) and (d)), does not exhibit a prominent shape change between 30 and 70°C. However the particle aggregates at the surface of drops are more numerous at the low temperature than at the high one. For both systems, the continuous phase seems to contain more particles at higher temperature and interfaces devoid of particles were observed at high temperatures.

3.5.1.2 Ultra Turrax homogenisation

The experiment detailed in section 3.5.1.1 was repeated with water-in-squalane emulsions prepared by 30 seconds homogenisation at 11000 rpm at room temperature. The findings reported in Figure 3.21 differ a lot from the handshaken emulsions ones. Firstly, it should be noted that for both wax particle systems, the emulsion stability at 20°C is significantly lower than that of the equivalent emulsions prepared by handshaking. This may be caused, as previously stated, by partial melting of the particles in the warmer regions close to the rotor-stator homogeniser head. Again, the Microklear 418-stabilised emulsion destabilises abruptly above 80°C, nearly reaching total phase separation at 95°C. For the Aquawax 114 emulsion, although there is virtually no change in the volume of separated water as a function of temperature, the average drop diameter observed visually increased with temperature due to coalescence.

Figure 3.21. Stability to coalescence after 1 h of water-in-squalane emulsions stabilised by 10 wt.% (◆) Microklear 418 and (▲) Aquawax 114 particles prepared by homogenisation at room temperature and subsequently heated.



3.5.2 *Effect of temperature during emulsification*

3.5.2.1 Wax particles

3.5.2.1.1 *Preparation and storage at high temperature*

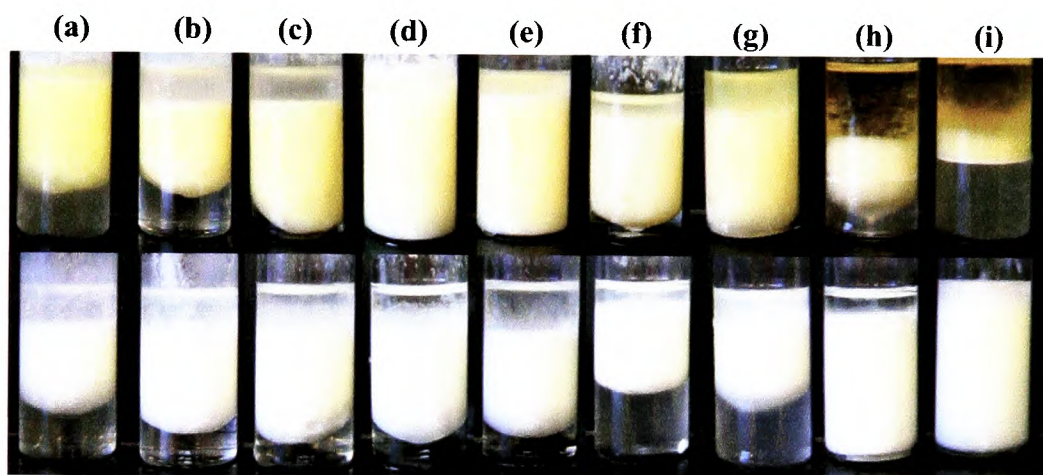
The importance of the wax particle state prior to emulsification was studied by preparing emulsions at different temperatures and assessing their stability at the same temperatures. 10 wt.% of particles were handshaken into oil to disperse them, and then the produced phase was heated to the appropriate temperature (from 20 to 90°C). An equal volume of water was brought to the same temperature, before being added to the wax dispersion followed by 11000 rpm thermostated homogenisation for 30 seconds. All emulsions were incubated at the emulsification temperature for 8 h, before being stored on the bench at room temperature.

All emulsions were water-in-squalane, but as Figure 3.22 shows, the fraction of aqueous phase resolved after 8 h varies with emulsification temperature. However, the fractions of coalescence were observed to stop changing after 4 h. The photograph of the vessels 8 h after emulsion formation illustrates the increase followed by a decrease in stability for the Microklear 418 system. Whereas the Aquawax 114 system presents two maxima separated by a decrease in stability. The subsequent cooling of the emulsions to room temperature did not induce any changes in the relative volumes of oil, emulsion or water phases.

Figure 3.23 shows that the Microklear 418-stabilised emulsions exhibit an increasing stability to coalescence from 20 to 60°C, above which it decreases significantly to 95°C. The increase in the extent of coalescence above 70°C is in agreement with the previous observation and starts at the onset of melting of a fraction of the particles (*cf.* § 3.3.1.2). However, the increase in stability approaching 60°C is surprising. From 20 to 60°C, the oil phase is a slightly turbid dispersion prior to emulsification, still showing a high concentration of particles. However at 70°C and above, this oil phase becomes clearer and more yellow with residual particles sedimenting very quickly. The increased stability could be due to dissolution of a small amount of surface-active molecules (ester or acid) from the particle surfaces, which are then available for adsorption at freshly created oil-water interfaces. Emulsions should

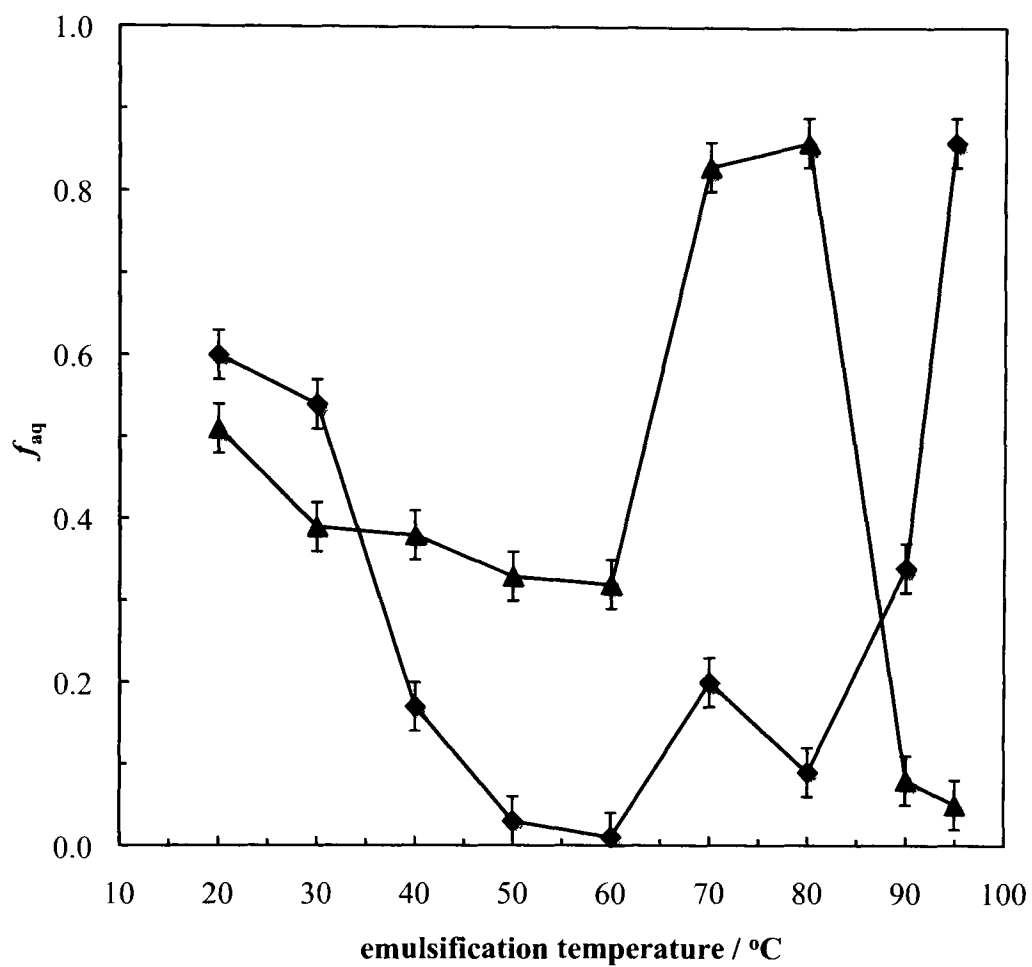
then be more stable at higher temperatures. However when all these molecules are melted, the opposite observation is made. This could be explained by smaller chain length molecules dissolving at lower temperature, that would be more effective emulsifiers than longer chain homologues liberated at higher temperature. This hypothesis still needs further investigation.

Figure 3.22. Photographs of vessels containing w/o emulsions stabilised by 10 wt.% Microklear 418 (upper) and Aquawax 114 (lower) particles homogenised and stored at (a) 20, (b) 30, (c) 40, (d) 50, (e) 60, (f) 70, (g) 80, (h) 90 and (i) 95°C, 30 min. after preparation.



By contrast, emulsions stabilised by Aquawax 114 particles show a small increase in coalescence stability up to 60°C, become very unstable at 70 and 80°C and re-stabilise above this (Figure 3.23). The oil phase before emulsion formation was observed to be slightly turbid between 20 and 60°C, and to become clearer above. Although no significant coalescence after emulsification was observed with temperature change in section 3.5.1.2, the alkane composition given by the manufacturer for the Aquawax 114 indicates that the emulsion should destabilise with increasing temperature. However our ATR-FTIR spectra of the Aquawax 114 revealed a band corresponding to either an ester or a carboxylic acid group, similarly present in the Microklear 418 spectrum (*cf.* § 3.1.3). Hence the polar molecules contained in the Aquawax 114 could adsorb at the squalane-water interface, resulting in the significant increase in instability occurring above 60°C. The following decrease in stability,

Figure 3.23. Variation of f_{aq} with emulsification temperature for emulsions in Figure 3.22 for (◆) Microklear 418 and (▲) Aquawax 114 particles.

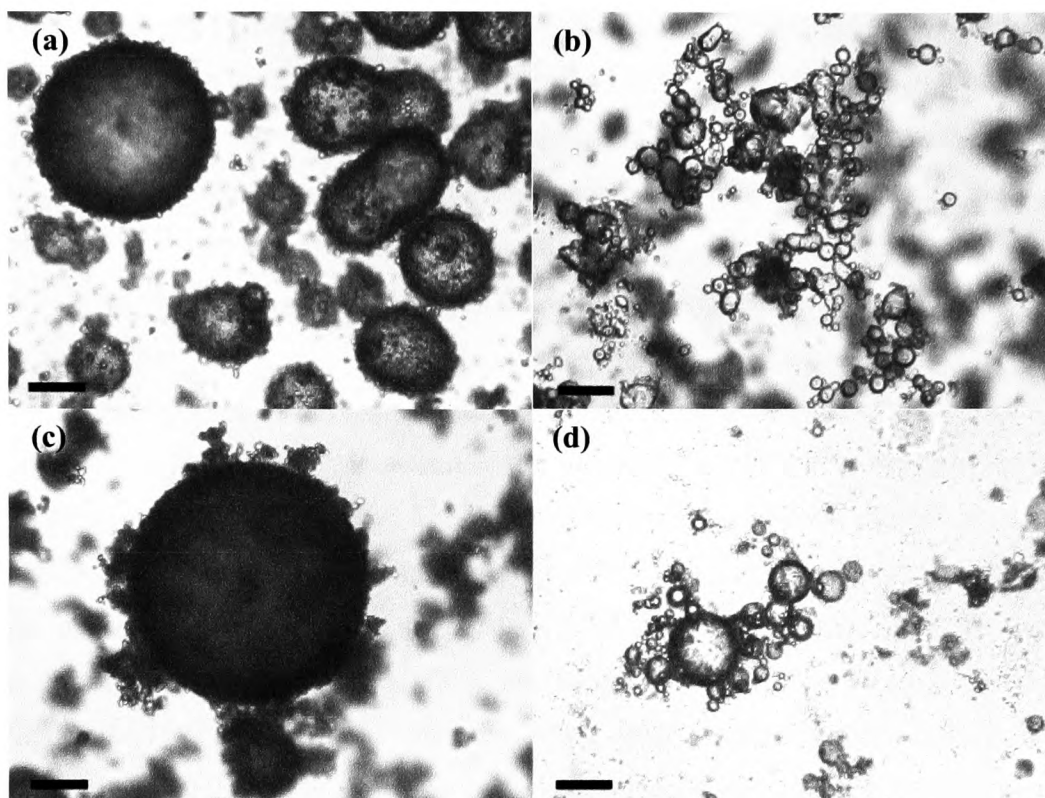


between 60 and 90°C, is probably due to the partial melting of the wax particles along with a concomitant change in their solid-like character and wettability. Adding surfactants to stable particle-stabilised emulsions has been observed previously to result in a decrease in stability.³⁸ The emulsion stability seems dependent on the concentration of surface-active molecules released from the particles in the system. Towards the upper end of the melting range, above 90°C, a significant proportion of the particles have melted and the hydrophobic molecular species dissolved in oil may act as efficient stabilisers of water drops.

The average drop sizes measured immediately after emulsification exhibit a minimum in line with the emulsion stability maximum for both series. The sizes in Microklear 418-stabilised emulsions pass through a minimum at 60°C: non-spherical drops with rough surfaces characteristic of particle-dominated interfaces are present at the lower temperatures, whereas at the optimum temperature, the drops become smaller and their surfaces are smoother, indicating the change in emulsifier type (Figure 3.24). The non-spherical drop shape observed at 60°C might be due to recrystallisation of the wax during microscopy. The micrographs of the Aquawax 114 emulsions at 40 and 90°C in Figure 3.24 show that the most stable emulsions also comprise the smallest drops.

Comparing sections 3.5.1 and 3.5.2 shows that the temperature history of wax particle-stabilised emulsions is very important with regard to their stability. If the temperature is changed once particles are adsorbed at the oil-water interface, the emulsion stability is quite different to that for which the temperature has been increased before emulsification.

Figure 3.24. Optical micrographs of water-in-squalane emulsions prepared and stored as in Figure 3.22 stabilised by Microklear 418 particles at (a) 40 and (b) 60°C and Aquawax 114 particles at (c) 40 and (d) 90°C. Scale bars represent 100 μm .



3.5.2.1.2 Preparation at high temperature and storage at room temperature

The basis of the method known as emulsification by the phase inversion temperature (PIT) method is investigated in this part by homogenising systems at different temperatures as described in section 3.1.1.1.1 but cooling within 5 min to room temperature. For non-ionic surfactant systems, the emulsion is made around the PIT where the drop size is least and then cooled, to yield very stable emulsions at the lower temperatures.³⁹ In our case, any melted material formed at higher temperatures should be solidified in oil on cooling, leading to potential enhancement of emulsion stability to sedimentation.

Figure 3.25 displays the resulting emulsion series with the two wax types for this experiment. Both series are similar to the series incubated at the emulsification temperatures. The Microklear 418 particle-stabilised emulsions exhibit an optimum stability followed by a decreasing stability with increasing temperature, but emulsions are invariably more stable and the most stable emulsions are formed at 60, 70 and 80°C as opposed to 60°C only when 8h of incubation at these temperatures is applied. For Aquawax 114 particles, the stability trend with increasing temperature is non-monotonic: stability to coalescence initially increases to 50°C, decreases progressively to 80 °C and increases again substantially to 95°C. This is also similar to the results obtained in section 3.1.1.1.1 but with generally higher stabilities. For both wax series, the immediate cooling after formation reduces the extent of drop sedimentation in the semi-solid oil phase, resulting in much better emulsions by lowering the probability of drop coalescence.

The average drop diameter with emulsification temperature, shown in Figure 3.26 for both particle types, fluctuates a lot for both series. This figure also underlines that the drop size is generally smaller with the Microklear 418 system than with the Aquawax 114 one, but this can be due to the smaller size of the Microklear 418 particles. A marked reduction in drop size at the highest temperature is noticeable which could be attributed to a more surfactant-stabilised emulsion system.

Figure 3.25. Photographs of vessels containing water-in-squalane emulsions stabilised by 10 wt.% Microklear 418 (upper) and Aquawax 114 (lower) particles, homogenised at (a) 20, (b) 30, (c) 40, (d) 50, (e) 60, (f) 70, (g) 80, (h) 90 and (i) 95°C and stored at room temperature. The photos were taken 1 day after emulsification.

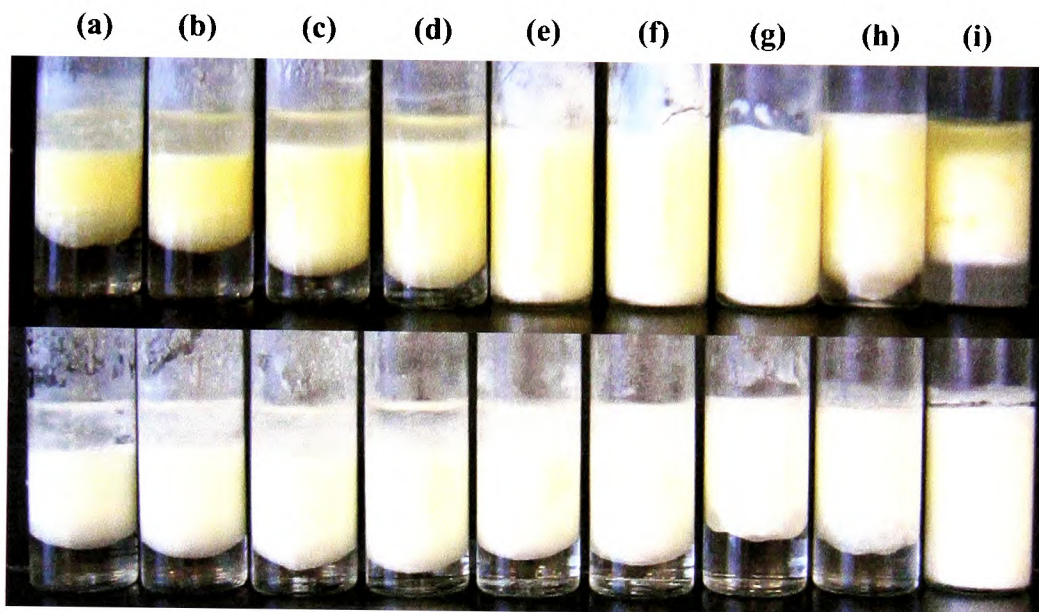
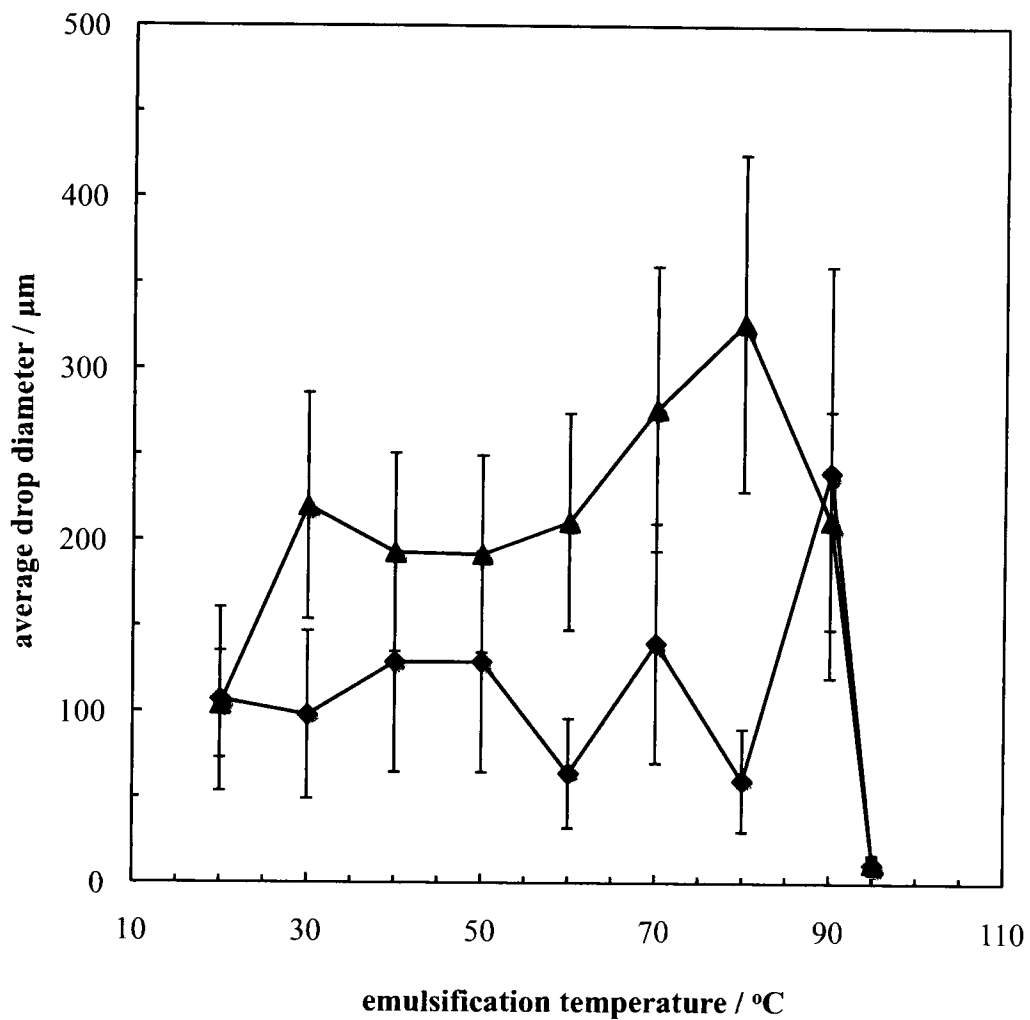


Figure 3.26. Variation of average drop diameter with emulsification temperature for w/o emulsions prepared as in Figure 3.25 and stabilised by either 10 wt.% (◆) Microklear 418 or (▲) Aquawax 114 particles.



3.5.2.2 Triglyceride crystals

The experiment carried out with the wax particles (*cf.* § 3.5.2.1) was replicated with emulsions stabilised by 3 wt.% glyceryl tripalmitate particles prepared by Ultra Turrax homogenisation at 11000 rpm for 30 seconds at 30, 50, 70 and 90°C. The emulsions were rapidly removed from the bath and cooled down to be stored at room temperature.

Photographs of the vessels after emulsification are shown in Figure 3.28. With increasing temperature, the stability to coalescence of the water-in-squalane emulsions decreases, and oil and water phases are almost totally separated from 70°C (Figure 3.29). This is close to the melting point of the glyceryl tripalmitate, which was measured with a capillary apparatus to be 66 ± 1 °C. The average drop diameter was measured on optical micrographs, and is observed to decrease with increasing temperature from about 200 μm at 30°C to 10 at 90°C.

Contrary to the wax particles, the partially or totally melted glyceryl tripalmitate crystals are not better emulsifiers for water-in-oil emulsions than the solid crystals. Comparing the wax particles with the triglyceride crystals might be equivalent to comparing impure to pure particles: the impure particles release a variety of surface active molecules when they melt, possibly leading to a better stabilisation of the emulsion.

Figure 3.28. Photographs of vessels containing water-in-squalane emulsions stabilised by 3 wt.% glyceryl tripalmitate homogenised at (a) 30, (b) 50, (c) 70 and (d) 90°C and stored at room temperature, 1 day after emulsification.

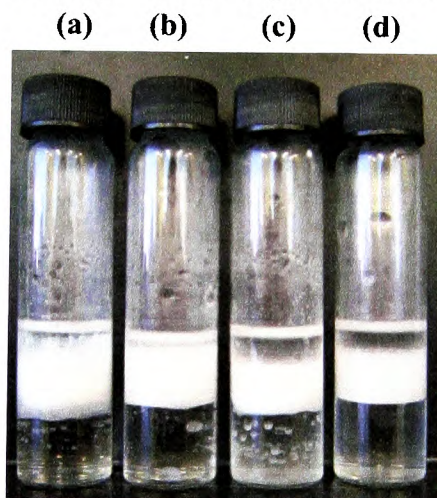
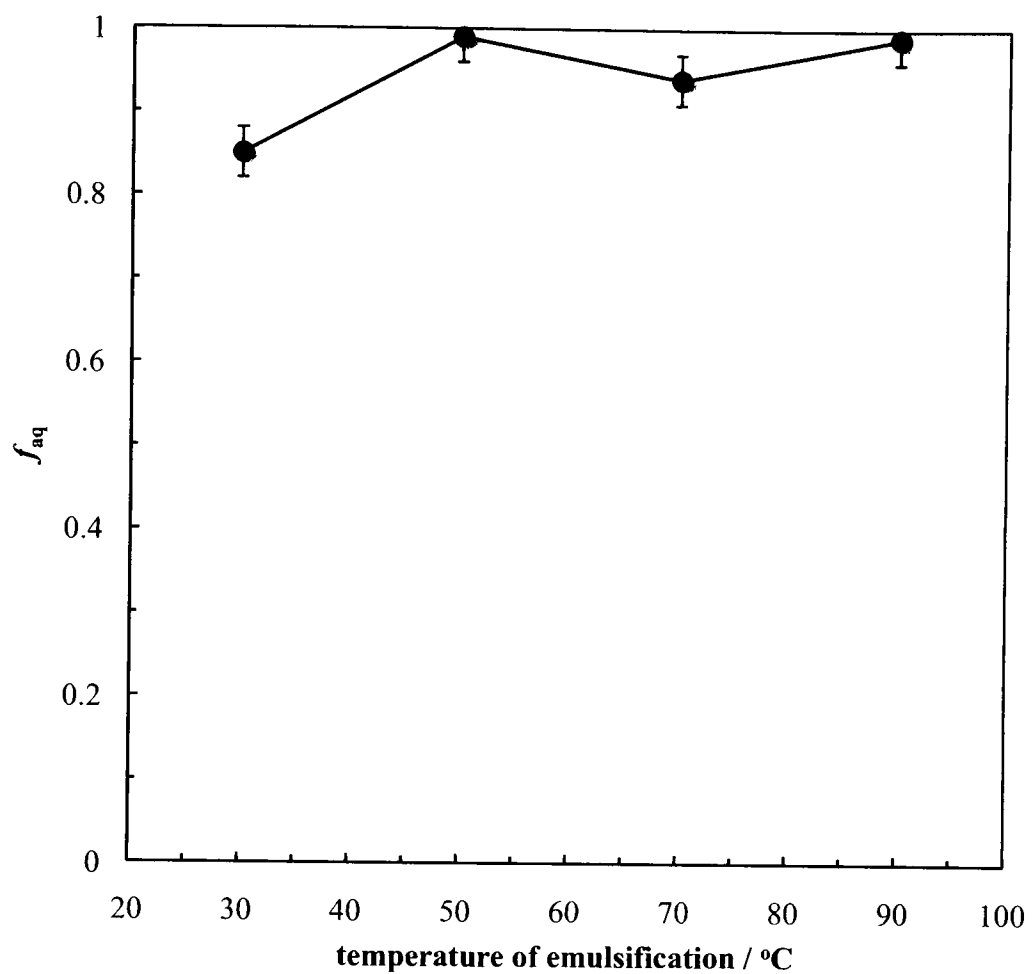


Figure 3.29. Stability to coalescence of water-in-squalane emulsions stabilised by 3 wt.% glyceryl tripalmitate particles prepared by homogenisation at room temperature and subsequently heated for 5 min.



3.6 Conclusions

Emulsions can be stabilised by micro-wax particles alone and, since particles are hydrophobic at the oil-water interface, such emulsions are water-in-oil. Different ways of dispersing the particles in oil and emulsifying the oil dispersion with water have been investigated. Sonication was observed to alter the particles either by breaking the network formed between them or by melting them, and Ultra Turrax homogenisation was seen to break the particles and probably partially melt them too. Large spherical wax particles gave water-in-oil emulsion when homogenised by the Ultra Turrax into fibers, whereas they are not able to stabilise any emulsion in their original shape. Emulsions stabilised by microwax particles (Aquawax 114 and Microklear 418) or triglyceride crystals alone were further investigated, and the influence of temperature on emulsion stability was described.²⁵ Upon increasing particle concentration, the wax-stabilised emulsions exhibit increasing stability and decreasing drop size, whereas the triglyceride-stabilised emulsions display a maximum in stability linked to crystal network formation.

The stability of the wax-stabilised emulsions at different temperatures to both sedimentation and coalescence depends on whether particles are adsorbed to drop interfaces or not prior to the temperature change. If drops are formed at room temperature, increasing the temperature of the emulsion subsequently leads to a progressive increase in the extent of coalescence as particles melt and cannot provide a sufficient barrier to drop fusion. By contrast, emulsions prepared and stored at elevated temperatures are particularly stable with respect to coalescence. It is thought that surface-active molecules, arising from the melting wax, adsorb to freshly created interfaces in these emulsions. It was concluded that the temperature variation might provide a means to control the coalescence tendency of wax particle-stabilised emulsions.

The temperature change affects the triglyceride-stabilised emulsion in a different way. Water-in-oil emulsions were observed to destabilise upon increasing the homogenisation temperature: almost total phase separation is reached above the melting point of the crystal, as the particles do not release any surface active molecules able to stabilise an emulsion.

3.7 References

1. R. Aveyard, B. P. Binks and J. H. Clint, *Adv. Colloid Interface Sci.*, **100**, 503 (2003).
2. B. P. Binks and S. O. Lumsdon, *Langmuir*, **16**, 8622 (2000).
3. B. P. Binks, A. K. F. Dyab and P. D. I. Fletcher, *Phys. Chem. Chem. Phys.*, **9**, 6391 (2007).
4. B. P. Binks, R. Murakami, S. P. Armes and S. Fujii, *Langmuir*, **22**, 2050 (2006).
5. S. Fujii, E. S. Read, B. P. Binks and S. P. Armes, *Adv. Mater.*, **17**, 1014 (2005).
6. B. P. Binks and S. O. Lumsdon, *Phys. Chem. Chem. Phys.*, **2**, 2959 (2000).
7. B. P. Binks and C. P. Whitby, *Colloid Surf. A*, **224**, 241 (2003).
8. B. P. Binks, R. Murakami, S. P. Armes and S. Fujii, *Angew. Chem. Int. Ed.*, **44**, 4795 (2005).
9. S. Tsuji and H. Kawaguchi, *Langmuir*, **24**, 3300 (2008).
10. J. R. Becker, *Crude oil waxes, emulsions and asphaltenes*, Pennwell Books, Tulsa, 1997.
11. B. J. Musser and P. K. Kilpatrick, *Energy Fuels*, **12**, 715 (1998).
12. T. A. Al-Sahhaf, M. A. Fahim and A. M. Elsharkawy, *J. Dispersion Sci. Technol.*, **30**, 597 (2009).
13. B. P. Binks and T. S. Horozov, *Colloidal Particles at Liquid Interfaces*, University Press, Cambridge, 2006.
14. S. M. Hodge and D. Rousseau, *Food Res. Int.*, **36**, 695 (2003).
15. S. M. Hodge and D. Rousseau, *J. Am. Oil Chem. Soc.*, **82**, 159 (2005).
16. D. Rousseau and S. M. Hodge, *Colloid Surf. A*, **260**, 229 (2005).
17. A. L. Campbell, B. L. Holt, S. D. Stoyanov and V. N. Paunov, *J. Mater. Chem.*, **18**, 4074 (2008).
18. D. Johansson, B. Bergenstahl and E. Lundgren, *J. Am. Oil Chem. Soc.*, **72**, 939 (1995).
19. E. H. Lucassen-Reynders and M. van den Tempel, *J. Phys. Chem.*, **67**, 731 (1963).

20. V. N. Paunov, O. J. Cayre, P. F. Noble, S. D. Stoyanov, K. P. Velikov and M. Golding, *J. Colloid Interface Sci.*, **312**, 381 (2007).
21. M. P. Aronson, *Langmuir*, **2**, 653 (1986).
22. C. Alkan, *Thermochimica Acta*, **451**, 126 (2006).
23. B. P. Binks and J. A. Rodrigues, *Langmuir*, **19**, 4905 (2003).
24. R. Aveyard, P. Cooper, P. D. I. Fletcher and C. E. Rutherford, *Langmuir*, **9**, 604 (1993).
25. B. P. Binks and A. Rocher, *J. Colloid Interface Sci.*, **335**, 94 (2009).
26. D. E. Tambe and M. M. Sharma, *Adv. Colloid Interface Sci.*, **52**, 1 (1994).
27. B. P. Binks and S. O. Lumsdon, *Langmuir*, **17**, 4540 (2001).
28. N. X. Yan, M. R. Gray and J. H. Masliyah, *Colloid Surf. A*, **193**, 97 (2001).
29. E. Vignati, R. Piazza and T. P. Lockhart, *Langmuir*, **19**, 6650 (2003).
30. B. P. Binks, J. H. Clint, P. D. I. Fletcher, T. J. G. Lees and P. Taylor, *Chem. Commun.*, 3531 (2006).
31. B. P. Binks, J. A. Rodrigues and W. J. Frith, *Langmuir*, **23**, 3626 (2007).
32. B. P. Binks and J. A. Rodrigues, *Langmuir*, **23**, 7436 (2007).
33. B. P. Binks and J. A. Rodrigues, *Angew. Chem. Int. Ed.*, **46**, 5389 (2007).
34. B. P. Binks, A. J. Johnson and J. A. Rodrigues, *Soft Matter*, **6**, 126 (2010).
35. D. E. Tambe and M. M. Sharma, *J. Colloid Interface Sci.*, **157**, 244 (1993).
36. M. de Ruijter, P. Koelsch, M. Voue, J. De Coninck and J. P. Rabe, *Colloid Surf. A*, **144**, 235 (1998).
37. B. P. Binks and C. P. Whitby, *Langmuir*, **20**, 1130 (2004).
38. B. P. Binks, A. Desforges and D. G. Duff, *Langmuir*, **23**, 1098 (2007).
39. H. Saito and K. Shinoda, *J. Colloid Interface Sci.*, **32**, 647 (1970).

CHAPTER 4 EMULSIONS STABILISED BY BIODEGRADABLE PARTICLES

4.1 Introduction

The stability of an emulsion is inevitably linked to the emulsifier used. The choice of the emulsifier is key in order to manipulate the emulsion: surfactants and wax particles (*cf.* Chapter 3) are often affected by temperature modification for example, which in turn affects the emulsion properties. Biodegradable particles, which have the property of degrading in many different environments, generate a growing interest among a wide variety of industries, and could supply a new solution to control emulsion properties.

Interest in biodegradable polymers have been firstly observed in the fields of medicine (degradable suture fibres) and agriculture (pesticide release), but today it is more focussed on environmental protection. Manufacturing biodegradable product packaging is a main target for cosmetics, food or homecare industries, in order to reduce the solid waste resulting.^{1, 2} Medical and pharmaceutical industries use biodegradable components for another purpose: polymers can degrade in the body without harming it, in the form of medical devices or drugs, the latter releasing their active ingredients in a controlled manner.^{3, 4}

Poly(lactic-co-glycolic) acid (PLGA) polymer as shown in Chapter 2, is known for its biodegradable and biocompatible properties and has been used for the past 20 years for drug delivery applications.⁵⁻⁷ It decomposes *in vivo*, by simple hydrolysis of the ester linkages, into lactic ($C_3H_6O_3$) and glycolic ($C_2H_4O_3$) acids, which are naturally present in the human body, before being eliminated as CO_2 and H_2O .^{8, 9} Hence PLGA exhibits very minimal toxicity.¹⁰ PLGA is often used as microsphere encapsulator, in which diverse drugs are contained, such as in Lupron Depot®, Decapeptyl® and Trelstar®.¹¹

Dunne *et al.* investigated the link between PLGA particle degradation, their size and the temperature: they concluded that particles between 9 and 120 μm degrade increasingly with increasing temperature, but the degradation rate is proportional to the particle diameter.¹² They described degradation as a two-step

process, which includes degradation of the polymer into water-soluble monomers and diffusion of these monomers to the particle surface and into the surrounding solution, causing mass loss. The produced monomers generate autocatalytic degradation of the particles: for large particles, it takes them more time to reach the surface, but they accelerate degradation. De and Robinson also studied the effect of incubation temperature on nano and micro-particles of PLGA: particle aggregation, more extensive for the smallest particles, was observed to increase with temperature.¹³ The pH of the solution was also reported by Yoo *et al.* to affect PLGA polymers.¹⁴ In their study, they measured the hydrolysis rate as a function of initial pH: the amount of monomer increases as the solution pH decreases, confirming a faster degradation at lower pH values. The degradation also depends on the composition of the PLGA in terms of lactic to glycolic monomer ratio. Shin *et al.* showed that PLGA 50:50 degraded quicker than the PLGA 75:25 due to a higher glycolic acid content, as the glycolic acid probably degrades faster than the lactic one.¹⁵

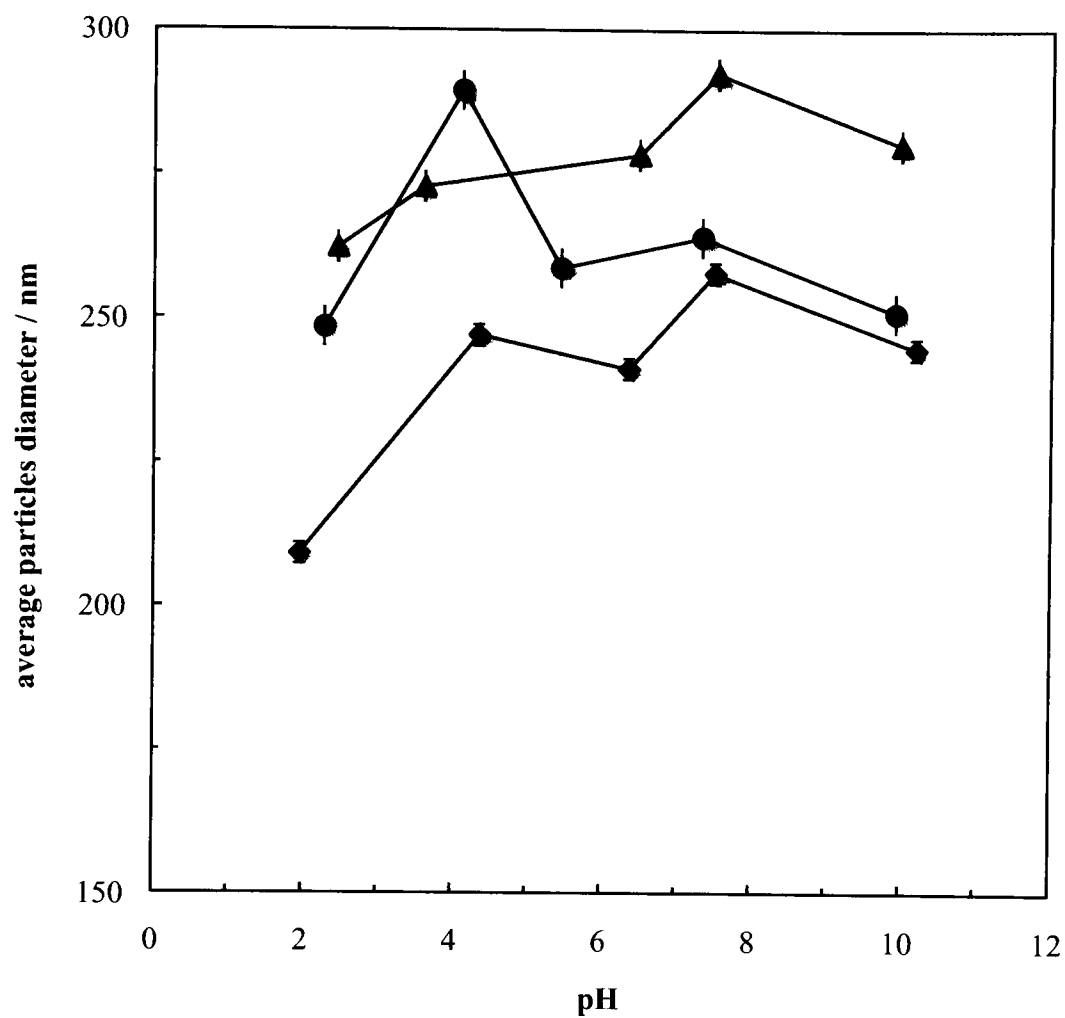
In this chapter, we study different ways of controlling PLGA particle-stabilised emulsions. The composition of the PLGA particles, in terms of variable surface chemistry or variable lactic to glycolic ratio, their concentration and their dispersion pH were observed to affect the short and long-term stability of the emulsions they stabilise.

4.2 Particle characterisation

4.2.1 *Dynamic light scattering*

Dynamic light scattering is a widespread technique for characterising colloidal suspensions. It is a non-destructive method used both to determine the size and the zeta potential of particles. PLGA particles were observed to be roughly spherical and are known to degrade as a function of temperature and pH.¹² It is therefore expected that their size might change with the pH of the particle dispersion. Figure 4.1 displays the change of the average diameter with pH for 3 different PLGA particles: particles were made from natural PLGA 50:50, with either carboxylic (PLGA-COOH) or amidine (PLGA-NH₂) groups attached on them. At their natural pH (~8), the three types of particles present equivalent diameters of 275 ± 25 nm. When the pH of the fresh dispersion is varied, none of the particles exhibit a clear alteration of size, even if PLGA-COOH particles seem to reach a maximum diameter of 280 nm at pH 4. However, PLGA particles go through a slight decrease in size when the dispersion pH is reduced to 2; the particle average diameter changes from 265 to 205 nm. If the change in size is not reversible, it could result from a partial degradation of the particles occurring at low pH, but more experiments should be done to confirm this. A similar but smaller effect of pH on PLGA-NH₂ is observed, the particle size decreasing slightly at low pH.

Figure 4.1. Average diameter of 0.002 wt.% (◆) PLGA, (●) PLGA-COOH and (▲) PLGA-NH₂ particles dispersed in Milli-Q water as a function of pH of the fresh dispersion.



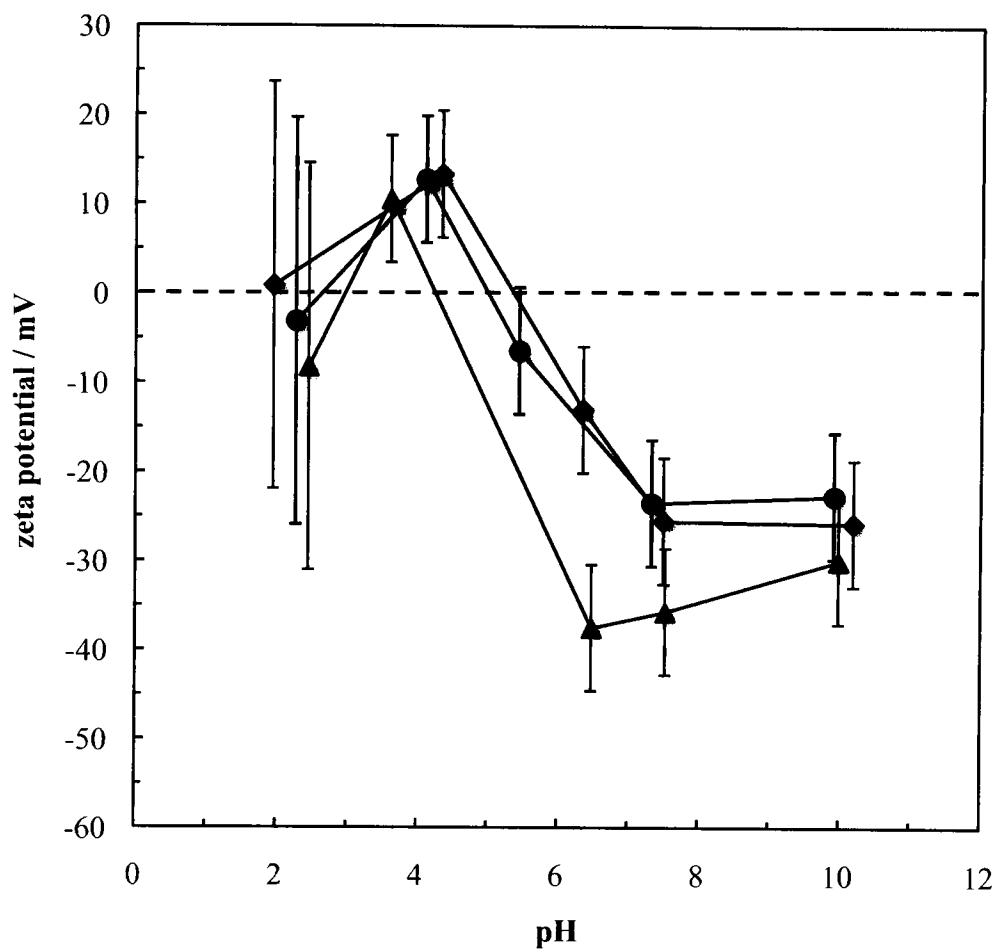
The zeta potential, which reflects the particle charge, was also measured using electrophoresis. PLGA, PLGA-COOH and PLGA-NH₂ were expected to be charged differently, due to their distinct surface groups: PLGA-NH₂ particles should be positively charged at low pH (PLGA-NH₃⁺), PLGA-COOH negatively charged at high pH (PLGA-COO⁻), whereas the unmodified PLGA particles should present a charge value in between the other two. As can be observed in Figure 4.2, all particle types are highly negatively charged at their natural pH, and they follow the same charge variation with pH: the positive zeta potential at pH 4 decreases upon increasing the pH, passing through zero around pH 5 and becoming increasingly negative up to pH 8, where it seems to plateau. The charge reversal is due to the weakly acidic groups on the particle surface losing their proton at high pH.¹⁶ The similar charges displayed by the modified and unmodified PLGA particles could be due to an insufficient group modification on the particle surface, rendering a change of charge unnoticeable. It is also believed that the large charge distribution at low pH could be due to an irregular chemical modification of the particles, as well as to particle degradation.¹³

The degradation of the unmodified PLGA particles was studied by measuring the average particle diameter as a function of pH and temperature. Table 1 shows the increase of the average diameter with incubation time: although the rate of size change is higher at 37°C for the first day, after a week the particles have reached the same degradation state at the two different temperatures. Simultaneous to the change of average diameter, the polydispersity of the size distribution increases. The increase of average diameter and of polydispersity can both be explained by the degradation process of the particles: degradation of PLGA particles occurs through a size decrease, due to loss of monomer from the particle surface, but also a size increase, when several particles fuse together forming a larger one.¹²

Table 1. Average diameter of PLGA particles at different incubation times at 25°C or 37°C. 0.002 wt.% particle dispersion was made at pH ~ 8.

temperature / °C	diameter / nm		
	initial	1 day	1 week
25	250 ± 60	290 ± 50	305 ± 150
37	250 ± 60	290 ± 150	285 ± 160

Figure 4.2. Variation of zeta potential of 0.002 wt.% (◆) PLGA, (●) PLGA-COOH and (▲) PLGA-NH₂ particles dispersed in water as a function of pH. The error bars represent the width of the zeta potential distribution.

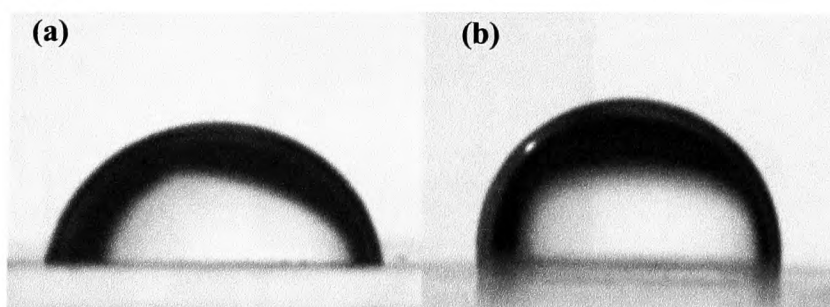


4.2.2 Contact angles

The PLGA, PLGA-COOH and PLGA-NH₂ particles previously characterised are composed of as much lactic acid as glycolic acid, *i.e.* 50:50 L:G ratio. PLGA particles with different ratio of lactic to glycolic acid (L:G) should present different wettability, as the glycolic acid is more hydrophilic than the lactic one.^{15, 17} Measuring the contact angle of different liquids enables the determination of the wettability of a solid. The PLGA 50:50 layer was made by spincoating a glass slide with a solution of the polymer in chloroform and letting the solvent to evaporate for 2 hours.

The contact angle in air of a drop of water on a layer of PLGA 50:50 was found to be $77 \pm 3^\circ$, which agrees with the values of Khorasani *et al.* and Paragkumar *et al.*^{18, 19} Under dodecane, this value increases to $82 \pm 5^\circ$. PLGA 65:35, which contains more lactic groups, exhibits higher contact angles through water: $79 \pm 3^\circ$ in air and $89 \pm 5^\circ$ under dodecane. Both PLGA types are hydrophilic, however PLGA 65:35 exhibits water drop contact angle under dodecane (Figure 4.3) closer to 90° , which would indicate a better adsorption of these particles at the dodecane-water interface than PLGA 50:50. With a contact angle of almost 90° , it is possible that particles made of PLGA 65:35 might stabilise water-in-oil emulsions as well as oil-in-water. Consequently, we expect that changing the polymer composition of the particles will change the behaviour of the particle at the oil-water interface.

Figure 4.3. Sessile water drop under dodecane (pH ~ 6.5) on (a) PLGA 50:50 and (b) PLGA 65:35 at $20 \pm 1^\circ\text{C}$.



4.3 Effect of particle type on emulsions

The effect of the surface chemistry of PLGA particles was investigated by producing emulsions of equal concentration of unmodified PLGA, PLGA-COOH or PLGA-NH₂ particles. At their natural pH, all the particles gave dodecane-in-water emulsions with equivalent stabilities. However, as Figure 4.4 displays, a little oil and large quantities of water are resolved from all the emulsions after 5 minutes. The emulsions are highly susceptible to creaming. It can also be observed that some emulsion drops display large diameter: drops between 50 and 450 μm were measured by optical microscopy. The emulsion drops stabilised by PLGA and PLGA-NH₂ are very polydisperse, with similar average diameters of 300 ± 150 μm, while the PLGA-COOH stabilised drops measure 120 ± 50 μm.

The three particle types do not present major differences in the emulsion they stabilise at their natural pH. The average drop diameters differ slightly, but the emulsion stabilities are comparable (Figure 4.5).

Figure 4.4. (a-c) Photograph and (d-f) optical microscopy images of dodecane-in-water emulsions stabilised with 0.1 wt.% of (a, d) PLGA, (b, e) PLGA-COOH and (c, f) PLGA-NH₂ particles 5 minutes after emulsification (pH ~ 8). Emulsions were made by 1 minute Ultra Turrax homogenisation at 11000 rpm. Scale bars represent 160 μm.

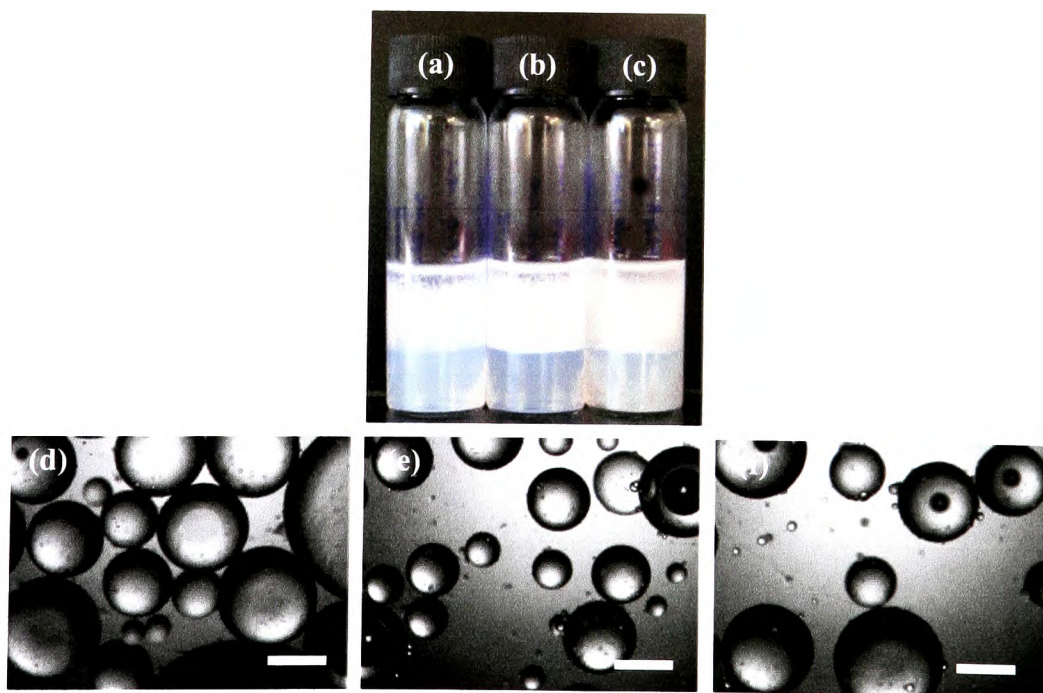
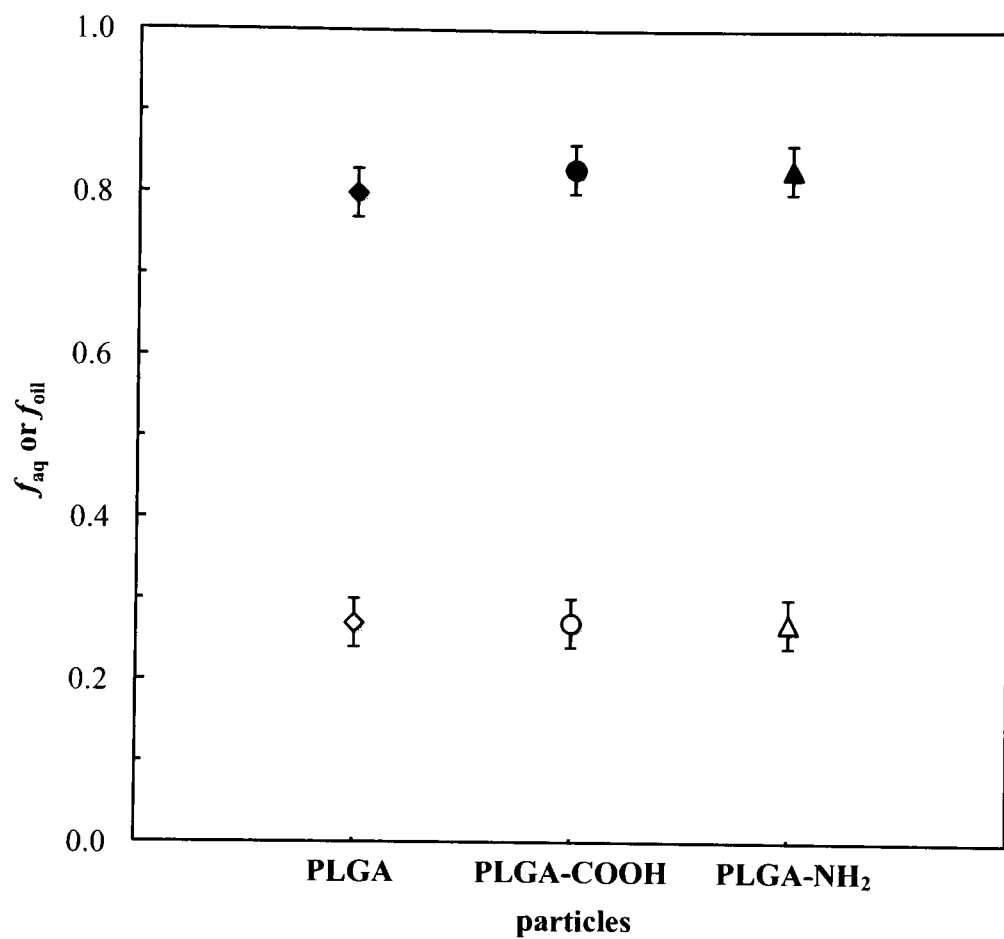


Figure 4.5. Stability of dodecane-in-water emulsions made with 0.1 wt.% (◆) PLGA, (●) PLGA-COOH and (▲) PLGA-NH₂ particles in terms of f_{oil} (open points) and f_{aq} (filled points) 1 day after emulsification.



4.4 Effect of particle concentration on emulsions

4.4.1 Variable surface chemistry

To investigate the effect of particle concentration on the PLGA 50:50 particles with different surface groups, the stability and drop size of the emulsion series with increasing particle concentration were measured. Emulsions were observed to be increasingly stable with particle concentration for the three types of particles. As Figure 4.6 displays, the emulsions are more stable at higher concentration: no coalescence is observed at 2 wt.% of particles, whereas only a few millimetre-size drops are stabilised at 0.01 wt.%. Figure 4.6 also illustrates the large amount of resolved water due to creaming of the emulsions, and that the creaming decreases with increasing particle concentration. The aqueous phase has an increasingly opaque and white appearance, probably resulting from a larger amount of free particles in the continuous phase. This can signify either that the concentration of particles non-adsorbed at the oil-water interface is increasing with the total particle concentration in the system, or that the aggregation state of the particles changes, affecting the turbidity of the subnatant. However, Figure 4.7 indicates that the average drop diameter decreases along the concentration series for all systems, implying that more particles are adsorbed at the oil-water interface. The three types of particles stabilise drops of equivalent size at and above 1 wt.%, of 75 to 50 μm in diameter. But at lower concentration (0.05 wt.%), the drop size increases and the different particles do not stabilise the same drop sizes anymore: drops are 840 μm in diameter with PLGA particles, 470 μm with PLGA-COOH and 350 μm with PLGA-NH₂.

Figure 4.6. Photograph of 1-day old dodecane-in-water emulsions stabilised with (a, e, l) 0.01, (b, f, m) 0.05, (g, n) 0.1, (c, h, o) 0.2, (i, p) 0.5, (d, j, q) 1 and (k, r) 2 wt.% of (a-d) PLGA, (e-k) PLGA-NH₂ and (l-r) PLGA-COOH particles (pH 8). Emulsions were made with 1 min. Ultra Turrax homogenisation at 11 000 rpm.

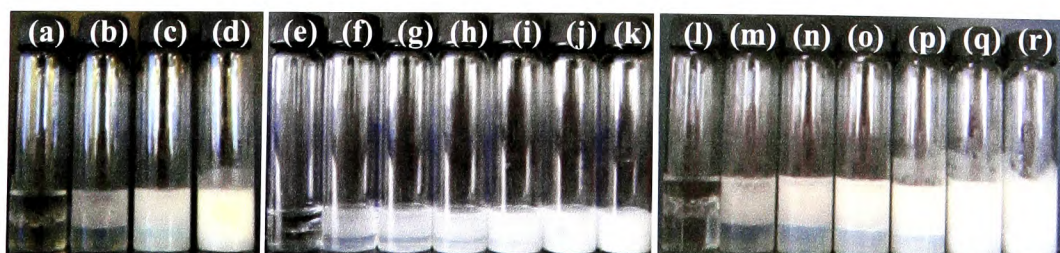
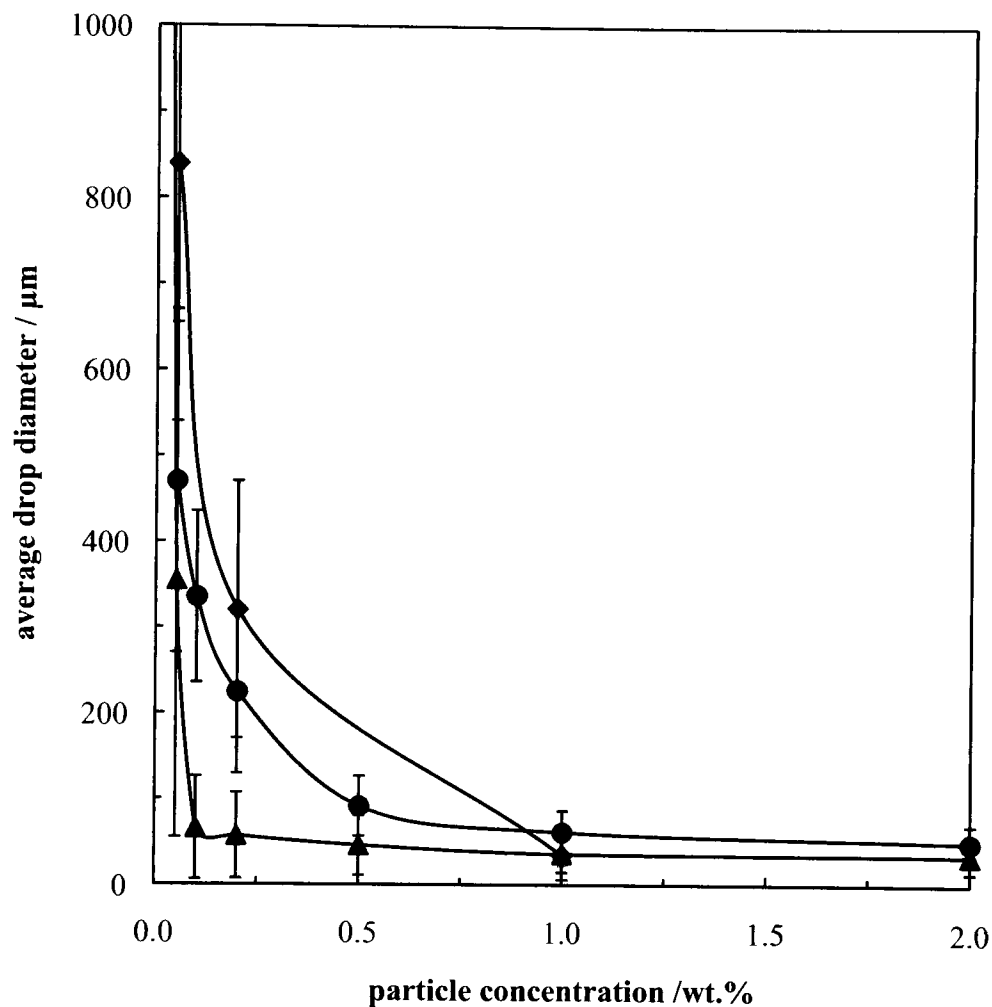


Figure 4.7. Average drop diameter measured by optical microscopy of dodecane-in-water emulsions made with (◆) PLGA, (●) PLGA-COOH and (▲) PLGA-NH₂ particles as a function of particle concentration. The size distribution of the emulsion drops is represented as an error bar.



PLGA, PLGA-COOH and PLGA-NH₂ particle-stabilised emulsions are composed of different size drops, but all emulsions exhibit increasing stability with increasing particle concentration.

4.4.2 Variable lactic/glycolic acid ratio

The effect of particle concentration was also studied for PLGA particles made of different ratio of lactic and glycolic acid. The unmodified PLGA particles from § 4.4.1 are composed of a 50:50 ratio of the two acids. Emulsions were made with the other types of PLGA particles: a 65:35 and a 75:25 L:G ratio. The three types of particle are around 250 nm in diameter. As the contact angles of water on the different PLGA ratio differ (*cf.* § 4.2.2), we expect the emulsion stability to vary as a function of particle composition.

As observed for particles of different surface chemistry, PLGA particles with different L:G ratio stabilise dodecane-in-water emulsions, which exhibit increased stability to creaming and coalescence with particle concentrations (Figure 4.8). The concentration of excess particles in the continuous phase also increases with the total particle concentration; the bottom phase becomes more opaque and white towards the end of the series.

Figure 4.8. Photographs of dodecane-in-water emulsions stabilised with (a, f) 0.01, (b, g) 0.05, (c, h) 0.1, (d, i) 0.2 and (e, j) 0.5 wt.% of (a-e) PLGA 75:25 and (f-j) PLGA 65:35 particles at pH 7.5, 5 min. after emulsification. Emulsions were made by 1 min. Ultra Turrax homogenisation at 11000 rpm.

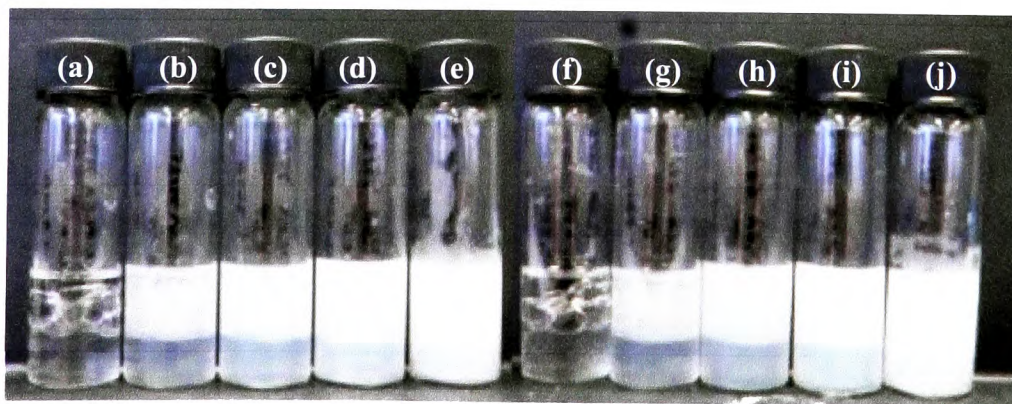


Figure 4.9 displays microscopy images of the emulsion drops for both series: all drops are spherical, and as a result of the higher particle concentration, the drop size is witnessed to decrease (compare Figure 4.9 a and c, or d and f). A quantitative representation of the change of drop size is shown in Figure 4.10: as the sampling of the emulsion is unfavourable to the large emulsion drops, which coalesce on the glass slide, a maximum drop size was measured with a ruler on the emulsion drops *in situ*. The minimum and average drops size were extracted from the microscopic measurement. The average drop size decreases sharply between 0.01 and 0.1 wt.% of particles, and an extrapolation of the curve would suggest that it would eventually plateau above 0.5 wt.%. The emulsion drops stabilised by PLGA 65:35 are slightly more polydisperse than those stabilised by PLGA 75:25. However, no significant difference can be seen between the emulsions stabilised by PLGA 65:35 and PLGA 75:25.

Figure 4.11 compares stabilities for PLGA 50:50, PLGA 65:35 and PLGA 75:25 stabilised emulsions. Stability to coalescence is observed to increase strongly at the start of the series for the three types of particles. This effect is stronger for PLGA 75:25 until 0.1 wt.% particles, after which a plateau is observed. The creaming stability also increases for all particle types, where again the emulsions made with PLGA 75:25 show the greatest stability at high particle concentration. The lactic-glycolic ratio has a small effect on the stability of emulsions formed: increasing the L:G ratio of the particles leads to improved emulsion stability to creaming and coalescence.

Figure 4.9. Optical microscopy images of dodecane-in-water emulsions stabilised with (a, d) 0.05, (b, e) 0.2 and (c, f) 0.5 wt.% of (a-c) PLGA 65:35 and (d-f) PLGA 75:25 particles. Emulsions were made by 1 min. Ultra Turrax homogenisation at 11000 rpm. Scale bars represent 400 μm .

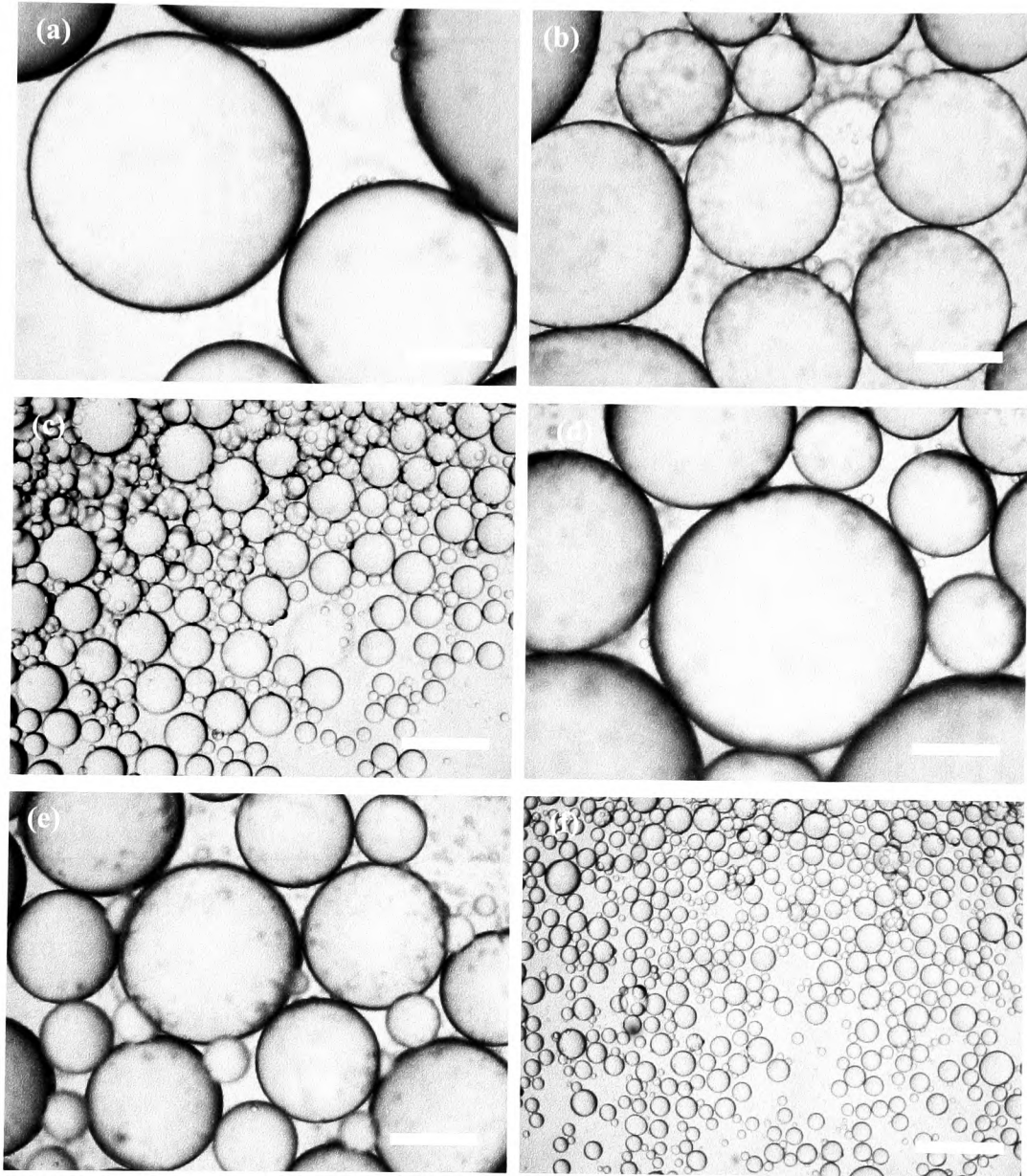


Figure 4.10. Average (■●), minimum (□○) and maximum (□○) drop diameter measured by optical microscopy of dodecane-in-water emulsions made with (●) PLGA 65:35 and (■) PLGA 75:25 as a function of particle concentration. The error bars represent the size distribution of the drops.

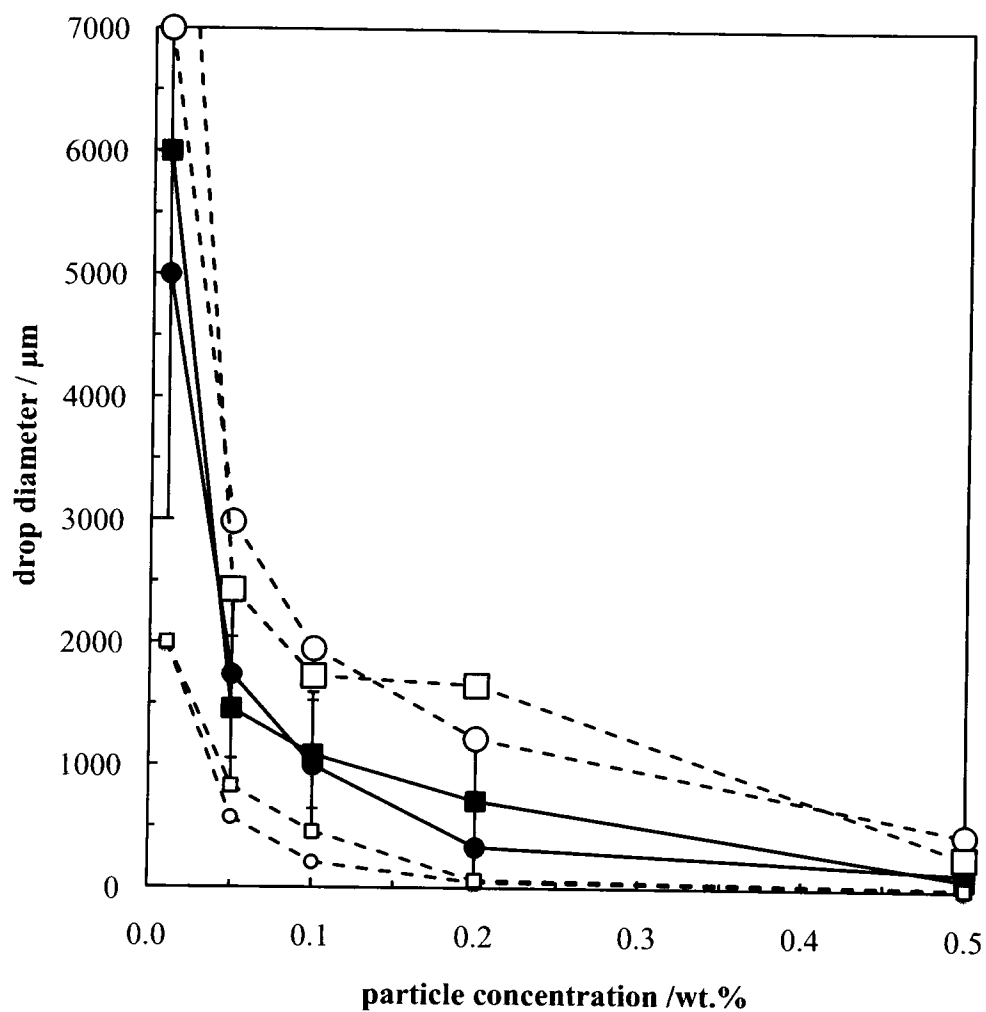
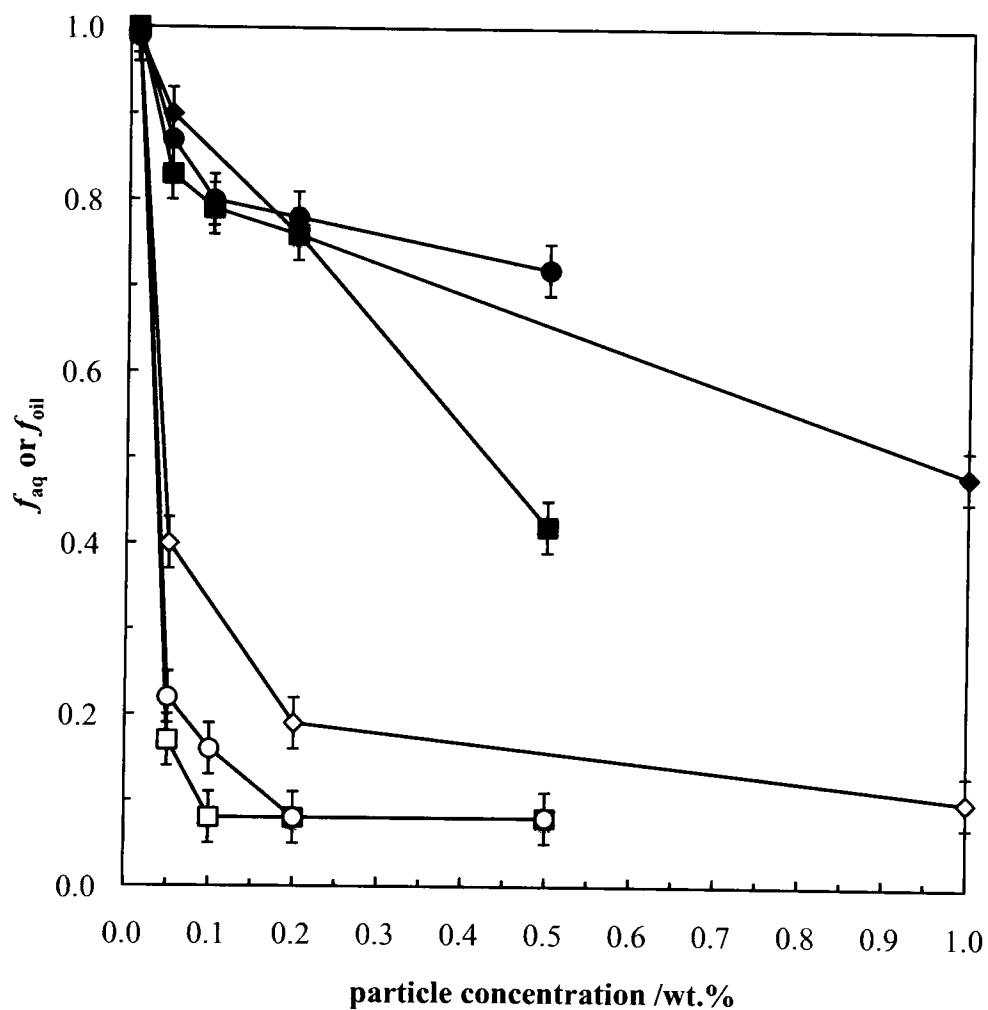


Figure 4.11. Stability of dodecane-in-water emulsions made with (◆) PLGA 50:50, (●) PLGA 65:35 and (■) PLGA 75:25 particles as a function of particle concentration in terms of f_{oil} (open points) and f_{aq} (filled points) 1 day after emulsification. Emulsions were made by 1 min. Ultra Turrax homogenisation at 11000 rpm.

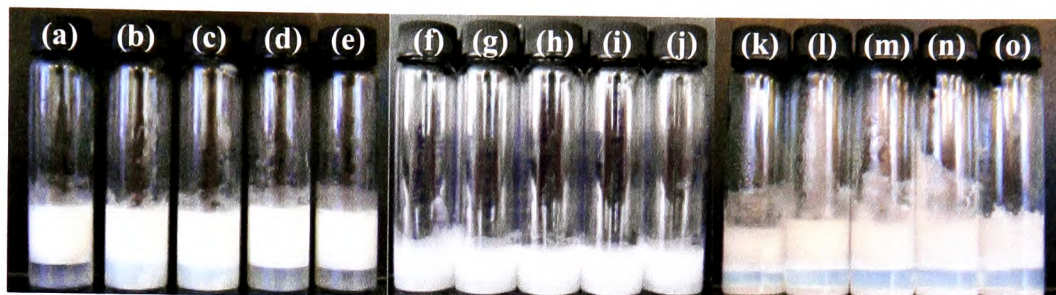


4.5 Effect of pH on emulsions

4.5.1 *Variable surface chemistry*

It has been shown in section 4.2.1 that changing the pH of the particle dispersion modifies the charge of the PLGA particles. Figure 4.12 displays the photograph of the series of emulsions made with PLGA, PLGA-COOH and PLGA-NH₂ particles at different pH. No major differences are noticed between the three series of dodecane-in-water emulsions: coalescence is not significant, while large amounts of water are resolved. A similar observation to the one made in section 4.4 can be made: Figure 4.12 shows evidence of free particles in the continuous phase. Their concentrations seem similar for the modified particles (comparable opacity of the bottom phase), however the PLGA series displays a whiter continuous phase at pH 4 and 6, indicating either that there is an increase of non-adsorbed particles or that particles are in an aggregated state (as they are close to their isoelectric point). The latter argument however does not work for the two other series, which exhibit a white phase at all pH values. Yet, there is no significant alteration of the emulsion stability compared to the emulsions at pH 2 or 8 for the PLGA series. Figure 4.13 reveals the high stability to coalescence of the unmodified PLGA-stabilised emulsions is not affected by the pH variation. However, it can also be noted that the pH slightly affects the emulsions stabilised by PLGA-COOH and PLGA-NH₂ particles: better emulsion stability seems to coincide with higher surface charge of the particles, with PLGA-COO⁻ and PLGA-NH₃⁺ giving more stable emulsions than their non-charged counterpart, at respectively high and low pH.

Figure 4.12. Photograph of 1-day old dodecane-in-water emulsions stabilised with 0.5 wt.% of (a-e) PLGA, (f-l) PLGA-COOH and (m-q) PLGA-NH₂ particles in aqueous dispersion at pH (a, f, k) 2, (b, g, l) 4, (c, h, m) 6, (d, i, n) 8 and (e, j, o) 10. Emulsions were made with 1 min. Ultra-Turrax homogenisation at 11 000 rpm.



The distinct concentration of free particles in emulsions stabilised by PLGA at pH 4 and 6 can be explained by examining the emulsion drop size. Figure 4.14 shows a slight increase in the average drop size at these pH values, indicating that the increase in particle hydrophilicity is counterbalanced by the decrease of water-oil interface needed to be stabilised. However, the large drop size of the PLGA emulsion at pH 2 contradicts this latter explanation. When comparing the three types of particles, it is noted that the PLGA-NH₂ particles stabilise the smallest drops (20 μm average diameter), while the PLGA and PLGA-COOH stabilise larger ones, of respectively 40 and 65 μm diameter. All emulsions exhibit high polydispersity in their drop size.

The different drop sizes resulting from the three types of particle is surprising, as it has been noted before (*cf.* § 4.2.1) that the three particles had similar charge as a function of pH. Also surprising is that when referring to the zeta potential measurements, the particles are highly charged at high pH, hence they should be less efficient at stabilising emulsions, which contradicts the findings for the PLGA-COOH series.²⁰ In these systems, the particles stabilise oil-in-water emulsions at all pH values, and are therefore hydrophilic. Hence, it is expected that an increase of the particle charge would further increase their hydrophilicity, causing a decrease in the emulsion stability. At low pH, PLGA-NH₃⁺ particles display a low charge, so they should give more stable emulsions, however the opposite is observed.

Figure 4.13. Stability of dodecane-in-water emulsions made with 0.5 wt.% (◆) PLGA 50:50, (●) PLGA-COOH and (▲) PLGA-NH₂ particles in terms of f_{oil} (open points) and f_{aq} (filled points) as a function of pH of the particle dispersion 1 day after emulsification.

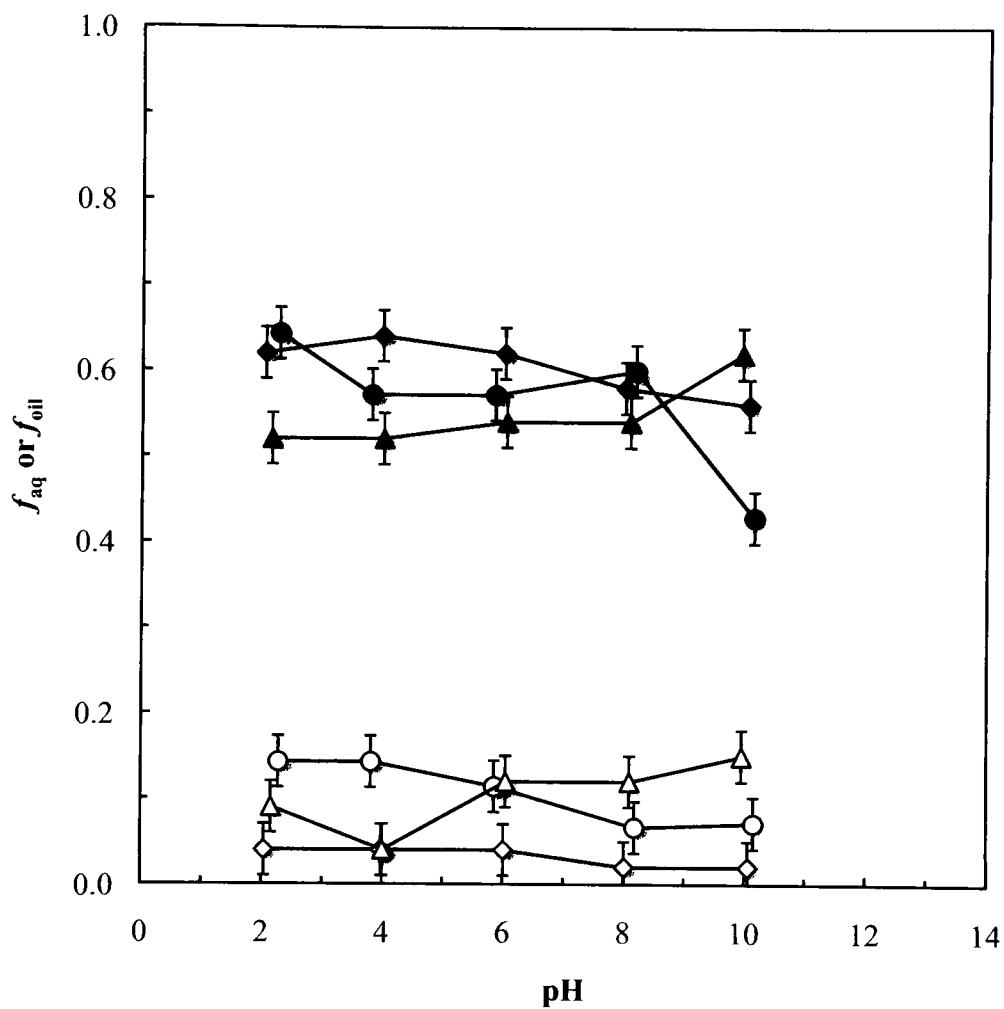
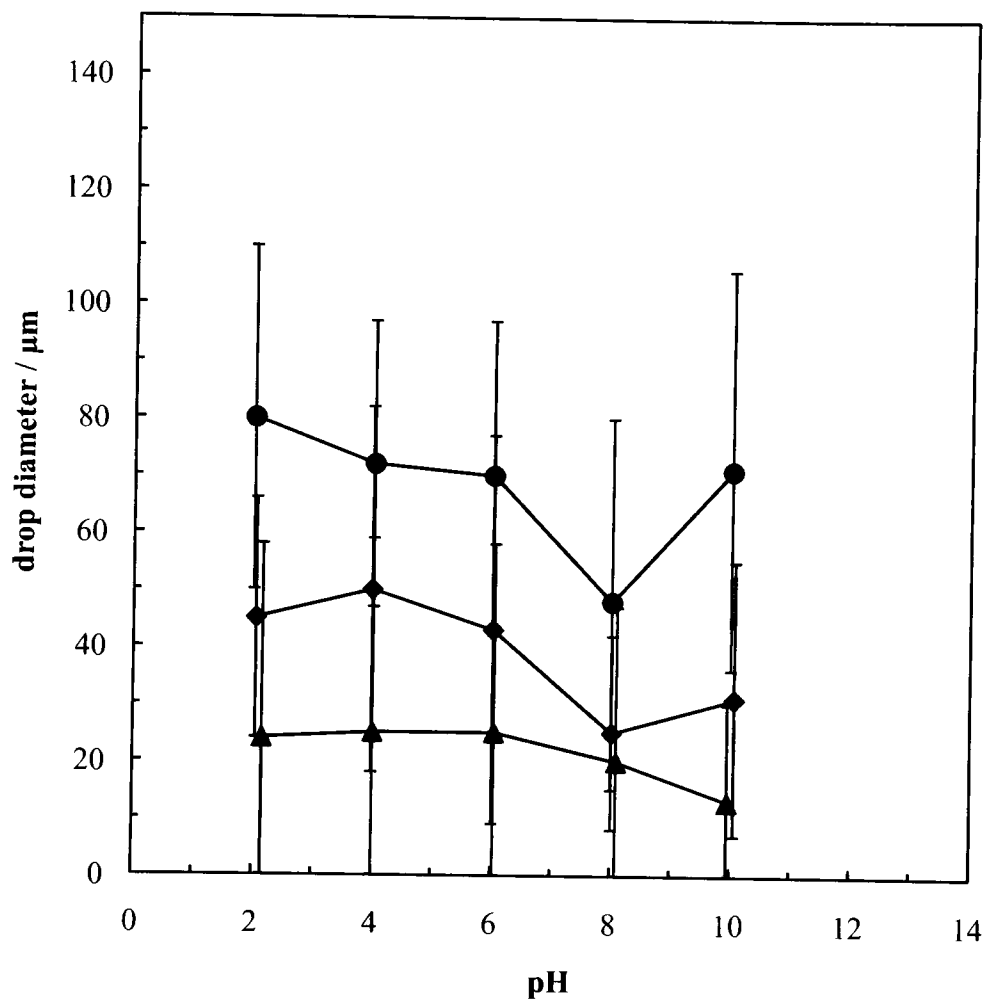


Figure 4.14. Average drop diameter measured by optical microscopy of dodecane-in-water emulsions made with 0.5 wt.% (◆) PLGA, (●) PLGA-COOH and (▲) PLGA-NH₂ as a function of the pH of the particle dispersion. The error bars represent the size distribution of the drops.



4.5.2 Variable lactic/glycolic acid ratio

PLGA particles with different L:G ratio are not expected to behave significantly differently with a change of pH, as the pK_a of lactic and glycolic acids are similar (respectively 3.86 and 3.83).²¹ The dodecane-in-water emulsions formed at all pH values displayed in Figure 4.15 exhibit equivalent stabilities: little coalescence is monitored ($f_{oil} \sim 0.15$), but large volumes of water containing excess particles are resolved ($f_{aq} \sim 0.55$). All the dodecane drops are spherical and present a high polydispersity, which can be observed from both Figures 4.15 and 4.16. The drop average diameter is dependent on the pH: for PLGA 75:25 particles, it decreases with pH due to the small drop population increasing compared to the big drop population, whereas it reaches a maximum at pH 8 for PLGA 65:35 particles. It can therefore be concluded that pH change affects emulsions stabilised with PLGA particles of higher L:G ratio more.

Figure 4.15. Photograph and optical microscopy of 1-day old dodecane-in-water emulsions stabilised with 0.5 wt.% of (a-e) PLGA 65:35 and (f-j) PLGA 75:25 particles in aqueous dispersion at pH (a, f) 2, (b, g) 4, (c, h) 6, (d, i) 8 and (e, j) 10. Emulsions were made with a 1 min. Ultra-Turrax homogenisation at 11 000 rpm. Scale bars represent 400 μm .

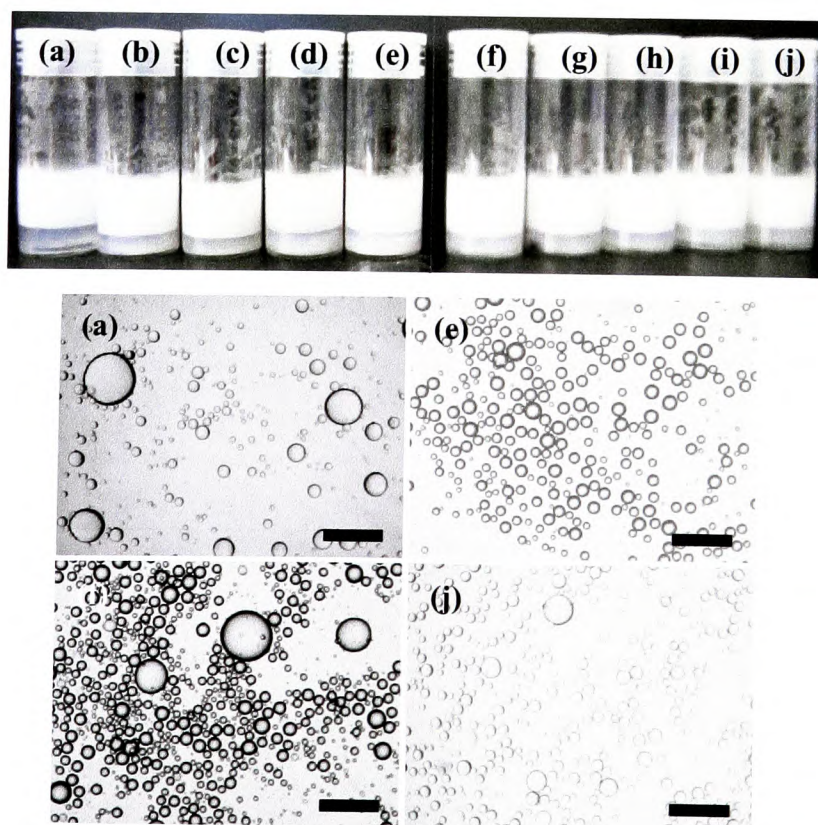
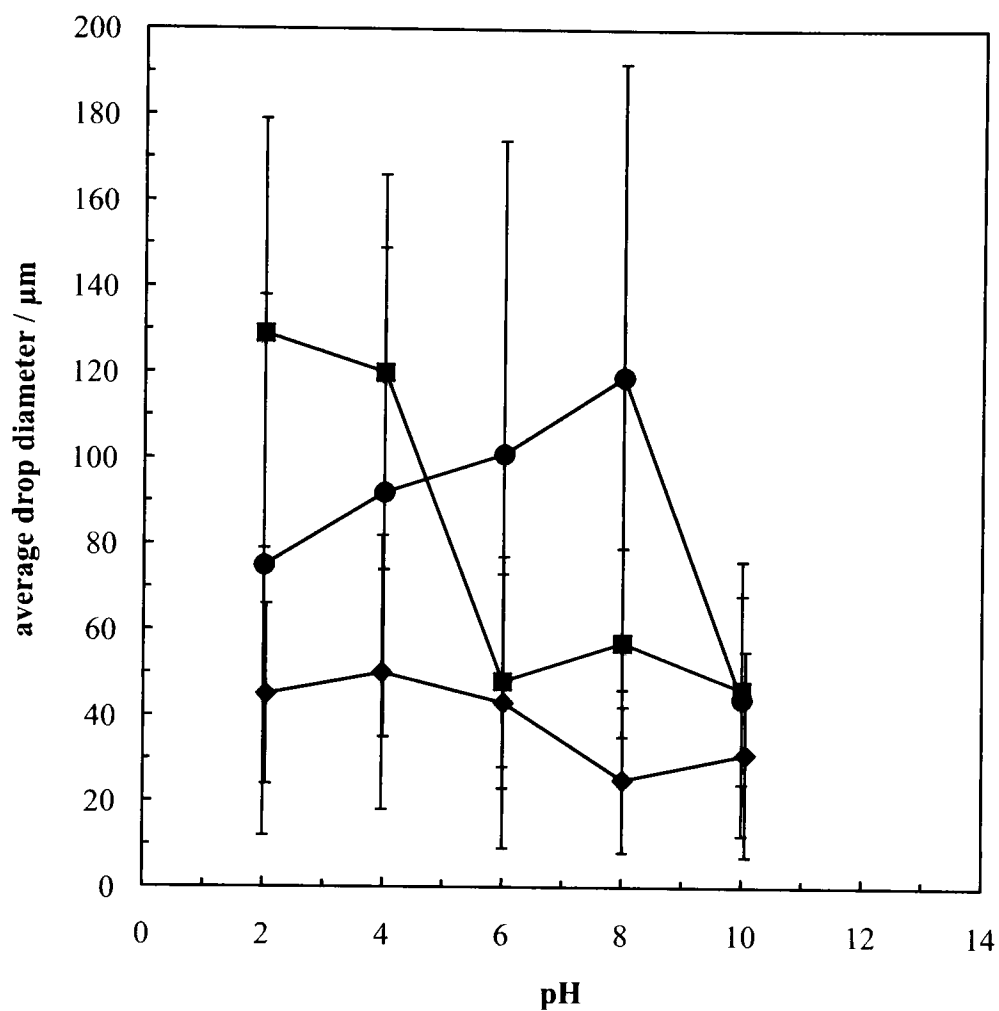


Figure 4.16. Average drop diameter measured by optical microscopy of dodecane-in-water emulsions made with 0.5 wt.% (◆) PLGA 50:50, (●) PLGA 65:35 and (■) PLGA 75:25 particles as a function of the pH of the particle dispersion. The error bars represent the size distribution of the drops.



4.6 Effect of time on emulsion degradation

The stability of emulsions stabilised with PLGA, PLGA-COOH or PLGA-NH₂ particles was monitored for 24 months for both the concentration (at pH ~ 8) and pH series. As the particles are biodegradable, it was expected that the emulsions should separate when stored at room temperature for significant lengths of time (*cf.* Table 1).

The concentration series made with PLGA exhibits evidence of degradation, whereas those made with PLGA-COOH and PLGA-NH₂ (not shown) do not show any change in appearance. Figure 4.17 enables comparison of the stable PLGA-COOH emulsions to the degrading PLGA-stabilised ones: initially the emulsions exhibited increasing stability with particle concentration, however after 6 months, the PLGA particles are unable to stabilise any emulsions even at the highest particle concentration, forming a bulk of amalgamated polymer particles attached to the oil-water interface (Figure 4.18). In addition, the resolved water phase exhibits a separation into clear water and sedimented particles at the bottom of the sample: for example compare Figures 4.17(c) and (d), where the clear water appears slightly blue, and the sedimented particle layer is white.

The change in stability to coalescence over time is represented in Figure 4.19 for the PLGA-stabilised emulsions. The increase in emulsion stability as a function of particle concentration is less evident after 2 months, and the emulsions are almost totally separated after 24 months. However the modified PLGA particles are still efficiently stabilising the emulsions, up to at least 24 months after initial formation. An example is shown in Figure 4.20 for emulsions stabilised by PLGA-NH₂. For almost all particle concentrations, destabilisation of the emulsions is limited to 24h after emulsification, indicating that it is caused by limited coalescence rather than degradation. At the highest particle concentration, 2 wt.%, this destabilisation occurs more gradually, agreeing with the idea that more particles slow down the coalescence process.

Figure 4.17. Photograph of (a, c) 1-day and (b, d) 6-months old dodecane-in-water emulsions stabilised with increasing concentration of (a, b) PLGA and (c, d) PLGA-COOH particles. Emulsion series are the same as in Figure 4.6(a-d).

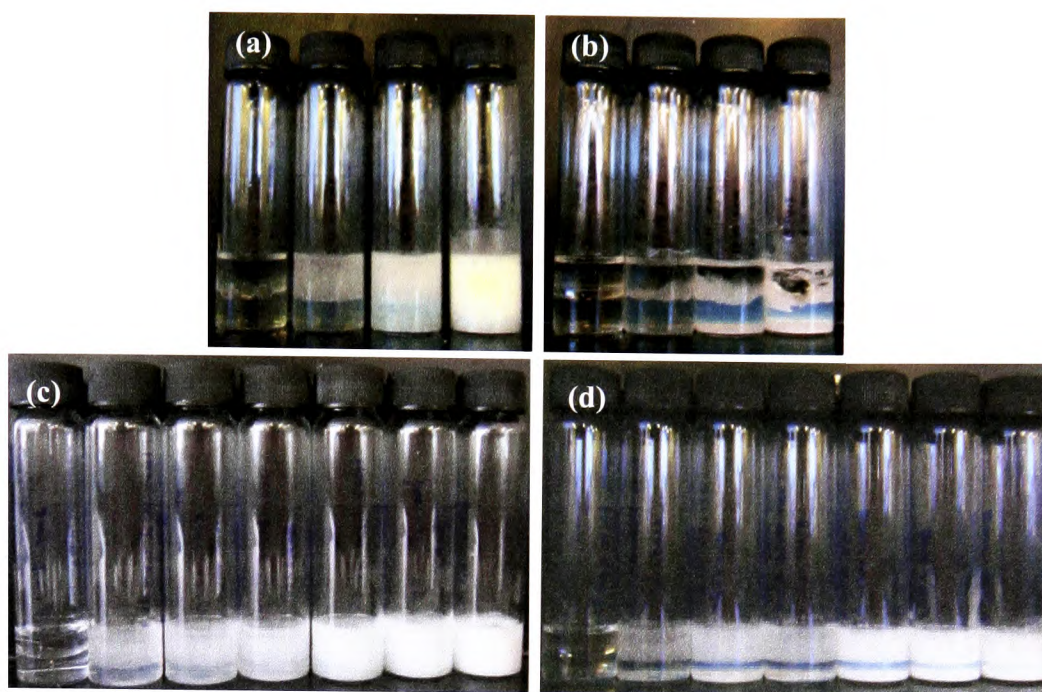


Figure 4.18. Optical microscopy images of a (a) 1-day and (b) 6-months old dodecane-in-water emulsions stabilised with 0.1 wt.% of PLGA particles. Scale bars represent 400 μm .

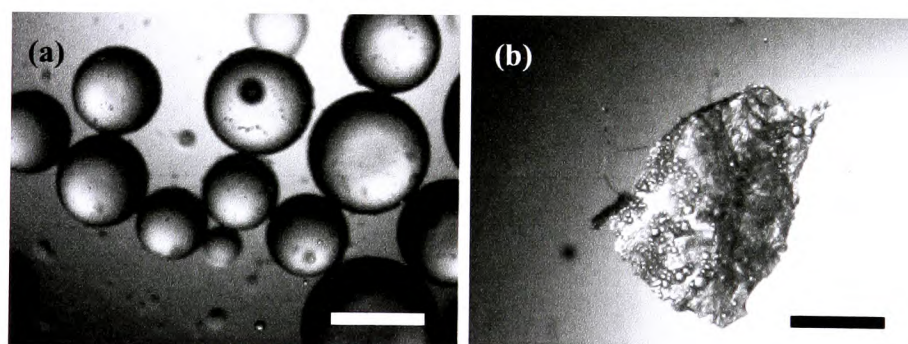


Figure 4.19. Stability to coalescence of dodecane-in-water emulsions stabilised by PLGA particles (—) 10 min., (- - -) 1 day, (- - -) 2 and (—) 24 months after emulsification. The stability is plotted in terms of f_{oil} as a function of PLGA particle concentration in wt.%. Emulsions were stored at room temperature ($20 \pm 5^\circ\text{C}$).

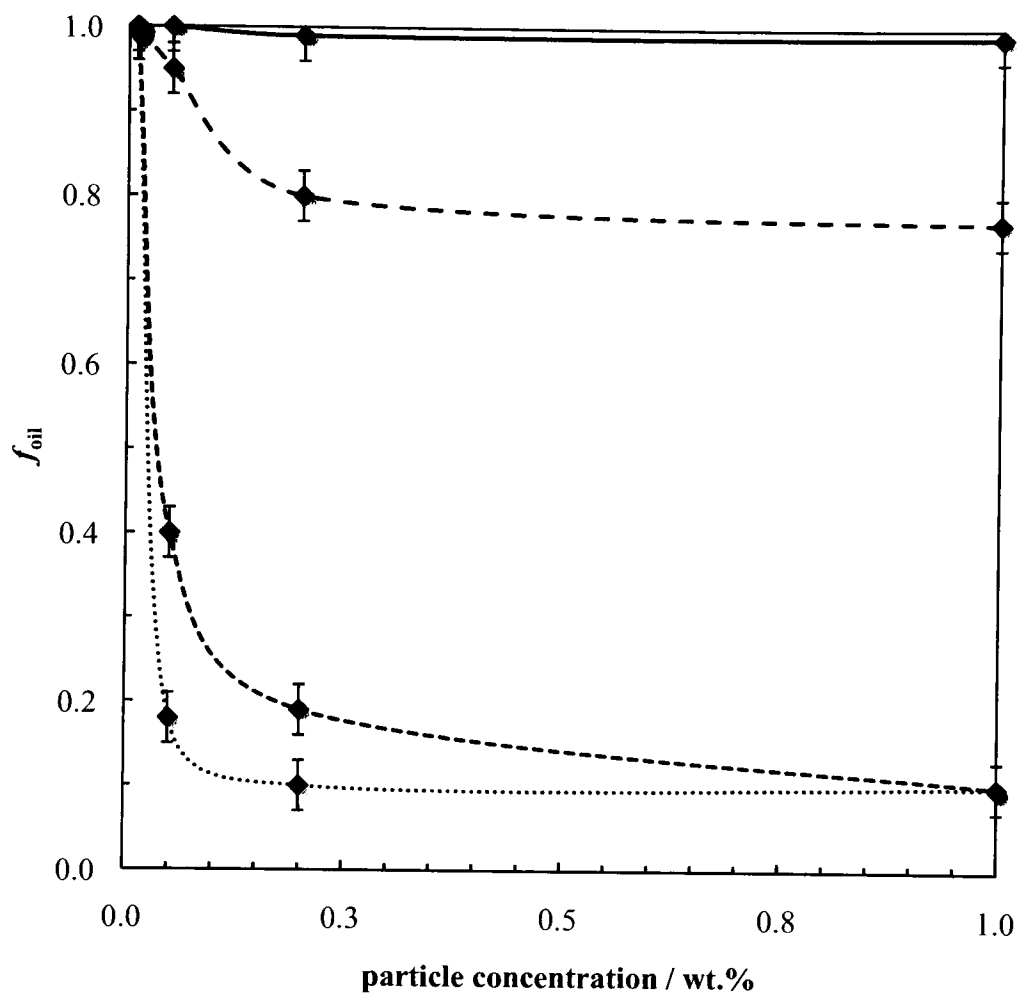


Figure 4.20. Stability to coalescence of dodecane-in-water emulsions stabilised by PLGA-NH₂ particles (") 10 min., (- - -) 1 day, (- - -) 2 and (—) 24 months after emulsification. The stability is plotted in terms of f_{oil} as a function of PLGA-NH₂ particle concentration in wt.%. Emulsions were stored at room temperature (20 ± 5°C).

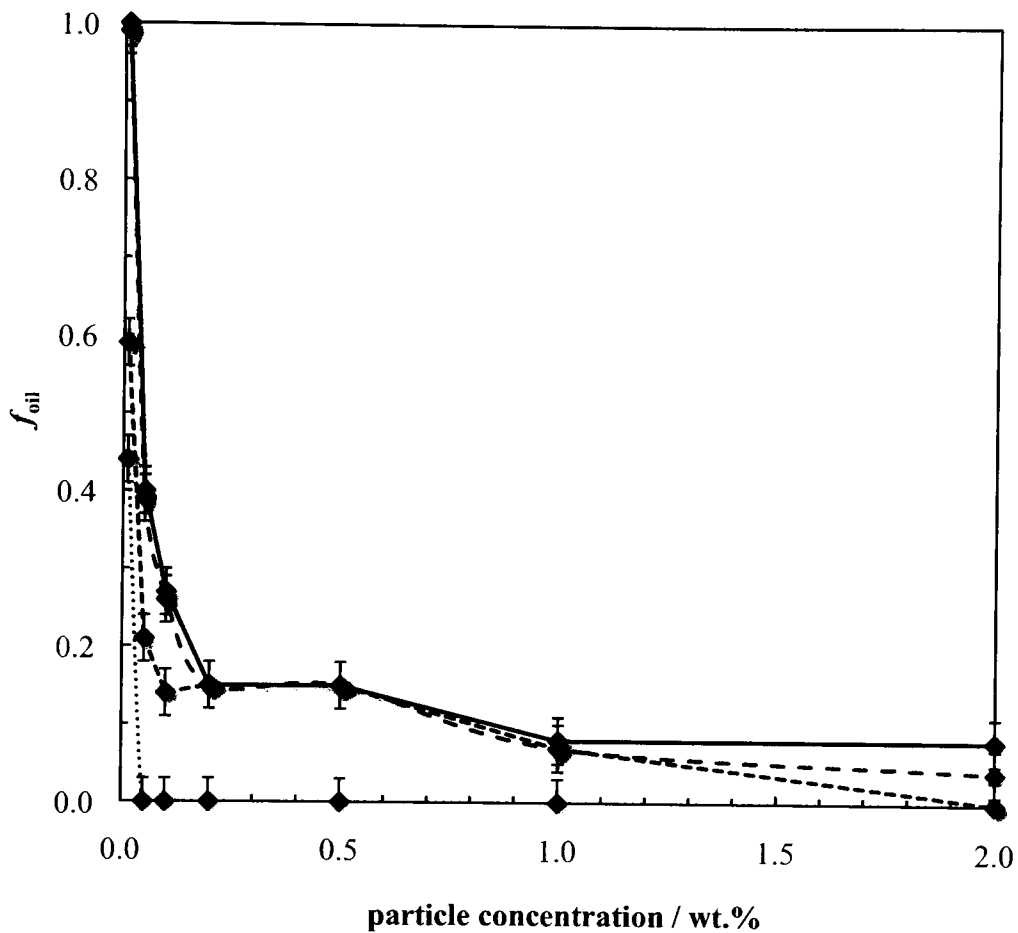


Figure 4.21 displays the appearance of the pH series of emulsions stabilised with either PLGA or PLGA-COOH particles. Whereas no obvious change in stability can be noted for emulsions stabilised with PLGA-COOH and PLGA-NH₂ (not shown), the PLGA series exhibits destabilisation after 6 months. The unmodified particles exhibit extensive emulsion degradation at low pH, in terms of the volume of oil and water resolved, which can be justified by the acid catalysis of the polymer decomposition.¹⁴ Similarly to the concentration series, a separated water phase can be observed in Figures 4.21(b) and (d), with a sedimented particle layer at the bottom of the sample. After 24 months, the PLGA systems are totally separated. The modified PLGA particles however seem to be resistant towards degradation, signifying that the particle surface modification has altered their degradability. Figure 4.22 displays the change in stability of the PLGA-NH₂-stabilised emulsions, where the coalescence is not observed to vary much after 2 months.

Figure 4.21. Photograph of (a, c) 1-day and (b, d) 6-month old dodecane-in-water emulsions stabilised with 0.5 wt.% of (a, b) PLGA and (c, d) PLGA-COOH particles in aqueous dispersion at different pH. Emulsion series are the same as in Figure 4.12(a-d).

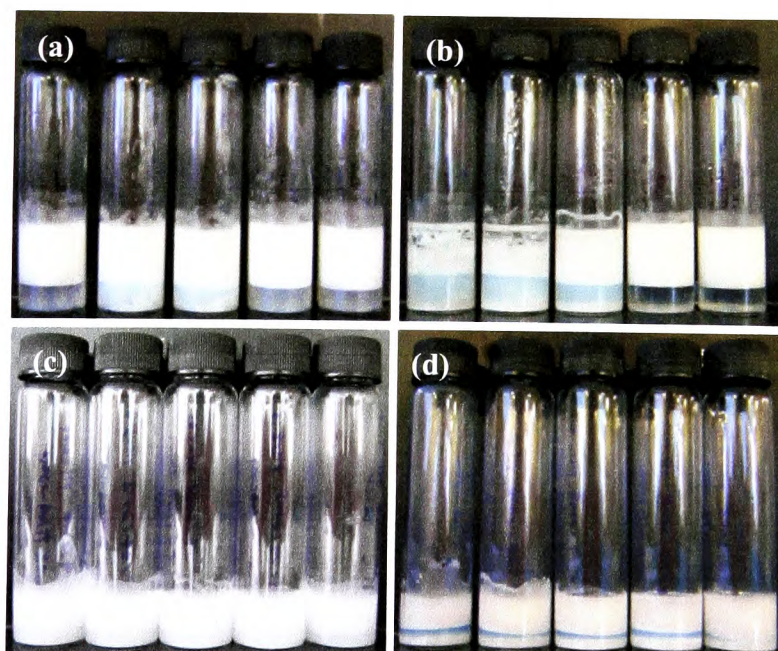
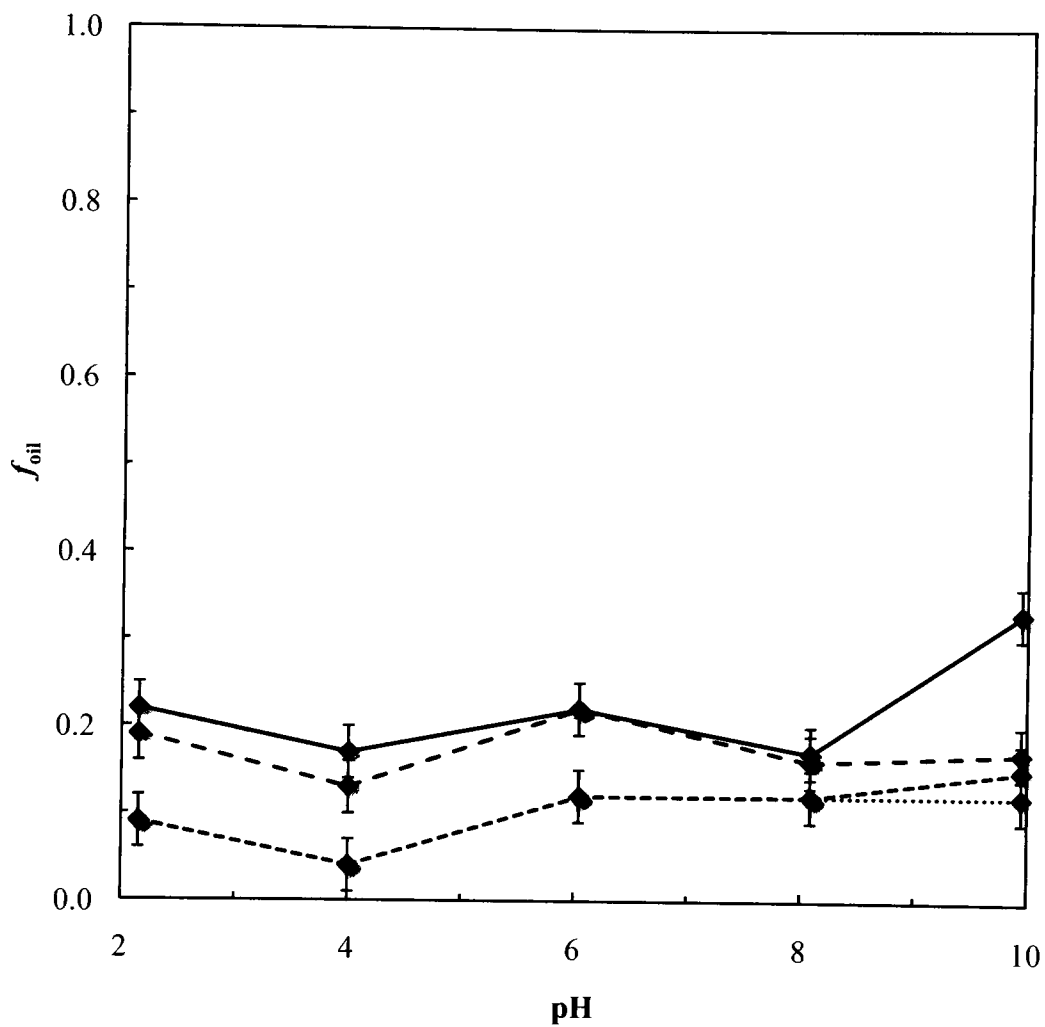


Figure 4.22. Stability to coalescence of dodecane-in-water emulsions stabilised by 0.5 wt.% of PLGA-NH₂ particles (---) 1 day, (- - -) 2 and (—) 24 months after emulsification. The stability is plotted in terms of f_{oil} as a function of particle dispersion pH. Emulsions were stored at room temperature ($20 \pm 5^\circ\text{C}$).



4.7 Conclusions

The ability of PLGA-based biodegradable particles to stabilise emulsions has been investigated in this chapter by using 5 different types of particles.

Unmodified PLGA, PLGA-COOH and PLGA-NH₂ particles, presenting different surface groups, were found to exhibit the same charge behaviour as a function of pH. This could be the result of insufficient surface modification, which is screened by the unmodified particle surface. The similar stability of the dodecane-in-water emulsions by the three particle types at neutral pH was expected. From the measured contact angle of water on PLGA substrates under dodecane, phase inversion from oil-in-water to water-in-oil emulsions with increasing L:G ratios could be expected. However these particles were observed to stabilise only dodecane-in-water emulsions at all concentrations and pH conditions.

Like other particle-stabilised systems (*cf.* § 3.4), the emulsion stability is affected by the particle concentration: increasing the particle quantity leads to reduced water and oil resolved, *i.e.* better stability, and smaller emulsion drops. The modified particles stabilise smaller drops and the higher L:G ratio PLGA particles also give more stable emulsions. In all cases it has been noted that the resolved water phase appears more turbid upon increasing total particle concentration, and this is believed to be due either to an increased free particle concentration or to a different aggregation state of the particles.

Changing the pH of the particle dispersions before emulsification slightly affects emulsions stabilised by the modified PLGA particles or those with high L:G ratio: the PLGA-stabilised emulsions seem unchanged over the pH range. PLGA-COOH and PLGA-NH₂-stabilised emulsions are more stable at high and low pH respectively, whereas the average drop diameter of PLGA 65:35 and PLGA 75:25-stabilised emulsions varies with pH.

When stored for 6 months, emulsions stabilised by unmodified PLGA particles exhibit significant destabilisation, which is more pronounced at low pH due to the acid-catalysed degradation of the particles. This emulsion destabilisation is similar to that of the wax-stabilised emulsions in Chapter 3: the degradation/melting of the particles causes them to become inefficient drop stabilisers, as they cannot hinder drop coalescence anymore. This is in stark contrast to those stabilised by either PLGA-COOH or PLGA-NH₂, which show little destabilisation up to at least 24 months after emulsification. It can be concluded therefore that the surface modification hinders, if not prevents, their degradability.

4.8 References

1. K. Leja and G. Lewandowicz, *Pol. J. Environ. Stud.*, **19**, 255 (2010).
2. J. W. Rhim, *Food Science and Biotechnology*, **16**, 691 (2007).
3. S. P. Lyu and D. Untereker, *Int. J. Molecular Sciences*, **10**, 4033 (2009).
4. A. Raval, J. Parikh and C. Engineer, *Brazilian J. Chem. Eng.*, **27**, 211 (2010).
5. J. Heller, *Adv. Drug Deliv. Rev.*, **10**, 163 (1993).
6. R. A. Kenley, M. O. Lee, T. R. Mahoney and L. M. Sanders, *Macromol.*, **20**, 2398 (1987).
7. S. S. Davis, L. Illum and S. Stolnik, *Curr. Opin. Colloid Interface Sci.*, **1**, 660 (1996).
8. A. Delgado, C. Evora and M. Llabres, *Int. J. Pharm.*, **140**, 219 (1996).
9. J. Siepman and F. Siepman, Microparticles used as drug delivery systems. In *Smart Colloidal Materials*; Springer-Verlag, Berlin, 2006.
10. L. K. Fung and W. M. Saltzman, *Adv. Drug Deliv. Rev.*, **26**, 209 (1997).
11. K. Koushik, D. S. Dhanda, N. P. S. Cheruvu and U. B. Kompella, *Pharm. Res.*, **21**, 1119 (2004).
12. M. Dunne, O. I. Corrigan and Z. Ramtoola, *Biomaterials*, **21**, 1659 (2000).
13. S. J. De and D. H. Robinson, *AAPS PharmSciTech*, **5**, 7 (2004).
14. J. Y. Yoo, J. M. Kim, K. S. Seo, Y. K. Jeong, H. B. Lee and G. Khang, *Bio-Med. Mater. Eng.*, **15**, 279 (2005).
15. H. J. Shin, C. H. Lee, I. H. Cho, Y. J. Kim, Y. J. Lee, I. A. Kim, K. D. Park, N. Yui and J. W. Shin, *J. Biomater. Sci.-Polym. Ed.*, **17**, 103 (2006).
16. P. Van der Meeren, H. Saveyn, S. B. Kassa, W. Doyen and R. Leysen, *Phys. Chem. Chem. Phys.*, **6**, 1408 (2004).
17. C. E. Holy, M. S. Shoichet and J. E. Davies, *Cells and Materials*, **7**, 223 (1997).
18. M. T. Khorasani, H. Mirzadeh and S. Irani, *Radiat. Phys. Chem.*, **77**, 280 (2008).
19. N. T. Paragkumar, E. Dellacherie and J. L. Six, *Appl. Surf. Sci.*, **253**, 2758 (2006).
20. B. P. Binks and J. A. Rodrigues, *Angew. Chem. Int. Ed.*, **44**, 441 (2005).

21. M. R. Rosen, *Delivery system handbook for personal care and cosmetic products: technology, applications, and formulation*, William Andrew Publishing, Norwich, 2005.

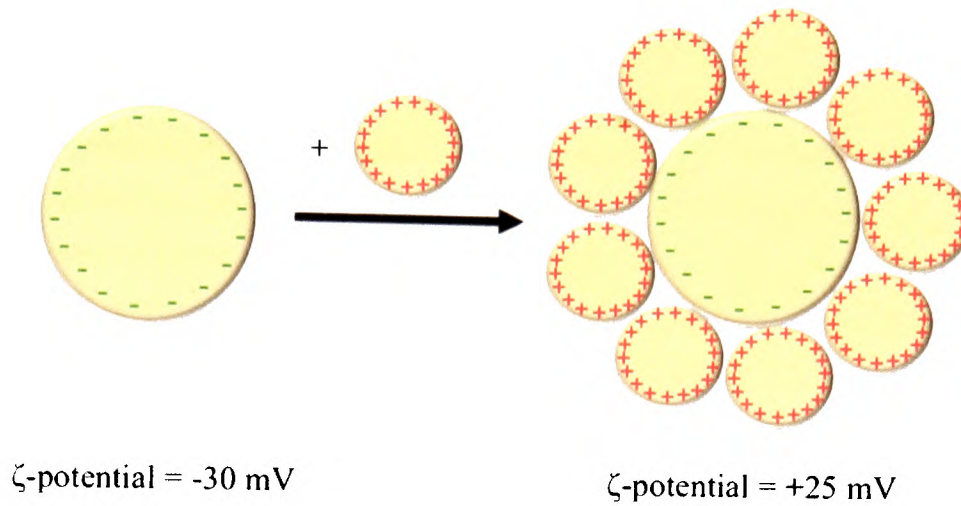
CHAPTER 5 HETEROAGGREGATION OF EMULSIONS STABILISED BY CHARGED COLLOIDAL SILICA PARTICLES

5.1 Introduction

Heteroaggregation corresponds to aggregation of unlike particles, which differ either by their size, charge, shape, charge density or composition. When oppositely charged particles meet, the electrical double layer attraction on the particles leads to bridging and charge neutralisation. Particle-stabilised emulsion drops can be considered like solid particles, as their surfaces are similar to the surfaces of the particles, which stabilise them. So it is expected that, like with particles, a size difference between drops will affect their aggregation and that hexagonal close packing will not occur due to charge repulsion.¹⁻³ Rasa *et al.*, who studied mixtures of positively and negatively charged Ludox particles in aqueous dispersions, observed heteroaggregation only for low content of positive particles, demonstrating that the ratio of the two type of particles affects their interaction.⁴ Binks *et al.* showed that flocculated dispersions of Ludox HS-30 and Ludox CL particles were reported to be efficient for stabilising emulsions and the optimum negative:positive particle ratio was found to be 2:1.⁵

Recently, Gu *et al.* described the formation of colloidosomes, microcapsules formed by colloidal particles, from large anionic droplets with small cationic droplets adsorbed on their surface.⁶ The charged droplets were obtained by stabilising oil-in-water emulsions with positively charged proteins, which could then be coated with pectin to reverse the surface charge of the drops. Mixed at a specific ratio, small droplets were observed to coat the surface of large, negatively charged, pectin modified droplets, causing a zeta potential inversion of the large drops (Figure 5.1). Emulsion mixture aggregation, observed at intermediate and high concentrations of small droplets, was attributed to either bridging or depletion flocculation of the drops.

Figure 5.1 Schematic representation of the charge reversal of a large, pectin-coated anionic drop upon addition of small, protein-stabilised cationic drops. Data taken from ref. 6.



The following study aims to create organised emulsion mixtures, with positive droplets aggregated around negative droplets or *vice-versa*. The work of Gu *et al.*, which managed the production of colloidosomes from emulsion droplets stabilised by charged proteins, opened the prospect to obtain similar aggregates with Ludox HS-30 and Ludox CL particles of opposite charge. The effect of pH, oil type, particle concentration and mixing protocol were considered to optimise heteroaggregation.

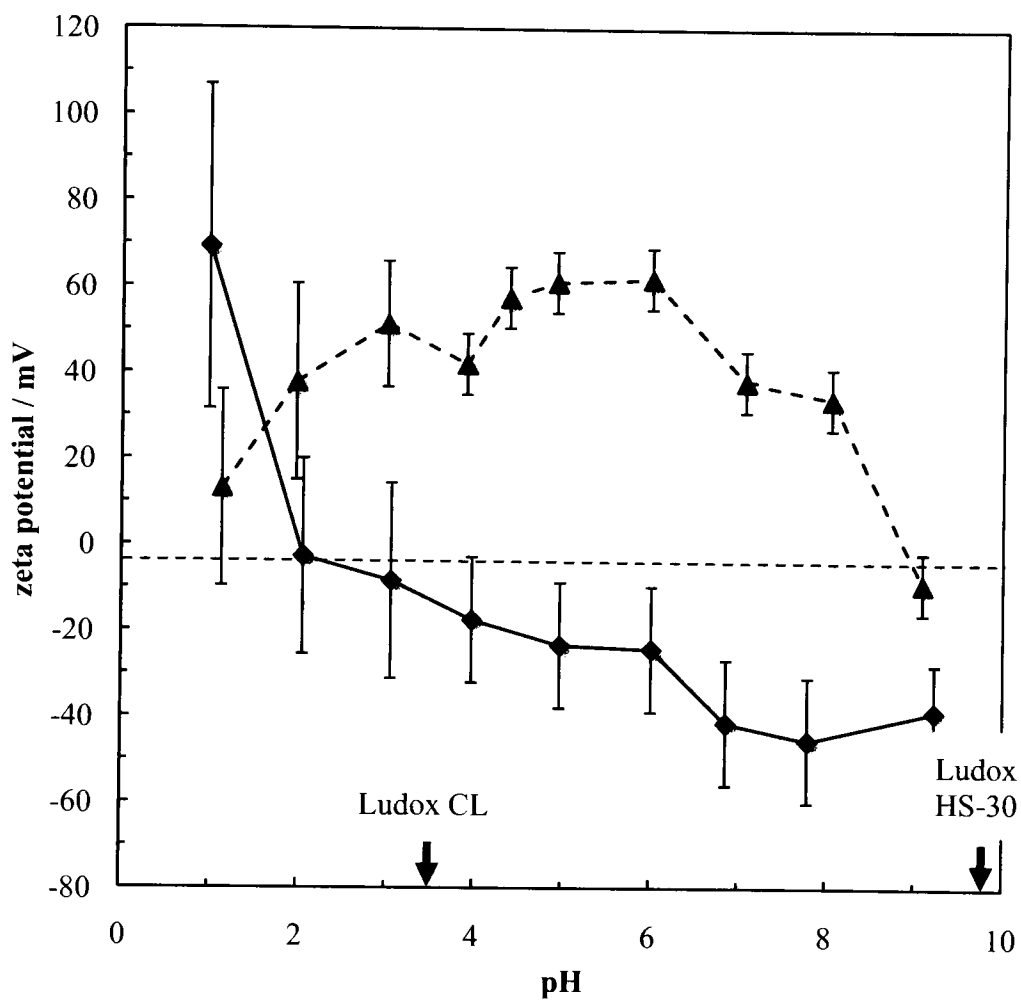
5.2 Zeta potential measurements of aqueous particle dispersions

Electrophoretic mobility measurements were carried out on Ludox HS-30 and Ludox CL aqueous particle dispersions. The two Ludox particles differ by their surfaces: the silanol groups on Ludox HS-30 makes it negatively charged at high pH, when the Si-OH group is deprotonated, whereas the alumina coating on Ludox CL provides a positive charge at low pH, Al dissociating into Al^{3+} .⁷ Figure 5.2 illustrates more accurately the influence of pH on the zeta potential of both particles.

Ludox HS-30 and CL particles are supplied at specific pH values, which render them respectively negative and positive: at pH 9.8, Ludox HS-30 particles display a high negative zeta potential of - 43 mV, while Ludox CL particles exhibit a positive zeta potential of + 43 mV at pH 3.5. The charge trends with pH for the two particles are different: the Ludox HS-30 charge decreases with increasing pH, while the Ludox CL exhibits a maximum around pH 5.5. Ludox HS-30 exhibits an isoelectric point around pH 2, being positively charged at pH 1, and increasingly negatively charged with increasing pH. The isoelectric point around pH 2 agrees with literature data for the isoelectric point of silica, and corresponds to the silanol group dissociation at high pH (Si-O^-) and protonation at low pH (Si-OH_2^+).^{8,9}

The aluminium coating on the silica surface shifts the isoelectric point of the Ludox CL particles towards high pH values. The surface chemistry of the particles follows that of the metal hydroxide precipitated on their surface, giving an isoelectric point at pH 8.5 close to that of aluminium hydroxide.¹⁰ Decreasing the pH of the Ludox CL particle dispersion leads to an increase of the particle charge, until around pH 5.5, when the charge reaches its maximum value. Below pH 5, the zeta potential decreases gradually, indicating proton desorption from the aluminium ions. As observed in Figure 5.2, a second charge reversal occurs around pH 1, which has been previously observed by van der Meeren *et al.* at pH 2.5.⁷

Figure 5.2. Variation of zeta potential of 1 wt.% (◆) Ludox HS-30 and (▲) Ludox CL particles dispersed in water under varying pH values from 1 to 9. The error bars represent the width of the zeta-potential distribution and the arrows the natural pH of dispersion of the particles.



5.3 Emulsions with dodecane

5.3.1. *Effect of pH in Ludox HS-30 systems*

The pH of the particle dispersion affects the charge on the Ludox HS-30 particles: they are positively charged below pH 2 and negatively charged above (*cf.* § 5.2). The particle wettability is expected to change accordingly, with highly charged particles adsorbing less to oil-water interfaces.¹¹⁻¹³ The aggregation state of the particles should also vary with their charge, as less charged particles exhibit less repulsion, often resulting in aggregation.

Figure 5.3 shows that all 1 wt.% Ludox HS-30 particle dispersions in water have the same appearance on standing for 24 hours throughout the pH range studied: the suspensions are clear and transparent, without any noticeable viscosity change. However, the dodecane-in-water emulsion series with equal oil and water volumes shows an optimum in stability at pH 3: the emulsion are almost totally separated at most pH values, but their stability increases sharply between pH 3 and 4. Interestingly, the emulsion drop size is observed to increase with pH when measured shortly after emulsification: the big and small drops, at respectively low and high pH, are unstable and coalesce quickly with the bulk oil phase (Figure 5.4).

This behaviour is slightly different to that expected from the zeta potential results: Ludox HS-30 particles, close to zero charge around pH 2, should be less hydrophilic and adsorb more easily at the oil-water interface. The low charge on the Ludox HS-30 surface should also enhance particle aggregation. It had been noted in several studies that stable emulsions are often generated by weak flocculation of particles, whereas extensive aggregation can cause emulsion destabilisation.¹⁴⁻¹⁶ The low stability of emulsions at pH 2 could be due to extensive aggregation of the Ludox HS-30 particles, unable to adsorb at the oil-water interface. The increase of pH might decrease the state of aggregation and enable stabilisation of the liquid interface at intermediate pH. However, the high charge density on the particle surface at high pH renders them too hydrophilic to stabilise an emulsion.

Addition of NaCl to the particle dispersion at pH 4 was studied in order to increase the particle aggregation prior to emulsification, as aggregated particle dispersions are better emulsifiers.¹⁴ However, it was observed that the presence of NaCl invariably decreased the emulsion stability (Figure 5.5). This might be due to formation of drop flocs, commonly observed for addition of salt in emulsion systems, which could accelerate drop-drop coalescence.^{17, 18}

Figure 5.3. Photographs of 1-day old 1 wt.% Ludox HS-30 particle dispersions (a-g) and dodecane-in-water emulsions (h-n) stabilised by them at pH (a, h) 1, (b, i) 2, (c, j) 3, (d, k) 4, (e, l) 5, (f, m) 6, and (g, n) 7. Emulsions were made with 1-day old particle dispersions by Ultra turrax homogenisation during 1 minute at 11 000 rpm, $\Phi_w = 0.5$.

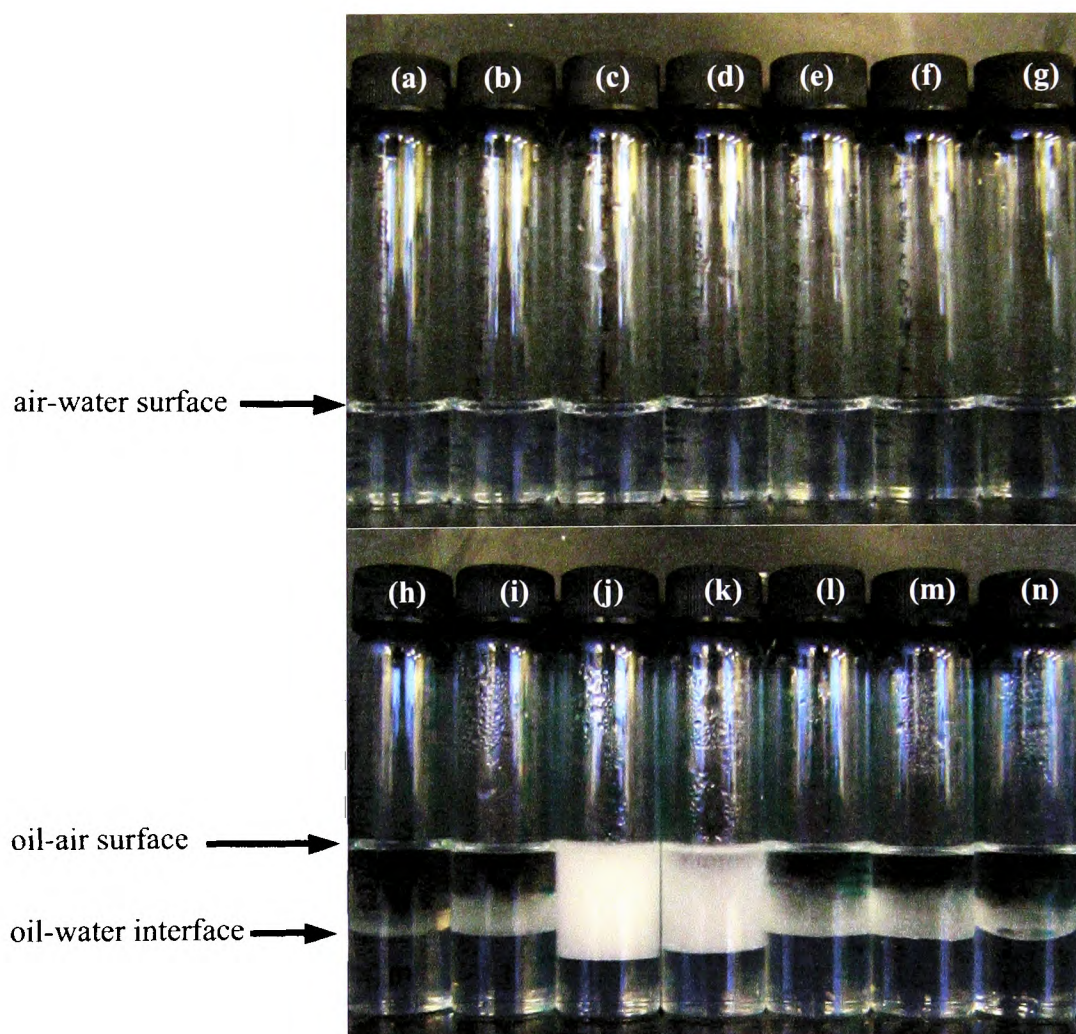


Figure 5.4. (◆) Average, (◊) minimum and (◇) maximum drop diameter measured by optical microscopy of fresh dodecane-in-water emulsions made with 1 wt.% Ludox HS-30 particles as a function of pH. The error bars represent the standard deviation in the mean drop size.

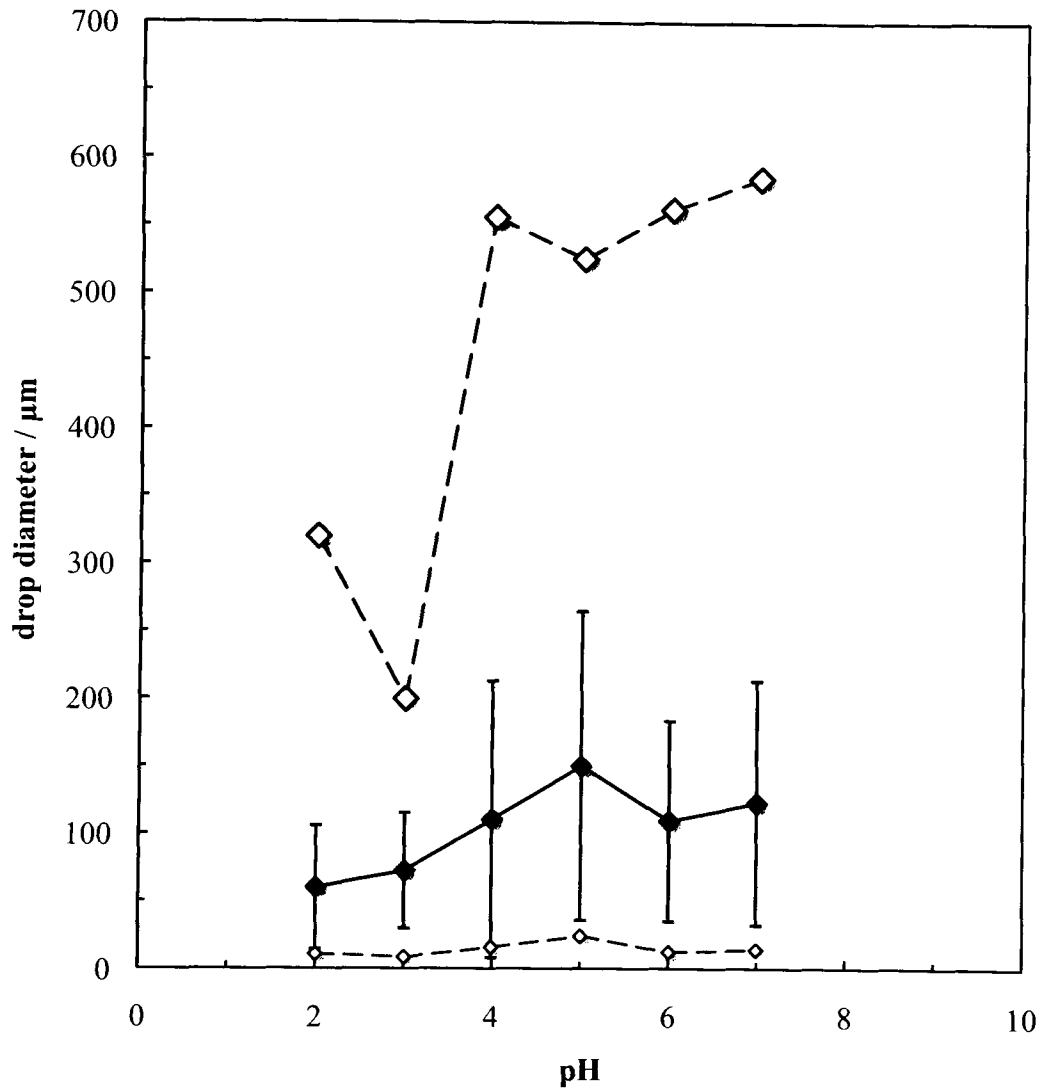
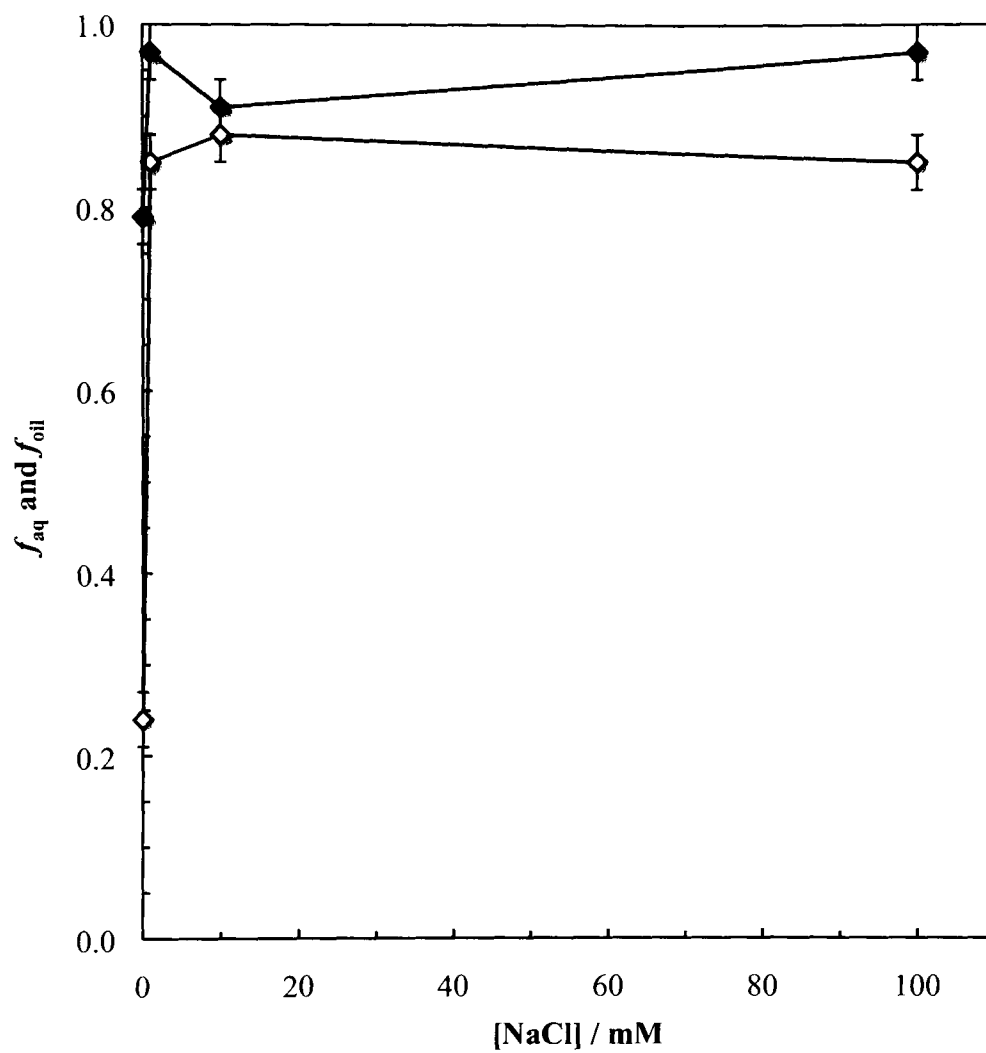


Figure 5.5. Stability of dodecane-in-water emulsion made with (◆) 1 wt.% Ludox HS-30 particles at pH 4 as a function of NaCl concentration in the aqueous phase in terms of (\diamond) f_{oil} and (\blacklozenge) f_{aq} 1 day after emulsification.



5.3.2. *Effect of pH in Ludox CL systems*

Unlike Ludox HS-30 suspensions, the appearance of Ludox CL particle dispersions is affected by the pH modification: the slightly positively charged particles form a clear transparent dispersion at low pH, which turns white and cloudy with increasing pH. Figure 5.6 displays the appearance of the particle dispersions after standing for 24 hours, which increase in viscosity and become gel-like. The aggregation state depends on the particle charge (Figure 5.2): the attraction forces dominate when particles exhibit low surface charge, causing an increase of particle aggregation and sedimentation at high pH.

The dodecane-in-water emulsions formed exhibit a stability dependent on pH: no stable emulsions are formed below pH 6, and emulsions with increasing stability towards coalescence are formed above this value. Figure 5.7 shows that maximum stability to both creaming and coalescence is reached at pH 7, which is close to the isoelectric point (~8.5). The optimum stability at pH 7 might also be due to the gel-like network formed by the particles in the continuous phase, protecting the oil drops from coalescing. As with the Ludox HS-30 emulsion series, emulsions stabilised by Ludox CL particles at the isoelectric point are less stable than those prepared close to the isoelectric point of the emulsifier. The change in drop diameter was also measured shortly after emulsification. Figure 5.8 displays the two successive increases and decreases in drop diameter. But it is worth noting that all drops formed below pH 6 coalesced quickly with the bulk oil. At pH above 8, emulsions were observed to display limited coalescence and the drops reached millimetre diameter. The particles might be too flocculated to undertake a significant area of oil-water stabilisation, as observed by Binks *et al.*¹⁴

Figure 5.6. Photographs of 1-day old 1 wt.% Ludox CL particle dispersions (a-i) and dodecane-in-water emulsions (j-r) stabilised with them at pH (a, j) 1, (b, k) 2, (c, l) 3, (d, m) 4, (e, n) 5, (f, o) 6, (g, p) 7, (h, q) 8 and (i, r) 9. Emulsions were made with 1-day old particle dispersions by Ultra turrax homogenisation during 1 minute at 11 000 rpm.

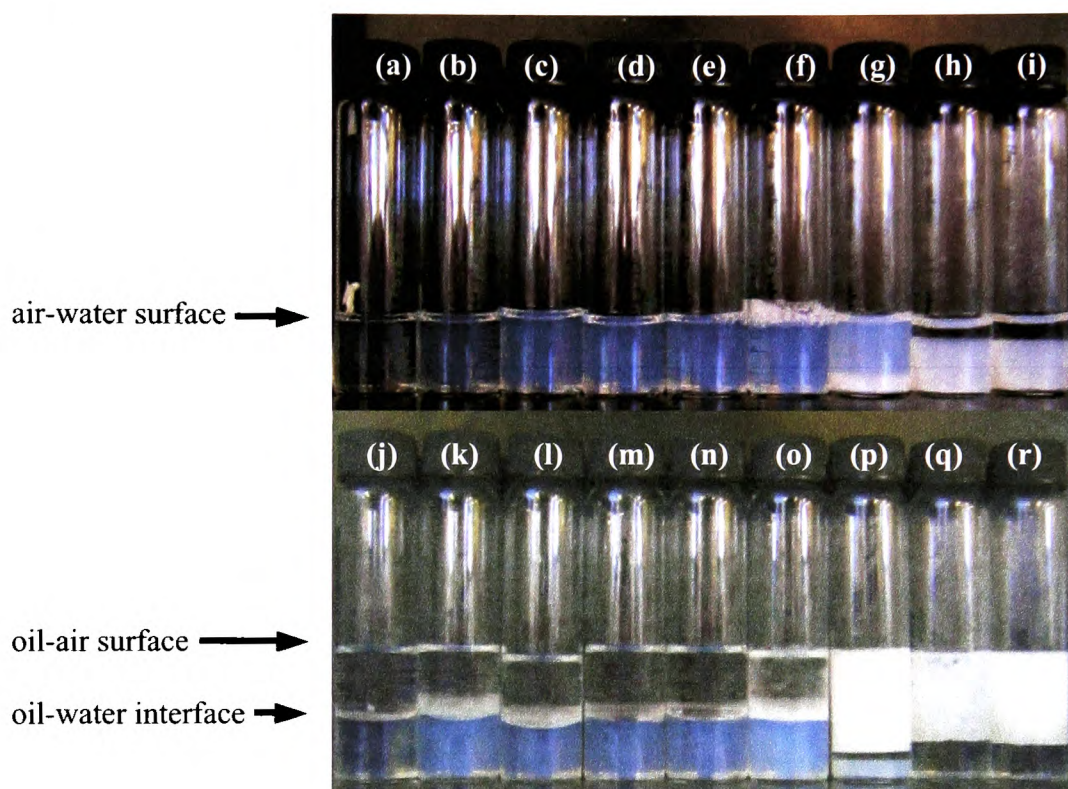


Figure 5.7. Stability of 1-day old dodecane-in-water emulsions made with (\blacktriangle) 1 wt.% Ludox CL particles as a function of pH in terms of f_{oil} (open points) and f_{aq} (filled points).

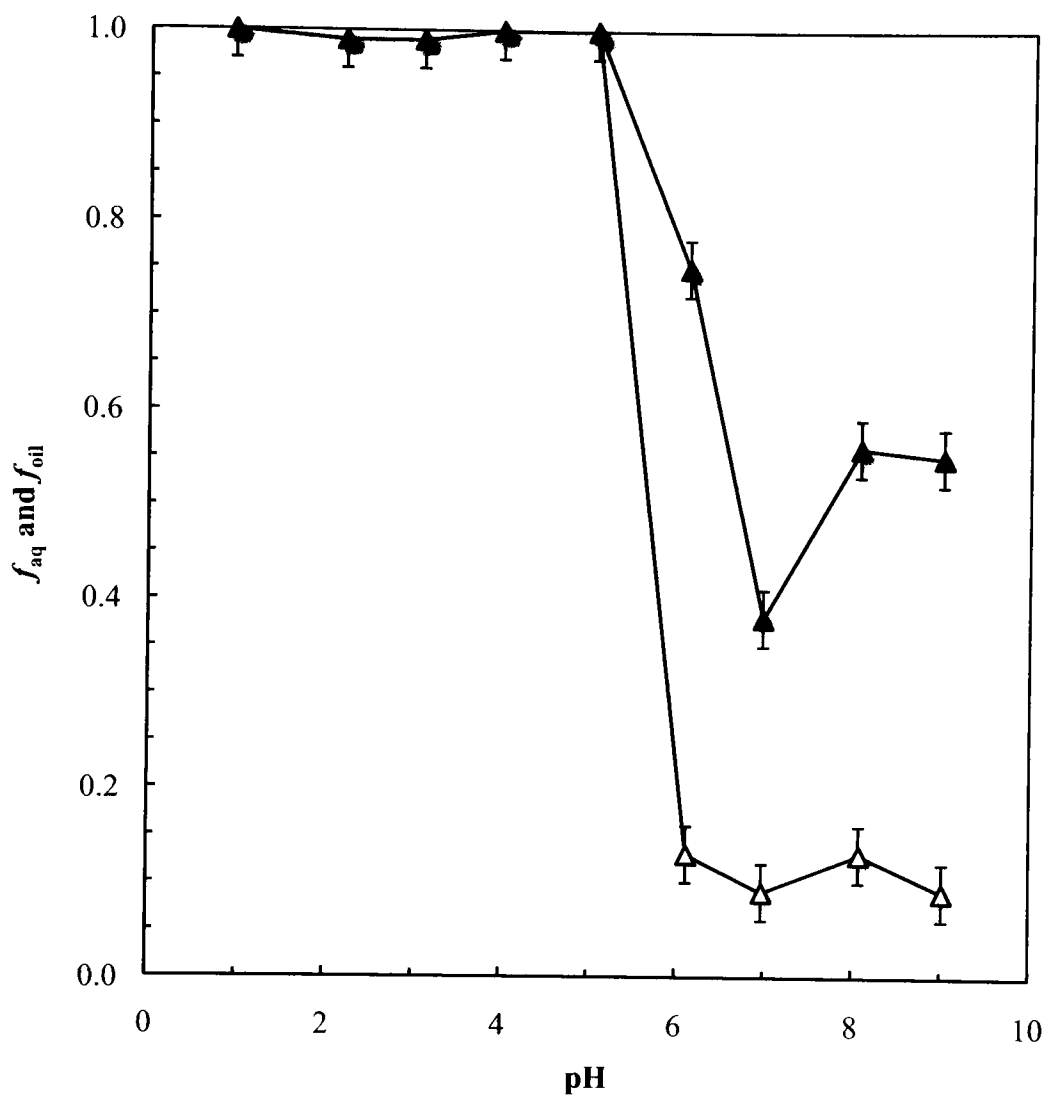
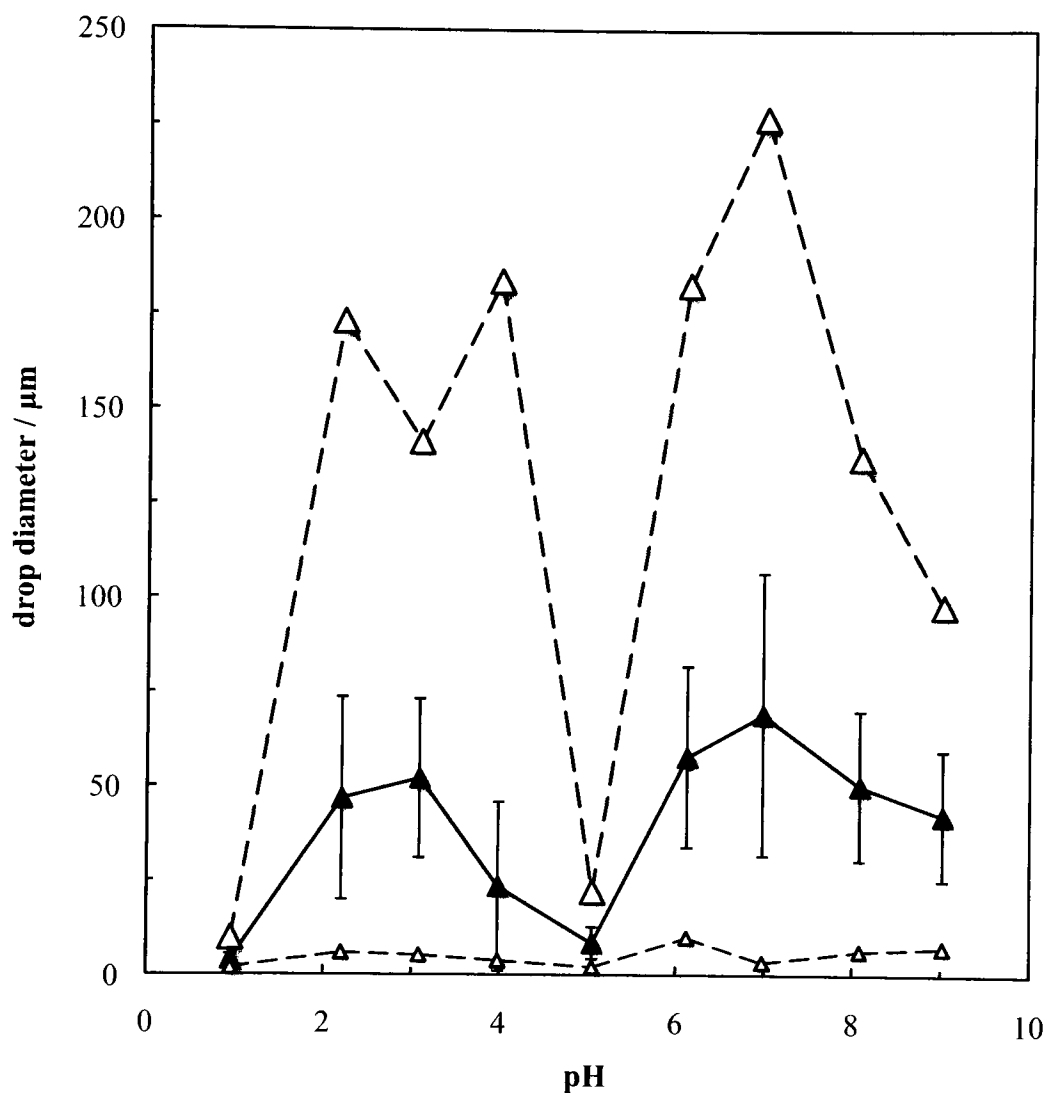


Figure 5.8. (▲) Average, (△) minimum and (△) maximum drop diameter measured by optical microscopy of fresh dodecane-in-water emulsions made with 1 wt.% Ludox CL as a function of pH. The error bars represent the standard deviation in the drop size distribution.



5.4 Emulsions with isopropyl myristate

In the previous emulsion series, the pH range at which emulsions were stable was limited due to the hydrophilicity of the charged colloidal particles. By replacing the non-polar dodecane oil with the slightly polar isopropyl myristate (IPM), it is thought that particle adsorption to the oil-water interface could be promoted through a reduction in the particle-oil tension.¹⁹

5.4.1. *Effect of pH in Ludox HS-30 systems*

The appearance of Ludox HS-30 dispersions prior to emulsification is unchanged and is as displayed in Figure 5.3. However, the IPM-in-water emulsion series in Figure 5.9 exhibits a different stability trend to that of dodecane. Emulsion stability decreases sequentially with increasing pH. It is also observed that the emulsions are now far more stable over a greater pH range. Figure 5.10 shows that both the resolved water and oil fractions increase upon increasing pH, with a maximum in stability at pH 1 and 2, and almost total separation at pH 8 and 9. Concurrently the increasing drop diameter with pH can be seen in Figure 5.11; the smallest IPM drops stabilise the largest oil volume, whereas large unstable drops coalesce quickly with the bulk oil phase. The optimum emulsion stability corresponds to the isoelectric point (pH ~2), and as the pH is increased the particles become more charged and so too hydrophilic to adsorb strongly at the oil-water interface. An IPM-in-water emulsion made at pH 7.5 (not shown) exhibits coalescence stability ($f_{oil} = 0.18$) and drop size (~50 μm) close to the one made at pH 7. This latter emulsion will be used in § 5.4.3 for the study of mixing oppositely charged emulsion drops.

Figure 5.9. Photographs of 1-day old isopropyl myristate-in-water emulsions stabilised with 1 wt.% Ludox HS-30 particles at pH (a) 1, (b) 2, (c) 3, (d) 4, (e) 5, (f) 6, (g) 7, (h) 8 and (i) 9. Emulsions were made with 1-day old particle dispersions by Ultra turrax homogenisation during 1 minute at 11 000 rpm.



Figure 5.10. Stability of 1-day old isopropyl myristate-in-water emulsions made with (◆) 1 wt.% Ludox HS-30 particles as a function of pH in terms of f_{oil} (open points) and f_{aq} (filled points).

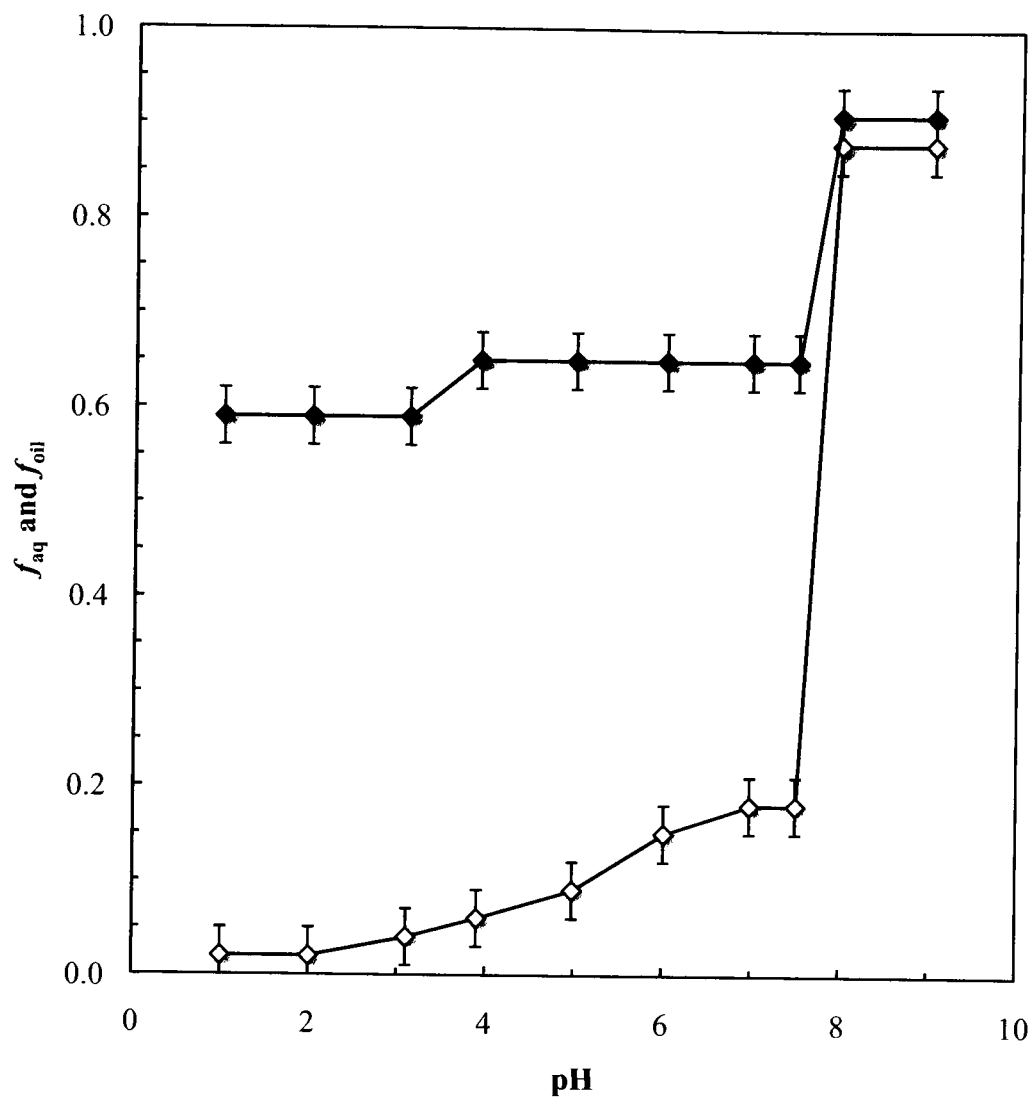
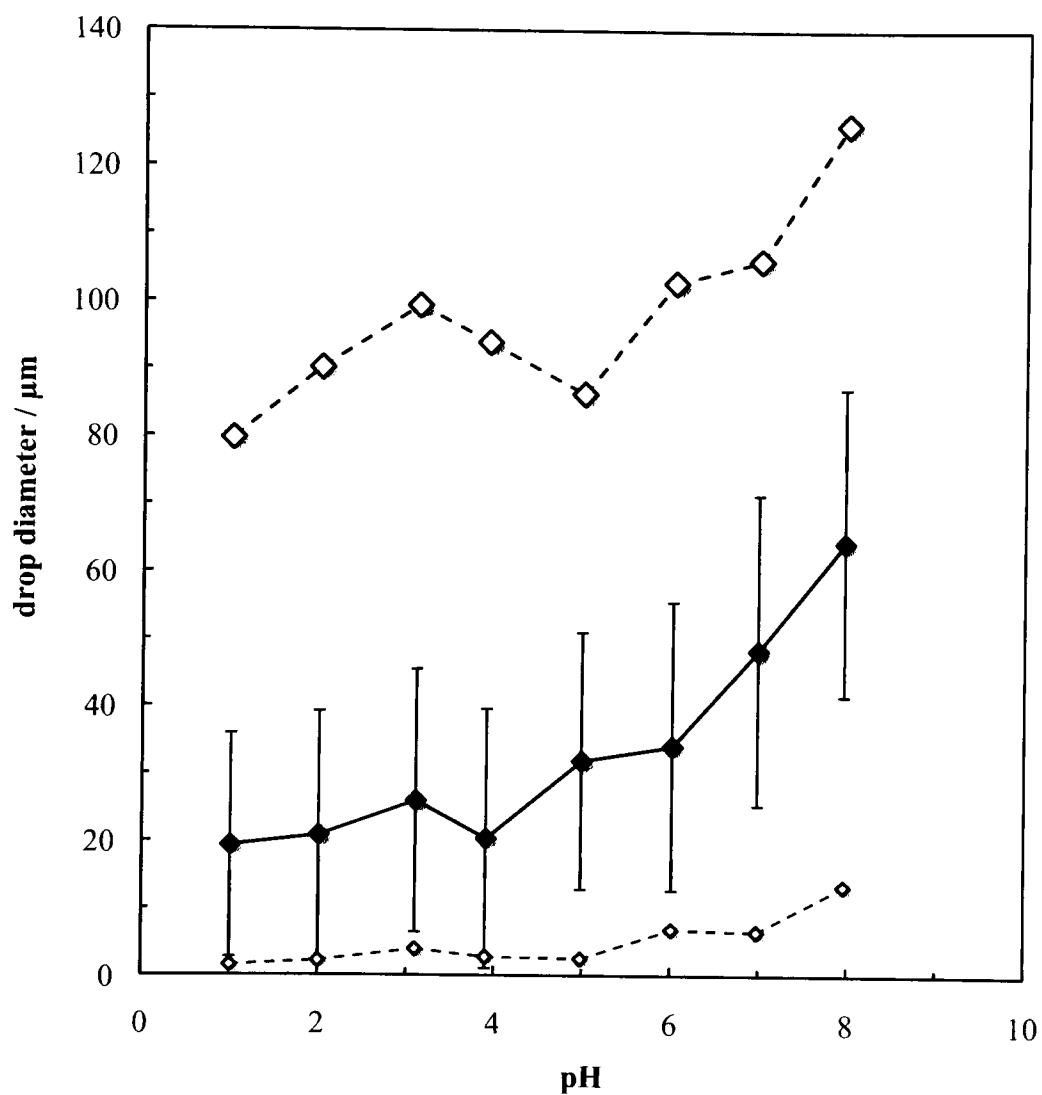


Figure 5.11. (◆) Average, (◇) minimum and (◇) maximum drop diameter measured by optical microscopy of fresh isopropyl myristate-in-water emulsions made with 1 wt.% Ludox HS-30 as a function of pH. The error bars represent the standard deviation in the drops size distribution.



5.4.2. Effect of pH in Ludox CL systems

IPM-in-water emulsions were made from the dispersions equivalent to those displayed in Figure 5.6. The emulsion series exhibited similar stabilities to the dodecane series, with the exception of high stability at pH 1 as evidenced in Figures 5.12 and 5.13. Below pH 6, emulsions are totally separated, but above it their stability increases with pH, reaching its maximum with minimum drop size at pH 8 (Figure 5.14). Like in the dodecane series, the best stability is linked to the isoelectric point. At this pH, particle dispersions exhibit intermediate stability (moderately flocculated) giving more stable emulsions than at higher pH, where the aggregation may be too extensive for particles to efficiently adsorb at the oil-water interface. However, the unexpected stability of the emulsion at low pH has to be explained otherwise. Parks stated that the Ludox CL zeta potential decrease below pH 6 is due to aluminium desorption from the silica surface.⁹ After losing their aluminium coating, Ludox CL particles behave like Ludox HS-30 particles and so stable emulsions can be formed at low pH.

Excluding the stable emulsions at low pH where the particles are likely to be modified, the most stable emulsion occurs at pH 8. However, an emulsion of intermediate stability was made at pH 7.5 ($f_{oil} = 0.15$) to be used in § 5.4.3 for the study of mixing oppositely charged emulsion drops.

Figure 5.12. Photographs of 1-day old isopropyl myristate-in-water emulsions stabilised with 1 wt.% Ludox CL particles at pH (a) 1, (b) 2, (c) 3, (d) 4, (e) 5, (f) 6, (g) 7, (h) 8 and (i) 9. Emulsions were made with 1-day old particle dispersions by Ultra turrax homogenisation during 1 minute at 11 000 rpm.

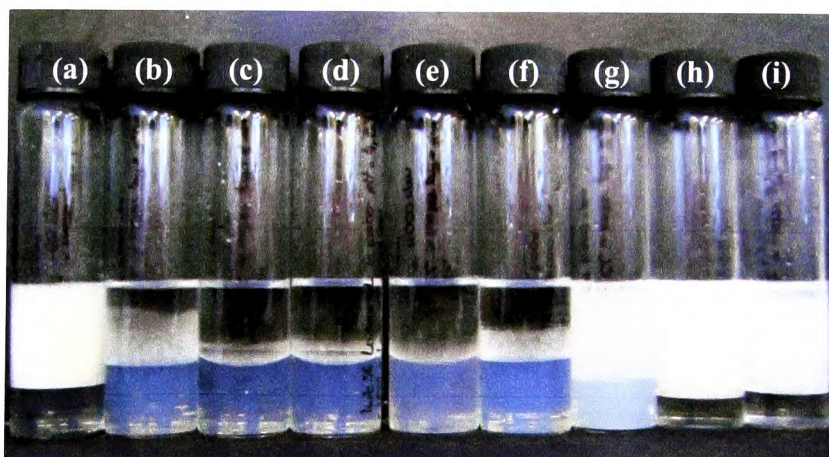


Figure 5.13. Stability of 1-day old isopropyl myristate-in-water emulsions made with (\blacktriangle) 1 wt.% Ludox CL particles as a function of pH in terms of f_{oil} (open points) and f_{aq} (filled points).

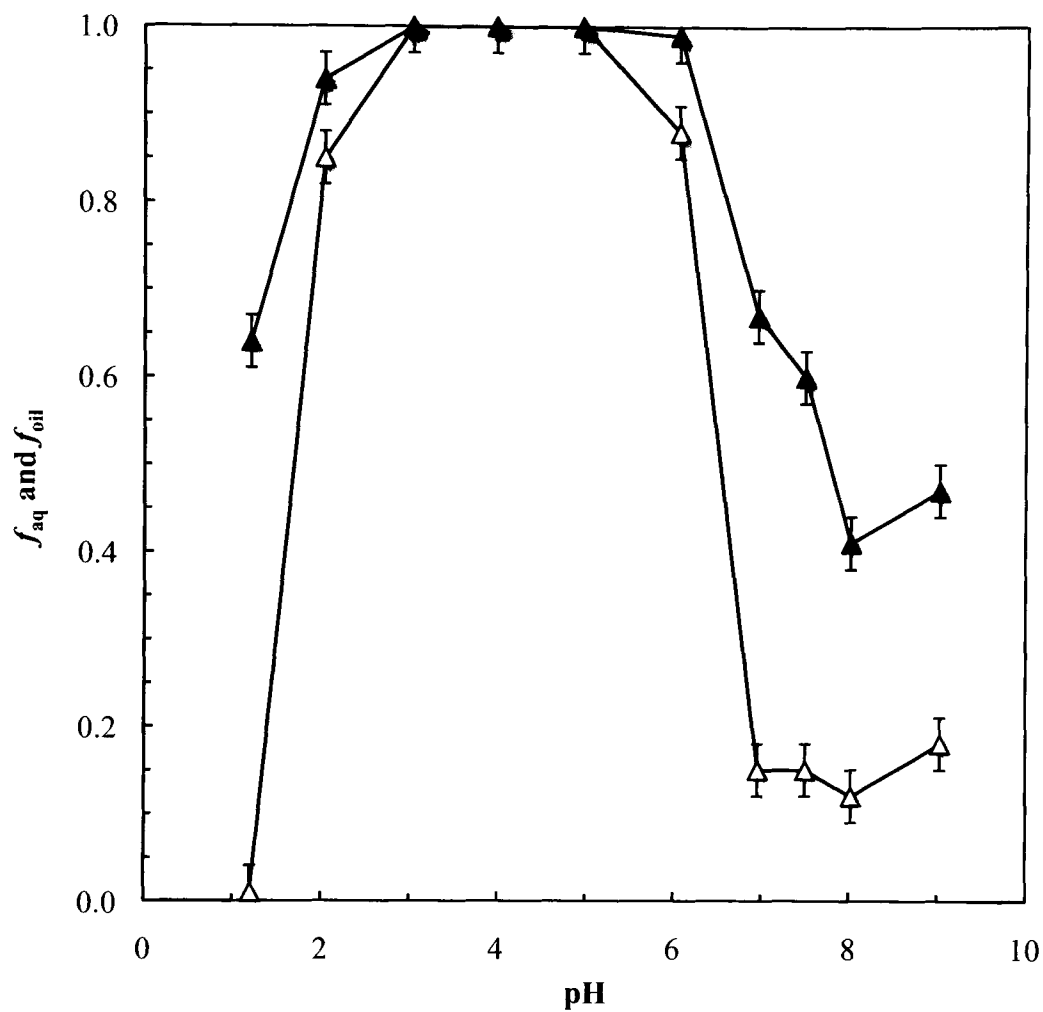
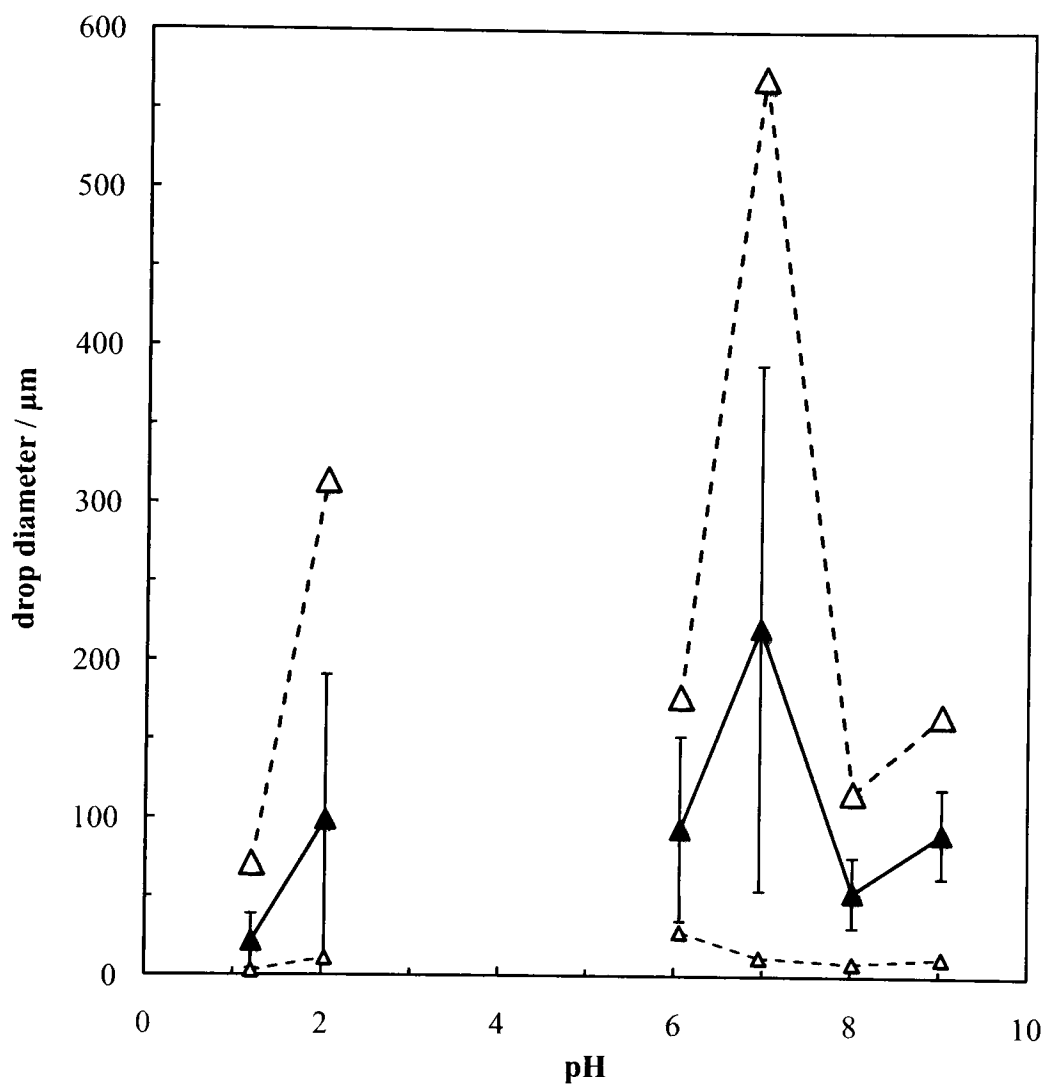


Figure 5.14. (▲) Average, (△) minimum and (△) maximum drop diameter measured by optical microscopy of fresh isopropyl myristate-in-water emulsions made with 1 wt.% Ludox CL as a function of pH. The error bars represent the standard deviation in the drop size distribution.



5.4.3. *Effect of oil volume fraction*

The initial oil volume fraction used to produce IPM-in-water emulsions was varied in order to change the emulsion drop size, which is of interest in controlling the mixed emulsion heteroaggregated structures. As Figures 5.15 and 5.16 show, the emulsion drop diameter decreases with increasing oil fraction. However the polydispersity increases. A way to control the drop size has been shown in recent publications, using a limited coalescence process:^{20, 21} by increasing the volume fraction of the disperse phase and using continuous emulsification, which consists of reemulsifying a system consecutively after sequential modification of its composition, it has been proven that the average drop size of the emulsion decreases simultaneously with the uniformity, a measure of the drop polydispersity.

For Ludox HS-30-stabilised emulsions, the drop size describes a bimodal distribution at the lowest oil fraction, which becomes monomodal at $\Phi_o = 0.4$ and 0.5 (Figure 5.15). The drops constantly have a wider size distribution for the Ludox CL-stabilised emulsions: Figure 5.16 displays drop diameters ranging from 1 to 1000 μm at the lowest oil fraction, with the size distribution becoming narrower at the highest. The microscopy of the emulsions made with different oil fraction evidence the decrease in polydispersity for both Ludox HS-30 and CL-stabilised emulsions with increasing Φ_o (Figures 5.17 and 5.18). Although the change in drop diameter is subtle for the Ludox HS-30 emulsions, the decrease in polydispersity can be noticed. Figure 5.18 confirms both the decrease in polydispersity and increase in size of the drops stabilised by Ludox CL particles with increasing Φ_o .

Even though the best emulsion in terms of drop polydispersity is found for 0.5 oil fraction, emulsions made with lower oil fraction exhibit smaller drops, which are more likely to show heteroaggregated structures when mixed with drops of opposite charge, due to their higher mobility and reduced buoyancy. Hence emulsions will be mixed at both high and low oil volume fraction.

Figure 5.15. Drop size distributions measured with the Mastersizer 2000 of 1-day old isopropyl myristate-in-water emulsions made with 0.5 wt.% Ludox HS-30 as a function of initial oil fraction (Φ_o) at pH 7.5. Emulsions were made with $\Phi_o =$ (···) 0.2, (---) 0.3, (— —) 0.4 and (—) 0.5 by 1 min. Ultra-Turrax homogenisation at 11000 rpm.

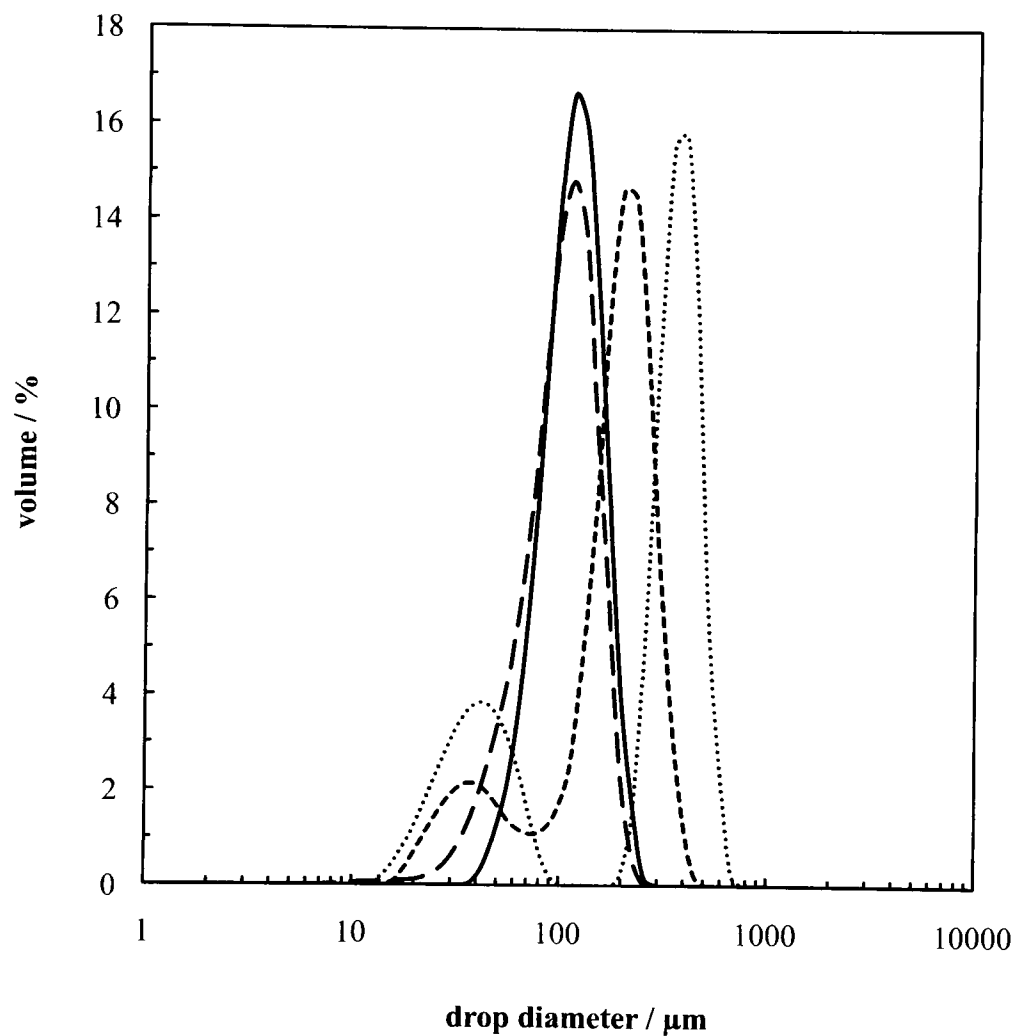


Figure 5.16. Drop size distributions measured with the Mastersizer 2000 of 1-day old isopropyl myristate-in-water emulsions made with 0.5 wt.% Ludox CL as a function of initial oil fraction (Φ_o) at pH 7.5. Emulsions were made with $\Phi_o =$ (···) 0.2, (---) 0.3, (— —) 0.4 and (—) 0.5 by 1 min. Ultra-Turrax homogenisation at 11000 rpm.

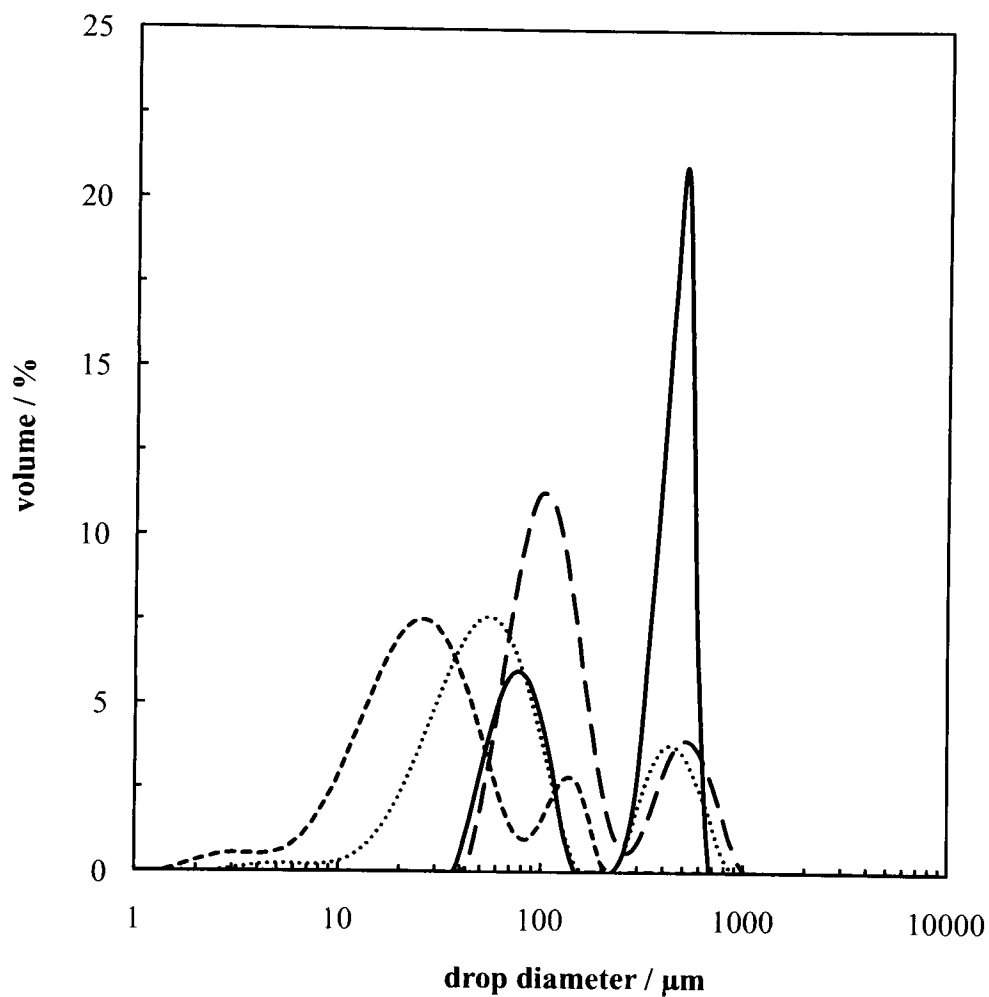


Figure 5.17. Optical microscopy images of IPM-in-water emulsions made with initial oil fraction $\Phi_o =$ (a) 0.2, (b) 0.3, (c) 0.4 and (d) 0.5, and stabilised with 0.5 wt.% of Ludox HS-30 at pH 7.5. Images were taken at 4 times magnifications 5 min after emulsification. Scale bars represent 400 μm .

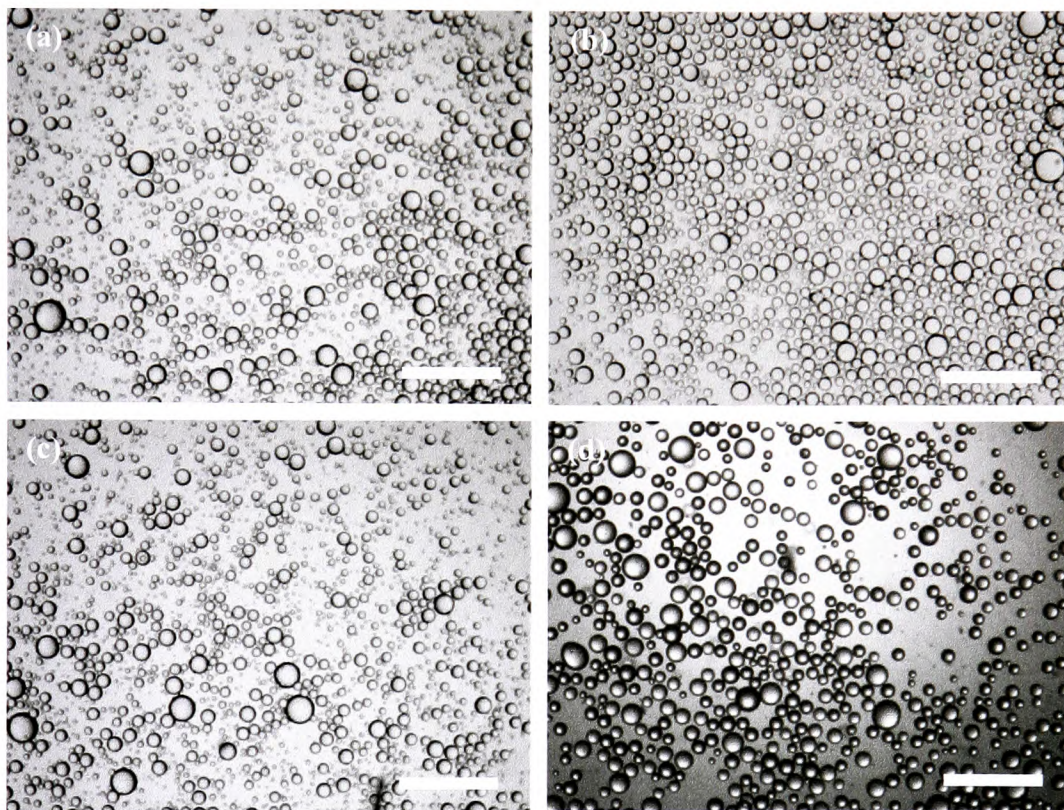
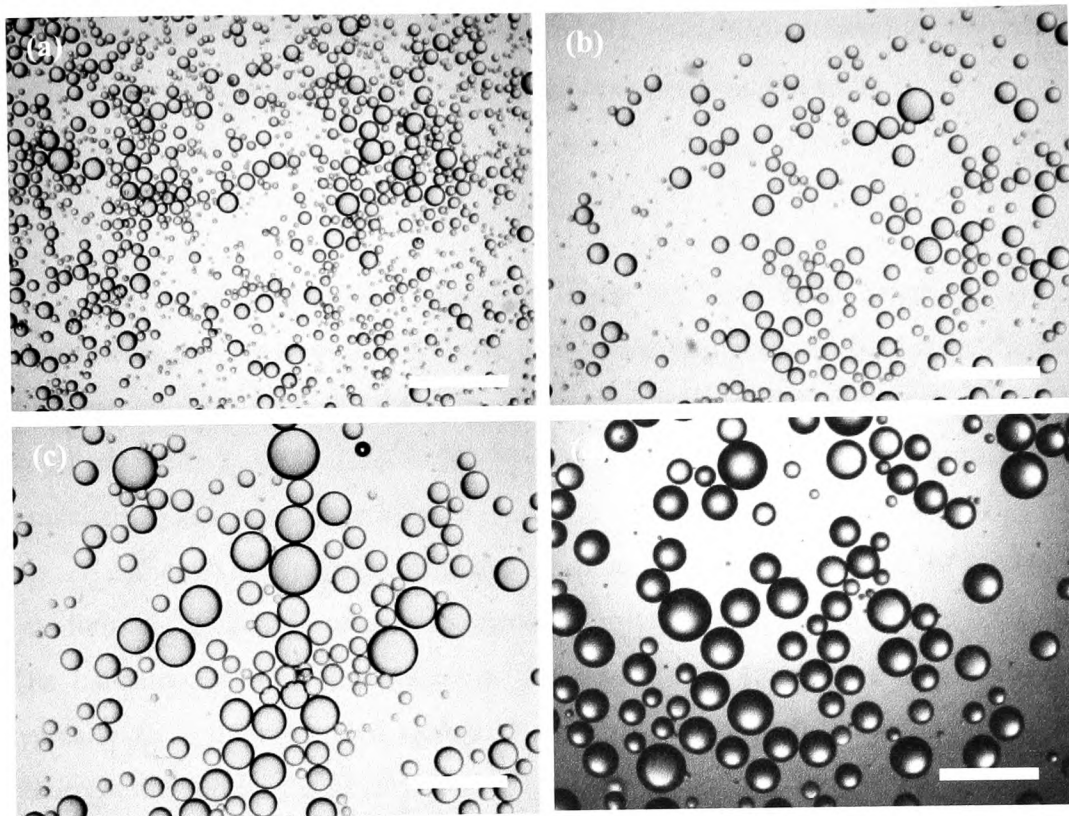


Figure 5.18. Optical microscopy images of IPM-in-water emulsions made with initial oil fraction $\Phi_o =$ (a) 0.2, (b) 0.3, (c) 0.4 and (d) 0.5, and stabilised with 0.5 wt.% of Ludox CL at pH 7.5. Images were taken at 4 times magnifications 5 min after emulsification. Scale bars represent 400 μm .



5.5 Mixing of oppositely charged emulsion drops

Separate emulsions stabilised by particles of opposite charge were mixed together in an attempt to organise emulsion drops with respect to each other.⁶ The most promising emulsions from § 5.3 and 5.4 were selected to undertake these experiments and to investigate the effects of pH, particle concentration, negative to positive drop ratio and drop size on emulsion drop heteroaggregation.

5.5.1. *Effect of mixing method*

Gu *et al.* employed a magnetic stirrer for their drop heteroaggregation experiments, which is reported to be a reproducible method.⁶ In our study, two different mixing methods were compared for mixing IPM-in-water emulsions stabilised with 1 wt.% Ludox HS-30 and 1 wt.% Ludox CL at identical pH: handshaking and magnetic stirring.

Although the magnetic stirring is a more reproducible method for mixing, it was found to greatly destabilise the emulsion mixture at its lowest speed (100 rpm). The handshaking method resulted in less coalescence from the mixed emulsion, typically $f_{oil} = 0.1$ compared with 0.35 from stirring, and so it was chosen as the recurrent method for the mixing process.

5.5.2. Dodecane-in-water emulsions

From the zeta potential measurements (*cf.* § 5.2), Ludox HS-30 particles are negatively charged at pH 3 and above, while Ludox CL particles are positively charged from pH 2 to 8. Hence, oil-in-water emulsion drops stabilised by an interfacial layer of these charged particles should also be charged within the same pH range, assuming the previously observed negative potential of bare oil-water interfaces has little influence, which is likely for close packed particle films.²² Therefore, when mixing Ludox HS-30-stabilised drops and Ludox-CL-stabilised drops at the correct pH, the two drop types should experience mutual attraction, forming heteroaggregated emulsion structures.

The dodecane-in-water emulsions were found to be stable at pH 3 when using Ludox HS-30 and 7 when using Ludox CL (*cf.* § 5.3). However neither was stable when prepared at the same pH. Consequently an emulsion of Ludox HS-30-stabilised dodecane drops at pH 3 was mixed with that stabilised by Ludox CL at pH 7. Equal volumes of the emulsions were taken within 15 minutes of their preparation and were mixed by gentle handshaking. The emulsion mixture was observed to quickly destabilise, displaying a $f_{oil} = 0.15$ and a $f_{aq} = 0.50$ within 5 minutes of mixing. As the resolved oil from the parent emulsions was not sampled into the emulsion mixture, the excess oil observed on top of the emulsion mixture can only result from coalescence during and after mixing. This instability may result from the pH change when mixing. At this pH, Ludox CL was not able to stabilise emulsions with dodecane and so it is likely that this emulsion would destabilise.

As displayed in Figure 5.19, the stability to creaming of the mixtures is similar to that of the parent-emulsions. Drop aggregation, either limited or extensive, should result in a change in the emulsion stability to creaming: if drops organise in close packed aggregates, the creaming should be more significant, whereas there would be less creaming if the drops form a 3-D network in the emulsion.²³⁻²⁵

Comparison of the micrograph images of the parent emulsions and the emulsion mixture, displayed in Figure 5.20, does not clearly show drop aggregation: the parent emulsions exhibit slight flocculation, which is also present in the emulsion mixture in the form of chains of drops. The large drops of the Ludox CL-stabilised emulsion are noticeably absent from the microscopy of the mixed emulsion 10

minutes after preparation. This again indicates that these emulsion drops are unstable and are now contributing to the coalesced oil observed on top of the emulsion mixture. After 1 day, some of the emulsion drops in the mixture show significant growth, likely due to coalescence as a result of particle desorption during the pH change.

Figure 5.19(d) shows the appearance of the emulsion mixture after 1 month. The emulsion shows significant destabilisation reminiscent of that observed from the optical microscopy. Also observed is particle sediment. At pH 3-4, both particle dispersions were stable, however when equal volumes of the two dispersions are mixed at the same particle concentration, and at pH 3 and 7 respectively for Ludox HS-30 and CL, giving a pH of 3-4, the particles are observed to heteroaggregate and sediment (e). The sediment shown in Figure 5.19(d) therefore results from heteroaggregation of free particles, which may be present during or as a result of mixing and destabilisation. Similar aggregates have been shown previously to stabilise emulsions if they are formed before emulsification.⁵

Figure 5.19. Photograph of dodecane-in-water emulsions stabilised with (a) 1 wt.% Ludox HS-30 at pH 3, (b) 1 wt.% Ludox CL at pH 7, (c & d) a 1:1 emulsion mixture at (c) 10 minutes and (d) 1 month after mixing. (e) Mixture of the two Ludox dispersions after 1 month. Photographs (a) and (b) were taken after sampling of the emulsion, which caused some coalescence. The mixture was prepared by handshaking two emulsions within 15 minutes of their initial preparation.

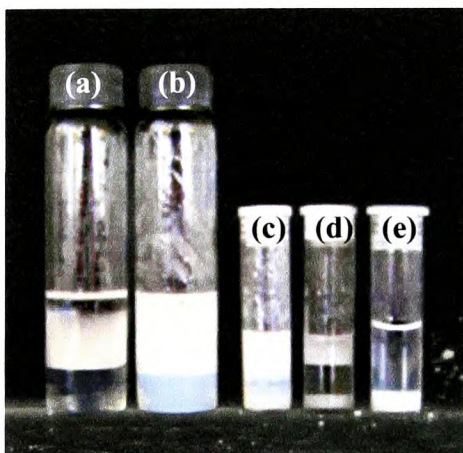
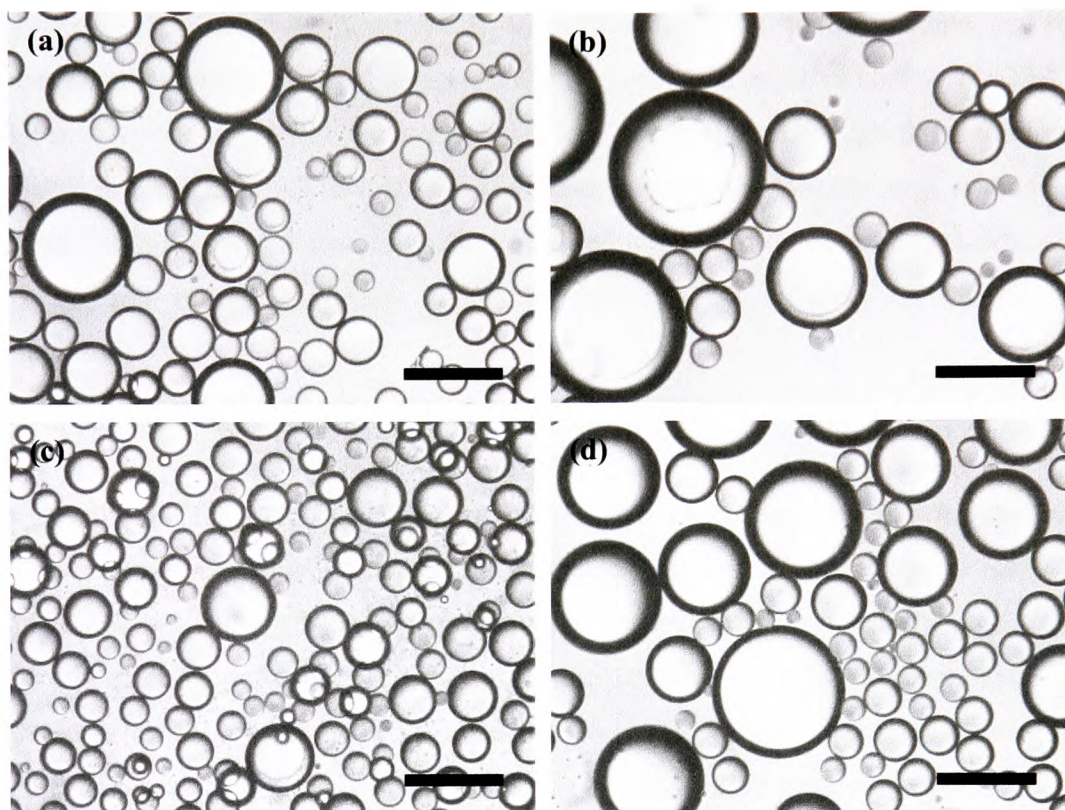


Figure 5.20. Optical microscopy images of dodecane-in-water emulsions stabilised with (a) 1 wt.% of Ludox HS-30 at pH 3 and (b) 1 wt.% of Ludox CL at pH 7, and (c, d) a 1:1 emulsion mixture as in Figure 5.18. Images are taken at 4 times magnifications (a,b) 5 min. after homogenisation, and (c) 10 min. and (d) 1 day after mixing. Scale bars represent 400 μm .



5.5.3. *Isopropyl myristate-in-water emulsions*

As shown in section 5.4, IPM-in-water emulsions with equal volumes of oil and water can be stabilised by Ludox HS-30 or Ludox CL in the same pH range. Zeta potential measurements done on the diluted emulsions at pH 7.5 confirmed that drops stabilised with 1 wt.% of the positive Ludox CL particles have a positive charge of $+38.6 \pm 6.4$ mV similar to that of the Ludox CL particles alone, and the ones stabilised with the negative Ludox HS-30 particles a negative charge of -27.4 ± 6.4 mV while the particles have a charge close to -40 mV. Although the sign of the charge is considered reliable, it has to be taken into account that the large size of the drops (between 20 and 100 μm in diameter) might cause saturation of the electrodes in the cell of the Zeta-sizer apparatus, reducing the accuracy of the charge magnitude.

The mixture of the IPM-in-water emulsions at identical pH (7.5) was observed to exhibit little destabilisation: around $f_{\text{oil}} = 0.1$ and $f_{\text{aq}} = 0.15$ 5 minutes after mixing (Figure 5.21). Stability to creaming of the mixture is not enhanced compared to the two parent emulsions; in fact, it seems to be an average of the two. After a month, the emulsion mixture remained stable, exhibiting no further coalesced oil and slightly more resolved water. A thin layer of particle sediment was also observed at the bottom of the emulsion mixture. However this was much smaller than the amount of sediment seen when the two particle dispersions were mixed at the same concentration: compare Figures 5.21 (d) and (e).

Limited drop aggregation can be observed in the micrographs in Figure 5.22: chains of 4 to more than 10 drops are arranged in a network manner, which indicates it is possible that oppositely charged droplets are subjected to attractive forces, electrostatic in this case, resulting in them gathering together. However, it is not significantly different to that observed in the parent emulsions. Contrary to the dodecane mixture, no change of drop size is observed after 1 day, which signifies that the emulsion drops remain stable on mixing them and afterwards. The small amount of sedimented particles supports this argument, as it means that fewer particles are present in the continuous phase, so there are more particles remaining at the oil-water interfaces.

Figure 5.21. Photograph of IPM-in-water emulsions stabilised with (a) 1 wt.% Ludox HS-30 and (b) 1 wt.% Ludox CL at pH 7.5, (c & d) a 1:1 emulsion mixture at (c) 10 min. and (d) 1 month after mixing. (e) Mixture of the two Ludox dispersions at 1 month. Photographs a and b were taken immediately after sampling.

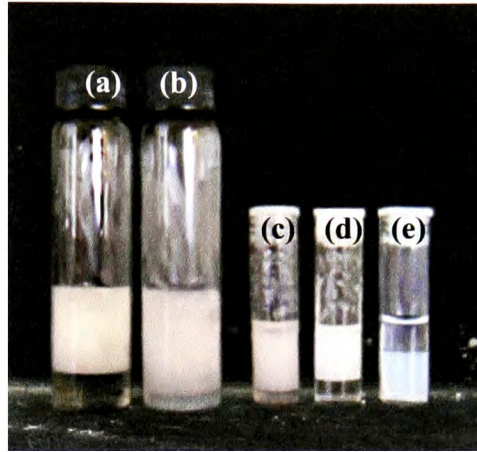
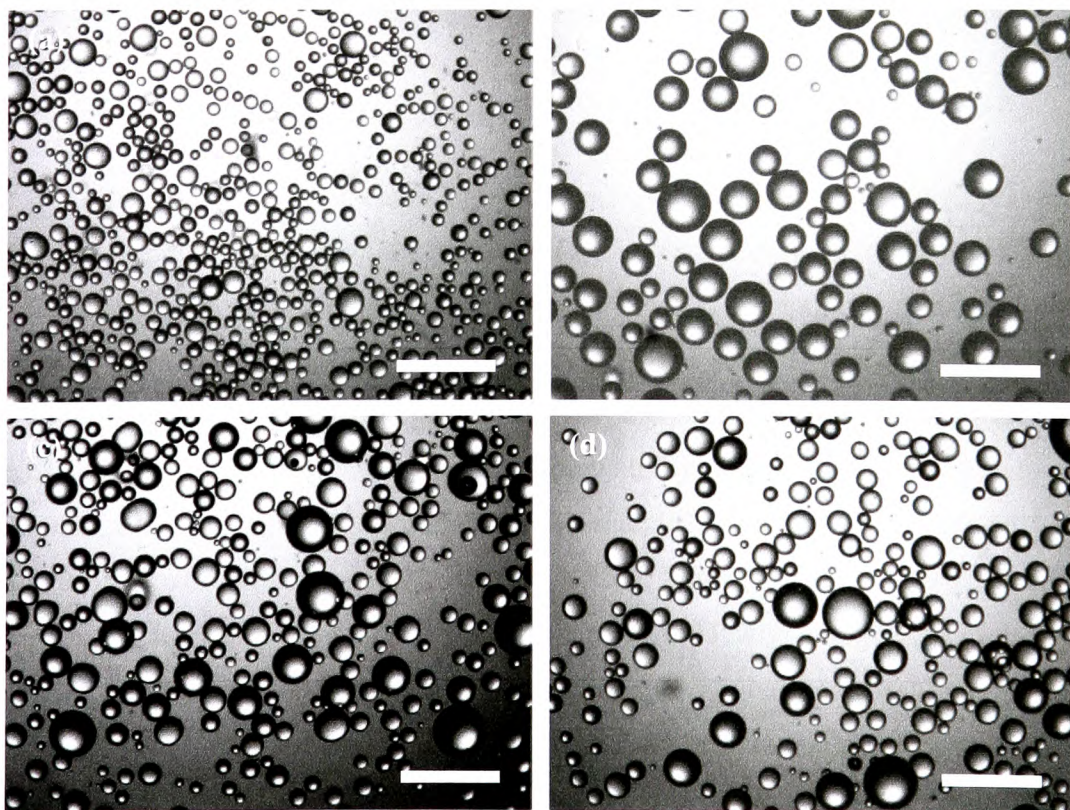


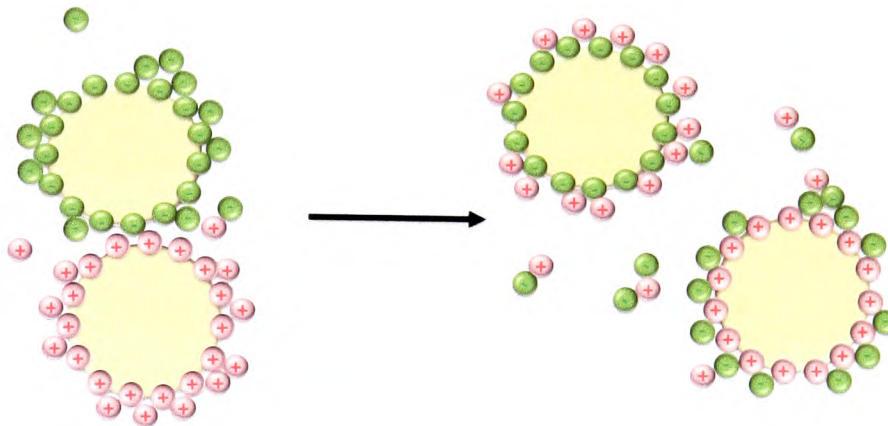
Figure 5.22. Optical microscopy images of fresh IPM-in-water emulsions stabilised with (a) 1 wt.% of Ludox HS-30 and (b) 1 wt.% of Ludox CL at pH 7.5, and (c, d) the emulsion mixture as in Figure 5.20 (c) 10 min. and (d) 1 day after mixing. Emulsions were made by 1 min. Scale bars represent 400 μm .



5.5.3.1 Effect of excess particles

Non-adsorbed particles in emulsion continuous phases have been evidenced by the formation of sedimented flocs in § 5.5.2. and 5.5.3. The drop aggregation can be reduced by the presence of free particles in the mixture, which conflicts with the aims of mixing the emulsions. Indeed, the free charged particles can adsorb as a neutralising layer on them, preventing electrostatic attraction between drops (Figure 5.23).

Figure 5.23 Schematic representation of the neutralisation of particle-stabilised oil drops in the presence of un-adsorbed particles of opposite charge. The free particles neutralise the emulsion drops through adsorption, reducing electrostatic drop attraction.



Prior to mixing, the emulsion continuous phases were replaced with water at pH 7.5 through removal of the resolved continuous phase after creaming and an addition of an equal volume of water several times. The resulting emulsions now showed completely clear subnatants (Figure 5.24). The stability to coalescence of the emulsion mixture was also enhanced. Compared with the non-washed mixture, the coalescence fraction is halved and no sedimented particles are observed up to 3 months after mixing. This confirms that the sediment in the previous mixture was due to free particles in the system prior to mixing. Furthermore, the creaming of the mixture is increased, from $f_{aq} = 0.15$ without to 0.43 with washing, indicating a change in emulsion density. The excess particles may have been structuring the continuous phase by creating a gel-like network between the oil drops, increasing the

viscosity and drop-drop separation. Removing the free particles also affected the drop packing in the emulsion, lowering the volume needed by the drops, hence increasing the amount of water resolved.

However, no significant increase in drop aggregation is witnessed using optical microscopy (Figure 5.25). On the right of Figure 5.25(d) however, some droplet clustering is apparent. In the dilute regime used for the microscopy, the buoyant drops are present at a concentration lower than that required to form a monolayer. The fact that some of the drops are present as clusters and are above or below each other, when their buoyancy should cause them to fill gaps in the creamed drop layer, signifies some attractive force between them, possibly as a result of heteroaggregation.

Figure 5.24. Photograph of IPM-in-water emulsions stabilised with (a) initially 1 wt.% Ludox HS-30 and (b) initially 1 wt.% Ludox CL at pH 7.5, whose aqueous phases have been replaced with water at pH 7.5. Photograph was taken after sampling. (c) Emulsion mixture (1:1) 1 month after mixing.

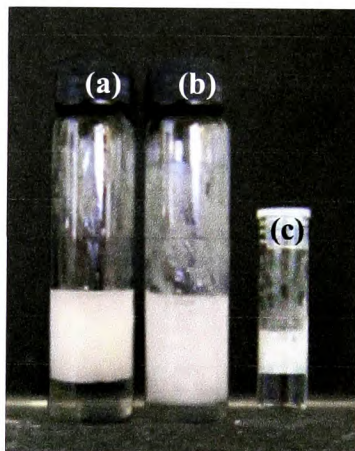
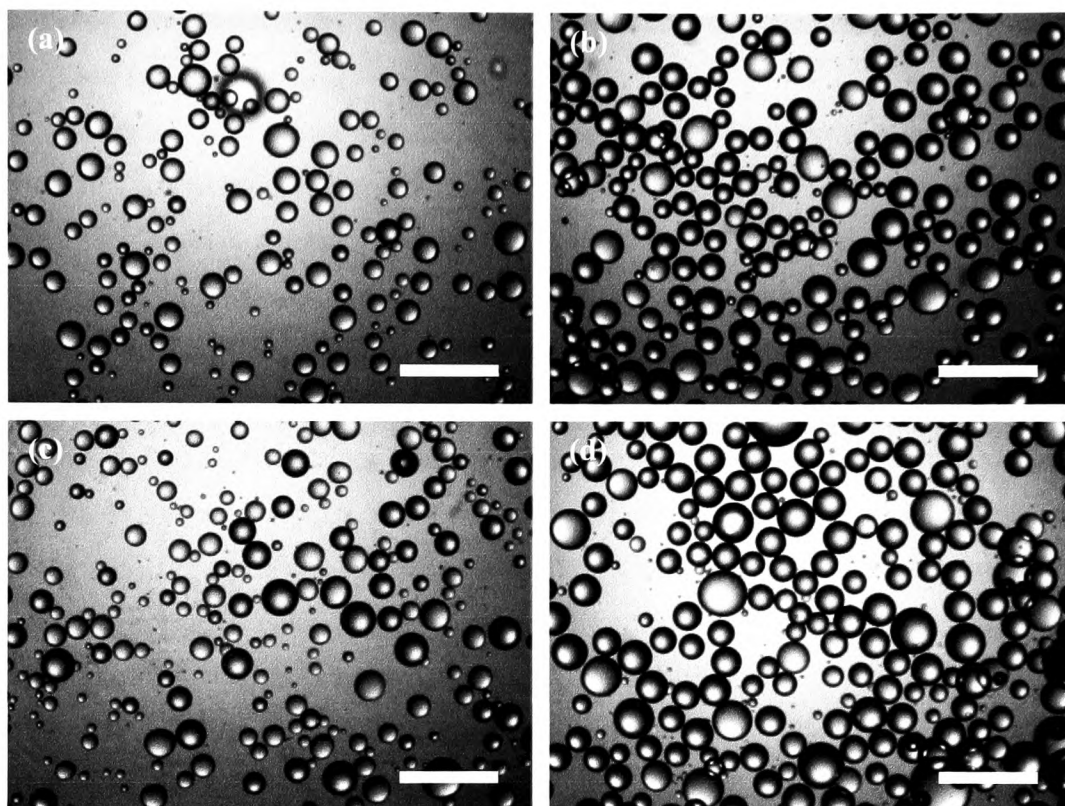


Figure 5.25. Optical microscopy images of IPM-in-water emulsions stabilised with (a) 1 wt.% of Ludox HS-30 and (b) 1 wt.% of Ludox CL after replacing with water at pH 7.5, and (c, d) a 1:1 emulsion mixture as in Figure 5.22 (c) 10 min. and (d) 1 day after mixing. Scale bars represent 400 μm .



As free particles are likely to affect both the emulsion mixture stability and the drop aggregation, the effect of adding more free particles in the separate emulsions before mixing was investigated, achieved through replacing a set volume of the resolved continuous phase with an aqueous particle dispersion. The emulsion stability was observed to decrease with the addition of particles: both types of emulsion are destabilised with increasing particle concentration, but complete emulsion separation was not observed.

Figure 5.26 shows that the coalescence in the emulsion mixtures increases with free particle concentration. At 4 wt.% however the Ludox CL particle dispersion is gel-like and, mixed with the 4 wt.% Ludox HS-30 stabilised emulsion, the coalescence exhibits a minimum, due to the increased viscosity of the continuous phase. For the other mixtures, the water fraction and the height of sedimented particles increase with the particle concentration. It should be noted that the small oil volume in Figure 5.26(d) results from difficulties in sampling the parent emulsions for which the addition of 2 wt.% particles caused significant coalescence. The microscopy images of the mixtures, shown in Figure 5.27, demonstrates that the free particles in the continuous phase do not enhance the drop aggregation. However, the average drop size is observed to increase with particle concentration in the continuous phase. This is probably due to larger drops present in the parent emulsions, which result from their destabilisation with excess particle addition.

Figure 5.26. Photographs of 1-day old IPM-in-water emulsion mixtures at pH 7.5. Emulsion mixtures were made from emulsions stabilised with initially 1 wt.% Ludox HS-30 and 1 wt.% Ludox CL at pH 7.5, then washed with pH 7.5 water at (a) 0, (b) 0.5, (c) 1, (d) 2 and (e) 4 wt.% of the same particle type.

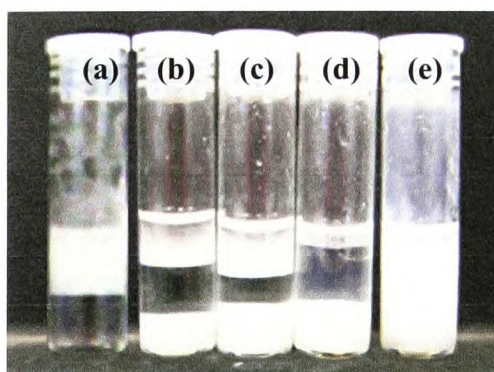
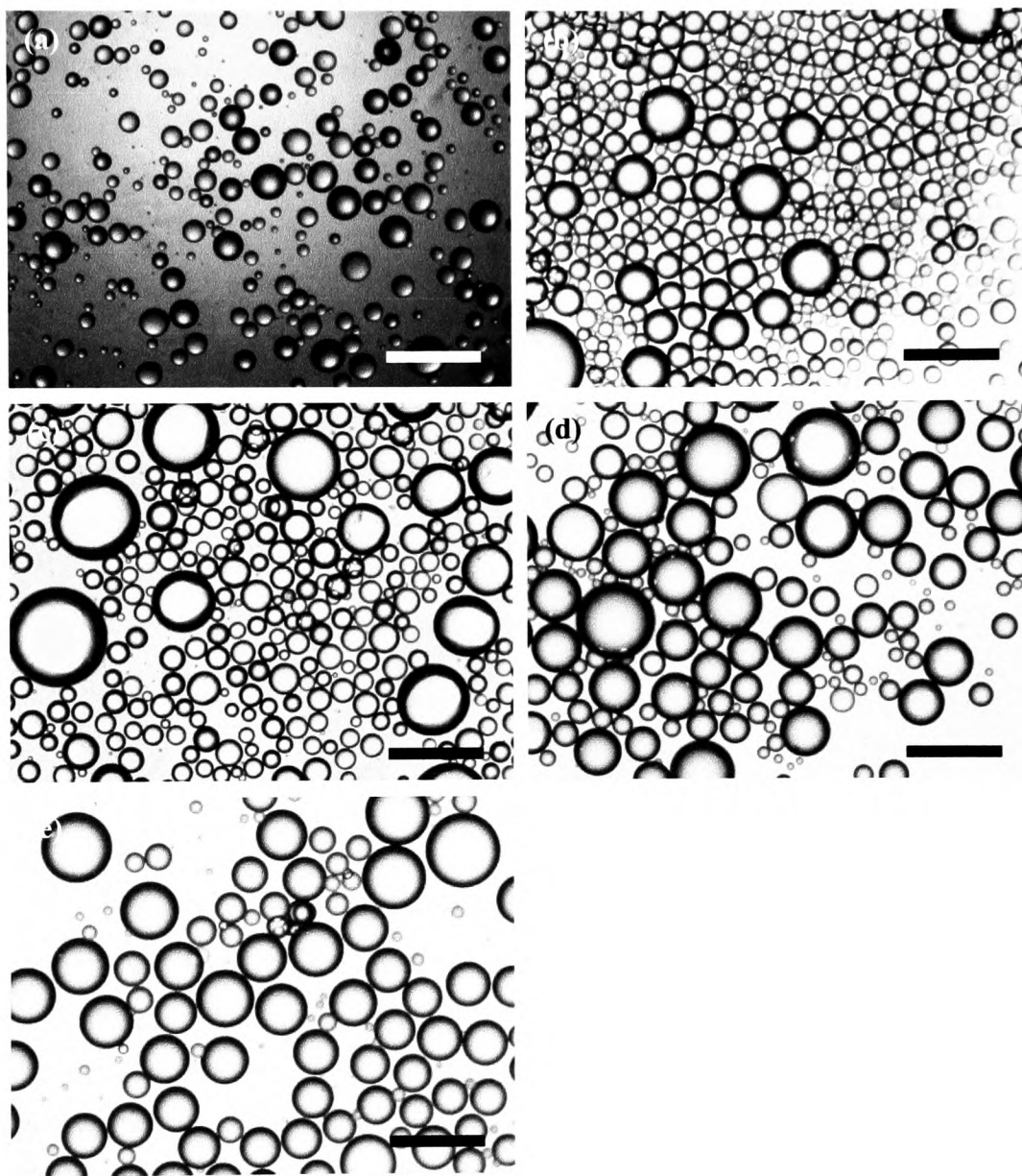


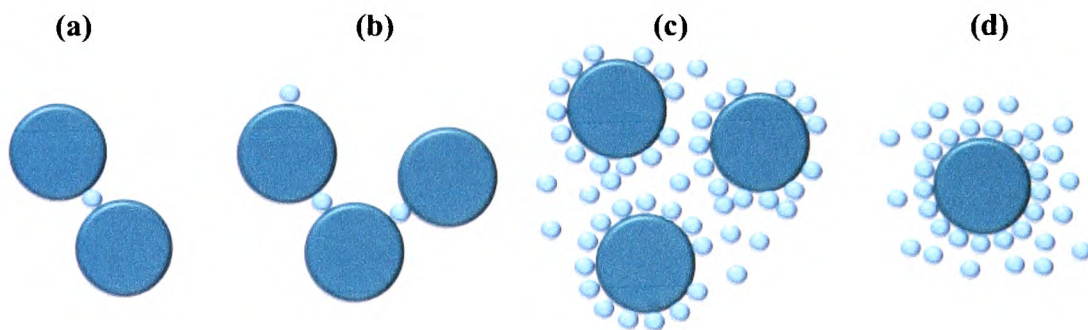
Figure 5.27. Optical microscopy images of IPM-in-water emulsion mixtures as in Figure 5.24. Emulsion mixtures were made from emulsions stabilised with initially 1 wt.% Ludox HS-30 and 1 wt.% Ludox CL at pH 7.5, then washed with pH 7.5 water at (a) 0, (b) 0.5, (c) 1, (d) 2 and (e) 4 wt.% of the same particle types. Scale bars represent 400 μm .



5.5.3.2 Effect of drop number ratio

As shown in Figure 5.22, the size of the positive drops stabilised with Ludox CL and of the negative ones stabilised with Ludox HS-30 are different: the latter are 3 times smaller in diameter than the former. For heteroaggregation of different size particles, it has been proven that the organisation of the particles was dependent on the ratio of large to small particles (Figure 5.28).^{4, 5} When equal volume concentrations of solution are mixed, as studied previously (*cf.* § 5.5.2), the number of small to large drops (S:L) is high. The effect of the number ratio of Ludox HS-30 to Ludox CL-stabilised drops mixed together is investigated here, in order to determine if the mixing ratio effects observed in particle heteroaggregation can also be applied to emulsion drop heteroaggregation.

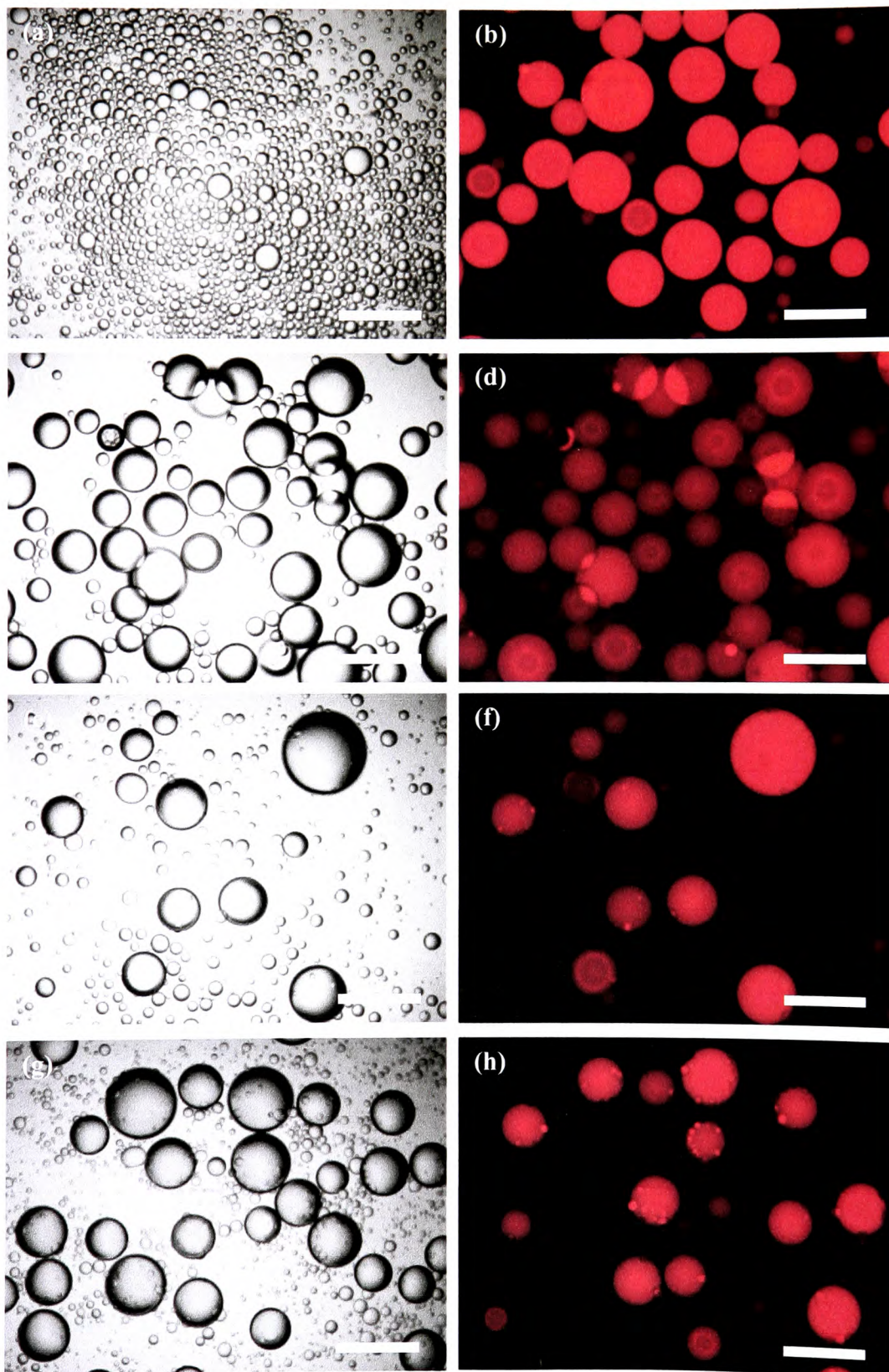
Figure 5.28 Schematic representation of the effect of the number ratio of large to small particles determining the morphology of the aggregates formed with increasing the small particles concentration from (a) to (d).



In order to differentiate between the HS-30 and CL-stabilised emulsions, the larger Ludox CL-stabilised emulsions were dyed with Nile Red in the IPM phase, rendering them fluorescent under UV irradiation. When the emulsions were re-made, the drop size ratio was different, possibly due to inclusion of the Nile Red dye, and now the negative drops were closer to 8 times smaller than the larger positive ones. Observation of the emulsion mixtures had to be done within 30 min after mixing to be able to differentiate the two types of drops, because the Nile Red diffusion into the other oil drops became significant above this length of time.

Varying the drop S:L number ratio from about 1:1 to 50:1 causes a change in the apparent drop aggregation observed in Figure 5.29. When the S:L number ratio is increased, large drops are observed to be surrounded by some small drops. At the maximum ratio 50:1, the large positive drops appear more covered in small negative droplets. However, this increase in coverage of large drop by small is expected, even without heteroaggregation, as there are simply more small drops available to separate the larger ones. At an S:L ratio number of 15:1, the largely uncovered positive drops in fact co-exist with free negatively charged ones indicating that the heteroaggregation is weak. As the emulsions are prepared close to the isoelectric point of the Ludox CL particles, it is likely that these particles are present as aggregates on the emulsion surface. It is possible that some of the Ludox HS-30-stabilised drops are able to remove some of the Ludox CL particles from their aggregates at the emulsion surfaces, resulting in reduced heteroaggregation.

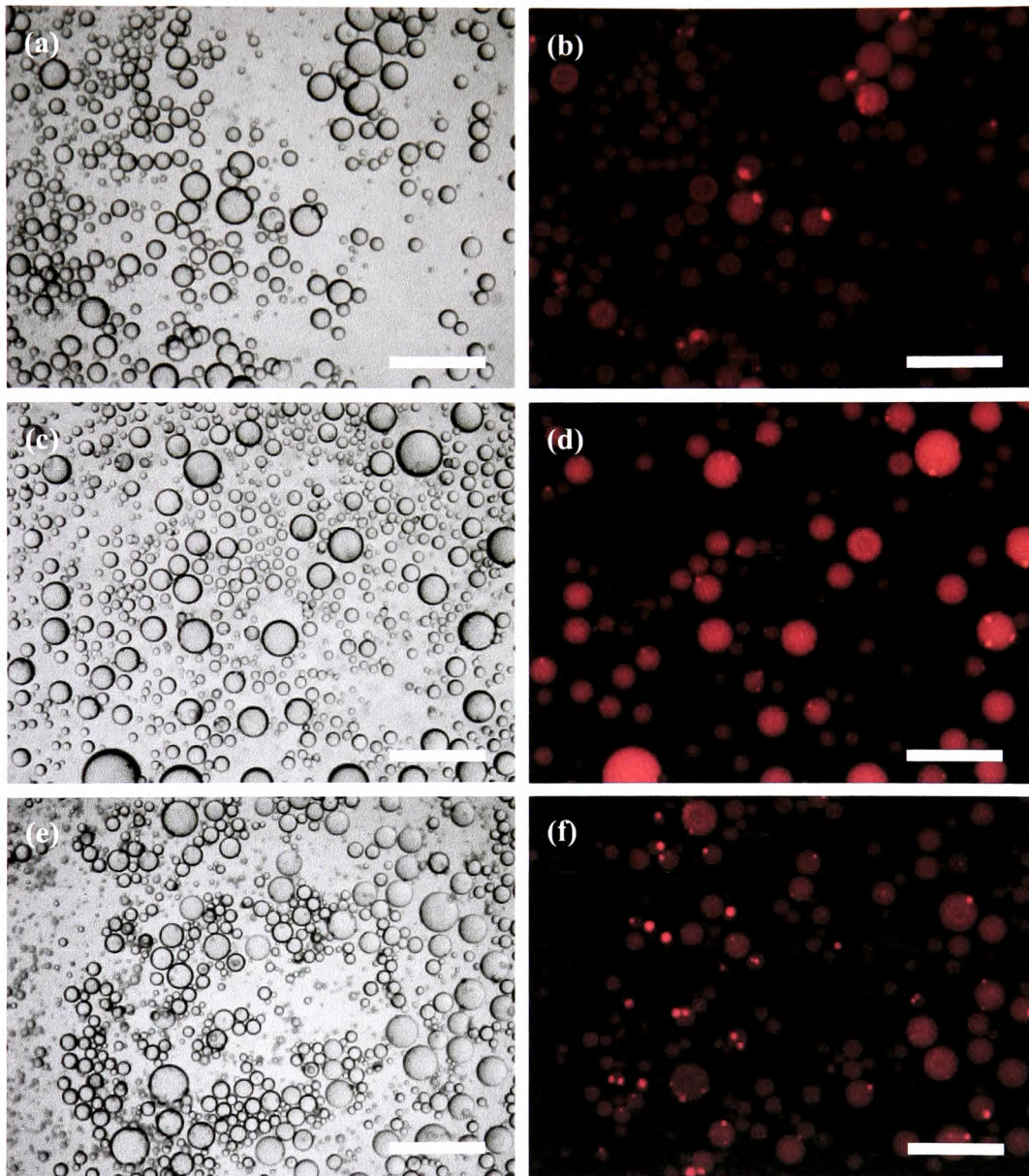
Figure 5.29. Optical microscopy images of IPM-in-water emulsion mixtures made with (c, d) 1:1, (e, f) 15:1 and (g, h) 50:1 S:L ratio of 1 wt.% (a) Ludox HS-30 to (b) Ludox CL (with Nile red)-stabilised emulsions drops. Images were taken with (a, c, e, g) transmitted and (b, d, f, h) UV light after 1 min. Scale bars represent 400 μm .



5.5.3.3 Effect of drop size

The initial oil fraction was shown to affect the emulsion drop size in § 5.4.3. However, changing the size of the emulsion drops before mixing them was observed to have little effect. Figure 5.30 reveals that the aggregation is higher at higher initial oil fraction, *i.e.* for larger oil drops. At 0.2 fraction of oil, only a few drop aggregates are witnessed and negative drops seemed aggregated together, whereas at 0.3 and 0.4 oil fraction, the aggregates comprise both positive and negative drops. It can be seen in Figures 5.30 (c) and (d) that the negative drops (in red) separated by positive ones form heteroaggregates. Some heteroaggregation is observed at 0.4 oil volume fraction, but only a few areas of the emulsion mixture exhibit this behaviour.

Figure 5.30. Optical microscopy images of IPM-in-water emulsion mixtures made with 1 wt.% Ludox HS-30 and Ludox CL-stabilised emulsions at (a, b) 0.2, (c, d) 0.3 and (e, f) 0.4 initial oil fraction. Images were taken with (a, c, e) transmitted and (b, d, f) UV light 1 min after mixing. Scale bars represent 400 μm .



5.6 Conclusions

The heteroaggregation of Ludox HS-30 and Ludox CL-stabilised emulsions has been attempted. Ludox HS-30 and Ludox CL particles were found to possess opposite charge at pH between 2 and 9. The dispersion pH was however observed to significantly affect dodecane-in-water emulsions. Ludox HS-30-stabilised dodecane drops in water were only stable at pH 3, whereas Ludox CL-stabilised ones were stable at pH 7. This leads to mixing of the emulsions at different pH values. The pH change experienced by the Ludox CL-stabilised emulsion led to destabilisation in terms of coalescence, and little drop aggregation was observed. When the polar isopropyl myristate oil was used, emulsions were stable over a larger range of pH, enabling the two emulsions to be mixed at identical pH. The mixture obtained displayed little destabilisation, but no real improvement in the drop heteroaggregation was witnessed. Particle sediments, due to aggregation of oppositely charged free particles in the continuous phase, were observed in both the dodecane-in-water and the IPM-in-water mixtures. Excess particles were observed to affect the stability of the emulsions and of their mixtures: when removed from the water phase, emulsion mixtures were more stable to coalescence but less to creaming, indicating the structuring role of the excess particles. Increasing the free particle concentration was proven to cause both coalescence and creaming. No enhancement of drop heteroaggregation was demonstrated with increasing or decreasing particle concentration in the mixtures. The use of a fluorescent dye and the change of small to large drop number ratio in the emulsion mixtures led to the observation of some heteroaggregation between drops of opposite charge. However, the use of large S:L size ratio made heteroaggregation difficult to distinguish from simple large drop separation with increasing amounts of smaller ones. The most promising result was found when both parent emulsions were prepared and mixed at a reduced volume fraction of oil giving smaller emulsion drops. Some significant heteroaggregation was observed, however this was restricted to only a few areas of the emulsion mixture.

5.7 References

1. K. Furusawa and C. Anzai, in *Heterocoagulation Behavior of Polymer Lattices with Spherical Silica*, Ralph K. Iler Memorial Symp. on Colloid Chemistry of Silica, at the 200th National Meeting of the American Chemical Soc., Washington, 1990.
2. C. A. Johnson and A. M. Lenhoff, *J. Colloid Interface Sci.*, **179**, 587 (1996).
3. G. Y. Onoda and E. G. Liniger, *Phys. Rev. A*, **33**, 715 (1986).
4. M. Rasa, A. P. Philipse and J. D. Meeldijk, *J. Colloid Interface Sci.*, **278**, 115 (2004).
5. B. P. Binks, W. Liu and J. A. Rodrigues, *Langmuir*, **24**, 4443 (2008).
6. Y. S. Gu, E. A. Decker and D. J. McClements, *Food Hydrocolloids*, **21**, 516 (2007).
7. P. Van der Meeren, H. Saveyn, S. B. Kassa, W. Doyen and R. Leysen, *Phys. Chem. Chem. Phys.*, **6**, 1408 (2004).
8. M. Kosmulski, in *A literature survey of the differences between the reported isoelectric points and their discussion*, International Symposium on Electrokinetic Phenomena, Krakow, Poland, 2002.
9. G. A. Parks, *Chem. Rev.*, **65**, 21 (1965).
10. R. O. James and T. W. Healy, *J. Colloid Interface Sci.*, **40**, 53 (1972).
11. B. P. Binks and J. A. Rodrigues, *Angew. Chem. Int. Ed.*, **46**, 5389 (2007).
12. B. P. Binks, J. A. Rodrigues and W. J. Frith, *Langmuir*, **23**, 3626 (2007).
13. B. P. Binks and J. A. Rodrigues, *Langmuir*, **23**, 7436 (2007).
14. B. P. Binks and S. O. Lumsdon, *Phys. Chem. Chem. Phys.*, **1**, 3007 (1999).
15. T. R. Briggs, *Ind. Eng. Chem. Res.*, **13**, 1008 (1921).
16. E. H. Lucassen-Reynerds and M. van den Tempel, *J. Phys. Chem.*, **67**, 731 (1963).
17. B. P. Binks, R. Murakami, S. P. Armes and S. Fujii, *Langmuir*, **22**, 2050 (2006).
18. A. Koh, G. Gillies, J. Gore and B. R. Saunders, *J. Colloid Interface Sci.*, **227**, 390 (2000).
19. B. P. Binks and S. O. Lumsdon, *Phys. Chem. Chem. Phys.*, **2**, 2959 (2000).

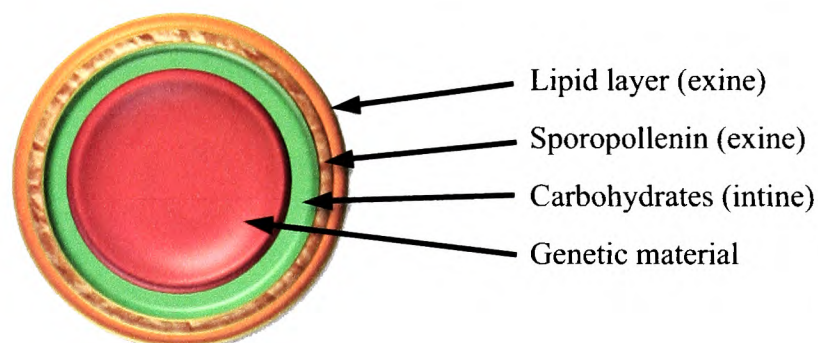
20. S. Arditty, C. P. Whitby, B. P. Binks, V. Schmitt and F. Leal-Calderon, *European Physical Journal E*, **11**, 273 (2003).
21. B. P. Binks and S. O. Lumsdon, *Langmuir*, **16**, 8622 (2000).
22. K. G. Marinova, R. G. Alargova, N. D. Denkov, O. D. Velev, D. N. Petsev, I. B. Ivanov and R. P. Borwankar, *Langmuir*, **12**, 2045 (1996).
23. S. Abend, N. Bonnke, U. Gutschner and G. Lagaly, *Colloid Polym. Sci.*, **276**, 730 (1998).
24. T. N. Hunter, R. J. Pugh, G. V. Franks and G. J. Jameson, *Adv. Colloid Interface Sci.*, **137**, 57 (2008).
25. J. L. Trompette and M. J. Clifton, *J. Colloid Interface Sci.*, **276**, 475 (2004).

CHAPTER 6 NATURAL SPOROPOLLENIN PARTICLES: TRANSITIONAL INVERSION OF EMULSIONS AND LIQUID MARBLES

6.1 Introduction

Spore particles are a reproductive organ composed of an internal sac, which contains the genetic material, and an external wall consisting of two layers: the intine or inner layer and the exine or outer layer. The latter is composed itself of sporopollenin coated by a layer of lipids, which contribute to ~ 27% of the total mass of the spore (Figure 6.1).¹⁻⁴ Of these, it is the sporopollenin which has received the most attention by demonstrating its remarkable stability towards chemical and physical degradation, having been discovered intact in fossil samples.⁵

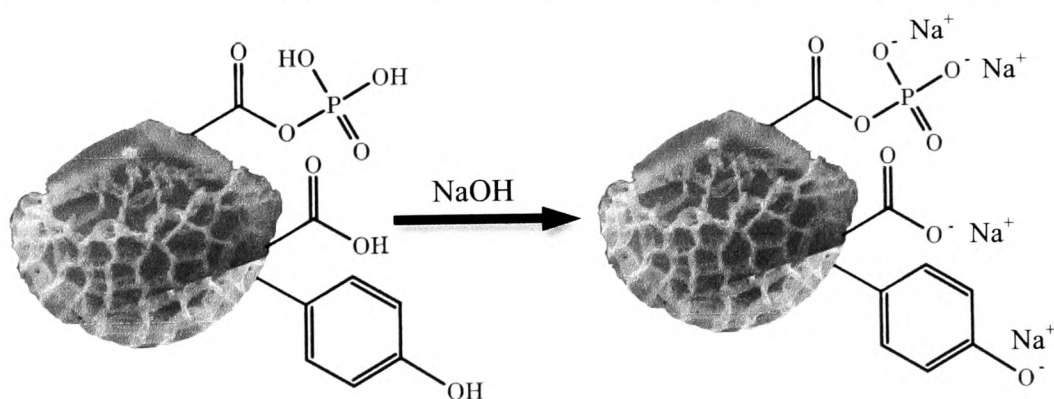
Figure 6.1. Schematic representation of a spore particle cross-section.



Sporopollenins have been extensively studied in plant reproduction and geology.⁵⁻⁷ In 1988, Shaw *et al.* also showed the possible application of the sporopollenin as an ion exchange medium.⁸ However, in the most recent years, its use has spread to the pharmaceutical and food industries, being loaded with active ingredients for controlled release in drug delivery or used as a gustative masker in food products.^{9, 10} By including them into shellac and ethyl cellulose rod-like microparticles, Campbell *et al.* observed that the lumpy food-grade microparticles have an enhanced efficiency as foam stabiliser compared to the equivalent smooth microparticles.¹¹

The spore particles used in this study originate from the *Lycopodium clavatum* plant, which is widespread in Nepal, where the spores are used in flash powder. The sporopollenin from this species, first studied by Zetzsche, was found to completely resist the harsh treatments used to remove the lipid layer, the exine and the intine contents.^{3, 4, 12} Zetzsche and Vicari were first to determine that the chemical composition of the sporopollenin includes an arbitrary C₉₀ subunit with methyl and hydroxyl groups on the surface.³ More recently, Kettley discussed the presence of unsaturated carbon chains, a high density of hydroxyl groups, phenolic and carboxylic acid, as well as carotenoid and carotenoid ester in the sporopollenin structure.¹² Williams also stated that the use of phosphoric acid in the extraction process is likely to cause the formation of phosphoric-carboxylic anhydrides.¹³ This acidic nature of the particle surface groups renders them pH sensitive; Figure 6.2 illustrates the final base washing effect on the sporopollenin, which creates ionised species.

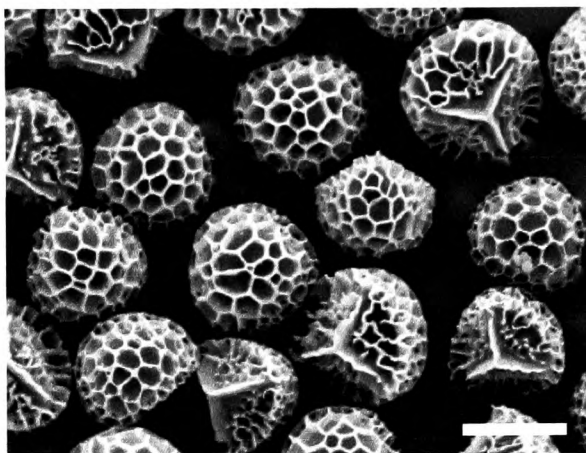
Figure 6.2. Schematic diagram of pH effect on surface groups of sporopollenin particles: the addition of NaOH renders the sporopollenin surface groups anionic.



Recently Binks *et al.* showed that the spore particles of *Lycopodium clavatum* can be used as sole emulsifiers in oil-water mixtures:¹⁴ the 30 μm diameter spores (Figure 6.3) adsorbed spontaneously at oil-water interfaces when initially dispersed in the oil, and stabilised oil-in-water emulsions with droplets as large as several millimetres in diameter. At 2 wt.% spores in the emulsions, microscopic observations showed that no more than 20% of the total drop surface was covered by spore

particles: large drops sparsely coated with particles remained stabilised as the interfacial particles moved to bridge between emulsion drops, preventing coalescence, similar to that witnessed by Vignati *et al.*¹⁵ The latter observation can be linked to the study by Horozov and Binks, who noted that hydrophobic silica particles arrange at a film interface in either a stable dimple surrounded by a particle ring or a dense crystalline bridging monolayer at the film centre.¹⁶

Figure 6.3. SEM image of dry *Lycopodium clavatum* spore particles from Binks *et al.*¹⁴ Scale bar represents 25 μm .



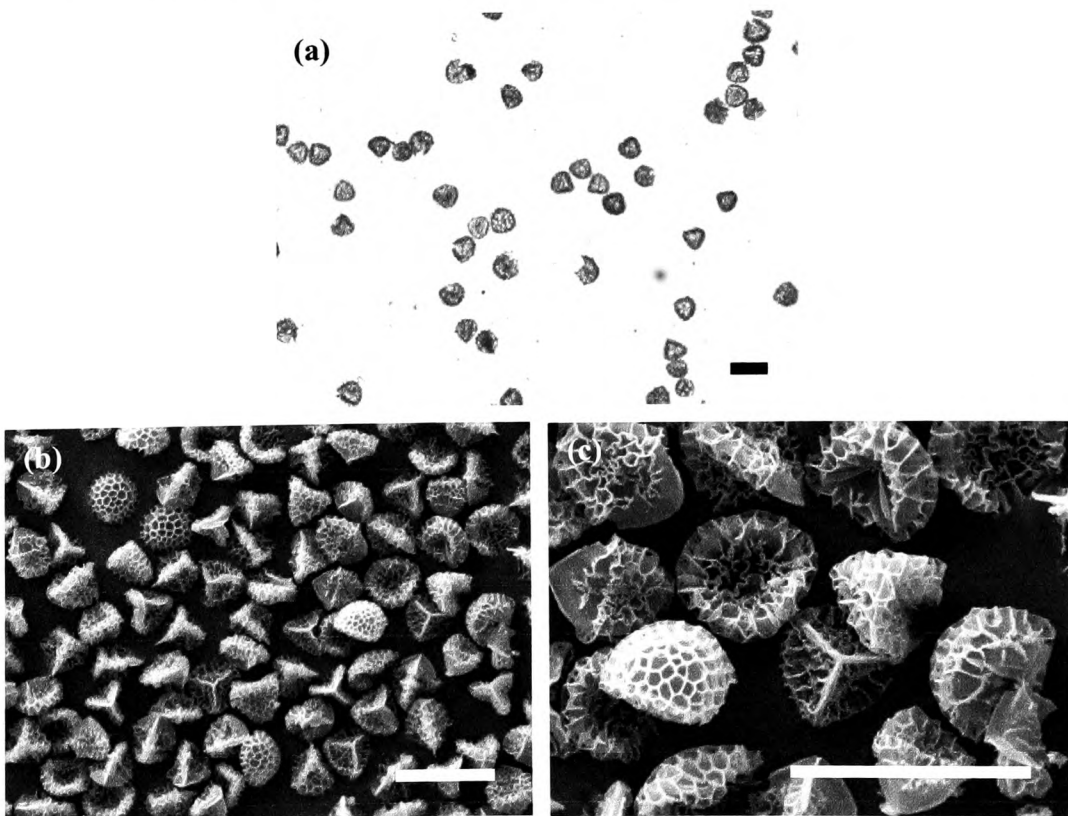
As sporopollenin has already raised the interest of the pharmaceutical and food industries, investigating their behaviour at fluid interfaces has become of importance. As the spores from *Lycopodium clavatum* are known to be able to stabilise emulsions, the ability of the hollow sporopollenin particles to also behave as good emulsifiers has been studied here: sporopollenin particles were first characterised in aqueous dispersion, before their emulsifying ability was investigated by studying the effect of their initial location, their concentration, the pH of their dispersion and the oil type used. Their surface activity at the air-water interface was also studied, through liquid marble production. Similarly, the effect of pH and salt concentration were considered, and the buckling of the liquid marble surface was examined.

6.2 Sporopollenin particle characterisation

6.2.1. Powdered particles

Lycopodium clavatum sporopollenin particles dispersed in water at their natural pH (~10) appear roughly spherical and seem relatively monodisperse (Figure 6.4(a)). They measure between 25 and 35 μm in diameter. When compared with SEM images of the *Lycopodium clavatum* spores (Figure 6.3) which they originate from, no major difference can be noted: as they are dispersed in water, the volume previously occupied by the removed intine is believed to be swollen by water, inducing a recovery of the spore-like spherical shape and causing the translucent appearance of the particles. However, dry sporopollenin particles exhibit a slightly different appearance: the SEM images in Figures 6.4(b) and (c) show collapsed and fragmented particles, probably resulting from the high vacuum pressure in the SEM chamber. They still present a rough surface, with the 3-fold marking (Y-shape) originating from the spore cell division, like the initial spores.

Figure 6.4. (a) Optical microscopy images of *Lycopodium clavatum* sporopollenin particles dispersed in water by 10 s hand shaking and (b, c) SEM images of the dry sporopollenin particles. Scale bar represents 50 μm .



6.2.2. Particle dispersions

The sporopollenin particles were always dispersed by 10 sec. handshaking, as the use of an Ultra Turrax was revealed to break the particles, and appeared as an orange-brown dispersion. When dispersed in water at their natural pH, the sporopollenin particles both sediment and cream simultaneously; optical microscopy of each layer reveals that the creaming particles stabilise several air bubbles of up to 5 times their diameter ($160 \pm 45 \mu\text{m}$), whereas the sedimenting ones are discrete particles swollen with water (Figure 6.5). This may indicate a difference in wettability within the same particle sample: the creaming particles may either be more hydrophobic or less porous than the sedimenting ones, due to the extraction process. This causes a disparate swelling of the particles, resulting in a difference in density within the aqueous dispersion. When the particles are dispersed in oil, no such observation is made and all particles sediment. This observation indicates that the cause of the foam is more likely due to differences in particle wettability.

Figure 6.5. Micrographs of sporopollenin particles dispersed in water: they separate into a cream layer (a) and a sedimented layer (b). The inset displays the vessel of the foaming sporopollenin dispersion. Scale bars represent $400 \mu\text{m}$.

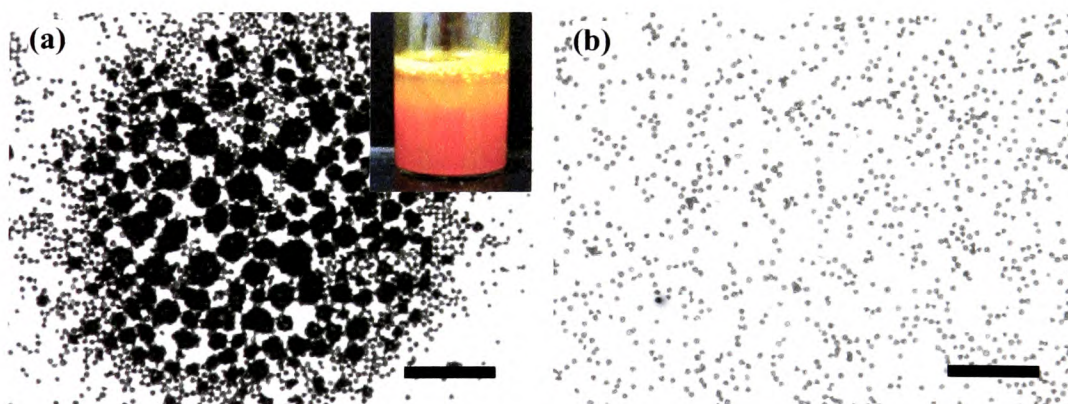


Figure 6.6 reveals that the sporopollenin particles are charged when dispersed in water and have basic surface groups: the conductivity doubles (from 25 to 55 $\mu\text{S cm}^{-1}$) when the particle concentration increases from 0.5 to 2 wt.%, while the solution pH rises slightly from 9.6 to 10.4. The basic groups may be due to deprotonation of the surface acid groups during the NaOH washing stage of the extraction, rendering the particle ionised at high pH.

The charge of the sporopollenin particles was determined more precisely by measuring the zeta potential with pH change: at natural pH (7.8 for 0.002 wt.%), sporopollenin particles exhibit a negative charge of ~ -50 mV, as Figure 6.7 displays. Sporopollenin particles exhibit monomodal charge distributions over the entire pH range, with the exception of pH 4, which causes the particles to express some positive charges (+75 mV) and some negative ones (-25 mV). The heterogeneous composition of the particles observed in the aqueous dispersion might be linked to this unusual behaviour. The large size of the sporopollenin particles might be responsible for saturating the zeta sizer electrode, which has a detection limit of approximately 10 μm . If an average of the particle charge at pH 4 is considered, the particle isoelectric point can be intrapolated to approximately pH 5.5: the majority of the particles are positively charged below this pH and negatively charged above it.

Figure 6.6. Variation of pH and conductivity of sporopollenin particle dispersions in water as a function of their concentration (wt.%).

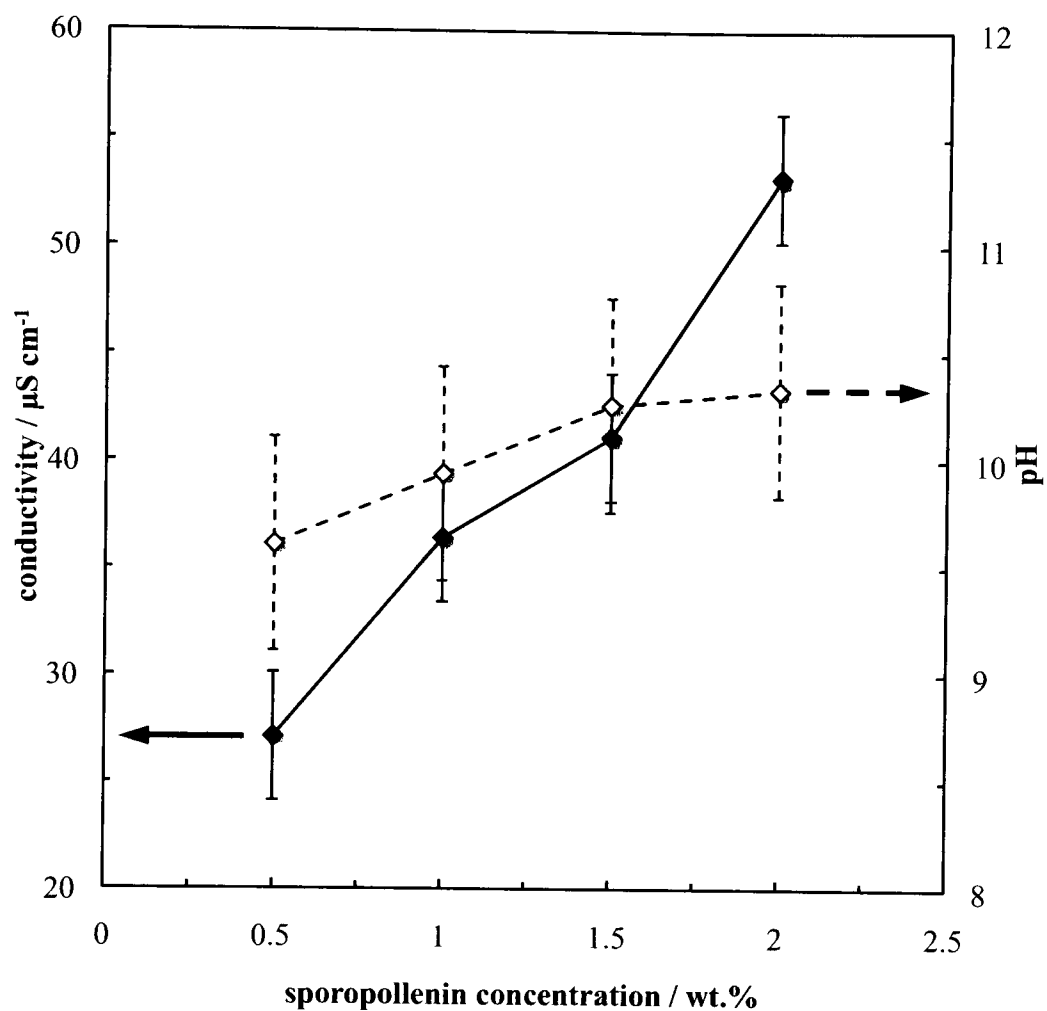
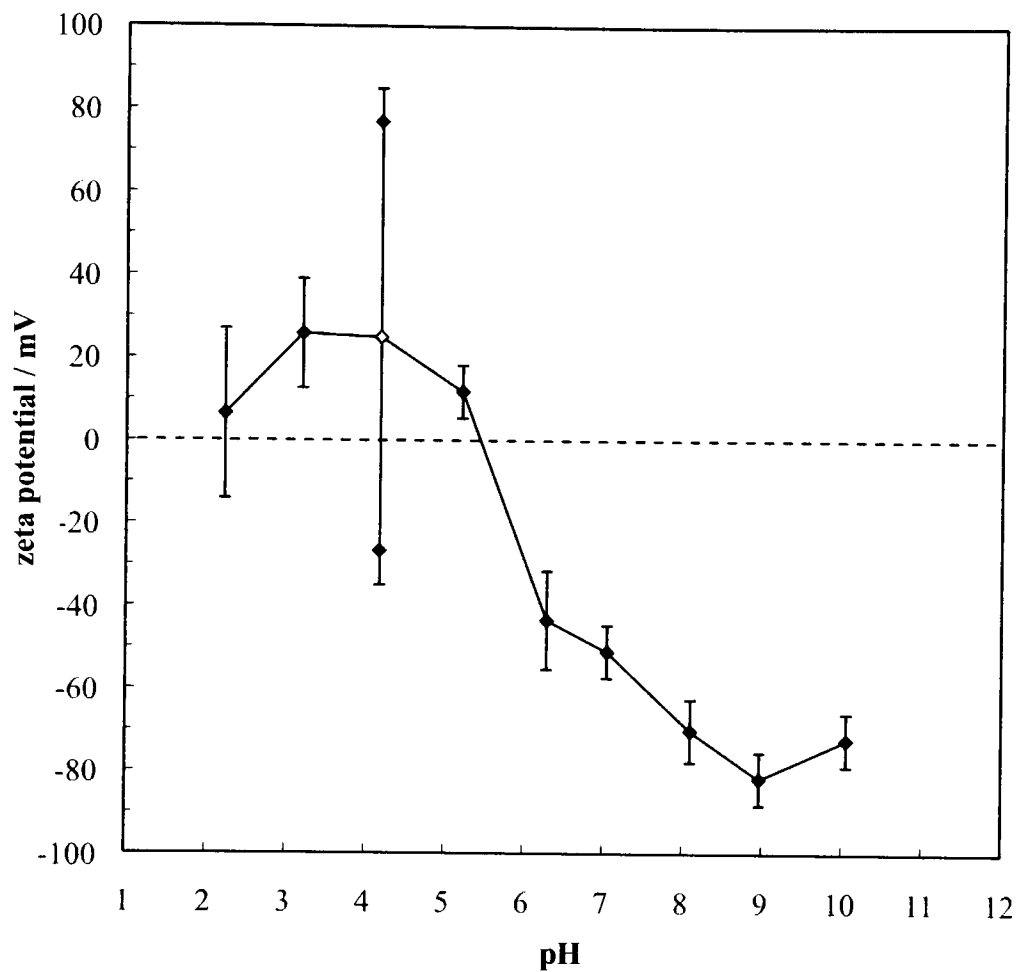


Figure 6.7. Variation of zeta potential of 0.02 wt.% sporopollenin particles dispersed in water under varying pH values from 1 to 10. The error bars represent the distribution of zeta potential, except at pH 4 where a bimodal charge distribution was found.



6.2.3. *Particles at planar fluid interfaces*

The Gel Trapping Technique (GTT) was used to image sporopollenin particles at fluid interfaces under SEM conditions. Both individual particles and aggregates of particles are observed when sporopollenin particles are spread at the water surface (at pH 6.5) and trapped in PDMS to be observed by SEM (Figure 6.8). The particles are immersed to different levels at the air-water interface and their orientations vary. The visible parts of the particles were initially in the water phase: diverse amounts of both the hemisphere side or the Y-fold opening side (or pyramidal side) can be observed, indicating that the particles orientate without preference toward water or air. The different extents of immersion might be due to the particle heterogeneous surface (affecting their wettability), their roughness or to a buoyancy effect resulting from different porosity. The latter effect may cause the sporopollenin to be filled with water to different extents, affecting their position at the interface.

When the particles are injected at the IPM-water interface, similar observations are made: the particles do not exhibit a preferred orientation. In Figure 6.9, the visible parts of the particles, which were initially in the water phase are again either the spherical or the pyramidal side.

Figure 6.8. SEM images at different magnifications of the dry sporopollenin particles spread at the air-water interface and trapped with the GTT. Scale bars represent 10 μm .

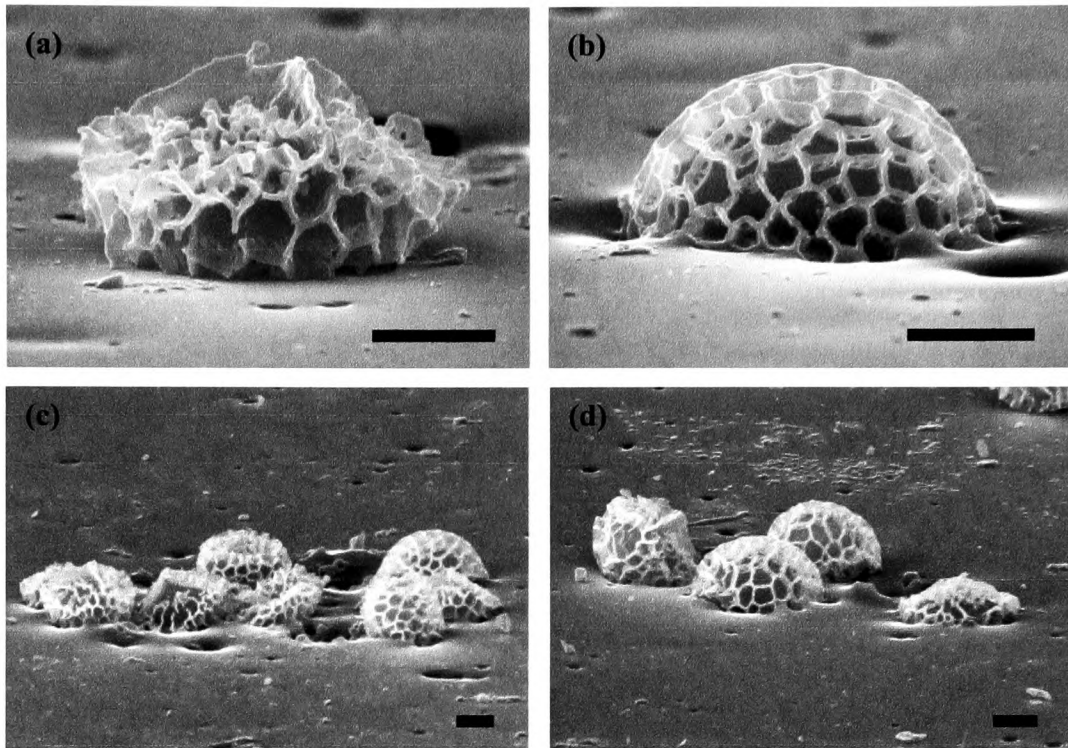
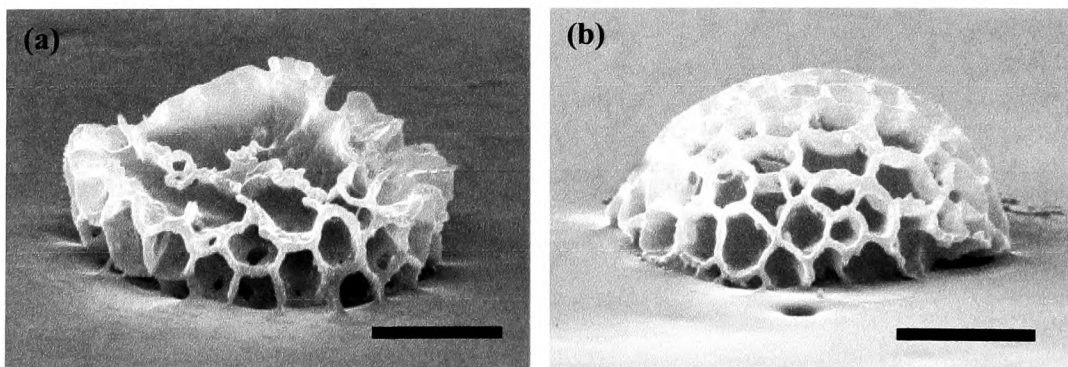


Figure 6.9. SEM images at different magnifications of the sporopollenin particles spread at the IPM-water interface and trapped with the GTT. Scale bars represent 10 μm .

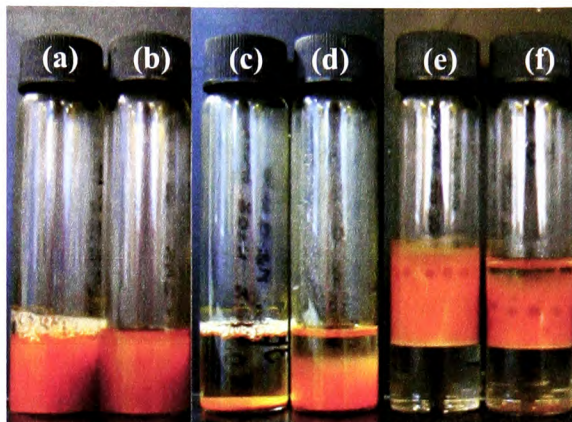


6.3 Emulsification with sporopollenin particles

6.3.1. *Effect of initial particle location*

1 wt.% of sporopollenin particles was either dispersed in isopropyl myristate (IPM) or in Milli-Q water before an equal volume of water or the opposing phase was added for emulsification. In water, some sporopollenin particles stabilised air bubbles, the others sedimented quickly to the bottom of the vessel, as shown in Figure 6.10. When the particles were dispersed in oil, the dispersion was more homogeneous, and the sedimentation although present happened slower. The resulting emulsions with identical composition exhibited really different stability: the emulsion made from the aqueous dispersion was more stable than the one from the oil dispersion. Although equivalent volumes of water were resolved in both cases ($f_{\text{aq}} = 0.82$ for water dispersion and 0.88 for oil), the oil volume originating from coalescence of the emulsion drops is a lot lower for the aqueous dispersion compared with the oil dispersion, respectively $f_{\text{oil}} = 0.06$ and 0.25. A larger concentration of particles sedimented in the water phase was also noted for the oil dispersion emulsion, indicating that the particles relocated from the oil to the water phase.

Figure 6.10. Photographs of 1 wt.% sporopollenin particle dispersions in (a, c) water and (b, d) isopropyl myristate and (e, f) IPM-in-water emulsions made with them respectively. Photographs were taken (a, b) 5 s and (c-f) 1 min. after handshaking. Emulsions were made by 30 s handshaking.



Similar observations have been made with silica-stabilised-emulsions, where the emulsion stability was observed to depend on the initial particle location.¹⁷ Binks and Lumsdon noted that the emulsions were more stable when the particles originated from the emulsion continuous phase. This behaviour is believed to be linked to the contact angle hysteresis of the particles: particles originated in the water and in the oil phase display different contact angles when they adsorb to the interface. Dispersions of the sporopollenin particles in water gave the best emulsion stability, so only this method is employed in the following study.

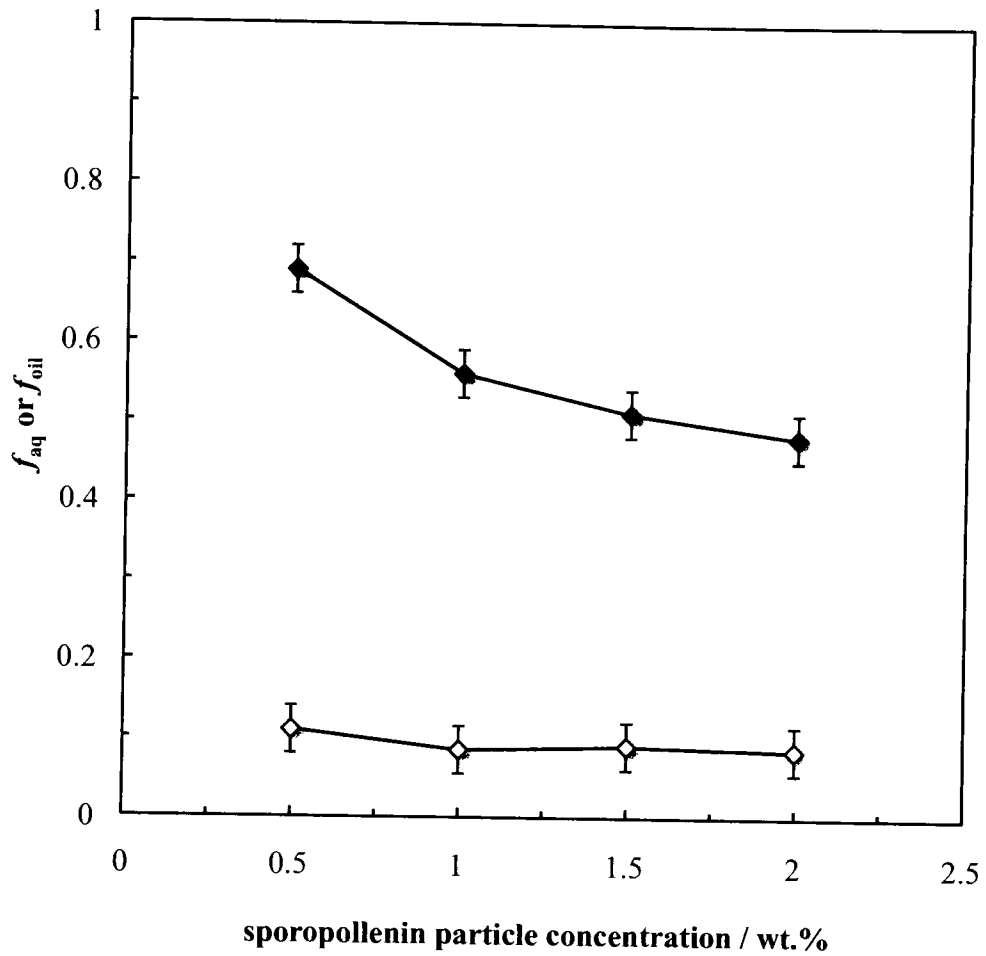
6.3.2. *Effect of particle concentration*

The effect of particle concentration was investigated by increasing the particle quantity in aqueous dispersions. As displayed in Figure 6.6, the natural pH of these particles in water varies with their concentration: from 9.6 at 0.5 wt.% to 10.3 at 2 wt.%. At these pH values, the particles are strongly negatively charged (~ -75 mV in Figure 6.7), so they are expected to stabilise oil-in-water drops regardless of their concentration as they are hydrophilic.¹⁸ All emulsions from the concentration series were IPM-in-water and their increasing stability with concentration can be observed even a month after their initial preparation in Figure 6.11. Figure 6.12 displays the stability of the emulsions after 1 day: with increasing concentration of particles from 0.5 to 2 wt.%, the fraction of coalesced oil diminishes slightly (from $f_{\text{oil}} = 0.11$ to 0.09), and the water resolved decreases sharply from $f_{\text{aq}} = 0.70$ to 0.45.

Figure 6.11. Photographs of 1-month old IPM-in-water emulsions stabilised with (a) 0.5, (b) 1, (c) 1.5, and (d) 2 wt.% sporopollenin particles at pH ~ 10 . Emulsions were made by 30 s handshaking.

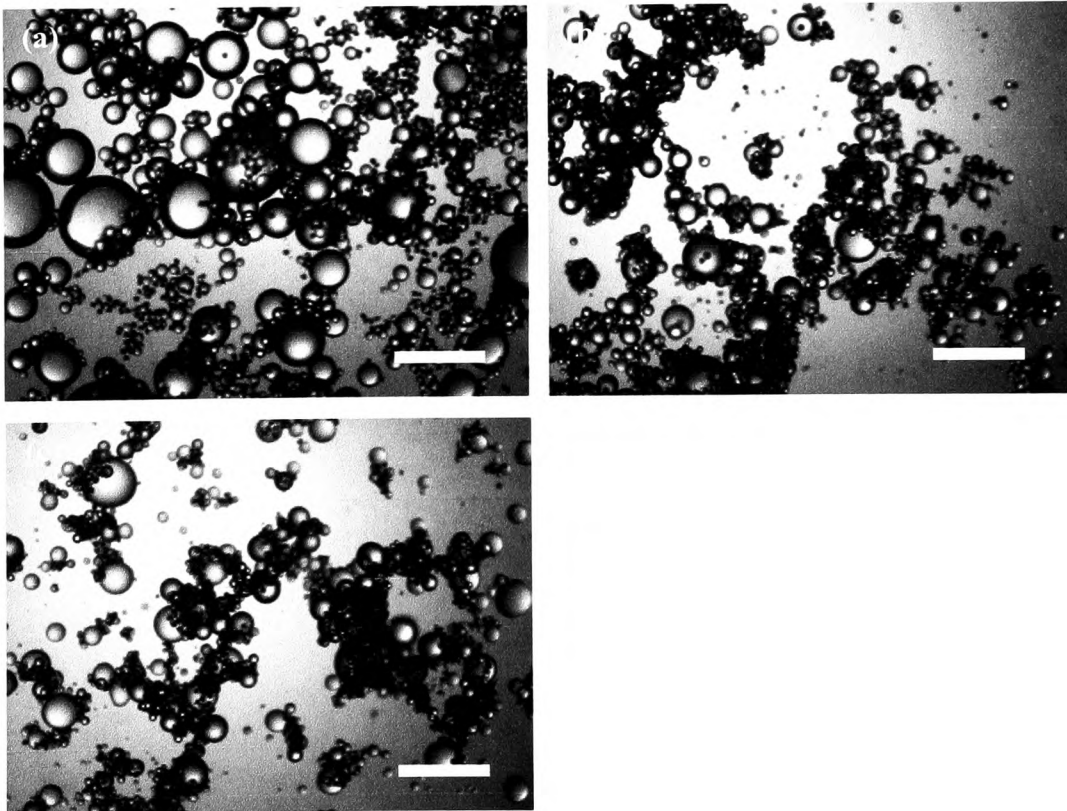


Figure 6.12. Stability of 1-day old IPM-in-water emulsions at pH ~ 10 in terms of (\blacklozenge) f_{aq} or (\diamond) f_{oil} as a function of particle concentration. Emulsions were made by 30 s handshaking.



Although the decrease of coalescence is not marked, the micrographs help explain the decrease in creaming seen in Figure 6.11. Figure 6.13 shows the decrease in emulsion drop diameter upon increasing particle concentration, which explains the subtle decrease in the volume of water resolved from the emulsions. The drops are also polydisperse and display strong aggregation, which appears to be due to particle bridging, as previously observed by Horozov and Binks.¹⁶ It is also interesting to note that the IPM droplets appear sparsely coated with particles, with some drops almost free of particles and some smaller than the particle size. Similar partial drop coverage has been described by Binks *et al.* for the *Lycopodium clavatum* spores in their study, but the possibility of surfactant-like molecules originating from the spores being present should not be totally refuted.¹⁴

Figure 6.13. Optical microscopy images of fresh IPM-in-water emulsions stabilised with 0.5 (a), 1.5 (b), and 2 wt.% (c) sporopollenin particles at pH ~ 10. Emulsions were made by 30 s handshaking. Scale bars represent 400 μm .



6.3.3. Effect of pH

The zeta potential measurements made previously (Figure 6.7) showed that the sporopollenin particle charge was close to zero at pH 5.5 and became increasingly negative above rendering the particles more hydrophilic. Figure 6.14 displays that a transitional type inversion appears to occur within the emulsion series with increasing pH: emulsions are water-in-oil at low pH and oil-in-water at high pH, the inversion happening close to the isoelectric point (between pH 6.5 and 7). A concomitant change in conductivity is observed in Figure 6.15: a slight decrease from pH 3 to 6.5 with lowering ionic strength where conductivity reaches a minimum, is followed by a sharp rise indicating the change to an aqueous continuous phase. This change in conductivity confirms the point of emulsion inversion between pH 6.5 and 7.0.

The stability of the emulsions with varying pH is displayed in Figure 6.16: the abrupt decrease of the fraction of oil resolved associated with the increase of water fraction indicates emulsion inversion above pH 6.5. Contrary to common observations, the stability of this series of emulsions reduced slightly towards the point of inversion:¹⁹⁻²¹ the more stable emulsions are observed at the extreme pH values. Although large drops are observed in the oil-in-water emulsions, they exhibit higher stabilities than the water-in-oil ones.

Figure 6.14. Photographs of 1-week old (a-e) water-in-IPM and (f-j) IPM-in-water emulsions stabilised with 0.5 wt.% sporopollenin particles at pH (a) 3, (b) 4, (c) 5, (d) 6, (e) 6.5, (f) 7, (g) 8, (h) 9, (i) 11 and (j) 12. Emulsions were made by 30 s handshaking.

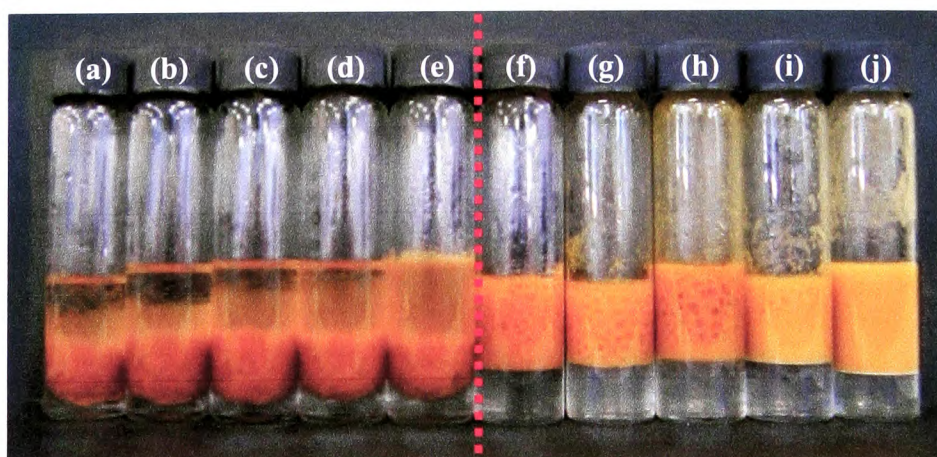


Figure 6.15. Conductivity of water-in-IPM and IPM-in-water emulsions stabilised with 0.5 wt.% sporopollenin particles as a function of pH. The red dotted line indicates phase inversion.

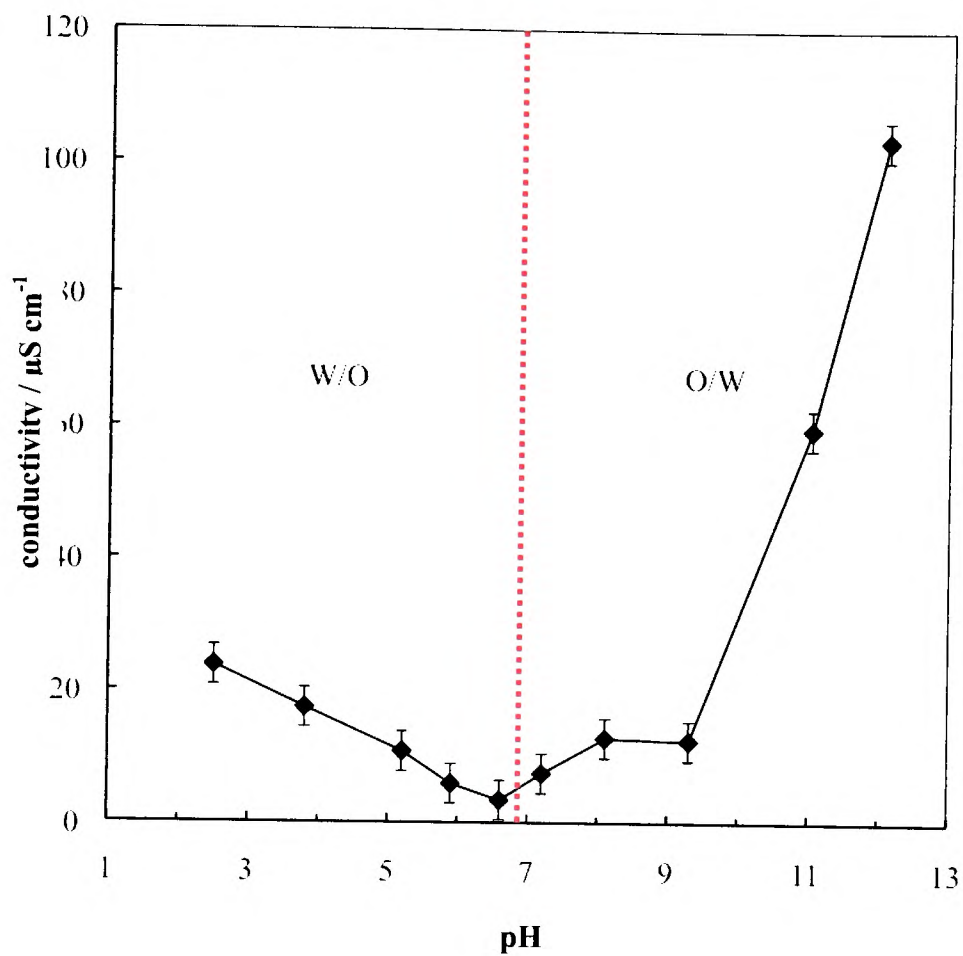
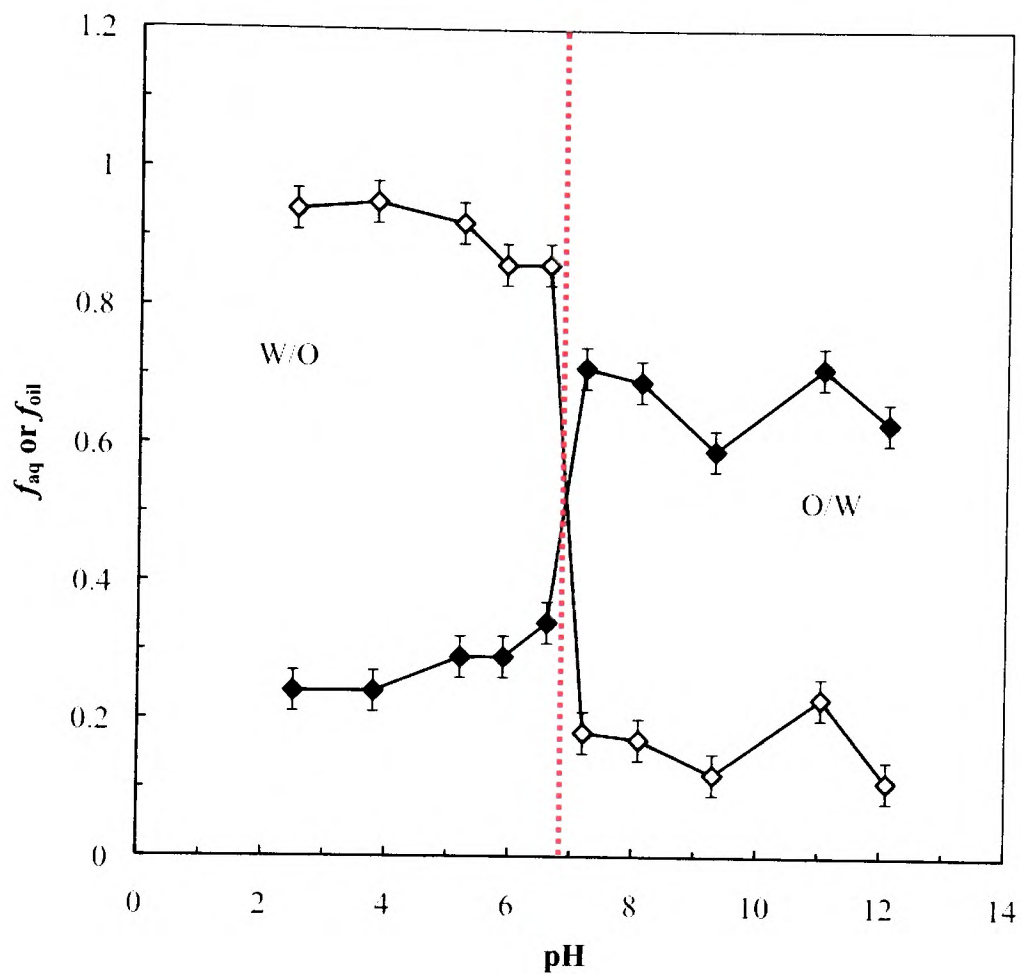
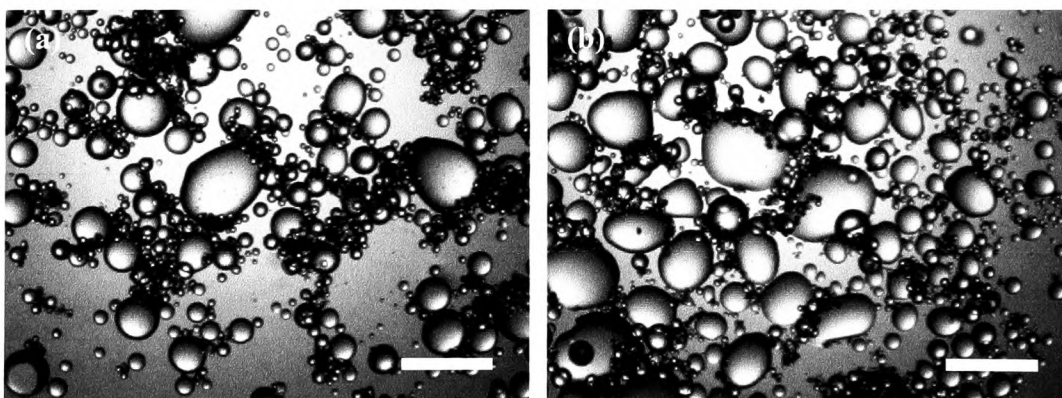


Figure 6.16. Stability of 1-week old water-in-IPM and IPM-in-water emulsions in terms of (\blacklozenge) f_{aq} or (\diamond) f_{oil} as a function of pH. Emulsions were made with 0.5 wt.% sporopollenin particles by 30 s handshaking.



Contrary to oil-in-water, the water-in-oil emulsions ($\text{pH} \leq 6.5$) were observed to undergo limited coalescence immediately after emulsification: the initially small droplets (0.5 mm diameter) coalesce in about 15 seconds to give large ones (4 mm diameter). The water drops covered by an orange particle layer are very stable *in situ* (within the glass vessel), but often break when sampled on microscope glass slides. Microscopy was only performed on the oil-in-water emulsions at high pH, as sampling was not possible for the large oil drops formed below pH 8 due to their instability. The micrograph images in Figure 6.17 show emulsions at pH 9 and 11 with very polydisperse and aggregated drops barely coated by particles. From the photos in Figure 6.14, the average drop size is believed to decrease with pH: the large drops at pH 7 cannot be observed at pH 12. However, in Figure 6.17 the drops display an increased size between pH 9 and 11, which might be due to coalescence of the drops onto the microscopy cell cover slip.

Figure 6.17. Optical microscopy images of fresh IPM-in-water emulsions stabilised with 0.5 wt.% sporopollenin particles at pH (a) 9 and (b) 11. Emulsions were made by 30 s handshaking. Scale bars represent 400 μm .



The pH series was reproduced at a higher particle concentration to enable sampling and microscopy observations: at 2 wt.% the emulsions stabilised with sporopollenin particles still display transitional inversion from water-in-IPM to IPM-in-water with increasing pH (Figure 6.18). The emulsions also exhibited visibly large drops close to the inversion point, as they did at 0.5 wt.% particles. The inversion point occurs at a slightly lower pH value, between pH 5 and 6, indicating that particle concentration affects the emulsion type.

The micrographs of these emulsions, displayed in Figure 6.19, highlight the difference between the water-in-IPM and the IPM-in-water emulsions: water drops, which underwent limited coalescence are densely coated with particles and exhibit larger diameters (0.4 and 2 μm), whereas the smaller oil drops are sparsely covered with particles. The latter observation is similar to the one made on spore-stabilised emulsions, and can explain the smaller size of the oil drops:¹⁴ as less particles are needed to stabilise the larger oil-water interface. The micrographs also show that the water drops are discrete, whereas the oil ones aggregate together, probably due to bridging of the droplets by the particles resulting in their stability at low particle coverage.

Figure 6.18. Photographs of 1-week old (a-c) water-in-IPM and (d-j) IPM-in-water emulsions stabilised with 2 wt.% sporopollenin particles at pH (a) 3, (b) 4, (c) 5, (d) 6, (e) 7, (f) 8, (g) 9, (h) 10, (i) 11 and (j) 12. Emulsions were made by 30 s handshaking.

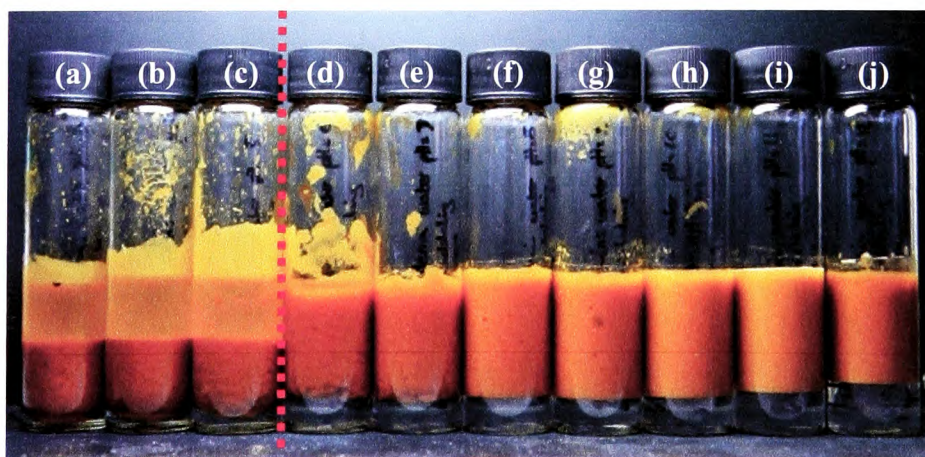
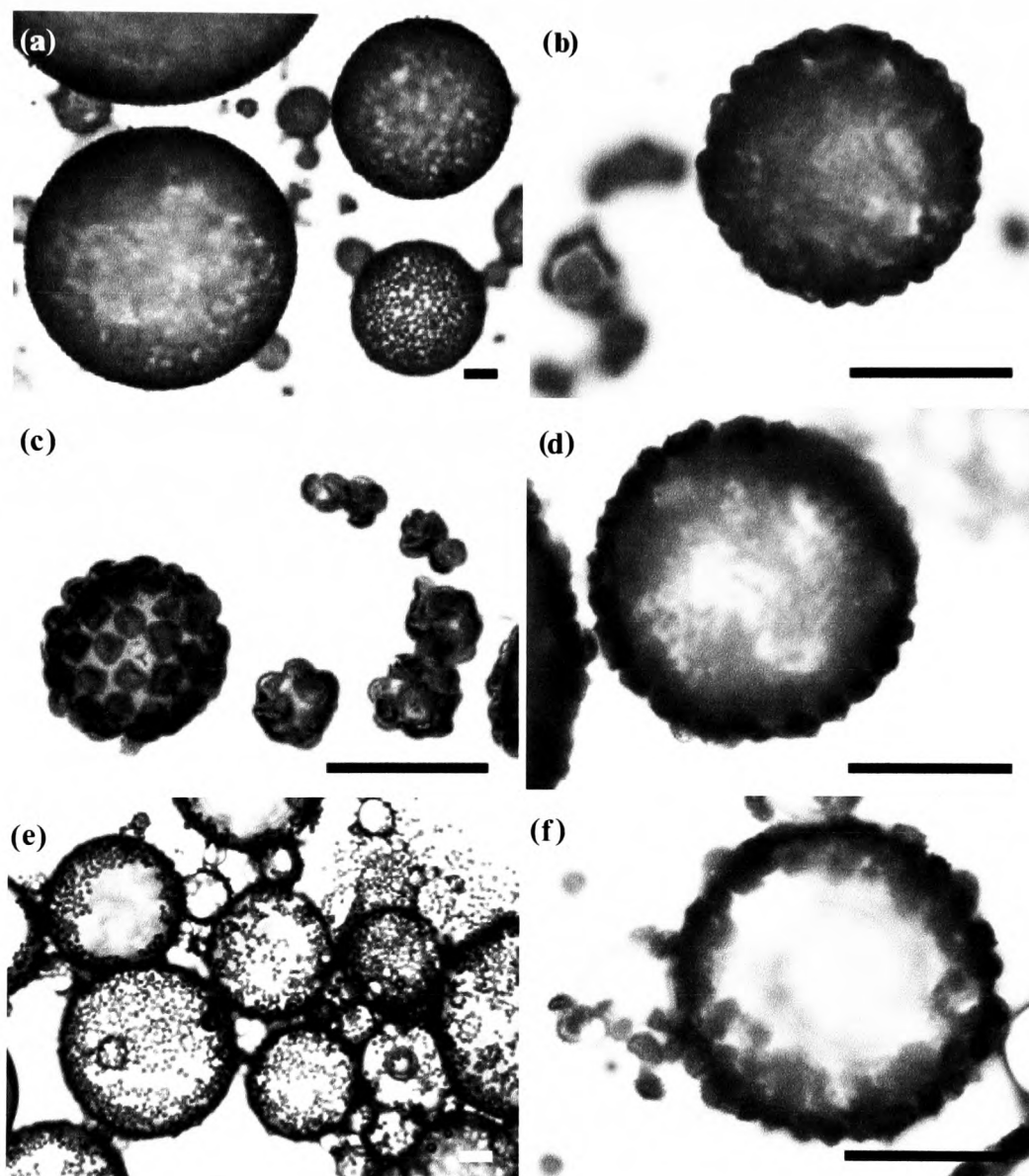


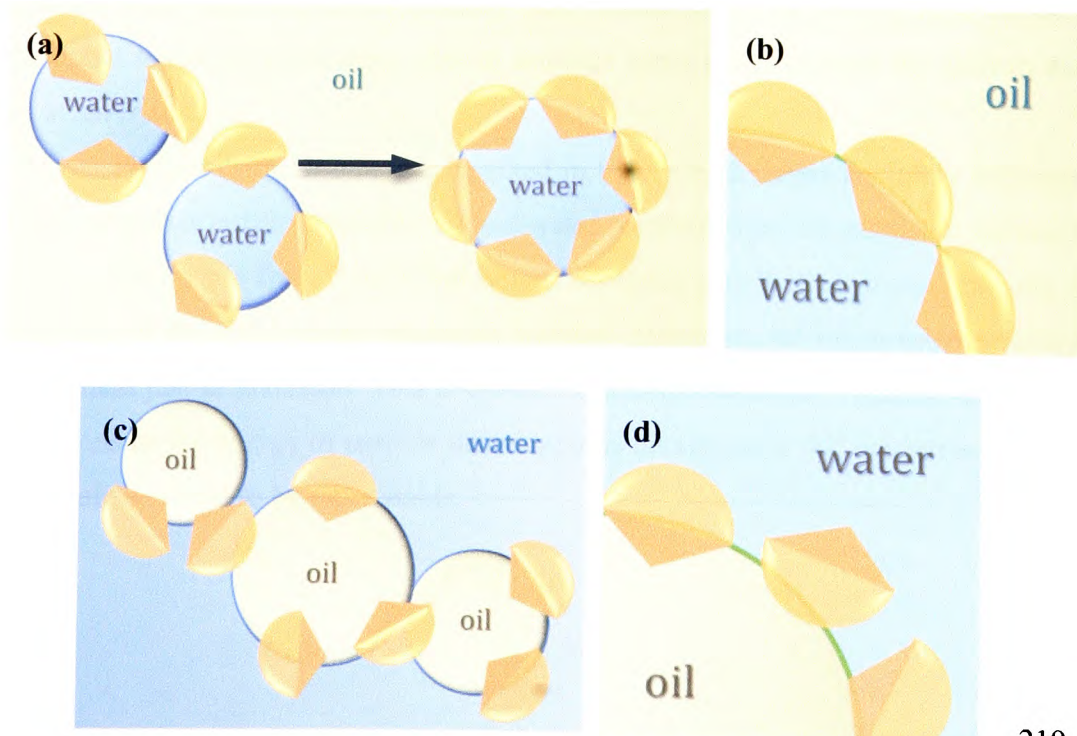
Figure 6.19. Optical microscopy images of fresh (a-d) water-in-IPM and (e-f) IPM-in-water emulsions stabilised by 2 wt.% sporopollenin particles at pH (a-b) 3, (c) 4, (d) 6 and (e-f) 8. Emulsions were made by 30 s handshaking. Scale bars represent 150 μm .



Another major difference between the particles at water and at oil drop surfaces appears by observing the micrographs in Figure 6.19: in the water-in-oil emulsions, the particles adsorb preferentially with their hemispherical side toward the oil phase and their Y-opening toward the water, while their orientation is random in the IPM-in-water emulsions. The preferred orientation around the water can be caused either by heterogeneity in the sporopollenin surface property, with the hemispherical side being perhaps more hydrophobic than the pyramidal one, or by the efficiency of close packing the particle with this geometry, as represented in Figure 6.20. The particles stabilising the oil drops, however, cannot exhibit a preferred orientation as they bridge several drops with different parts of their surface and the particles are not close-packed.

No preferred orientation was noticed when particles were spread and then trapped at the IPM-water interface at pH 6.5 (*cf.* § 6.2.3): either the method did not reproduce the same mechanism of adsorption as in the emulsion or the pH above that of phase inversion meant that no definitive orientation was preferred.

Figure 6.20. Representation of (a) the limited coalescence process occurring in the water-in-IPM emulsions which may cause the (b) preferred orientation of the sporopollenin particles, and of (c) the drop bridging by the sporopollenin particles in IPM-in-water emulsions rendering the (d) particle orientation random.



Increasing the concentration of particles in the IPM system causes a decrease in drop size, but also a decrease of the inversion pH. This latter decrease means that more hydrogen ions are needed to render particles hydrophobic, possibly due to a different aggregation state of the particles which alter their wettability.^{22, 23}

6.3.4. Effect of oil type

The effect of oil type was studied by replacing the isopropyl myristate, an ester oil with an interfacial tension with water of 28.6 mJ m^{-2} , by the straight-chain alkane dodecane ($\gamma_{ow} = 52.5 \text{ mJ m}^{-2}$) or the triglyceride tricaprylin ($\gamma_{ow} = 13.3 \text{ mJ m}^{-2}$). These series were produced with 0.5 wt.% of sporopollenin and can be compared with the IPM series in Figure 6.14.

6.3.4.1 Tricaprylin

Replacing IPM by tricaprylin was expected to lead to better emulsion stability and smaller drop diameter because of the lower interfacial tension with water which should assist drop break-up during handshaking.¹⁷ Like the IPM series, the tricaprylin emulsions exhibit transitional inversion from water-in-oil to oil-in-water, but at a higher pH value (Figure 6. 21), exhibiting greater hydrophobicity at the tricaprylin-water interface. This can be rationalised through consideration of the particle-oil tension. It is likely that more polar tricaprylin wets the surface active particles more than the lower polarity oils, consequently increasing their contact angle and rendering them more able to stabilise water drops causing the shift in the pH at inversion.

The emulsion stability represented in Figure 6.22 shows a slightly different trend compared to IPM: both the oil and water resolved from the emulsion decrease with increasing pH from 3 to 9, but before inversion they both increase, causing a minimum in the water-in-oil emulsions stability. However, the oil-in-water stability is maximal just at inversion. This is classic behaviour observed in particle-stabilised emulsions as the energy of particle detachment is maximum at 90° contact angle and the emulsions tend to be more stable.

Due to the low particle concentration used, it was difficult to compare the IPM and the tricaprylin series: the emulsion drops of the latter exhibit very low stability in terms of mechanical resistance to motion, big water drops coalescing easily during sampling. The fact that this behaviour is more evident in the tricaprylin series is likely due to the lower oil-water interfacial tension, which results in lower particle attachment energy particularly away from the phase inversion point.

Figure 6.21. Photographs of 1-week old (a-h) water-in-tricaprylin and (i-j) tricaprylin-in-water emulsions stabilised with 0.5 wt.% sporopollenin particles at pH (a) 3, (b) 4, (c) 5, (d) 6, (e) 7, (f) 8, (g) 9, (h) 10, (i) 11 and (j) 12. Emulsions were made by 30 s handshaking.

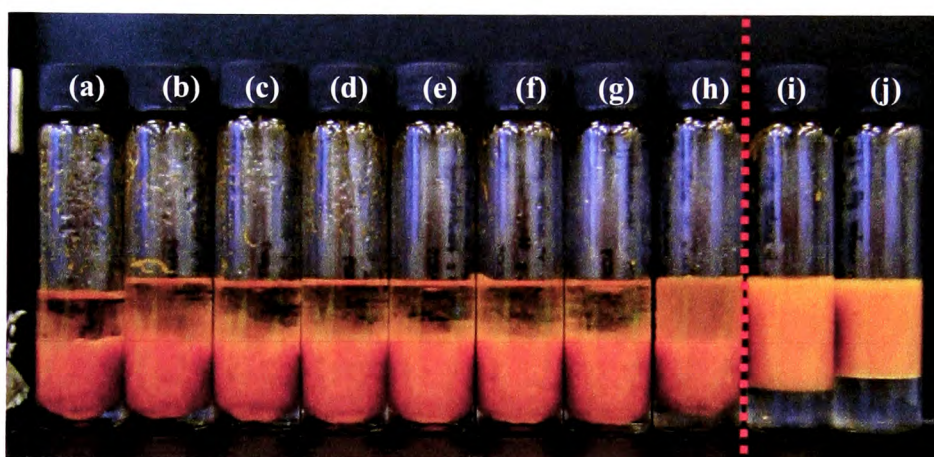
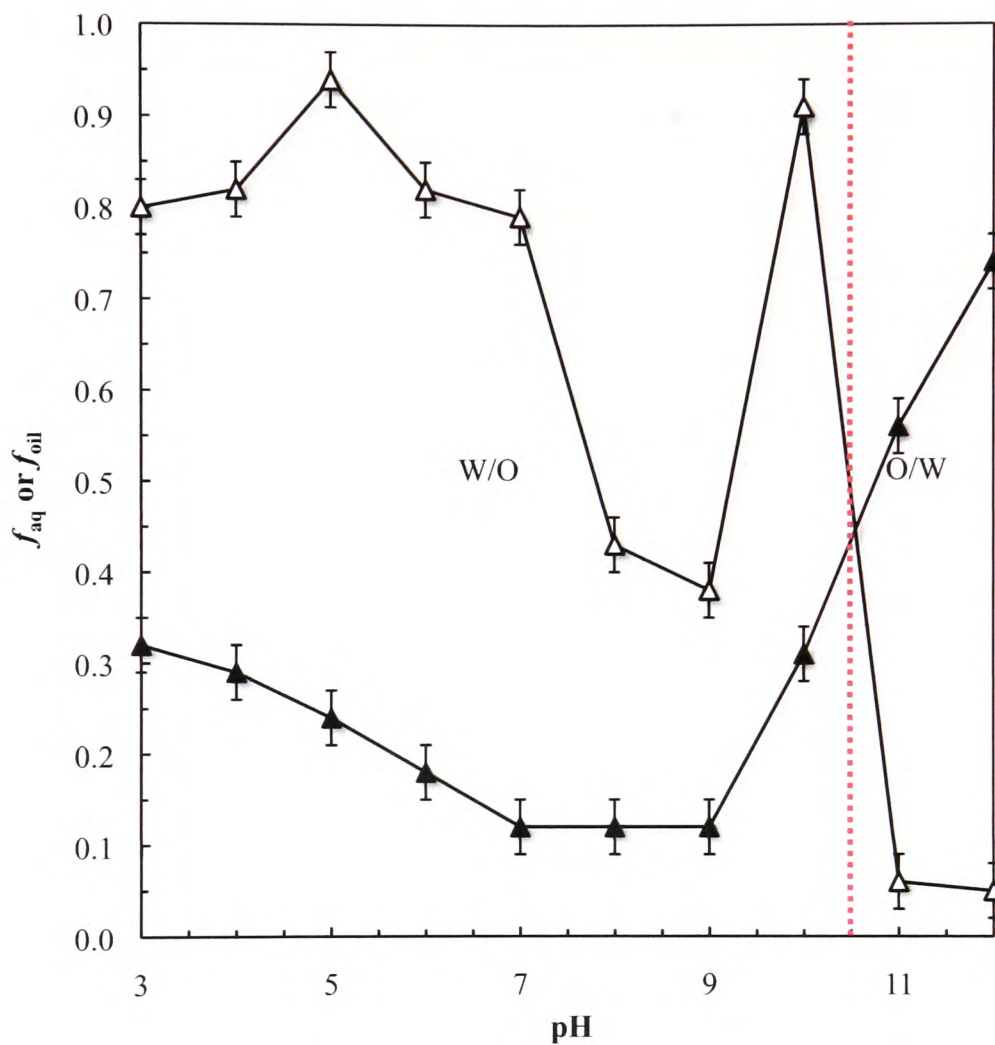


Figure 6.22. Stability of 1-week old water-in-tricaprylin and tricaprylin-in-water emulsions in terms of (\blacklozenge) f_{aq} or (\blacktriangle) f_{oil} as a function of pH. Emulsions were made with 0.5 wt.% sporopollenin particles by 30 s handshaking.



The microscopy images are not representative of the drop size as the sampling process favours the small drop populations. However, Figure 6.23 enables comparison between water and oil drops: water-in-oil emulsion drops are more densely covered with particles than the oil drops, and as a result smaller oil drops can be stabilised. Like previously observed (*cf.* § 6.3.3), particles adsorbing around water drops orientate preferentially their hemispherical side toward the oil phase (Figure 6.23b), while no preference is observed for the tricaprylin-in-water emulsions.

When Figures 6.14 and 6.21 are compared, the drop diameter of the visible water drops appears to be larger for the tricaprylin series. In Figure 6.24, measurements of the tricaprylin emulsion drops was realised by two different means: the large water drops, which were not stable to sampling, were measured with a ruler, while the stable small drop population was measured *via* microscopy. Along with the volumes of water and oil resolved, the large and small drop diameters both decrease with increasing pH up to pH 9, then a slight increase in size for the water-in-oil emulsion drops happens before inversion. The oil drops display smaller size than the corresponding water drops in oil, as can be expected from the high stability of the emulsions and the small number of particles needed to stabilise the sparsely covered drops.

Figure 6.23. Optical microscopy images of fresh (a, b) water-in-tricaprylin and (c-f) tricaprylin-in-water emulsions stabilised with 0.5 wt.% sporopollenin particles at pH (a, b) 3, (c, d) 11 and (e, f) 12. Emulsions were made by 30 s handshaking. Scale bars represent 200 μm .

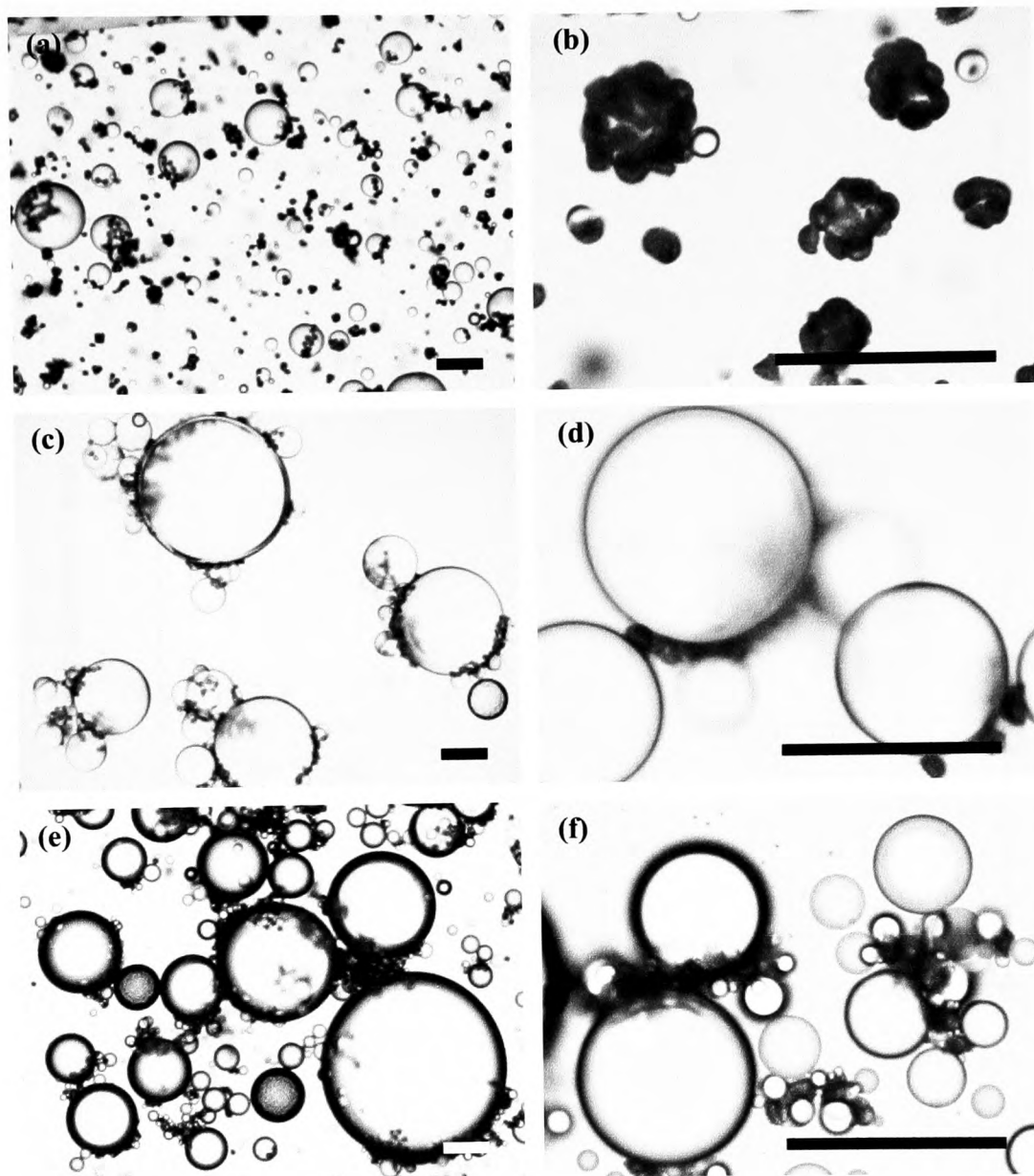
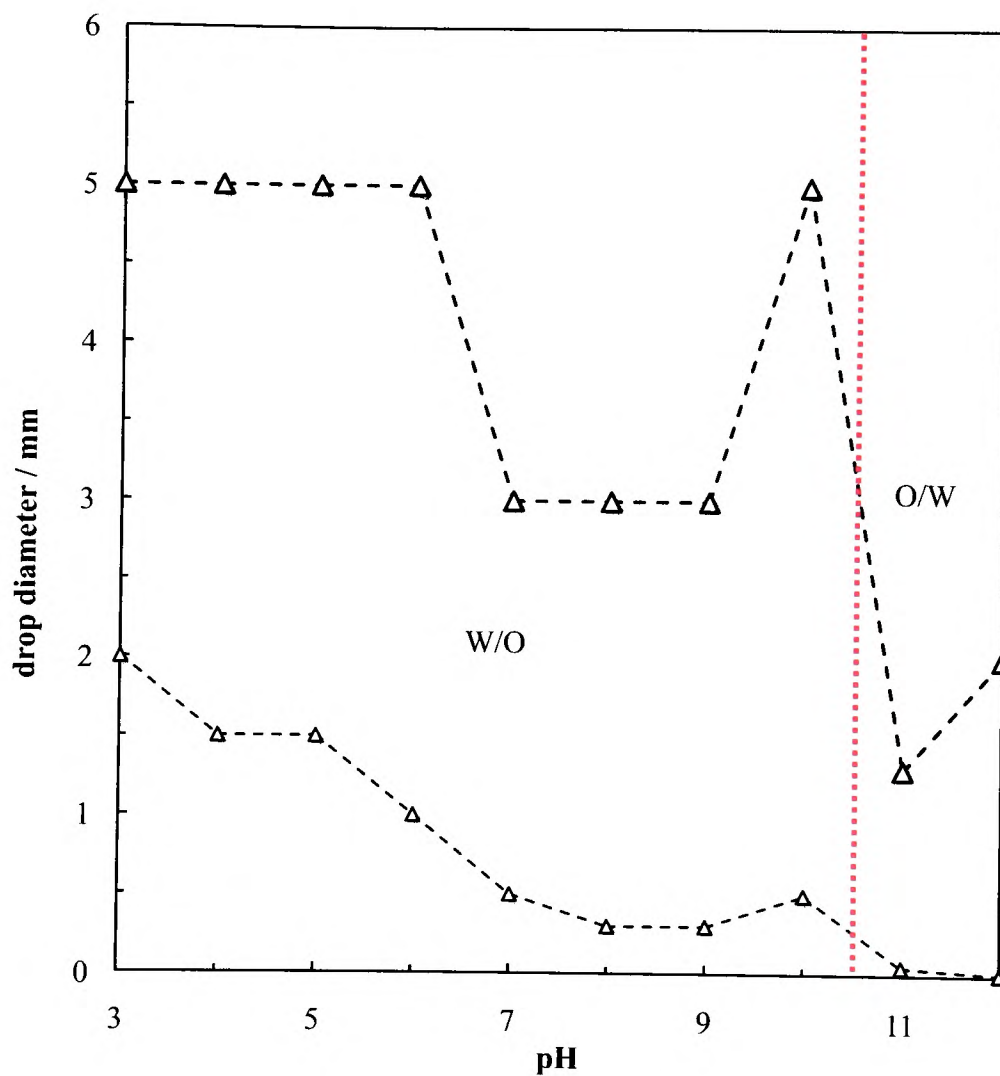


Figure 6.24. Small (\triangle) and large (Δ) drop diameters of water-in-tricaprylin and tricapylin-in-water emulsions as a function of pH, 5 minutes after emulsification. The small drop diameters were taken from microscopy images, the large diameters were taken with a ruler *in situ*. Emulsions were made with 0.5 wt.% sporopollenin particles by 30 s handshaking.



6.3.4.2 Dodecane

Emulsions made with the high oil-water tension dodecane oil exhibit transitional inversion from water-in-dodecane to dodecane-in-water emulsions at lower pH values than the two other oils as confirmed by drop test analysis. The affinity of the particles for dodecane is lower than for IPM or tricaprylin. In this case, more hydrons are needed to render the particle hydrophobic enough to stabilise water-in-oil emulsions. It can also be noted in Figure 6.25 that the volume of water resolved in the water-in-oil emulsions is much larger than in the two other oils series, indicating that the higher interfacial tension of the dodecane with water renders the rupture of the oil-water interface more difficult with handshaking, so less water can be emulsified.

Figure 6.25. Photographs of 1-week old (a-c) water-in-dodecane and (d-j) dodecane-in-water emulsions stabilised with 0.5 wt.% sporopollenin particles at pH (a) 3, (b) 4, (c) 5, (d) 6, (e) 7, (f) 8, (g) 9, (h) 10, (i) 11 and (j) 12. Emulsions were made by 30 s handshaking. Scale bar represents 1 cm.

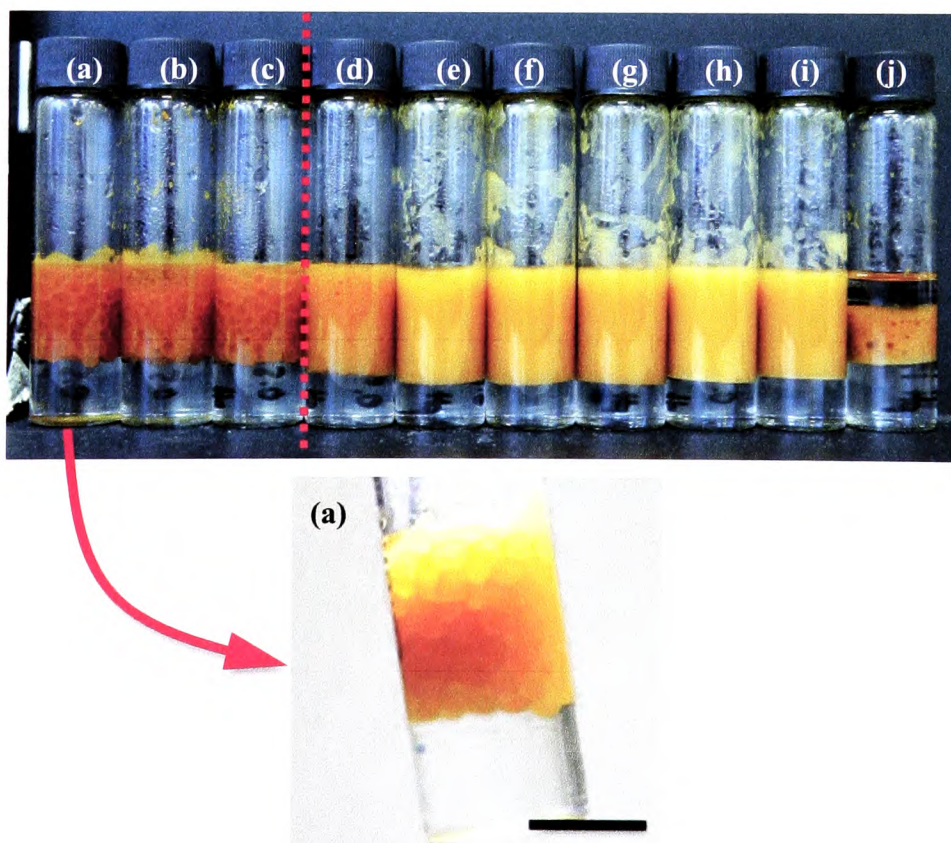


Figure 6.26 displays the emulsion stability: both the water-in-oil and the oil-in-water emulsions exhibit constant stabilities to coalescence over most of the pH range, with the oil-in-water being slightly more stable to creaming than the water-in-oil. This constant stability fits what was expected, in a similar manner to the IPM series, as in high oil-water tension systems the detachment energy of the particle is high for all contact angles. At high pH however, the oil-in-water emulsions are very unstable, which could be due to the particles being too hydrophilic to adsorb strongly at the oil-water interface.

The large water drops, which are shown in the close-up photograph of Figure 6.25(a), were highly stable *in situ* but could not be sampled for microscopy. Figure 6.27 displays only the micrographs of dodecane-in-water emulsion drops. Similarly to the two previous series, the oil drops exhibit a sparse coverage by the sporopollenin particles and no preferred orientation of the particles is observed. However, the drops are highly polydisperse and form aggregates; polydispersity, aggregate size and drop size seem to concomitantly decrease with increasing pH.

This observation is confirmed by the drop diameter measurements in Figure 6.28: the diameter of the emulsion drops decreases constantly along the pH series, with water drops displaying diameters up to 20 times larger than those of oil. Although smaller, the oil drops exhibit much higher polydispersity than the water-in-oil drops. This is expected as the water drops have undergone limited coalescence to a greater extent, which has been shown previously to provide quite monodisperse particle-stabilised droplets.²⁴

Figure 6.26. Stability of 1-week old water-in-dodecane and dodecane-in-water emulsions in terms of (■) f_{aq} or (□) f_{oil} as a function of pH. Emulsions were made with 0.5 wt.% sporopollenin particles by 30 s handshaking.

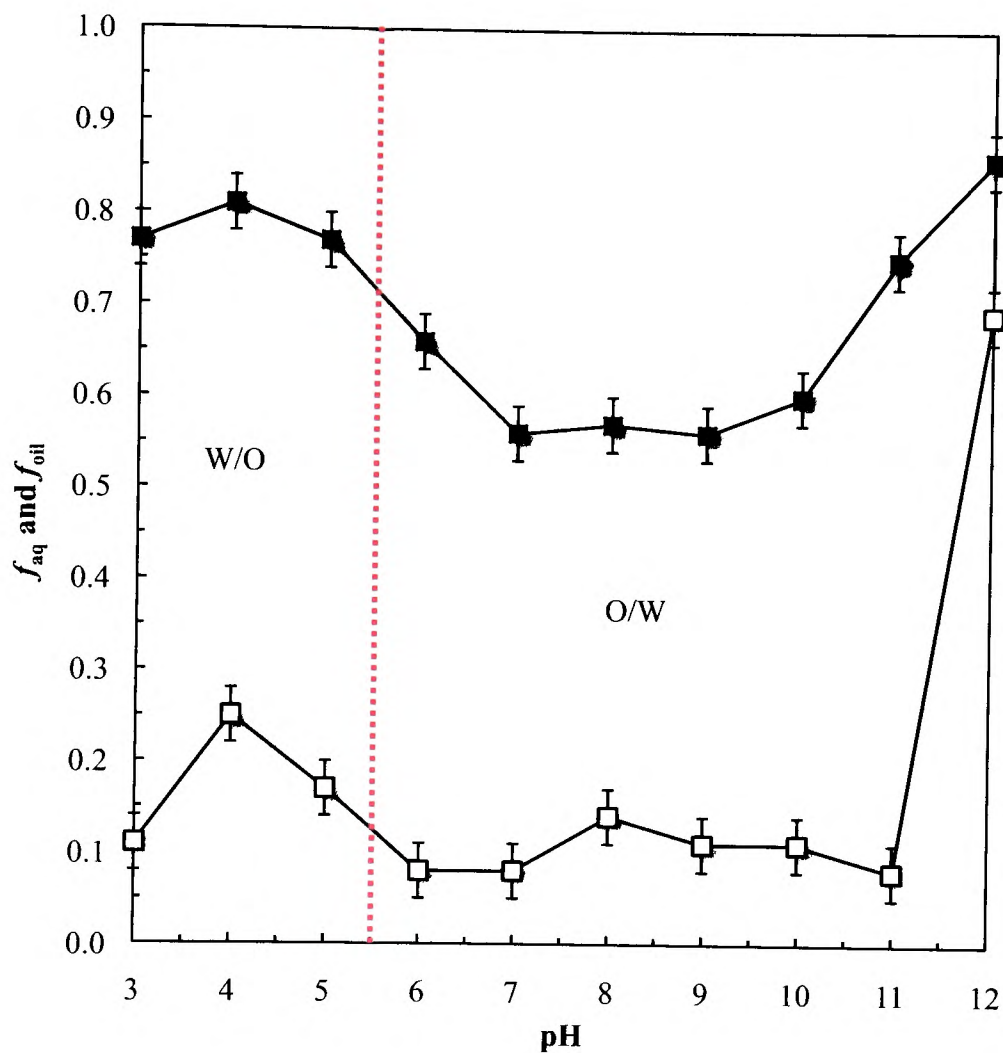


Figure 6.27. Optical microscopy images of fresh dodecane-in-water emulsions at pH (a) 6, (c) 9, (d) 10 and (d) 12. Emulsions were made with 0.5 wt.% sporopollenin particles by 30 s handshaking. Scale bars represent 400 μm .

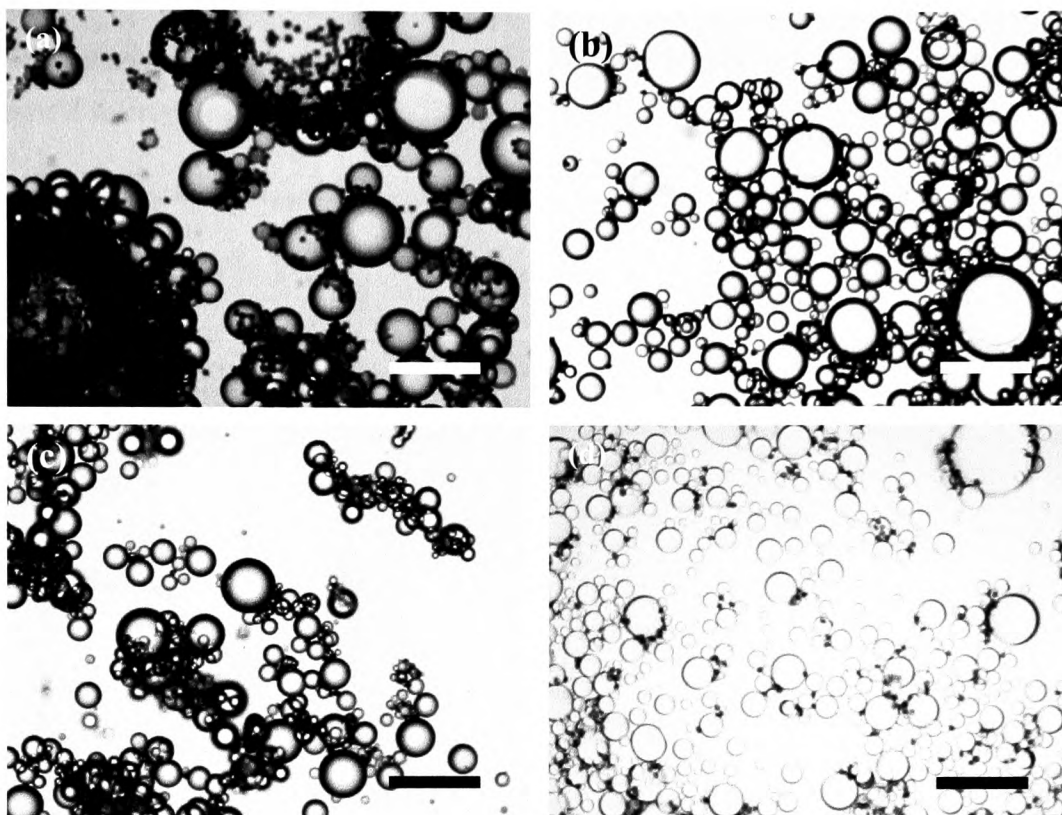
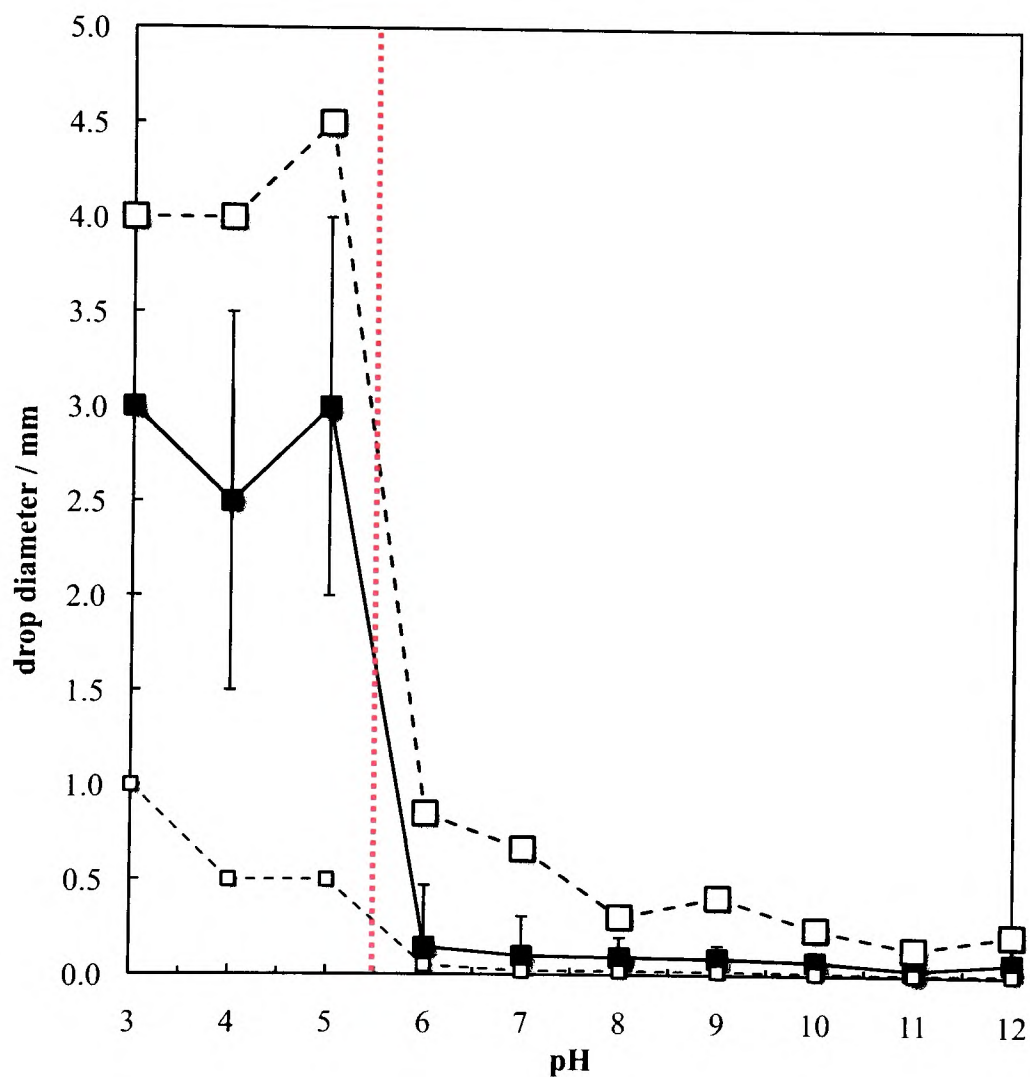


Figure 6.28. (■) Average, (□) minimum and (□) maximum drop diameter of water-in-dodecane and dodecane-in-water emulsions as a function of pH, 5 minutes after emulsification. The error bars represent the standard deviation. Emulsions were made with 0.5 wt.% sporopollenin particles by 30 s handshaking. The water drops at pH 3 to 5 were measured *in situ*, whereas the oil drops at pH above 6 were measured from optical micrographs.



6.4 Liquid marbles with sporopollenin particles at the air-water surface

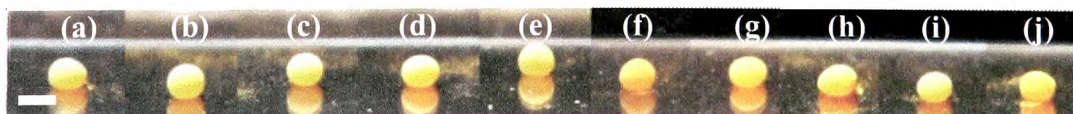
As they were observed to adsorb at the air-water surface when dispersed in water (*cf.* Figure 6.5), it was believed that sporopollenin particles might stabilise liquid drops coated with particles, also known as “liquid marbles”. The effect of pH was investigated to enable comparison between the emulsions and the liquid marbles systems: the sporopollenin particles stabilise opposite types of emulsion at high and low pH, so they might be able to stabilise liquid marbles only upon a narrow pH range. As a buckling phenomenon linked to water evaporation was observed, the effect of salt concentration on this phenomenon was investigated.

6.4.1. Effect of pH

In the previous part, sporopollenin particles were used to stabilise emulsions at different pH and it was observed that transitional inversion of the emulsion occurred linked to their charge change (*cf.* § 6.2.2). It was believed that the pH of the liquid marbles should therefore affect their stability in that at high pH the particles maybe too hydrophilic to stabilise water-in-air systems.²⁵

Liquid marbles were produced over a large range of pH (1-10), and as Figure 6.29 displays, they exhibited similar stabilities: all of them were easy to form, and they were able to roll on a clean glass slide, as well as bounce against a glass wall or against other liquid marbles without breaking. However, another aspect of the liquid marbles was noted after several minutes: as the encapsulated water evaporated, the marbles were seen to shrink with their surface buckling.

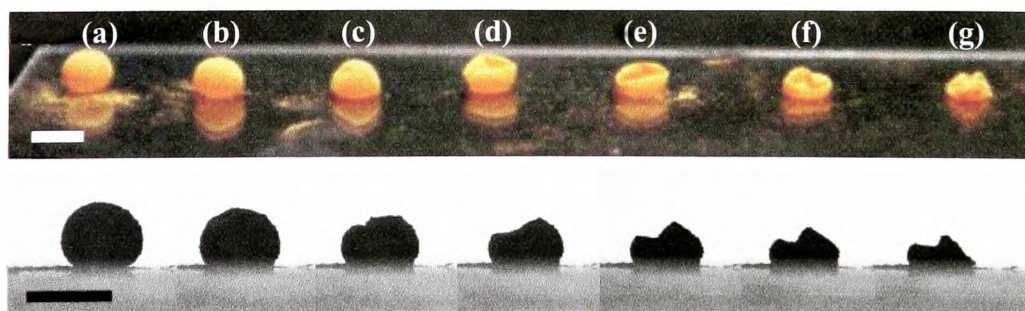
Figure 6.29. Photographs of liquid marbles on glass slide stabilised by sporopollenin particles 30 s after formation, at pH (a) 1, (b) 2, (c) 3, (d) 4, (e) 5, (f) 6, (g) 7, (h) 8, (i) 9, and (j) 10. Scale bar represents 2 mm.



6.4.2. Evaporation and buckling

Xu *et al.* have studied the shrinkage of water droplets covered with polystyrene particles in decane oil.²⁶ They found that upon reducing the volume of the drops, which leads to a surface area decrease, the interfacial particles undergo a liquid film to solid film transition: collapse of the drop shell happened when deflating the drop, but was noted to be reversible. The onset of buckling occurred at the top of the emulsion drop for drops which were large relative to the capillary diameter, whereas dimpling occurs at random locations for small drops. The liquid marbles stabilised with the sporopollenin particles can be compared with the drops of this study: as displayed in Figure 6.30, liquid marbles collapse and the drop surface buckles as the water evaporates as the drop size is close to the capillary length (~ 2 mm). The interface containing the sporopollenin particles closes as the water within the marble evaporates and the particles become denser on the liquid surface. Finally the marble buckles because the particles have reached their maximum packing density. Dandan and Erbil noticed this same buckling phenomenon with graphite liquid marbles, and observed that the evaporation rate of the water was slowed down, nearly by half the time, thanks to the presence of the particles at the water drop surface.²⁷

Figure 6.30. Upper-photographs and lower-DSA images of the change with time of a liquid marble at pH 6.5 stabilised by sporopollenin particles let to dry (evaporate) at 25°C and 66% relative humidity at (a) 30 s, (b) 5, (c) 10, (d) 15, (e) 20, (f) 25, and (g) 30 min. Scale bars represent 2 mm.



Evaporation and shrinking of the liquid marbles was estimated by eye and the effect of the pH on them was investigated. Figure 6.31 shows the change of liquid marble shape during 30 min. at 5 different pH values: the quickest evaporation and shrinking was recorded for the liquid marble at pH 8 and the lowest at pH 6. The total buckling time, corresponding to the time after which the shape of the marble does not change, was found to be 90 minutes at pH 8 decreasing to 60 at pH 6 (Table 6.1). However, although the temperature was kept constant at 19 ± 1 °C the relative humidity (ratio of the partial pressure of water vapour to the saturated vapour pressure of water) varied from $24 \pm 5\%$ at pH 8 to $55 \pm 5\%$ at pH 6, rendering it difficult to conclude if the effect of pH or that of relative humidity was prevailing. The little effect of pH might be because the water does not equilibrate with the entire particle surface during formation.

The shape change of the liquid marbles was observed to be affected by the rate of evaporation: the drops kept a uniform shape while shrinking at the lowest evaporation rate (comparing Figures 6.31 at pH 2 and 8), possibly by a rearrangement of the particles at the drop surface to occupy less space and not deform the water film.

Figure 6.31. Photographs of time evolution of 10 μL liquid marbles stabilised by sporopollenin particles, at pH given. Photographs were taken at (a) 30 s, (b) 5, (c) 10, (d) 15, (e) 20, (f) 25 and (g) 30 min. after formation. The room temperature was 19 $^{\circ}\text{C}$ and variable humidity 24-55%.

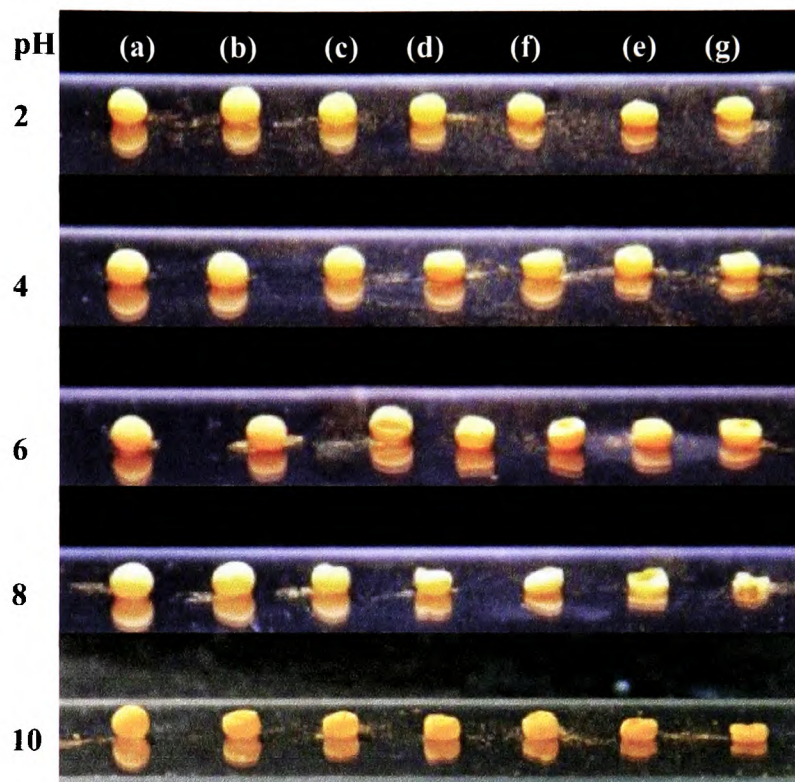
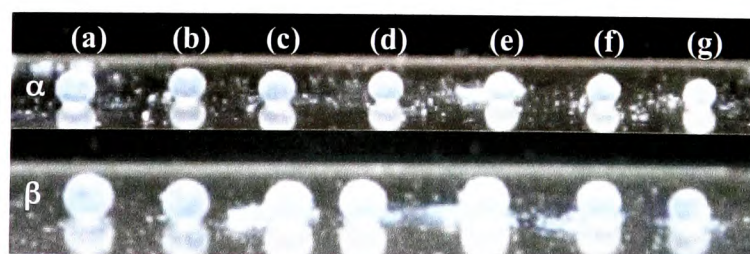


Table 6.1. Time of total buckling of the sporopollenin liquid marble at different internal pH values.

pH	2	4	6	8	10
Total buckling time / min.	75	80	90	60	65

To understand the origin of the buckling, a short investigation of liquid marbles stabilised by hydrophobic silica particles was done. Their production was found to be more difficult than that made with the sporopollenin particles: they exhibit a weaker stability on glass substrates and break under the smallest shock. These observations could result from a lower surface activity of the silica particles compared to the sporopollenin ones at the air-water interface. The better stability of the sporopollenin-stabilised liquid marbles might be due to their large size resulting in both a stronger adsorption and a larger distance between the water surface and the glass substrate. The evaporation and shrinking of the silica-stabilised liquid marbles are slower and appear different to that observed with the sporopollenins: Figure 6.32 shows that the liquid marbles keep a spherical shape during their evaporation and some desorbed particles can be observed under the marbles. It was also noted that their total shrinking took twice the time needed by the sporopollenin stabilised ones, in equivalent temperature and humidity conditions; this might be caused by a closer packing of the silica particles on the drop surface, hindering the water evaporation. However, their lower stability and persistent spherical shape might indicate a less strong adsorption of silica particles onto the drop surface: the particles do not cause buckling of the drop surface instead they desorb from the interface, enabling it to keep its spherical shape.

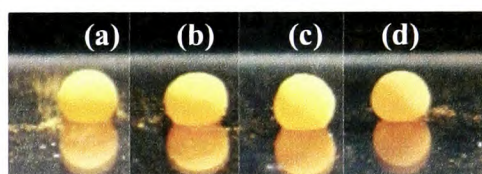
Figure 6.32. Photographs of a time evolution of liquid marbles stabilised by (α) 20 and (β) 14% SiOH silica particles at pH 6. Photographs were taken at (a) 30 s, (b) 5, (c) 10, (d) 15, (e) 20, (f) 25 and (g) 30 min. after formation. The room temperature was 19 °C and the humidity 32 %.



6.4.3. *Effect of salt concentration*

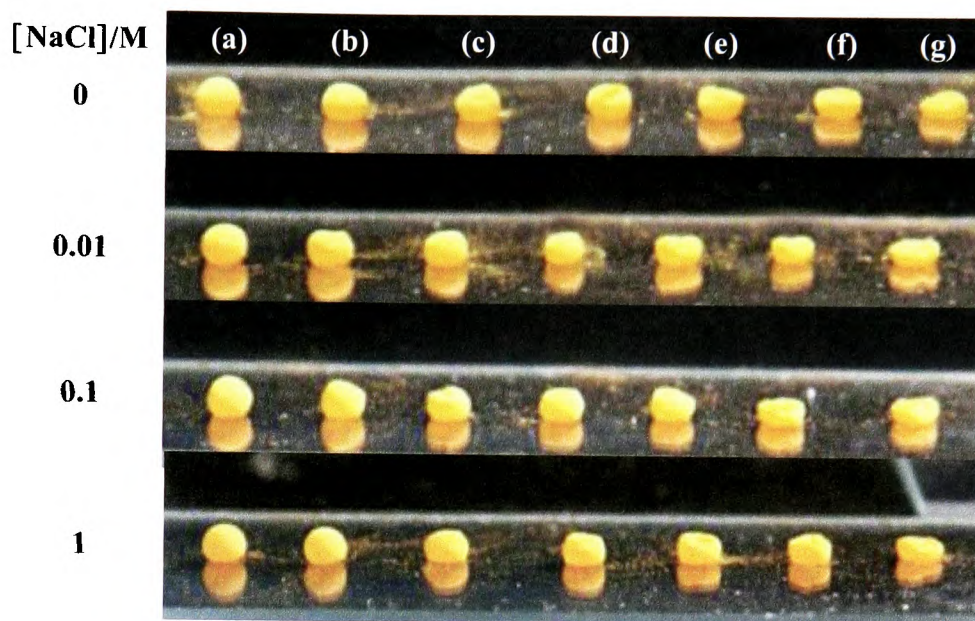
The presence of electrolyte in the water phase of the liquid marbles is expected to slow down the evaporation from the drop and so to change their buckling shape. Relative humidity and temperature were kept constant to avoid conflicts. As represented in Figure 6.33, the salt concentration did not affect the formation and the stability of the liquid marbles. When the change over time was monitored as in Figure 6.34, no significant difference in the evaporation rate was observed as a function of the NaCl concentration. Comparing the time of total buckling of the marbles enables deduction that the quickest evaporation occurs for 0.01 M of NaCl and the slowest for 1 M. However, these differences are really small.

Figure 6.33. Photographs of liquid marbles stabilised by sporopollenin particles 30 s after formation, at pH 6.5 and (a) 0, (b) 0.01, (c) 0.1 and (d) 1 M of NaCl.



Contrary to observations made at the oil-water interface, neither the pH nor the salt concentration seems to affect the adsorption of the sporopollenin particles at the air-water interface. This may be due to the contact angle hysteresis, in which the particle contact angle at an interface will depend on the phase from which it adsorbs:²⁸ when adsorbed at the oil-water interface from an aqueous dispersion, particles are more in contact with water so more of their surface will be available to modification by ions in the water. However when adsorbed from air, a smaller area of the particle is in contact with the water which will render this same modification more difficult.

Figure 6.34. Photographs of time evolution of 10 μL liquid marbles stabilised by sporopollenin particles at pH 6.5 and NaCl concentrations given. Photographs were taken at (a) 30 s, (b) 5, (c) 10, (d) 15, (e) 20, (f) 25 and (g) 30 min. after formation. The room temperature was 19 $^{\circ}\text{C}$ and the humidity 39 %.



6.5 Conclusions

Hollow *Lycopodium clavatum* sporopollenin particles were prepared from the spore particles by removal of all but the most resistant part of the particle exine. They were shown to resemble the unmodified spores of the same species when swollen with water in aqueous dispersion. Modification of the particle surface during the intine removal caused the particles to exhibit pH sensitive behaviour in aqueous dispersions, being increasingly charged at high pH. They are surface active at the air-water interface as they were observed to stabilise air bubbles, and at the oil-water interface stabilising emulsions. IPM-water emulsion inversion from water-in-oil at low pH to oil-in-water at high pH coincides with the isoelectric point of the particles. The pH of inversion was also affected by the type of oil: transitional phase inversion being occurring at low pH for the non-polar dodecane systems, while it happens at high pH for the polar tricaprylin oil systems. The lower particle-oil tension in the tricaprylin series is likely to provide a higher contact angle explaining this high pH of inversion. Interestingly in all systems, water-in-oil emulsions exhibited limited coalescence after emulsification leading to large water drops, and sporopollenin particles were observed to adsorb with a preferred orientation onto the drop surface. The oil-in-water drops however were consistently sparsely covered and showed no preferred particle orientation. Instead drops were stabilised through bridging particles.

The surface activity of sporopollenin particles at the air-water interface also rendered them able to stabilise liquid marbles: stable and shock resistant, the liquid marbles produced were neither affected by the pH or the salt concentration of the encapsulated water. The contact angle hysteresis might be responsible for this lack of effect, with the particle originating from the air here, rather than an aqueous dispersion as used in the emulsions. Sporopollenin-stabilised liquid marbles exhibited shrinking as the water evaporated, with the marble surface showing strong buckling. The temperature and relative humidity was found to determine the rate of evaporation of the liquid marbles, which affected the shrinking shape of the marbles.

6.6 References

1. G. Shaw and A. Yeadon, *J. Chem. Soc. Perkin 1*, **1**, 16 (1966).
2. R. G. Stanley and H. F. Linskens, *Pollen: Biology, Biochemistry, Management*, Springer-Verlag, 1974.
3. F. Zetzsche and H. Vicari, *Helvetica Chimica Acta*, **14**, 5 (1931).
4. F. Zetzsche and H. Vicari, *Helvetica Chimica Acta*, **14**, 5 (1931).
5. A. R. Hemsley, P. J. Barrie and A. C. Scott, *Fuel*, **74**, 1009 (1995).
6. R. J. Scott, Pollen Exine - The Sporopollenin Enigma and the Physics of Pattern, in *Molecular and Cellular Aspects of Plant Reproduction*; Cambridge Univ. Press, Cambridge, 1994.
7. R. Wiermann and S. Gubatz, *Int. Rev. Cytol.*, **140**, 35 (1992).
8. G. Shaw, M. Sykes, R. W. Humble, G. Mackenzie, D. Marsden and E. Pehlivan, *React. Polym.*, **9**, 211 (1988).
9. S. Barrier, A. S. Rigby, A. Diego-Taboada, M. J. Thomasson, G. Mackenzie and S. L. Atkin, *LWT-Food Sci. Technol.*, **43**, 73 (2010).
10. M. Lorch, M. J. Thomasson, A. Diego-Taboada, S. Barrier, S. L. Atkin, G. Mackenzie and S. J. Archibald, *Chem. Commun.*, 6442 (2009).
11. A. L. Campbell, S. D. Stoyanov and V. N. Paunov, *Soft Matter*, **5**, 1019 (2009).
12. S. J. Kettley, Ph.D, University of Hull, Hull, 2001.
13. S. Williams, B.Sc., University of Hull, Hull, 2008.
14. B. P. Binks, J. H. Clint, G. Mackenzie, C. Simcock and C. P. Whitby, *Langmuir*, **21**, 8161 (2005).
15. E. Vignati, R. Piazza and T. P. Lockhart, *Langmuir*, **19**, 6650 (2003).
16. T. S. Horozov and B. P. Binks, *Angew. Chem. Int. Ed.*, **118**, 787 (2006).
17. B. P. Binks and S. O. Lumsdon, *Phys. Chem. Chem. Phys.*, **2**, 2959 (2000).
18. B. P. Binks and J. A. Rodrigues, *Angew. Chem. Int. Ed.*, **44**, 441 (2005).
19. B. P. Binks and J. A. Rodrigues, *Angew. Chem. Int. Ed.*, **46**, 5389 (2007).
20. B. P. Binks, J. A. Rodrigues and W. J. Frith, *Langmuir*, **23**, 3626 (2007).
21. B. P. Binks and J. A. Rodrigues, *Langmuir*, **23**, 7436 (2007).

22. B. P. Binks, P. D. I. Fletcher, B. L. Holt, J. Parker, P. Beaussoubre and K. Wong, *Phys. Chem. Chem. Phys.*, **12**, 11967 (2010).
23. B. P. Binks, W. Liu and J. A. Rodrigues, *Langmuir*, **24**, 4443 (2008).
24. B. P. Binks and C. P. Whitby, *Langmuir*, **20**, 1130 (2004).
25. D. Dupin, S. P. Armes and S. Fujii, *J. Am. Chem. Soc.*, **131**, 5386 (2009).
26. H. Xu, S. Melle, K. Golemanov and G. Fuller, *Langmuir*, **21**, 10016 (2005).
27. M. Dandan and H. Y. Erbil, *Langmuir*, **25**, 8362 (2009).
28. B. P. Binks and J. A. Rodrigues, *Langmuir*, **19**, 4905 (2003).

CHAPTER 7 NON-AQUEOUS FOAMS AND DRY LIQUIDS STABILISED SOLELY BY TEFLON® PARTICLES

7.1 Introduction

Foam is characterised by its high area of interface, similarly to other dispersed systems (suspensions and emulsions). The foam film, which is the fluid region separating two air bubbles, is the main structural element of the foam and will determine the foam stability. Foams are widely applied in a large variety of industries, from the food to the material production industry or in wastewater treatment.¹ Consequently, it becomes important to study the parameters and processes responsible for foam formation and stability in order to optimise or indeed hinder their production. Like emulsion drops, bubbles formed in pure liquid are very unstable, necessitating the addition of a surface-active substance to confer stability.²

Surfactant-stabilised foams, like soap-foams, have been thoroughly studied as far back as a hundred years ago, but the possibility of stabilising foams with particles has only been observed more recently.^{3,4} However, several conditions are necessary for particles to act as foam stabilisers and not as de-stabilisers: in solid-liquid-air systems, particle adsorption is thermodynamically favourable if the sum of the solid-air tension (γ_{sa}) and the solid-liquid tension (γ_{sl}) is less than the original liquid-air tension (γ_{la}). This balance of interfacial tensions results in adsorbed particles displaying a contact angle at the liquid-air interface: if the angle is close to 60° , the particles are observed to help stabilise surfactant-stabilised foams, whereas above it and close to 90° they often cause foam collapse.⁵⁻⁸ Industrial foams often contain mixtures of particles and surfactant, which makes the understanding of their interaction of importance: Subramaniam *et al.* observed that addition of surfactant to particles-stabilised air bubbles in water caused the gas to dissolve, and colloidosomes were formed, possibly due to the change in curvature of the air-water surface.^{9, 10} Particles like silicon carbide were also demonstrated to act as effective stabilisers of metal foams, used in the automotive industry.¹¹ In the case of aqueous foams in the absence of surfactant, Binks and Murakami varied the particle contact angle θ by using silica particles coated to different extents with a hydrophobising agent:¹²

increasing θ through 90° caused phase inversion from air-in-water foams to water-in-air powders, similar to that of particle-stabilised emulsion inversion.¹³ Silica particle-stabilised foams have also been observed to exhibit better stability to disproportionation than protein-stabilised ones, but the nanoparticles had to be partially aggregated for this purpose.¹⁴⁻¹⁶ Other particles, like latex or food grade microrods, have also been shown to be good aqueous foam stabilisers.¹⁷⁻²¹

Non-aqueous foams are much less common than aqueous foams, although they appear transiently in various applications in the oil industry.²² Their stabilisation by surfactant has been reported to occur thanks to various types of aggregated phases formed around bubbles.^{23, 24}

In order to adsorb at oil-air surfaces, particles must be partially oleophobic. This idea can be understood by relating it to the stabilisation of “dry water” by hydrophobic silica particles. Polytetrafluoroethylene (PTFE), which possesses a very low surface energy due to fluorine content, can be used for this purpose. Other particles with similar surfaces have been incorporated into cotton textiles to provide oil repellency properties.²⁵ Their high hydrophobicity also made them good foam destabilisers in surfactant-stabilised foam systems.⁵ PTFE particles have been used to stabilise liquid marbles, and in the last year to produce hollow capsules or macroporous materials, via emulsion or foam templating.²⁶⁻²⁹ Fox and Zisman investigated the wetting of low energy surfaces in air and established that $\cos \theta$ increased linearly with a decrease in γ_{la} for homologous liquids.³⁰ They defined the critical surface tension γ_c for PTFE to be of 18 mN m^{-1} at 20°C : liquids with surface tensions under this value wetted the solid completely, whereas those with values above did not.³¹ On smooth PTFE, θ was observed to increase as the interactions between solid molecules and liquid ones changed from exclusively dispersion forces to a mixture of dispersion and hydrogen bonding forces: θ increased from 0° for pentane to 46° for hexadecane and 108° for water. Murakami and Bismark have demonstrated that stable non-aqueous foams can be stabilised by oligomeric tetrafluoroethylene (OTFE) particles, which exhibit a high surface roughness rendering them very hydrophobic.³²

This study aims at investigating the wettability of 5 different fluorinated particles (varying size and shape) by a large range of liquids. Different bulk materials (dispersions, foams or dry powder) were formed by the mixing of a liquid, air and those particles, and the materials produced were observed to depend on the initial wettability of the particles. The production methods were also compared and the effect of the liquid type, particle type and particle concentration were investigated.

7.2 Tetrafluoroethylene particle characterisation

7.2.1 SEM imaging

Five types of particles were used for this study: four of polytetrafluoroethylene (PTFE) and one of oligomeric tetrafluoroethylene (OTFE). The scanning electron microscopy (SEM) images, given in Figure 7.1, show that the particles range from 0.3 to 10 μm (mean diameter) and present different shapes and surfaces. The PTFE particles can be organised into two categories: Zonyl MP1100 and Ultraflon UF-8TA particles (Figures 7.1(a) and (d)), measuring approximately 0.3 μm in diameter, have smooth surfaces and rounded shape and are fairly monodisperse, whereas the Zonyl MP1400 and Ultraflon MP-8T (Figures 7.1(b) and (c)), of respectively 10 and 2.5 μm in diameter, are rough-surfaced and irregular-shaped polydispersed particles. The OTFE particles, displayed in Figure 7.1(e), are similar to the Zonyl MP1100, with a larger diameter ($\sim 1.3 \mu\text{m}$) and an almost spherical shape.

7.2.2 Light scattering

The size distributions of the particles dispersed in methanol are displayed in Figure 7.2: Zonyl MP1100 and Ultraflon UF-8TA powders contain the smallest particles ($\sim 0.15 \mu\text{m}$), while Zonyl MP1400 contain the largest PTFE particles ($\sim 15 \mu\text{m}$) with the highest polydispersity. The volume weighted mean diameters calculated from the size distribution mostly agree with the SEM data. However the Ultraflon UF-8TA particles are measured with light scattering to be 1.3 μm in diameter. This is slightly larger than that shown by SEM and so they are likely to be partially aggregated. The OTFE particles are measured to be 1 μm by SEM, however

the dispersion in methanol reveals a much larger mean of 57.1 μm . The quality of the particle dispersion in methanol is therefore poor, and it is likely that the dispersion contains mostly large aggregates of particles which have not been broken by sonication.

Figure 7.1. SEM images of (a) Zonyl MP1100, (b) Zonyl MP1400, (c) Ultraflon MP-8T, (d) Ultraflon UF-8TA and (e) OTFE particles. Scale bars represent 1 μm .

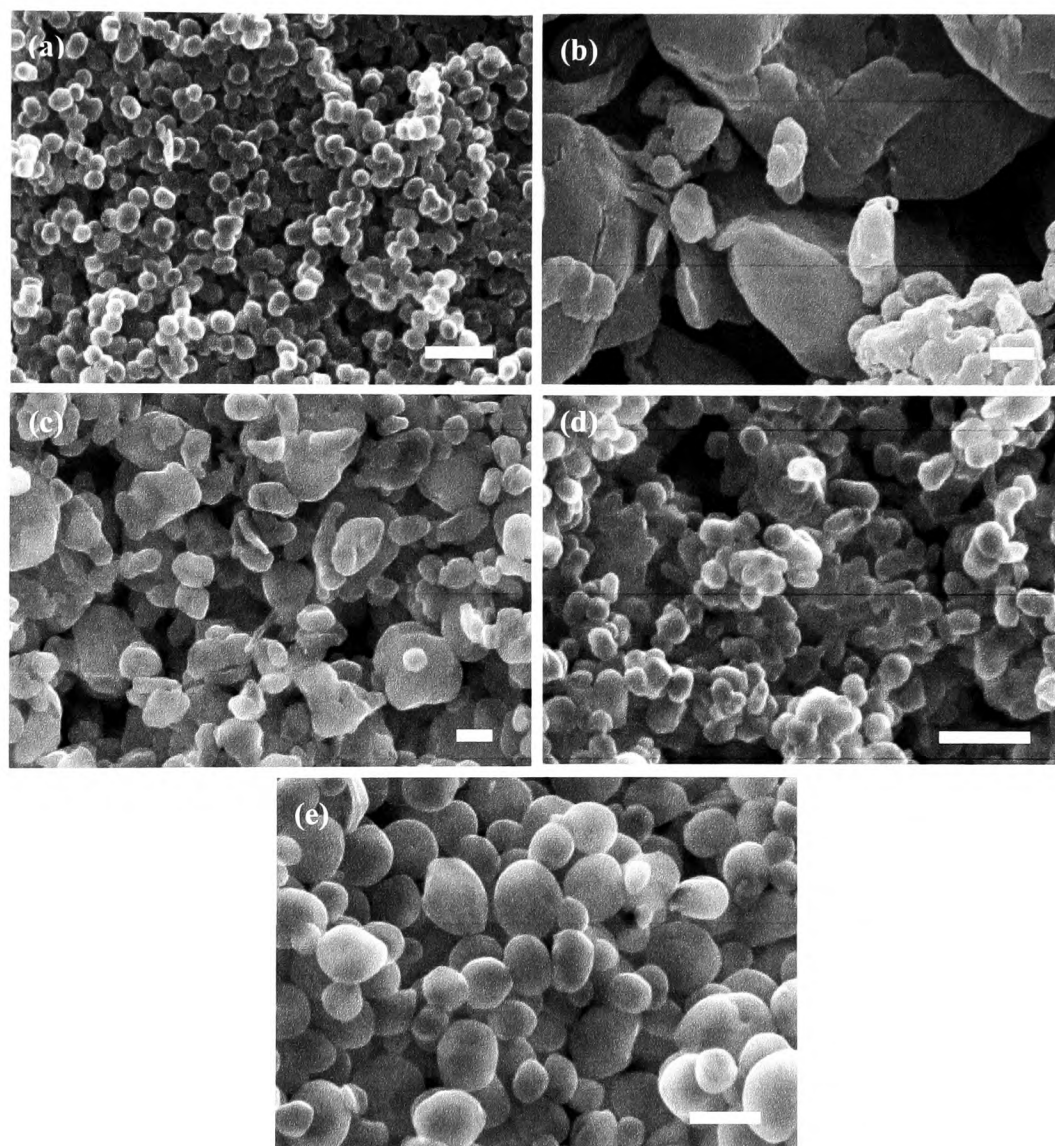
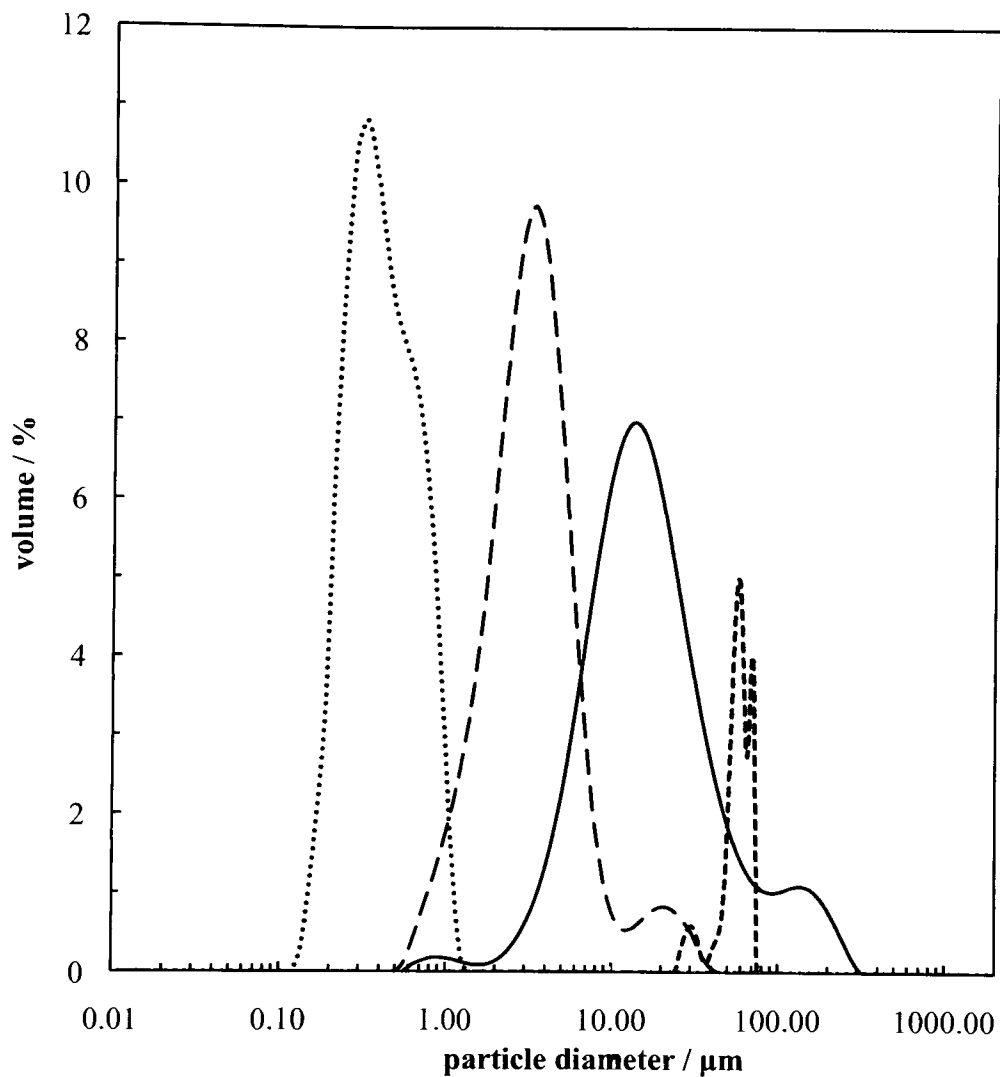


Figure 7.2. Size distribution of the (...) Zonyl MP1100, (—) Zonyl MP1400, (---) Ultraflon MP-8T and (·) Ultraflon UF-8TA PTFE particles, and the (- - -) OTFE particles. Particles were dispersed at 0.05 wt.% in methanol by 2 min. sonication, and then sized in the Mastersizer 2000.



7.2.3 Powder immersion tests

In order to estimate the pre-disposition of the different particles to stabilise foam, static and dynamic immersion tests were done: the behaviour of particles spread onto 34 oils of different structure, glycerol and water was observed where they either enter the liquid completely, are partially wet by it or remain completely non-wet. Figure 7.3 displays some of the samples, in which Zonyl MP1400 particles were totally wetted by the short alkanes and perfluorohexane (a and e), partially wetted by the long alkanes, toluene and some alcohols (b, d, g and i) or non-wetted at all by water, esters and triglyceride oil (f, h and j) 24 h after particle addition.

When the samples were handshaken for 10 s to apply energy to the powdered particles (particle bulk density 0.42 g cm^{-3}), the system formed either particle dispersions, foams or a dry material, as described in Table 7.1. For liquids with a liquid-air surface tension (γ_{la}) under 29 mN m^{-1} , particles were wetted or partially wetted when at rest, whereas they dispersed in the liquid and eventually sedimented after handshaking. For liquids of $29 < \gamma_{la} < 45 \text{ mN m}^{-1}$, particles exhibit both wetted and non-wetted behaviour, but interestingly they also stabilised bubbles within the liquid. For liquids with $\gamma_{la} > 45 \text{ mN m}^{-1}$, like glycerol and water, non-wetting persisted even after handshaking.

Figure 7.3. Photographs of vessels containing 2.5 mg of Zonyl MP1400 particles spread onto 1 mL of (a) pentane, (b) tetradecane, (c) cyclohexane, (d) toluene, (e) water, (f) perfluorohexane, (g) linalool, (h) benzyl acetate, (i) cis-3-hexenol and (j) sunflower oil 24 h after particle addition.

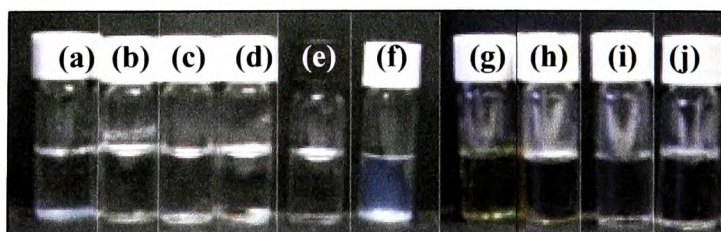


Table 7.1. Behaviour of PTFE or OTFE particles on various liquids, in terms of static and dynamic wettability. The surface tensions (γ_{la}) of the different liquids at 20°C, either determined in our laboratory or from literature values, are also given.

Liquid (γ_{la} / mN m ⁻¹)	Particle	Static wettability at 24 h	Dynamic wettability
Perfluorohexane (11.9) ³³ Pentane (15.0) ³⁴ Hexane (18.4) ³⁵ n-heptane (20.1) ³⁶ 0.65-500 cS PDMS (16-21.1) Dodecane (25.4) ³⁷ Tetradecane (26.3) ³⁸	Zonyl MP1100	Wetted	Dispersed
	Zonyl MP1400		
	Ultraflon MP-8T		
	Ultraflon UF-8TA		
	OTFE		
Hexadecane (27.6) ³⁷ Cyclohexane (25.5) ³⁹ Toluene (28.4) Cis-3-hexenol (28.7)	Zonyl MP1100	Partially wetted	Dispersed
	Zonyl MP1400		
	Ultraflon MP-8T		
	Ultraflon UF-8TA		
	OTFE		
Benzene (28.9) ⁴⁰ Limonene (29.0) Linalool (29.2) Isopropyl myristate (29.4) Tricaprylin (29.5) Miglyol (30.3) Squalane (31.1) ⁴¹ Geraniol (31.6)	Zonyl MP1100	Partially wetted	Few bubbles + Dispersed
	Zonyl MP1400		
	Ultraflon MP-8T		
	Ultraflon UF-8TA		
	OTFE		
Peanut oil (33.8) Sunflower oil (33.9) Rapeseed oil (33.9) α -hexyl cinnamaldehyde (35.3) Benzyl acetate (38.0) Eugenol (36.4) Tricresyl phosphate (40.9) α -bromo naphthalene (44.6)	Zonyl MP1100	Partially wetted	Bubbles
	Zonyl MP1400	Non-wetted	
	Ultraflon MP-8T		
	Ultraflon UF-8TA		
	OTFE		
Ethylene glycol (47.7) Diiodomethane (50.8) Formamide (58.2) Glycerol (63.4) Water (72.5)	Zonyl MP1100	Non-wetted	Dry material
	Zonyl MP1400		
	Ultraflon MP-8T		
	Ultraflon UF-8TA		
	OTFE		

7.2.4 Contact angles

As the contact angle of a micro-particle at a liquid-air interface is difficult to measure, it was chosen to do measurements of the advancing and receding contact angles of the different liquids used onto solid pellets of compressed particles, displayed in Figure 7.4 for Zonyl MP1100.⁵ Both angles are relevant, as the homogenisation process implies that the particles are moved in and out of the liquid, experiencing both the advancing and the receding of the liquid on their surfaces. For PTFE particles we assumed that the contact angles measured should be the same as those of pellets made with the other PTFE particles, as they are of the same chemical nature.

The measurements of the contact angle of 19 different liquids on the PTFE pellets are shown in Table 7.2. Figure 7.5 illustrates the drop shape of three liquids exhibiting a low (a), intermediate (b) and high (c) contact angle onto the Zonyl MP1100 particle pellet. The contact angles support the immersion test results: the oils with the lowest surface tension, and in which particles entered readily, are the ones exhibiting the lowest contact angle (perfluorohexane, PDMS and dodecane), whereas the ones with the highest γ_{la} and which did not wet the particles display the highest contact angle (glycerol, diiodomethane and water). A large range of oils exhibits intermediate contact angles (between 40 and 90°) and the particles seemed to stabilise foam with them (*cf.* § 7.2.3). Figure 7.6 displays the correlation between the cosine of the liquid contact angle on Zonyl MP1100 particles and γ_{la} . As seen in previous studies, a linear correlation is observed:³⁰ lines (for advancing and receding θ) can be traced for the liquids of surface tension smaller than 50 mN m⁻¹, however with liquids of higher surface tension, the lines curve indicating that non-homologous liquids do not obey the exact same trend.

Figure 7.4. Photographs of a (a) side and a (b) top view of a Zonyl MP1100 pellet made by compressing the particle powder with a hydraulic press under 10 Tons of pressure for 30 s.

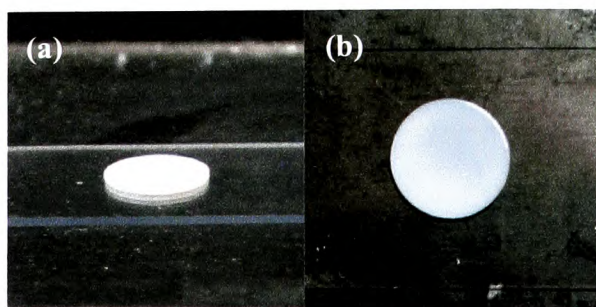


Figure 7.5. DSA images of advancing 0.05 mL drops of (a) rapeseed, (b) tricresyl phosphate and (c) glycerol in air and on Zonyl MP1100 particle pellets.

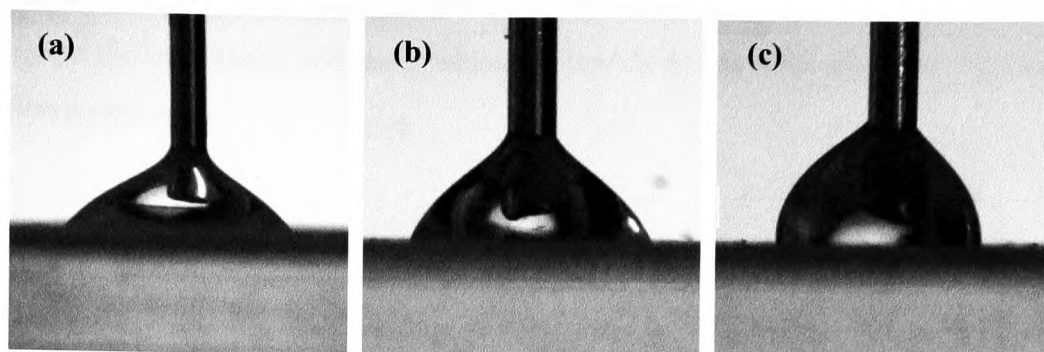
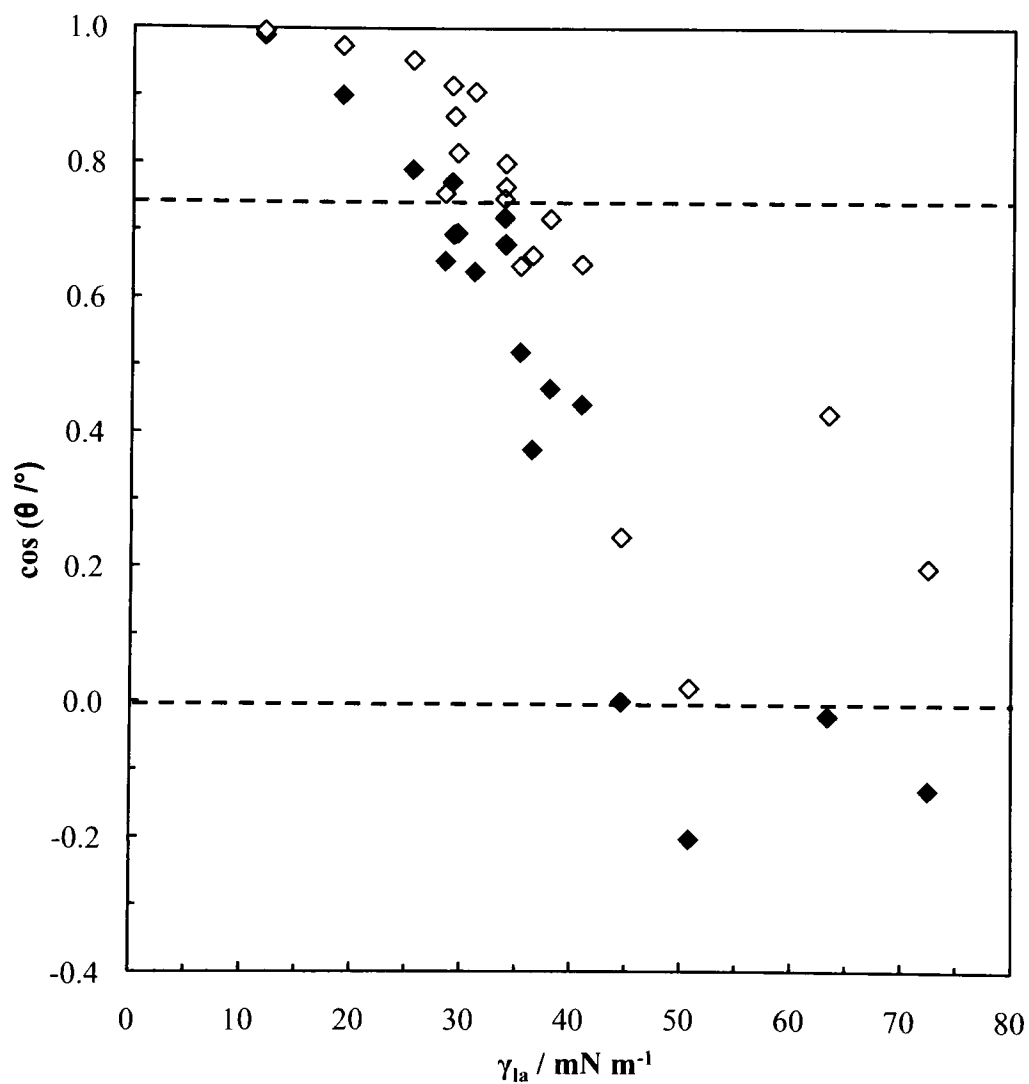


Table 7.2. Advancing and receding contact angles of 0.05 mL drops of liquid in air and on pellets made from Zonyl MP1100 particles. The grey boxes represent the contact angle range for which the particles may stabilise a foam, whereas those with bold lining represent liquids which did not wet the particle at all.

Liquid	Advancing contact angle / °	Receding contact angle / °
Perfluorohexane	8.38 ± 0.51	5.25 ± 1.83
10 cS PDMS	25.73 ± 3.37	13.10 ± 3.81
Dodecane	37.83 ± 1.10	17.68 ± 2.01
Limonene	39.50 ± 2.13	23.75 ± 1.49
Peanut	44.05 ± 1.38	41.68 ± 2.60
Tricaprylin	45.90 ± 3.20	35.40 ± 0.32
Linalool	46.05 ± 4.42	29.53 ± 1.85
Sunflower	47.28 ± 2.68	40.10 ± 0.84
Rapeseed	47.08 ± 0.73	36.88 ± 0.80
Toluene	49.15 ± 1.38	40.98 ± 1.30
Squalane	50.30 ± 1.19	25.03 ± 2.45
Hexyl-cinnamaldehyde	58.73 ± 1.08	49.68 ± 1.57
Benzyl Acetate	62.30 ± 0.35	44.15 ± 1.46
Tricresyl Phosphate	63.78 ± 0.43	49.45 ± 0.60
Eugenol	67.95 ± 0.54	48.45 ± 1.21
α-bromonaphtalene	89.98 ± 0.26	75.83 ± 1.47
Glycerol	91.20 ± 0.43	64.65 ± 3.15
Water	97.50 ± 5.40	78.50 ± 2.62
Diiodomethane	101.73 ± 1.44	88.83 ± 1.66

Figure 7.6. Cosine of (\blacklozenge) advancing and (\diamond) receding contact angles, θ , of liquids in Table 7.2 on compressed powder pellets of Zonyl MP1100 particles as a function of the liquid surface tension (both literature and measured γ_{la} values). The dashed lines represent the limit above and under which the liquids do not form any foam with the Teflon particles.



7.3 Non-aqueous foams with TFE particles

7.3.1 Effect of mixing method on foams

Four different methods were investigated for producing foams stabilised by Zonyl MP1400 particles: homogenisation in a jug blender, with a rotor-stator, handshaking or aeration with a bubble diffuser. The foams produced were compared in order to choose the best method for subsequent study.

7.3.1.1 Blender homogenisation

The blender homogenisation either gave particle dispersions or particle-stabilised foams with the 9 different liquids used, these being sunflower oil, rapeseed oil, eugenol, α -hexylcinnamaldehyde, benzyl acetate, hexadecane, hexane, isopropyl myristate and 10 cS PDMS. Oils with surface tensions below 30 mN m^{-1} , which wet the powder in immersion tests (*cf.* § 7.2.3) like hexadecane, hexane, PDMS and isopropyl myristate, formed dispersions of particles within 10 s of homogenisation. As can be seen in Figure 7.7, the particles eventually sediment to the bottom of the vessels.

For the higher surface tension liquids, which were not observed previously to generate foams, air-in-oil foams were produced with the Zonyl MP1400 particles using the blender. The appearance of the foams was different for the long triglyceride oils (Figures 7.7(a) and (b)) and for the perfume oils (Figures 7.7(c) and (d)): the foams creamed quicker in eugenol and α -hexyl cinnamaldehyde than in the vegetable oils, probably due the viscosity difference of these oils. Although the transfer from the glass jug of the blender to the glass jar resulted in a loss of foam, all foams were observed to stay stable for up to 2 months.

The microscopy images in Figure 7.8 enable a more detailed examination of the foam bubbles: spherical and non-spherical bubbles from 30 to 300 μm in diameter are observed and their average size is smaller for the liquids exhibiting the highest contact angle with PTFE (Table 7.2). The air-in-eugenol bubbles appear non-spherical, similarly to observations made on emulsion drops, with a dense, rigid layer of jammed particles preventing relaxation to a spherical shape.¹⁴

Figure 7.7. Photographs of 5-minutes old (a) air-in-sunflower oil, (b) air-in-rapeseed oil, (c) air-in-eugenol and (d) air-in- α -hexylcinnamaldehyde stabilised with Zonyl MP1400 particles. Zonyl MP1400 particles form a dispersion in (e) hexadecane, (f) hexane, (g) isopropyl myristate and (h) 10 cS PDMS. (a-d) Foams and (e-h) particle dispersions were made with 5 wt.% particles by 30 s blender homogenisation at 25000 rpm.

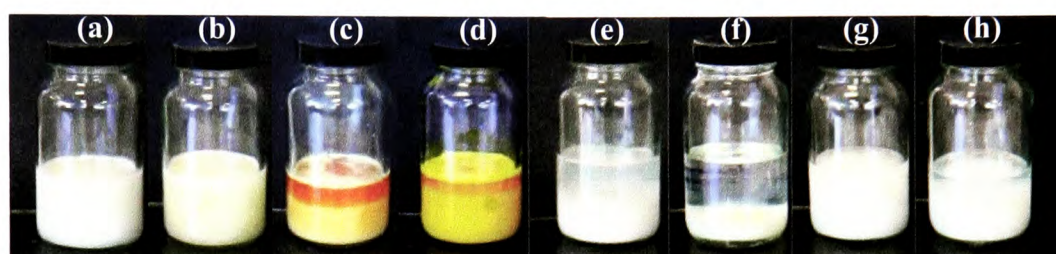
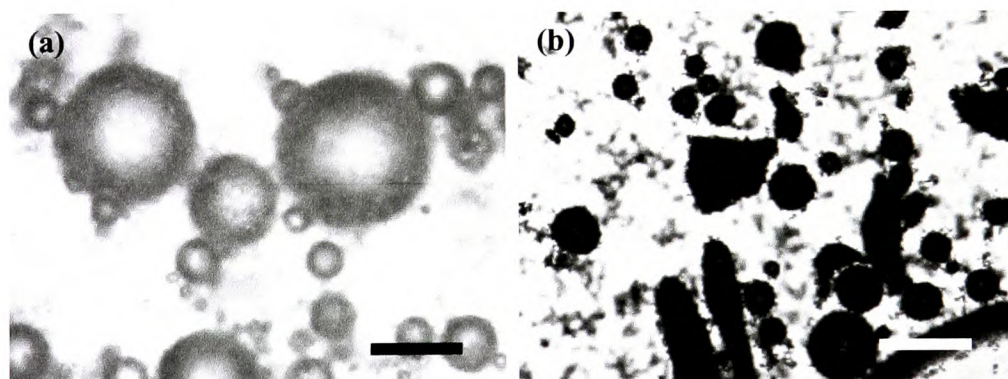


Figure 7.8. Optical microscopy images of (a) air-in-sunflower oil and (b) air-in-eugenol bubbles stabilised with Zonyl MP1400 particles 5 min after homogenisation. Foams were made with 5 wt.% particles by 30 s blender homogenisation at 25000 rpm. Scale bars represent 160 μm .



7.3.1.2 Ultra Turrax homogenisation

Rotor-stator Ultra Turrax homogenisation was observed to give similar results to blender homogenisation with slightly lower foam volumes: Zonyl MP1400 particles were observed to disperse in low surface tension oils, while the foam formed with the other oils seems to last up to two months after homogenisation.

In Figure 7.9 the foam bubbles appear dispersed throughout the liquid for the two triglyceride oils, resembling those produced by blender homogenisation; the perfume oil (eugenol, α -hexyl cinnamaldehyde and bezyol acetate) foams creamed a lot quicker, and the volume of foam generated again seems higher for lower surface tension oils. The particles are observed to sediment in the low surface tension oil dispersions, with the rate of sedimentation depending on the liquid viscosity.

The micrographs in Figure 7.10 again illustrate the difference in shape between the vegetable oils and the perfume oils: the bubbles observed in the long triglycerides oils are spherical, whereas the ones in the eugenol oil deform into long irregular tube shapes, in excess of 500 μm . Although the drops look different to those made with the blender homogenisation, the spherical versus non-spherical shape of the drops is consistently observed. This demonstrates that particle-stabilised bubbles can exhibit similar non-spherical shapes to those of particle-stabilised emulsion drops, proving strong particle adsorption to the air-liquid interface.^{42, 43} The change in bubble shape may also highlight stronger particle adsorption to the higher surface tension liquids resulting in more dense particle packing.

Figure 7.9. Photographs of 5-minutes old (a) air-in-sunflower oil, (b) air-in-rapeseed oil, (c) air-in-eugenol, (d) air-in- α -hexylcinnamaldehyde and (e) air-in-benzyl acetate bubbles stabilised with Zonyl MP1400 particles. Zonyl MP1400 particles form a dispersion in (f) hexadecane, (g) hexane, (h) isopropyl myristate and (i) 10 cS PDMS. (a-d) Foams and (e-h) particle dispersions were made with 5 wt.% particles by 1 min. Ultra Turrax homogenisation at 13000 rpm.

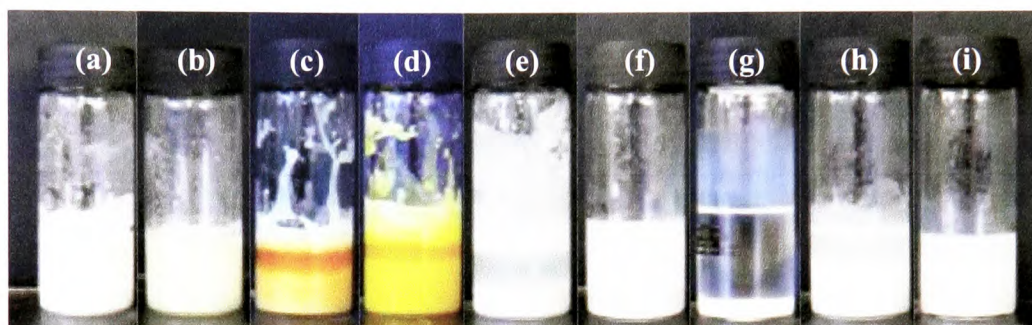
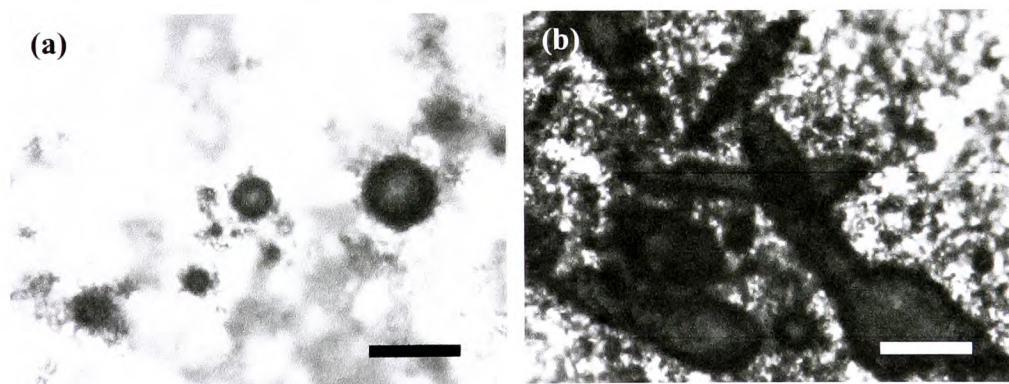


Figure 7.10. Optical microscopy images of (a) air-in-sunflower oil and (b) air-in-eugenol bubbles stabilised with Zonyl MP1400 particles 5 min after homogenisation. Foams were made with 5 wt.% particles by 1 min. Ultra Turrax homogenisation at 13000 rpm. Scale bars represent 160 μm .



7.3.1.3 Handshaking

Handshaking was found to give better foam volumes than systems studied in sections 7.3.1.1 and 7.3.1.2: compared with the high shear produced by the blender or the Ultra Turrax homogenisation, handshaking was believed to generate more foam by entraining more air.

Figure 7.11 displays a series of foams using the liquids previously noted to give foam (*cf.* § 7.2.3) and stabilised by Zonyl MP1400 particles: the foam bubbles were observed to cream slowly upwards and to remain stable to disproportionation and coalescence for many days despite their large volume fraction. Particle-stabilised aqueous foams have previously been revealed to behave similarly due to the close-packed particle layer hindering these processes.^{15, 21} Similar to previous observations, the creaming happened slower for the vegetable oils.

The micrograph images of the foam bubbles show once again that eugenol foam contains a large number of non-spherical bubbles, however some irregular bubbles are also observed in sunflower oil (Figure 7.12). The bubble surfaces appear textured due to packing of irregular-shaped and polydisperse particles, and free particles can also be seen in the continuous oil phase. These bubbles are noticeably smaller than those typically observed in aqueous foams possibly due to lower surface tension of the liquids.⁴⁴ Here they measure 20 to 160 μm in diameter for the sunflower oil and 20 to 100 μm for the eugenol.

Handshaking clearly shows advantages in terms of the simplicity of the method, as well as the better quality of the foam produced (in terms of volume and stability) compared to the blender or Ultra Turrax homogenisation.

Figure 7.11. Photographs of 5-minutes old (a) air-in-sunflower oil, (b) air-in-rapeseed oil, (c) air-in-eugenol, (d) air-in- α -hexylcinnamaldehyde and (e) air-in-benzyl acetate foams, stabilised with Zonyl MP1400 particles. Foams were made with 5 wt.% particles by 30 s strong handshaking.

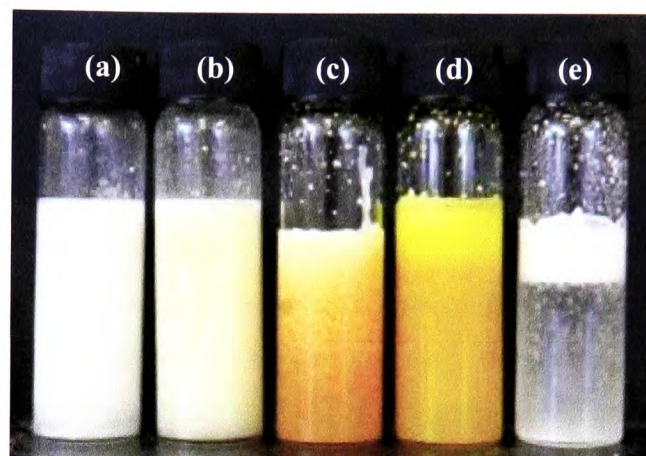
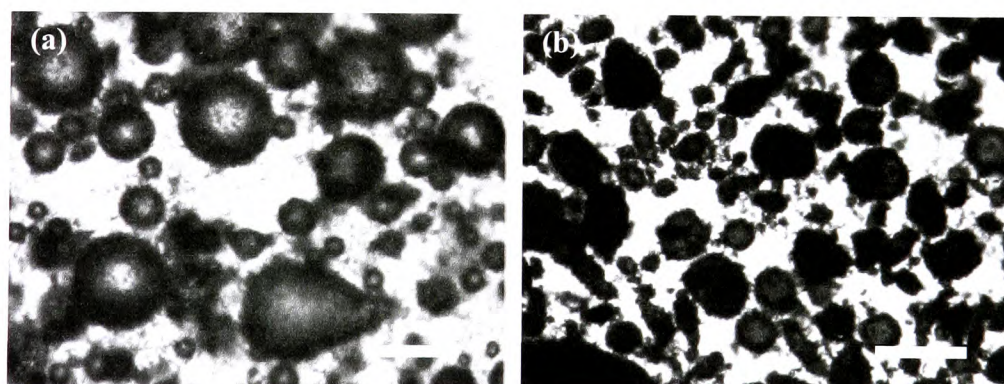


Figure 7.12. Optical microscopy images of (a) air-in-sunflower oil and (b) air-in-eugenol bubbles stabilised with Zonyl MP1400 particles 5 min after homogenisation. Foams were made with 5 wt.% particles by 30 s strong handshaking. Scale bars represent 160 μm .

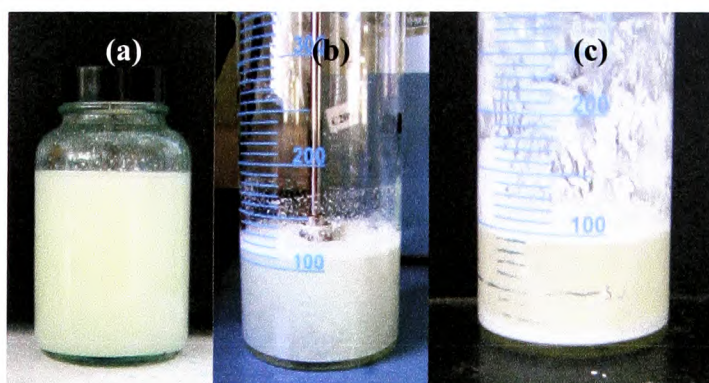


7.3.1.4 Diffuser aeration

Diffuser aeration was tested as a method to produce foam with the same systems studied in sections 7.3.1.1 to 7.3.1.3. As the air was injected into the liquid the Zonyl MP1400 particles had to be dispersed by sonication in it prior to aeration in order for them to adsorb (Figure 7.13(a)). The foam produced during aeration is significantly different from foams made in non-aqueous surfactant systems:⁴⁵ Figure 7.13(b) displays the dense appearance of the particle-stabilised foam, which contains small bubbles, while lubricating oils studied by Binks *et al.* exhibited large volumes of millimetre-sized bubbles. However, the diffuser aeration method is shown to produce poor foams for systems proven to give good foam volumes previously: comparing Figures 7.11(a) and 7.13 illustrates the different appearance and volume of foam formed by handshaking and diffuser aeration method respectively when using sunflower oil. The particle dispersion preceding aeration is believed to have modified the particle wettability: sonication might have removed the air from the powdered particles, rendering them more oleophilic so easily dispersible in the oil, but less surface active, hence not able to stabilise an air-oil interface anymore. Furthermore, when originated from the oil phase, instead of air, the particles will display a receding contact angle and will therefore be less strongly adsorbed in the case of the sunflower-air interface (see Table 7.2).

This method was not used further in this study, as it was observed to be a poor means to produce non-aqueous foams with the Zonyl MP1400 particles, and was relatively laborious.

Figure 7.13. Photographs of 5 wt.% Zonyl MP1400 particles (a) dispersion in sunflower oil, (b) during aeration with the diffuser and (c) 30 s after stopping aeration and removing the diffuser.

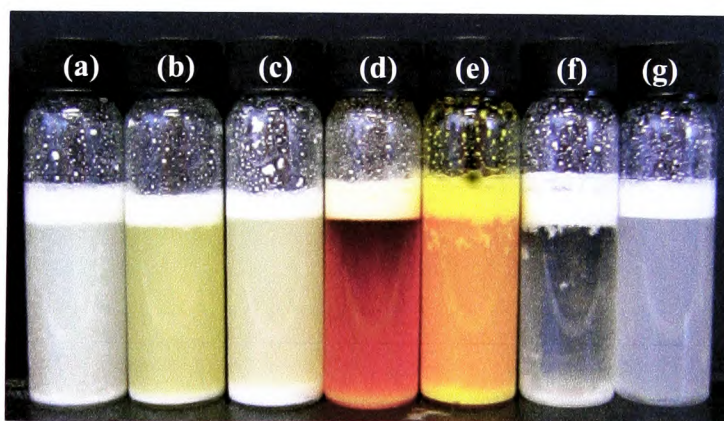


7.3.2 Effect of liquid type on foams

In order to investigate the effect of the oil type on the foam formed, the foam series made with Ultraflon MP-8T particles by handshaking was monitored in terms of stability over time. Ultraflon MP-8T particles were chosen for their intermediate size (compared to the other particles in Figure 7.2) and their low wettability, which enable them to stabilise bubbles with the oils used here (Table 7.1).

Figure 7.14 displays the foam series an hour after handshaking: the three perfumes oils (eugenol, α -hexyl cinnamaldehyde and benzyl acetate) seem to give a slightly larger volume of the white dense foam than the vegetable oils. A sediment of particles can be observed at the bottom of the samples and their volumes seem to depend on the oils: the peanut oil, which gives the lowest contact angle with PTFE particles (*cf.* Table 7.2), displays the highest volume of sedimented particles, whereas the tricresyl phosphate with its higher contact angle on PTFE exhibits no sedimented particles. However no linear trend linking the height of sediment and the contact angle of the oil is observed.

Figure 7.14. Photographs of 1-hour-old air-in- (a) sunflower, (b) rapeseed oil, (c) peanut, (d) eugenol, (e) α -hexyl cinnamaldehyde, (f) benzyl acetate and (g) tricresyl phosphate foams stabilised with Ultraflon MP-8T PTFE particles. Foams were made with 5 wt.% particles by 30 s strong handshaking.



The foamability and foam stability as a function of time are represented in Figures 7.15 and 7.16. The foam volume, liquid volume and total volume of the system are displayed in Figure 7.15: the foam bubbles were observed to remain stable to disproportionation and coalescence after monitoring for several weeks despite their large volume fraction. The increase in foam volume over the first 10 minutes results from depletion of the remaining air bubbles in the liquid fraction, which act to increase the volume of the air-bubble dense region, classified as the foam. For both oils represented, peanut and α -hexyl cinnamaldehyde, the total volume stayed fixed after handshaking, indicating that no air is lost from the system the bubbles do not coalesce. However, it can be noted that the peanut oil gives less foam than the α -hexyl cinnamaldehyde; this observation should be linked with the high amount of sedimented particles found for the peanut oil, implying that less particles are adsorbed at the oil-air interface, so less foam can be stabilised.

Figure 7.16 shows only the foam volume for the different oils: the foamability, which refers to the foam volume after 30 minutes, is observed to be equivalent for most oils. The vegetable oils, like the peanut previously discussed, gave a slightly smaller volume of foam and the creaming happened slower than for the other oils.

Figure 7.15. Volume of foam stabilised with Ultraflon MP-8T particles after homogenisation as a function of time. Foams were made with 5 wt.% particles in (\diamond) peanut oil and (\blacklozenge) α -hexyl cinnamaldehyde by 30 s handshaking. The (—) foam, (---) liquid and (---) total volume of the system are represented on this graph.

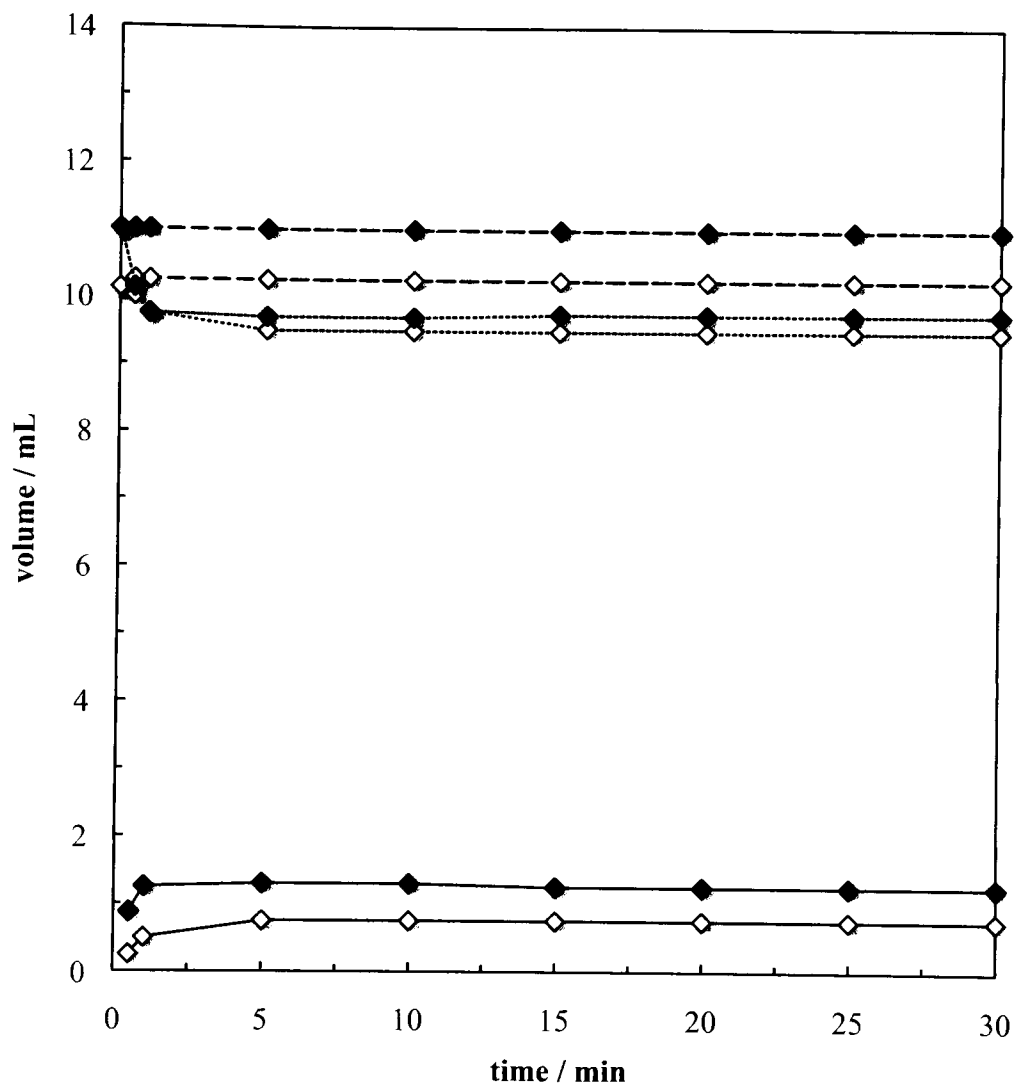
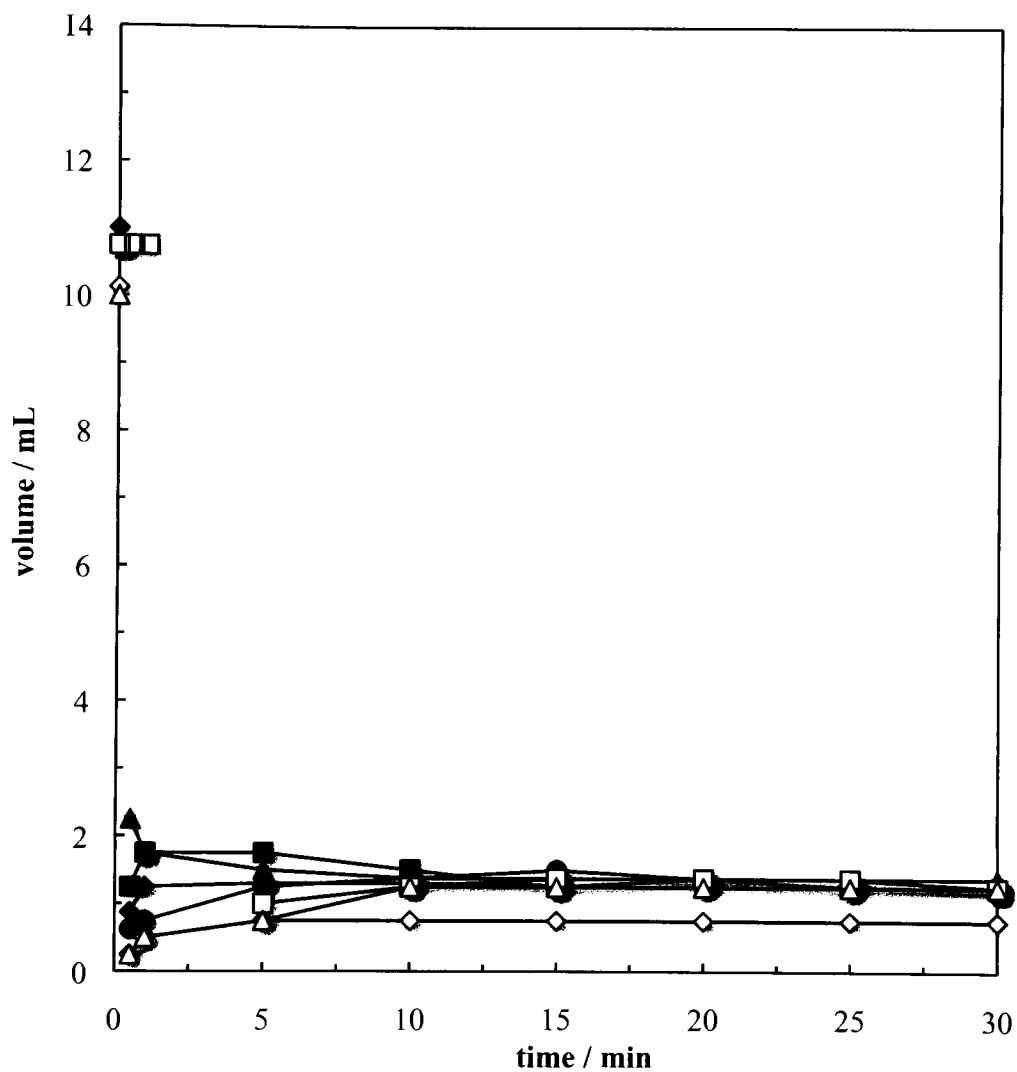


Figure 7.16. Volume of foam stabilised with Ultraflon MP-8T particles after homogenisation as a function of time. Foams were made with 5 wt.% particles by 30 s handshaking. The foam volumes for the (□) sunflower, (△) rapeseed, (◇) peanut, (■) eugenol, (◆) α -hexyl cinnamaldehyde, (▲) benzyl acetate and (●) tricresyl phosphate systems are represented on this graph.



A similar series was reproduced with the small spherical Zonyl MP1100 particles (*cf.* Figure 7.1(a)), which is displayed in Figure 7.17: after one week, only the eugenol and the benzyl acetate display large amounts of foam. However, cryo-SEM imaging was carried out on the freshly formed foams, and evidences particles at the surface of air bubbles in rapeseed oil, eugenol and α -hexyl cinnamaldehyde. SEM images in Figures 7.18(a) and (d) show sections of non-spherical air bubbles for rapeseed oil and α -hexyl cinnamaldehyde: the surfaces of the particle-coated bubbles display a wavy appearance, which might be due to the high surface density of the strongly adsorbed particles, or to the freezing process. At higher resolution, in Figures 7.18(b), (c) and (f), close packed particle monolayers are observed along with small areas devoid of particles. The bubbles in α -hexyl cinnamaldehyde appear to be more densely covered with particles and it is also noted that the particles seem to protrude more in the air than those in peanut oil (Figures 7.18(b) and (f)); this latter observation is consistent with the contact angle of the peanut oil on PTFE being smaller than that of α -hexyl cinnamaldehyde (~ 44 and 59° respectively).

Figure 7.17. Photographs of 1-week old air-in-(a) sunflower, (b) rapeseed oil, (c) eugenol, (d) α -hexyl cinnamaldehyde and (e) benzyl acetate foams stabilised with Zonyl MP 1100 PTFE particles. Foams were made with 5 wt.% particles by 30 s strong handshaking.

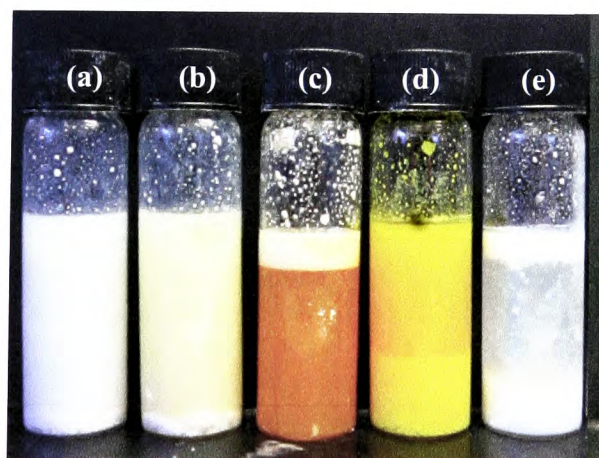
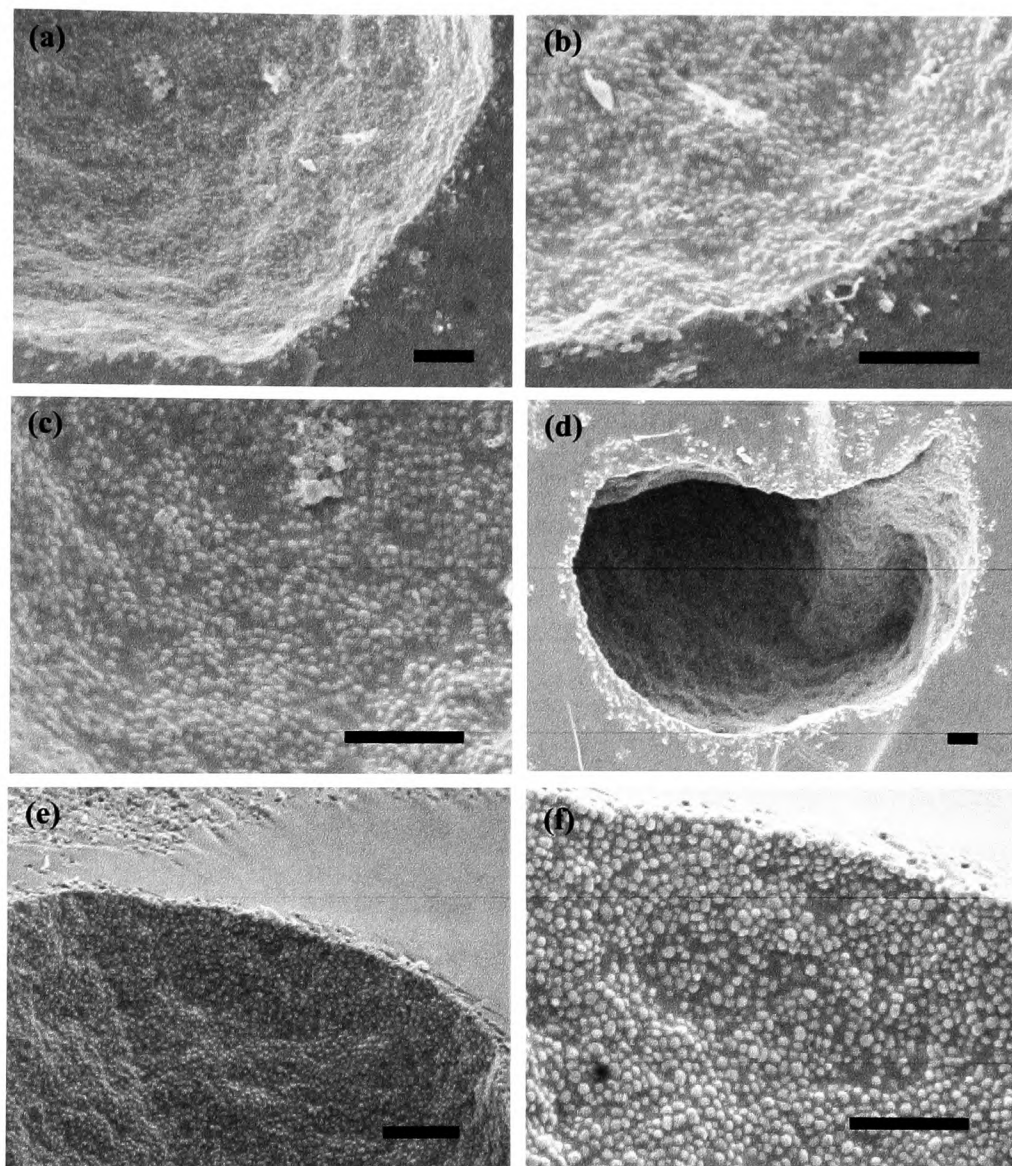


Figure 7.18. Cryo-SEM images of frozen non-aqueous foams of (a-c) air-in-rapeseed oil and (d-f) air-in- α -hexyl cinnamaldehyde stabilised with Zonyl MP 1100 as in Figures 7.17(b) and (d) respectively. Foams were made with 5 wt.% particles by 30 s strong handshaking. Scale bars represent 2 μ m.



7.3.3 *Effect of particle type on foams*

The foams made with the 5 different particle types were compared in the series shown in Figure 7.19. All particles were observed to give air-in-eugenol foam, and the creaming rate seemed to depend on the particle type: although the foam volume was not monitored constantly, it was observed that the bubbles stabilised by the large Zonyl MP1400 particles creamed slower than those stabilised by the small Zonyl MP1100. It also seems that the small OTFE and Ultraflon UF-8TA stabilised larger volumes of foams than the other particles, suggesting that at the air-eugenol interface the small particles are better stabilisers than the large ones, as observed commonly in particle-stabilised emulsions.¹³ It can also be due to aggregates formed by those particles rendering them very oleophobic.³² An OTFE particle-stabilised oil film is observed to form on the wall of the vessel, and can be compared to similar films seen previously in hydrophobic particle-water systems (*cf.* Chapter 3).⁴⁶ The Zonyl MP1100 particles however do not stabilise a large volume of foam. It was noticed previously that the particles were partially wetted by eugenol, indicating a lower surface activity at the eugenol-air interface (*cf.* Table 7.1).

The cryo-SEM micrographs displayed in Figure 7.20 show that all particle types adsorb at the air-eugenol interface: all bubbles exhibit irregular surfaces, which may be either due to the particle size and shape (Figures 7.20(b) and (d)), to the dense particle packing at the oil surface (Figures 7.20(c) and (f)), to particle aggregation (Figure 7.20(h)), or simply to freezing of the oil. It is also interesting to note that the highly polydisperse Zonyl MP1400 and the small irregular-shaped Ultraflon MP-8T particles are organised at the eugenol-air interface into a close-packed layer, with very little interface free of particles (Figures 7.20(b) and (d)); similar behaviour is often observed in particle-stabilised emulsions and attributed to their high stability. The small spherical-shaped particles exhibit similar behaviour: Zonyl MP1100 and Ultraflon UF-8TA adsorb at the eugenol-air interface as a dense wavy monolayer (Figures 7.20(c) and (f)), whereas the OTFE are seen to form large particle aggregates producing a very irregular bubble surface (Figure 7.20(h)). The latter particles were also observed previously to form aggregates in methanol (*cf.* § 7.2.2).

Figure 7.19. Photographs of 5-minutes old air-in-eugenol foams stabilised by Zonyl (a) MP 1400, (b) MP 1100, Ultraflon (c) MP-8T, (d) UF-8TA PTFE particles and (e) OTFE particles. Foams were made with 5 wt.% particles by 30 s strong handshaking.

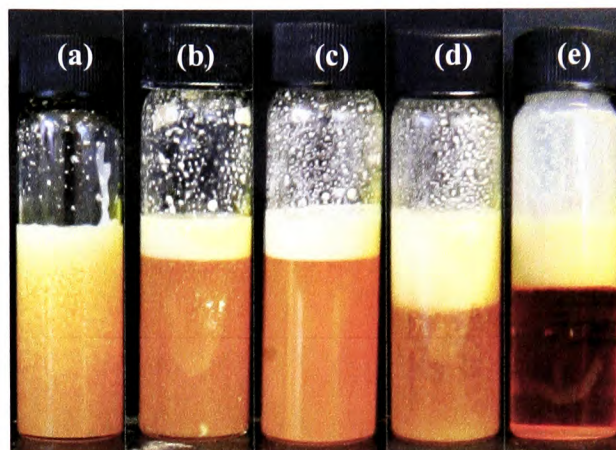
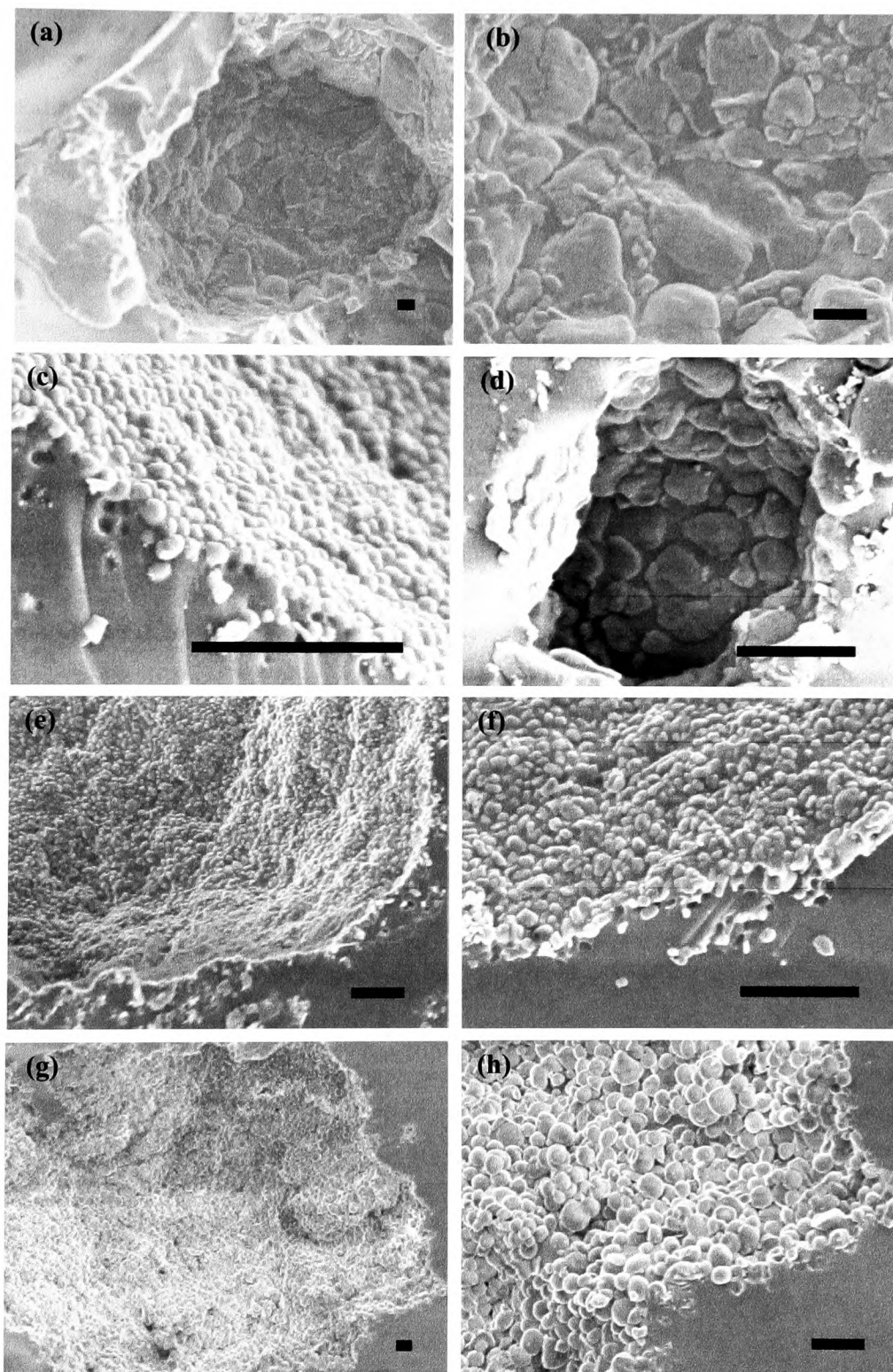


Figure 7.20. Cryo-SEM images of frozen air-in-eugenol foams stabilised with Zonyl (a, b) MP 1400, (c) MP 1100, Ultraflon (d) MP-8T, (e, f) UF-8TA PTFE particles and (g, h) OTFE particles as in Figure 7.19. Foams were made with 5 wt.% particles by 30 s strong handshaking. Scale bars represent 2 μm .



7.3.4 Effect of particle concentration on foams

To study the influence of the particle concentration on foamability and foam stability, two series were made with increasing Ultraflon MP-8T particle concentration in either sunflower oil or eugenol. Figure 7.21 displays the foam series an hour after handshaking, and as expected, the foam volume is observed to increase with increasing particle concentration in both series. It was also noted that the height of sedimented particles, at the bottom of the sample, is more elevated at high particle concentration, with more sediment observed for the sunflower oil than for the eugenol (as in § 7.3.2).

Figure 7.22 enables comparison of the foamability and foam stability as a function of time, for the highest concentration of particles in both the sunflower oil and the eugenol systems. The total volume is observed to stay constant during the 30 minutes of monitoring, while the volume of foam increases slowly for the sunflower oil and decreases for the eugenol: this latter difference in behaviour is probably due to the different viscosities of the two oil, the bubbles creamed slowly in the sunflower oil, gradually contributing to the foam layer, but they creamed quickly in the eugenol, leading to continuous compression of the foam layer formed. The evolution of the foam layer volume with particle concentration is illustrated in Figures 7.23 and 7.24 for sunflower oil and eugenol respectively: the increase in foam volume with increasing particle concentration is observed for both series, with the air-in-eugenol foam volume consistently larger than that of the sunflower oil, as observed previously (*cf.* § 7.3.2).

Figure 7.21. Photographs of 1-hour old (a-e) air-in-sunflower oil and (f-j) air-in-eugenol foams stabilised with Ultraflon MP-8T PTFE particles. Foams were made with (a, f) 0.5, (b, g) 1, (c, h) 2, (d, i) 5 and (e, j) 10 wt.% particles by 30 s strong handshaking.

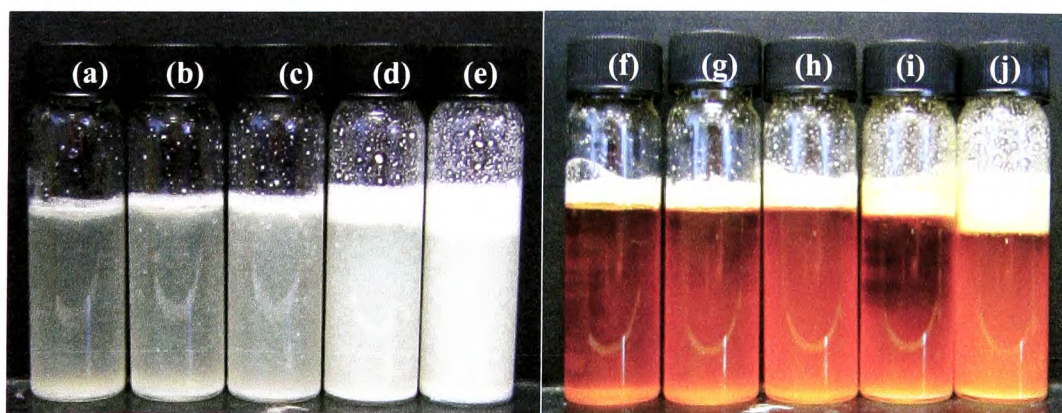


Figure 7.22. Volume of foam stabilised with Ultraflon MP-8T particles after homogenisation as a function of time. Foams were made with 10 wt.% particles in (□) sunflower oil and (■) eugenol by 30 s handshaking. The (—) foam, (····) liquid and (---) total volume of the system are represented on this graph.

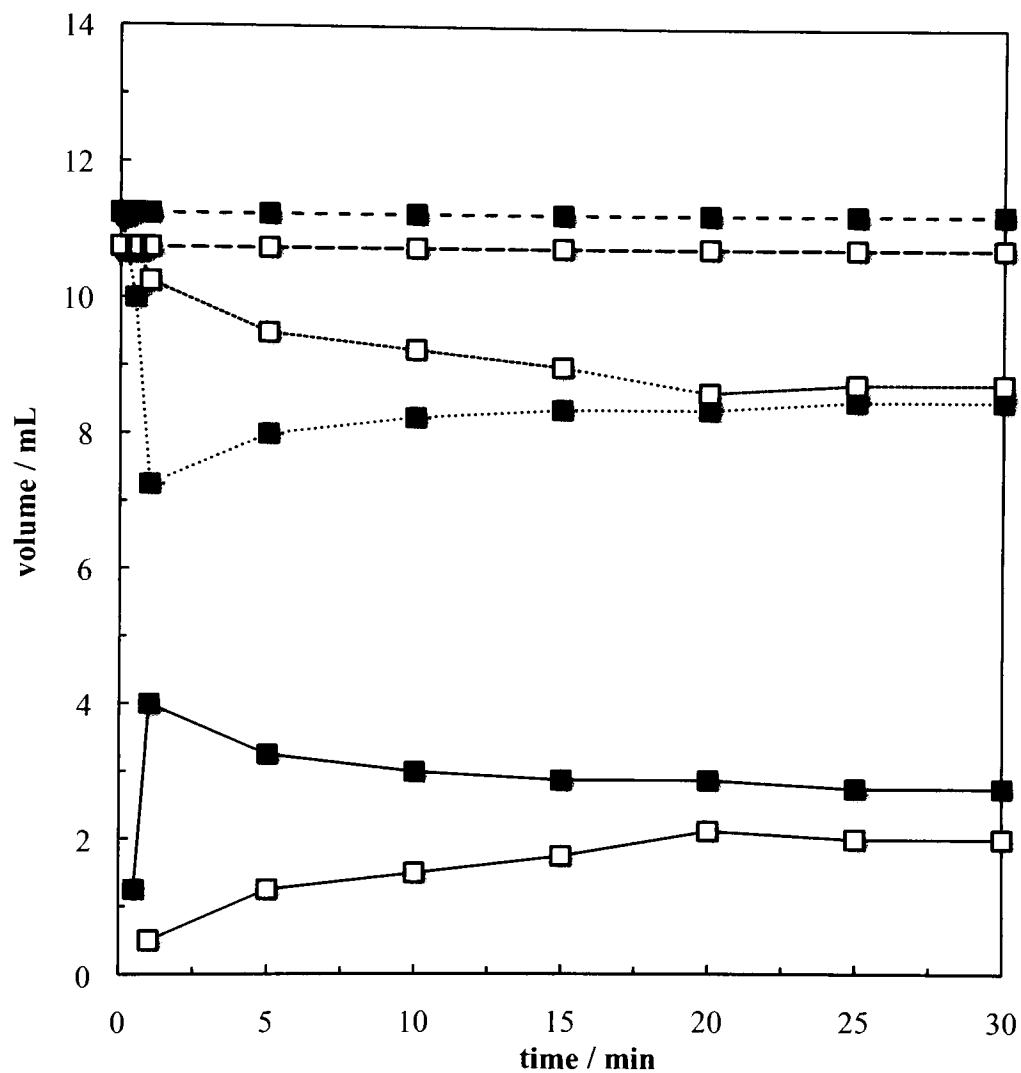


Figure 7.23. Volume of foam stabilised with Ultraflon MP-8T particles after homogenisation as a function of time. Foams were made in sunflower oil by 30 s handshaking. The foam volumes of the system are represented on this graph for (□) 0.5, (◇) 1, (△) 2, (○) 5 and (*) 10 wt.%.

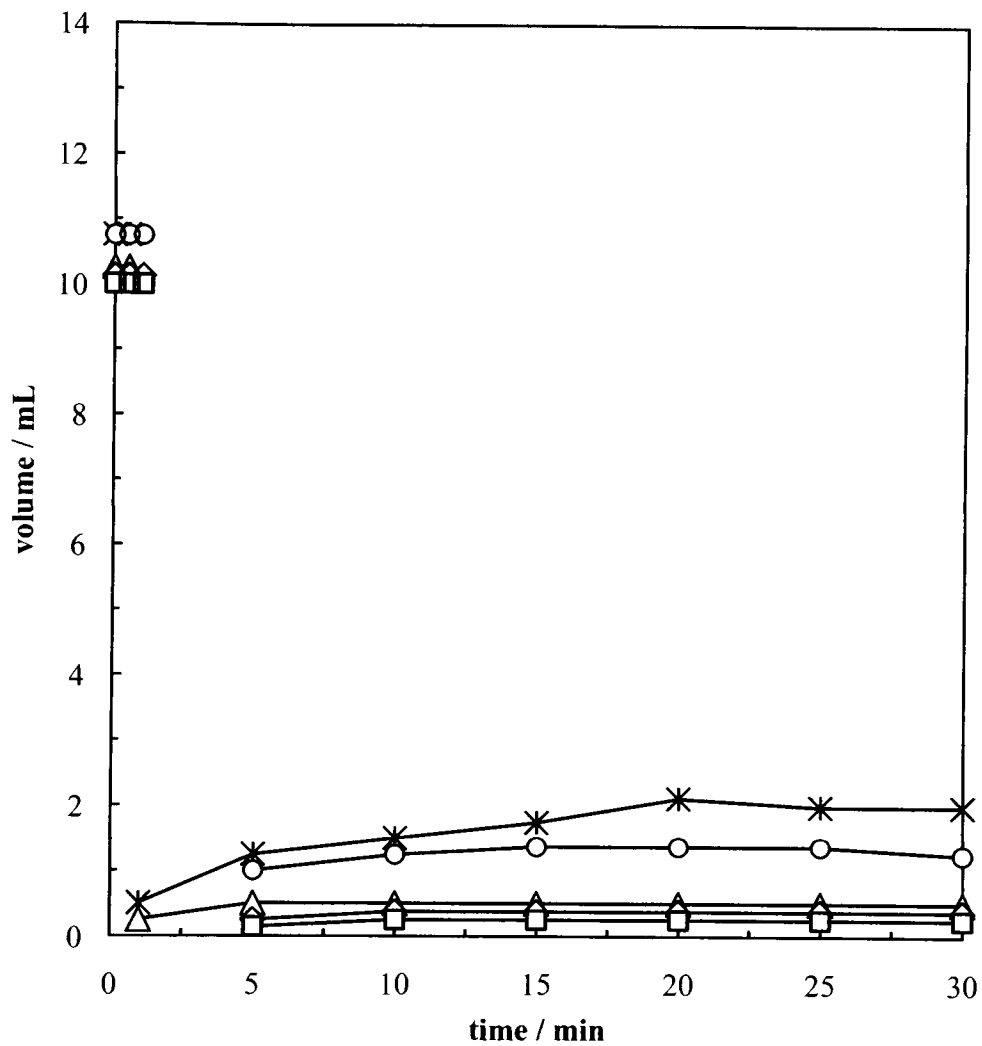
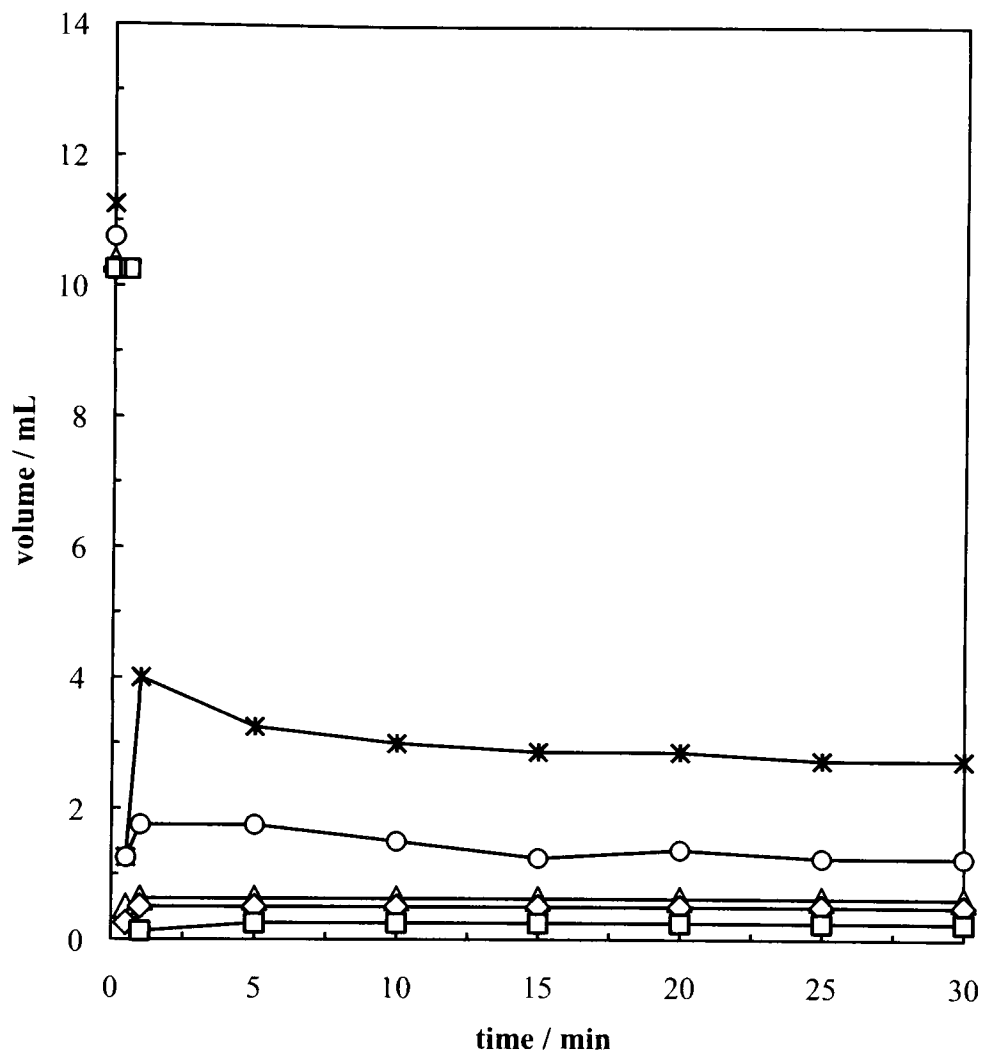


Figure 7.24. Volume of foam stabilised with Ultraflon MP-8T particles after homogenisation as a function of time. Foams were made in eugenol by 30 s handshaking. The foam volumes of the system are represented on this graph for (\square) 0.5, (\diamond) 1, (\triangle) 2, (\circ) 5 and ($*$) 10 wt.%.



7.4 Dry powder with PTFE particles

It was observed that for liquids of much higher tension than the oils studied in section 7.3, like glycerol and water, the curvature of the liquid-air surface inverted and materials termed dry liquid or soufflé were formed containing droplets of liquid coated by particles dispersed in air.

A material similar to powdered dry water was formed, which does not immerse in water and can be shaped in a pile.¹² Figure 7.25 displays this powder resulting from blending water with Zonyl MP1400 particles. Very little water seems to have been encapsulated within the powder (around 5% of the initial volume of water) and the dry liquid does not flow like dry water, as application of shear causes rupture of the droplets and the release of bulk water.⁹ However, water drops covered in particles (liquid marbles) were observed on the powder, and their formation was reproduced, as shown in Figure 7.26(a), by rolling a macroscopic water drop on a bed of Zonyl MP1400 particles.⁴⁷ The adsorbed particle layer prevents the spreading of water on a hydrophilic glass slide, as seen previously (*cf.* Chapter 6). Although they do not form spontaneously when sunflower oil is handshaken with PTFE particles, liquid marbles of sunflower oil can still be stabilised with Zonyl MP1400 particles when rolled on a bed of particles (Figure 7.26(b)).

Figure 7.25. Photographs of 5-minutes old dry water stabilised with Zonyl MP1400 (a) from the side and (b) top of the vessel. The obtained powder is (c) not wet by water and (d) can be shaped in a pile. Dry water was made with 5 wt.% particles by 30 s blender homogenisation at 25000 rpm.

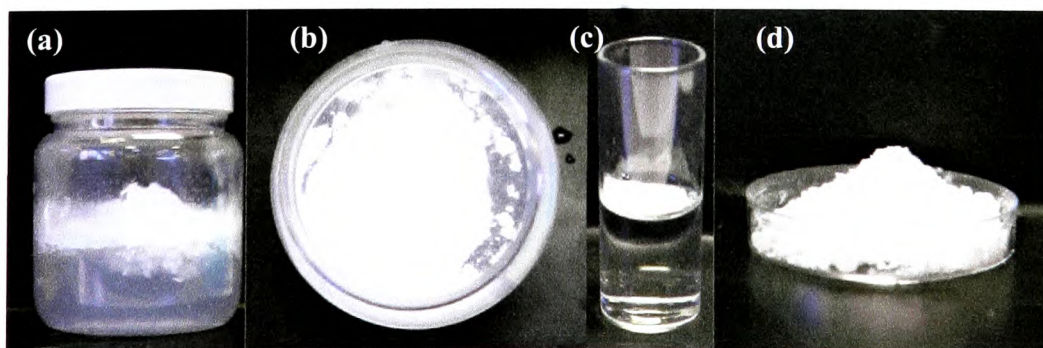
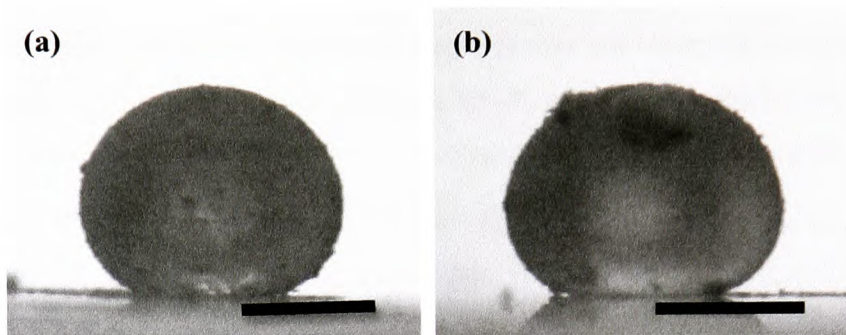
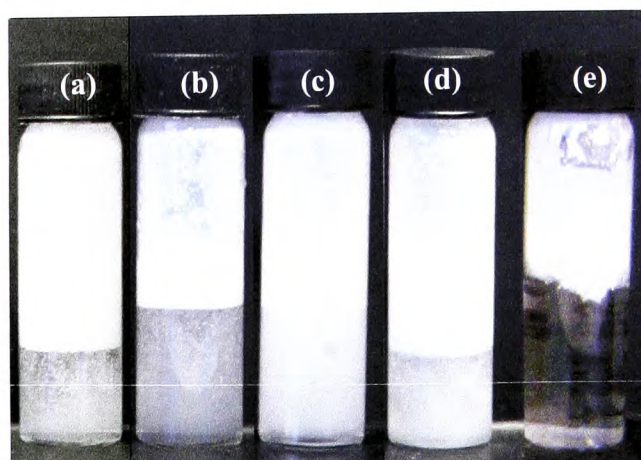


Figure 7.26. Photograph of a (a) water and (b) sunflower oil liquid marble stabilised with Zonyl MP1400 particles in air and on a glass substrate. Scale bars represent 1 mm.



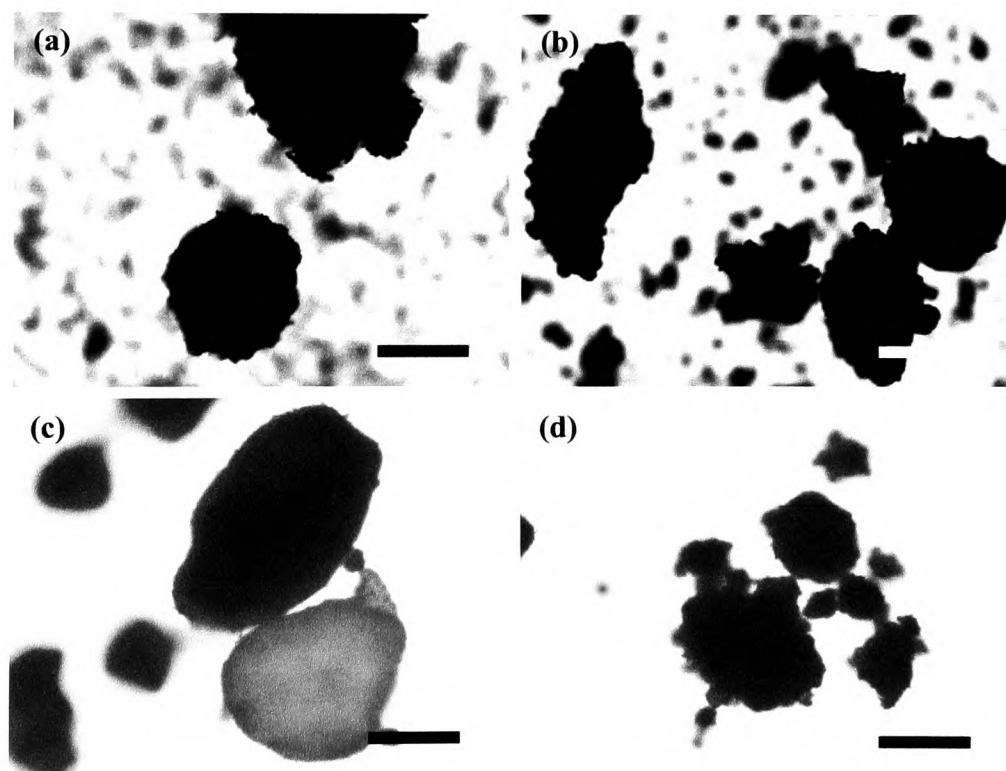
Glycerol handshaken with any of the TFE particles gave a soufflé, which could be described as an intermediate material between a foam and a dry liquid: the soufflé contains liquid encapsulated by particles, but does not exhibit the flowing behaviour of the powder, as it seems to have a high viscosity and gel-like reaction to shaking. The glycerol soufflé series with the different TFE particles is represented in Figure 7.27: as observed for the dry water, the soufflé does not seem to encapsulate a large volume of glycerol. Particles are also spread by the glycerol onto the glass wall of the vessel, however a difference was noted between the particles: some of the PTFE particles disperse a little in the glycerol stabilising some air bubbles before creaming, whereas the OTFE does not go in the glycerol at all, indicating a lower hydrophobicity than the PTFE particles.

Figure 7.27. Photographs of 1-week old glycerol soufflé stabilised with (a) Zonyl MP1400, (b) Zonyl MP 1100, (c) Ultraflon MP-8T, (d) Ultraflon UF-8TA PTFE and (e) OTFE particles. Glycerol soufflé was made with 5 wt.% particles by 30 s handshaking.



The microscopy images of the glycerol soufflé, in Figure 7.28, show that the liquid drops are non-spherical and highly covered with particles. Some drops are believed to be aggregated via non-adsorbed particles, particle aggregates or glycerol films, as in Figure 7.28(b), explaining the higher viscosity displayed by this material compared to the dry powder. The liquid drop size was not observed to depend on the particle type. Drops stabilised by Ultraflon UF-8TA particles, which have the most regular surface, appear more transparent than drops stabilised by other particles, indicating a possibly thinner layer of particles stabilising them.

Figure 7.28. Optical microscopy of glycerol-in-air stabilised with (a) Zonyl MP1400, (b) Zonyl MP1100, (c) Ultraflon UF-8TA and (d) OTFE particles 5 min after homogenisation. Glycerol soufflé was made with 5 wt.% particles by 30 s handshaking. Scale bars represent 160 μm .



7.5 Conclusions

The activity of PTFE and OTFE microparticles at the liquid-air surface has been investigated for a variety of liquids. The five type of particles investigated, four PTFE and one OTFE, presented different size and shape but behaved similarly at the liquid-air surface. When exposed to the liquid surface as a dry powder, it was observed that oils of surface tension under 30 mN m^{-1} wet the particles, whereas relatively high tension oils ($> 30 \text{ mN m}^{-1}$) did not, and they allowed preparation of particle-stabilised air-in-oil foams.

Several mixing methods were employed to produce the non-aqueous foams, with handshaking found to give the larger volumes of foam, probably due to better air entraining. This was also the simplest method to make foams. All foams were stable to coalescence and disproportionation, and formed a dense white layer. Optical and cryo-SEM microscopy revealed that the bubbles formed were non-spherical, with a wavy surface covered with close-packed layers of particles, whether the particle were spherical or not.

Foams produced with oils of intermediate surface tension were observed to be slightly affected by the type of oil used: the volume of foam formed was approximately equivalent, although the perfume oils seemed to produce a little more foam, and exhibited less sedimented particles than the vegetable oils. The non-spherical nature of the air bubbles in the perfume oils also indicated strong particle adsorption during shear. The type of particle was also observed to affect the foam: the bubbles stabilised were bigger for larger particles, and the small particles stabilised larger foam volumes. It was also noted that the OTFE particles were able to stabilise oil films on the glass wall of the sample vessel, indicating higher oleophobicity. Like in particle-stabilised emulsions, the volume of foam was shown to depend on the concentration of particles: the foam volume increased with increasing particle concentration.

With liquids of higher surface tension, different materials were formed: dry liquids were produced with water, and a soufflé (foam-dry liquid intermediate material) was made with glycerol. The increased viscosity of the soufflé is probably caused by aggregation of the liquid drops, either through particles or through liquid films.

7.6 References

1. T. N. Hunter, R. J. Pugh, G. V. Franks and G. J. Jameson, *Adv. Colloid Interface Sci.*, **137**, 57 (2008).
2. B. P. Binks and T. S. Horozov, *Colloidal Particles at Liquid Interfaces*, University Press, Cambridge, 2006.
3. D. R. Exerowa and P. M. Kruglyakov, *Foam and foam films: theory, experiment, application*, Elsevier, Amsterdam, 1998.
4. T. S. Horozov, *Curr. Opin. Colloid Interface Sci.*, **13**, 134 (2008).
5. R. Aveyard, P. Cooper, P. D. I. Fletcher and C. E. Rutherford, *Langmuir*, **9**, 604 (1993).
6. G. Johansson and R. J. Pugh, *Int. J. Miner. Process.*, **34**, 1 (1992).
7. S. Schwarz and S. Grano, *Colloids Surf. A*, **263**, V (2005).
8. A. van der Zon, P. J. Hamersma, E. K. Poels and A. Blik, *Chem. Eng. Sci.*, **57**, 4845 (2002).
9. A. B. Subramaniam, M. Abkarian and H. A. Stone, *Nature Mater.*, **4**, 553 (2005).
10. A. B. Subramaniam, C. Mejean, M. Abkarian and H. A. Stone, *Langmuir*, **22**, 5986 (2006).
11. G. S. Vinod Kumar, F. Garcia-Moreno, N. Babcsan, A. H. Brothers, B. S. Murty and J. Banhart, *Phys. Chem. Chem. Phys.*, **9**, 6415 (2007).
12. B. P. Binks and R. Murakami, *Nature Mater.*, **5**, 865 (2006).
13. B. P. Binks and S. O. Lumsdon, *Langmuir*, **16**, 8622 (2000).
14. S. K. Bindal, G. Sethumadhavan, A. D. Nikolov and D. T. Wasan, *AIChE J.*, **48**, 2307 (2002).
15. B. P. Binks and T. S. Horozov, *Angew. Chem. Int. Ed.*, **44**, 3722 (2005).
16. E. Dickinson, R. Ettelaie, T. Kostakis and B. S. Murray, *Langmuir*, **20**, 8517 (2004).
17. B. P. Binks, R. Murakami, S. P. Armes, S. Fujii and A. Schmid, *Langmuir*, **23**, 8691 (2007).
18. A. L. Campbell, S. D. Stoyanov and V. N. Paunov, *Soft Matter*, **5**, 1019 (2009).

19. Z. P. Du, M. P. Bilbao-Montoya, B. P. Binks, E. Dickinson, R. Ettelaie and B. S. Murray, *Langmuir*, **19**, 3106 (2003).
20. S. Fujii, P. D. Iddon, A. J. Ryan and S. P. Armes, *Langmuir*, **22**, 7512 (2006).
21. S. Fujii, A. J. Ryan and S. P. Armes, *J. Am. Chem. Soc.*, **128**, 7882 (2006).
22. R. H. Ottewill, D. L. Segal and R. C. Watkins, *Chemistry & Industry*, 57 (1981).
23. S. E. Friberg, C. S. Wohn, B. Greene and R. Vangilder, *J. Colloid Interface Sci.*, **101**, 593 (1984).
24. L. K. Shrestha, K. Aramaki, H. Kato, Y. Takase and H. Kunieda, *Langmuir*, **22**, 8337 (2006).
25. A. Tuteja, W. Choi, M. L. Ma, J. M. Mabry, S. A. Mazzella, G. C. Rutledge, G. H. McKinley and R. E. Cohen, *Science*, **318**, 1618 (2007).
26. I. Akartuna, E. Tervoort, J. C. H. Wong, A. R. Studart and L. J. Gauckler, *Polymer*, **50**, 3645 (2009).
27. P. S. Bhosale, M. V. Panchagnula and H. A. Stretz, *Appl. Phys. Lett.*, **93**, (2008).
28. E. Bormashenko, T. Stein, G. Whyman, Y. Bormashenko and R. Pogreb, *Langmuir*, **22**, 9982 (2006).
29. J. C. H. Wong, E. Tervoort, S. Busato, U. T. Gonzenbach, A. R. Studart, P. Ermanni and L. J. Gauckler, *J. Mater. Chem.*, **20**, 5628 (2010).
30. H. W. Fox and W. A. Zisman, *J. Colloid Sci.*, **5**, 514 (1950).
31. E. G. Shafrin and W. A. Zisman, *J. Phys. Chem.*, **64**, 519 (1960).
32. R. Murakami and A. Bismarck, *Adv. Funct. Mater.*, **20**, 732 (2010).
33. R. Thomas, Material Properties of Fluoropolymers and Perfluoroalkyl-based Polymers, in *Fluoropolymers 2*; Hougham, G.; Cassidy, P.; Johns, K.; Davidson, T. ed., Springer, New York, 2002.
34. R. Wagner, L. Richter, Y. Wu, J. Weißmüller, J. Reiners, E. Hengge, A. Kleewein and K. Hassler, *Applied Organometallic Chemistry*, **11**, 645 (1997).
35. D. L. Goldfarb, J. J. de Pablo, P. F. Nealey, J. P. Simons, W. M. Moreau and M. Angelopoulos, in *Aqueous-based photoresist drying using supercritical carbon dioxide to prevent pattern collapse*, Rancho Mirage, California, 3313, 2000.
36. S. A. Brewer and C. R. Willis, *Appl. Surf. Sci.*, **254**, 6450 (2008).

37. A. F. Thünemann, *Polymer International*, **49**, 636 (2000).
38. J.-M. Corpart, S. Girault and D. Juhu, *Langmuir*, **17**, 7237 (2001).
39. S. M. Iveson, S. Holt and S. Biggs, *Colloids Surf. A*, **166**, 203 (2000).
40. L. R. Fisher and J. N. Israelachvili, *Chem. Phys. Let.*, **76**, 325 (1980).
41. S. Semal, T. D. Blake, V. Geskin, M. J. de Ruijter, G. Castelein and J. De Coninck, *Langmuir*, **15**, 8765 (1999).
42. B. P. Binks, A. J. Johnson and J. A. Rodrigues, *Soft Matter*, **6**, 126 (2010).
43. B. P. Binks and A. Rocher, *J. Colloid Interface Sci.*, **335**, 94 (2009).
44. A. C. Martinez, E. Rio, G. Delon, A. Saint-Jalmes, D. Langevin and B. P. Binks, *Soft Matter*, **4**, 1531 (2008).
45. B. P. Binks, C. A. Davies, P. D. I. Fletcher and E. L. Sharp, *Colloids Surf. A*, **360**, 198 (2010).
46. B. P. Binks, J. H. Clint, P. D. I. Fletcher, T. J. G. Lees and P. Taylor, *Chem. Commun.*, **33**, 3531 (2006).
47. P. Aussillous and D. Quere, *Nature*, **411**, 924 (2001).

CHAPTER 8 POWDERED EMULSIONS STABILISED BY FUMED SILICA PARTICLES

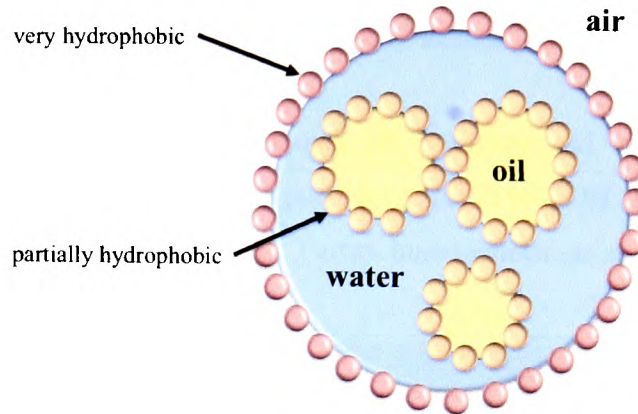
8.1 Introduction

Liquid drops in air encapsulated by particles can be produced on a macroscopic or on a microscopic scale: liquid marbles measure up to several millimetres while dry water drops are as little as 50 μm .^{1, 2} Binks and Murakami showed that the mixing of air, water and silica powder gave different materials depending on the silica particle wettability: aqueous dispersions were made with hydrophilic silica particles ($\theta < 20^\circ$), stable air-in-water foams were made with silica of intermediate hydrophobicity ($32^\circ < \theta < 62^\circ$) and stable drops of water-in-air with very hydrophobic silica ($\theta > 66^\circ$). The water-in-air material is called “dry water” as it behaves like a free-flowing powder, containing non-spherical drops of water piled on top of each other. Such water encapsulation is believed to have cosmetic applications, and can be used as gas storage or reactor cells.^{3, 4} Liquid marbles, which have been produced with a wide variety of particles (from latex to PTFE), can be thought of as the macroscopic equivalent of “dry water”, with potential applications in microfluidics as liquid or particle carriers.^{1, 5, 6}

Murakami and Bismark achieved encapsulation of squalane and hexadecane into OTFE oleophobic particle capsules by spraying oils onto a bed of particles.⁷ However, the content of oil was only up to 15 wt.% of the material, while dry water can contain up to 98 wt.% water.² It follows that the encapsulation of an oil-in-water emulsion may provide a means to improve this uptake.

This study aims at determining the processes which enable production of powdered emulsions or emulsions encapsulated in the form of a free-flowing powder. This material will be an oil-in-water-in-air material (Figure 8.1). Toward this objective, the emulsion to encapsulate was first optimised in terms of the particles used and their concentration, before optimising the process and particles used for the emulsion encapsulation. The maximum concentration of oil in encapsulated emulsions in a flowing powder form was then determined.

Figure 8.1 Schematic representation of the oil-in-water-in-air material: the oil drops are stabilised in water with partially hydrophobic silica particles, while the water drop are stabilised in air with very hydrophobic silica particles.



8.2 Oil-in-water emulsions

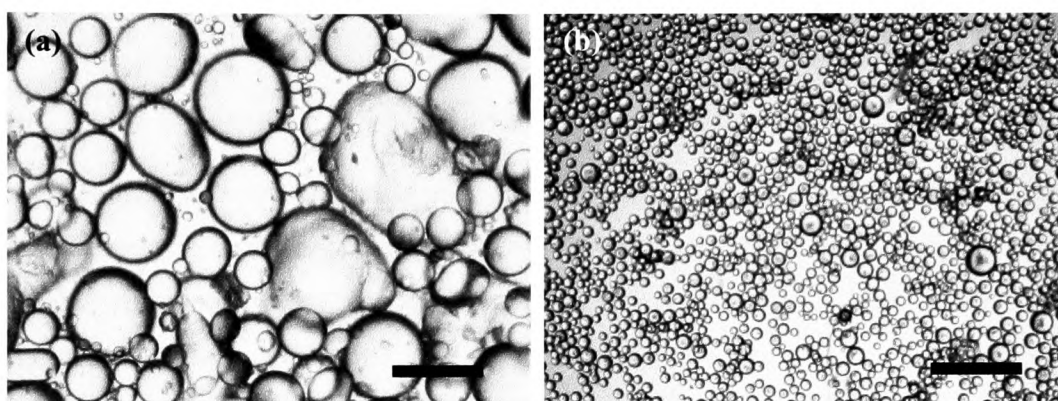
Production of a powdered emulsion to encapsulate oil requires a stable oil-in-water emulsion, which will remain stable to dilution in its continuous phase and a second short homogenisation. For this purpose, the following part investigates the particle wettability and concentration of the silica particles in order to obtain a stable emulsion. A range of silica particles was used with varying remaining surface silanol content (%SiOH) after partial hydrophobisation. Higher %SiOH denotes more hydrophilic less modified particles.

8.2.1 Effect of particle hydrophobicity on emulsions

Silica particles with a high content of silanol were chosen as they should not affect the second homogenisation by adsorbing at the air-water interface.² Tricaprylin-in-water emulsions were made with 1 wt.% of 71% and 80% SiOH silica particles with equal volumes of oil and water. The tricaprylin-in-water emulsion stabilised with 80% SiOH silica particles shows little coalescence 5 minutes after preparation, with $f_{oil} = 0.01$. However, the emulsion stabilised with 71% SiOH exhibits resolved oil ($f_{oil} = 0.35$) after 5 minutes and the drops reach millimetre sizes. Figure 8.2 displays the microscopic images of the two emulsions: the one stabilised by 71% SiOH presents large ($d = 364 \mu\text{m}$ on average) non-spherical drops

polydisperse in size, whereas the 80% SiOH stabilised one exhibits small spherical drops of 39 μm average diameter with a low polydispersity. Although it shows evidence of a little coalescence, observations of both emulsion stability, drop appearance and size demonstrate that the 80% SiOH-stabilised emulsion displays more ideal characteristics for production of the powdered emulsion.

Figure 8.2. Optical microscopy images of 5-minute old tricaprylin-in-water emulsions stabilised with 1 wt.% silica particles at (a) 71% SiOH and (b) 80% SiOH. Emulsions were made by 2 min. Ultra Turrax homogenisation at 13000 rpm. Scale bars represent 400 μm .



8.2.2 Effect of particle concentration on emulsions

To optimise the stability of tricaprylin-in-water emulsions stabilised with 80% SiOH silica particles, the effect of particle concentration is studied. It has already been shown that an increasing concentration of particles leads usually to an increase in the emulsion stability,⁸ however too high a particle concentration has to be avoided as the excess of hydrophilic particles could interact with the hydrophobic particles added later on for producing of the powdered emulsion. Mixtures of hydrophilic and hydrophobic particles are known to be antagonistic in terms of emulsion stability and so this is to be avoided here.⁹ The initial particle concentration at 1 wt.% was increased to 2 and 3 wt.-%: the fraction of coalesced oil decreased from 0.01 to less than 0.01 with 2 wt.-% particles, and no coalescence was observed for the emulsion at 3 wt.-% particles. The emulsion drops were also observed to diminish in size. Figure 8.3 shows that the drops for emulsions stabilised with 1 wt.-% ($d = 39$

μm) are larger than the 2 wt.% ones ($d = 28 \mu\text{m}$) and the 3 wt.% ones ($d = 22 \mu\text{m}$) when observed by optical microscopy. However, all emulsion drops were spherical with little polydispersity.

The tricaprylin-in-water emulsion stabilised by 3 wt.% of 80% SiOH silica particles was chosen to be the potential disperse phase in powdered emulsions due to its stability to coalescence and creaming, as can be seen in Figure 8.3. The white emulsion exhibits a high viscosity, probably responsible for the low creaming observed.¹⁰ The monomodal size distribution of its oil drops is given in Figure 8.4: the drop size ranges from 5 to 100 μm diameter, with an average of 25 μm . The small size of these drops also meant that this emulsion in particular was required for powdered emulsion preparation, as dry water drops are often as little as 50 μm in diameter themselves.²

Figure 8.3. (a, b and c) Optical microscopy images and (d) photographs of 5-minute old tricaprylin-in-water emulsions stabilised with (a) 1, (b) 2 and (c and d) 3 wt.% silica particles at 80% SiOH. Emulsions were made by 2 min. Ultra Turrax homogenisation at 13000 rpm. Scale bars represent 160 μm .

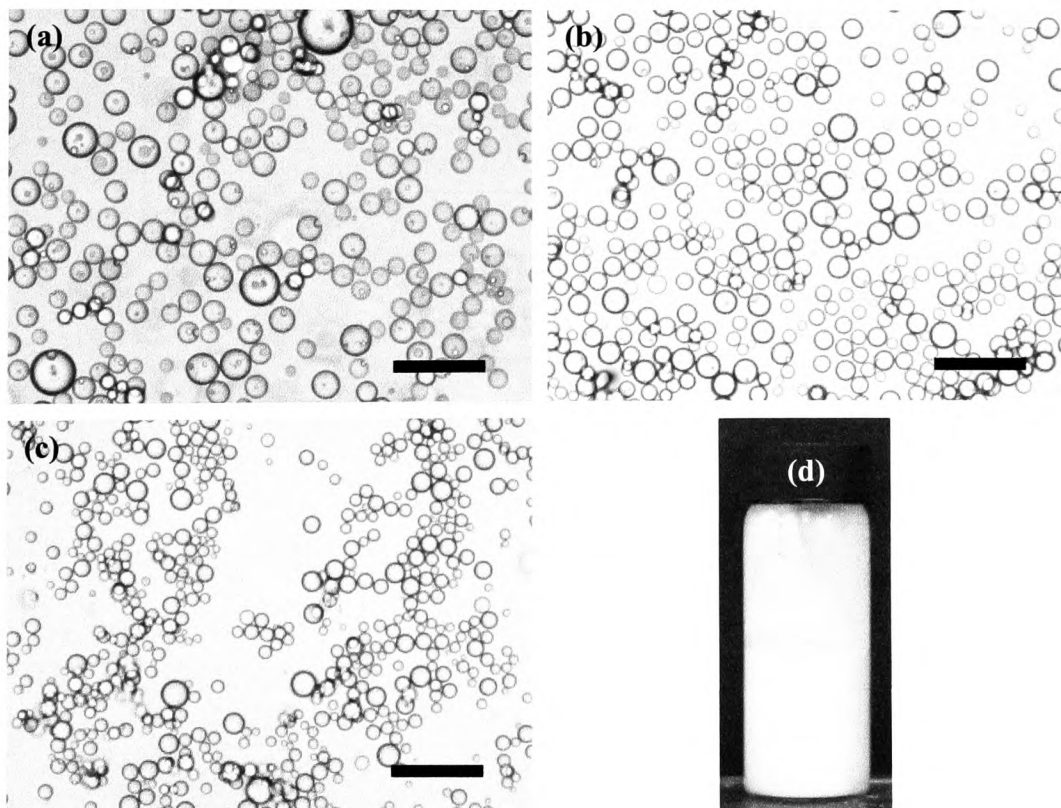
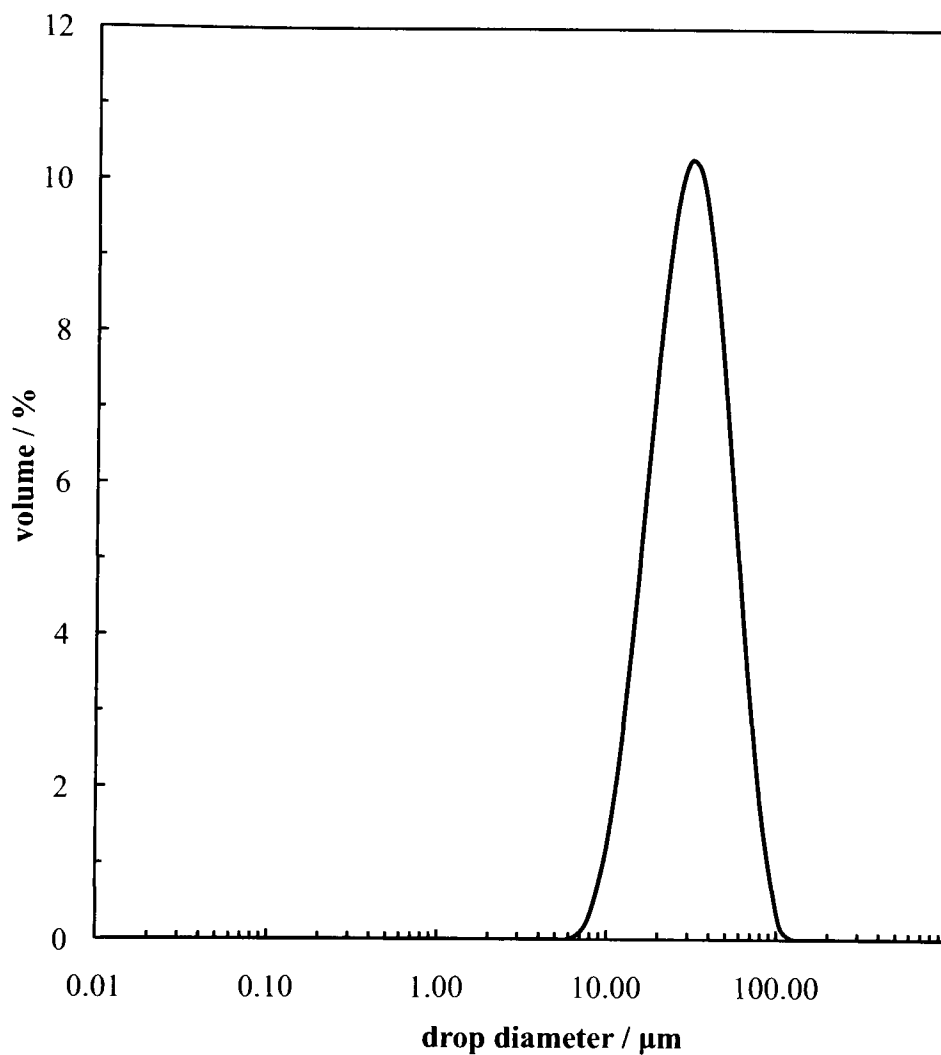


Figure 8.4. Size distribution of 5-minutes old tricaprylin-in-water emulsion drops stabilised with 3 wt.% silica particles at 80% SiOH. The emulsion was made by 2 min. Ultra Turrax homogenisation at 13000 rpm and was measured with a Mastersizer 2000.



8.3 Oil-in-water-in-air powdered emulsions

Various parameters were investigated in order to make a powdered emulsion: the silanol content of the hydrophobic particles used to encapsulate the emulsion, the homogenisation time and the maximum fraction of oil, which can be encapsulated.

8.3.1 Effect of particle hydrophobicity on powdered emulsions

Binks and Murakami produced dry water using 20% SiOH silica particles by homogenising the three components in a blender.² When their experiment is repeated with 14% SiOH silica particles, a material similar to their description is obtained: a flowing powder, which releases water when rubbed, displayed in Figure 8.5. The powder can be shaped into a mountain-like pile and remains stable to coalescence for more than 4 weeks. Optical microscopy in Figure 8.6 shows the non-spherical and polydisperse water capsules produced.

Figure 8.5. Photographs of dry water with 5 wt.% silica particles at 14% SiOH. Dry water was made by 30 seconds homogenisation in a blender jug at 25000 rpm. Photographs show the (a) side and (b) top of the vessel and (c) a pile of the resulting material.

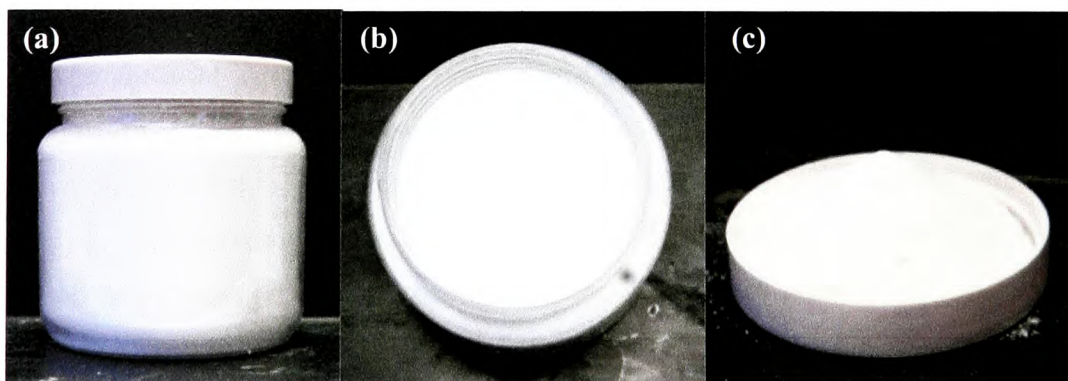
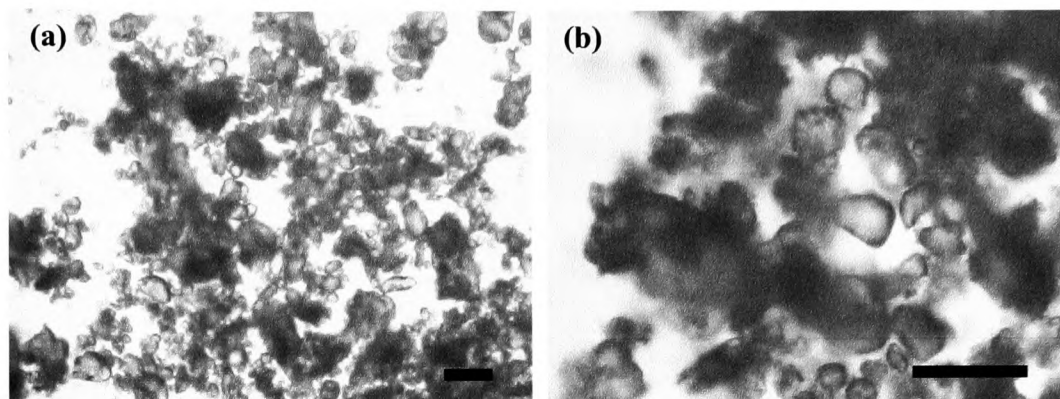


Figure 8.6. Optical microscopy images of a 5-minute old water-in-air powder stabilised with 5 wt.% silica particles at 14% SiOH. Dry water was made by 30 s. blender homogenisation at 25000 rpm. Scale bars represent 200 μm .



The tricaprylin-in-water emulsion shown in Figure 8.3 was diluted 10 times with Milli-Q water to a volume of 95 mL and then blended with either 5 wt.% of 20% SiOH silica particles, like Binks and Murakami, or with 14% SiOH silica particles. The obtained materials are displayed in Figure 8.7: both products display a smaller volume than the dry water shown in Figure 8.5, also containing 95 mL of fluid phase, and exhibit different rheology to the dry water. The materials are compact and act like a foam when agitated (gel-like behaviour), but they also contain a small amount of dry material which delivers liquid when rubbed. It is close to the soufflé material described by Binks and Murakami, which occurs close to the inversion point of the air-water systems.² The material formed with the 20% SiOH silica particles has a wetter appearance, and some excess liquid was observed after mixing. The microscopy image in Figure 8.8b shows that it contains large round water drops most probably stabilised by a rough layer of particle aggregates. The sample seemed to contain both dry and wet material. However, the material stabilised with the 14% SiOH particles appeared more similar to a dry powder: the micrographs in Figure 8.8(a) displays the non-spherical capsules of liquid, larger but similar to those in Figure 8.6. Although the thick layer of particles restricts observation inside the capsule, it is believed that they contain the original emulsion drops.

Figure 8.7. Photographs of 5-minute old tricaprylin-water-air soufflés stabilised with 5 wt.% silica particles at (a, d) 14% and (b, e) 20% SiOH. Tricaprylin-in-water emulsions were stabilised by 3 wt.% of 80% SiOH silica particles at $\Phi_o = 0.5$ before dilution to $\Phi_o = 0.05$. Soufflés were made by 30 s homogenisation in a blender jug at 25000 rpm. Photographs show the (a-b) side and (d-e) top of the vessel.

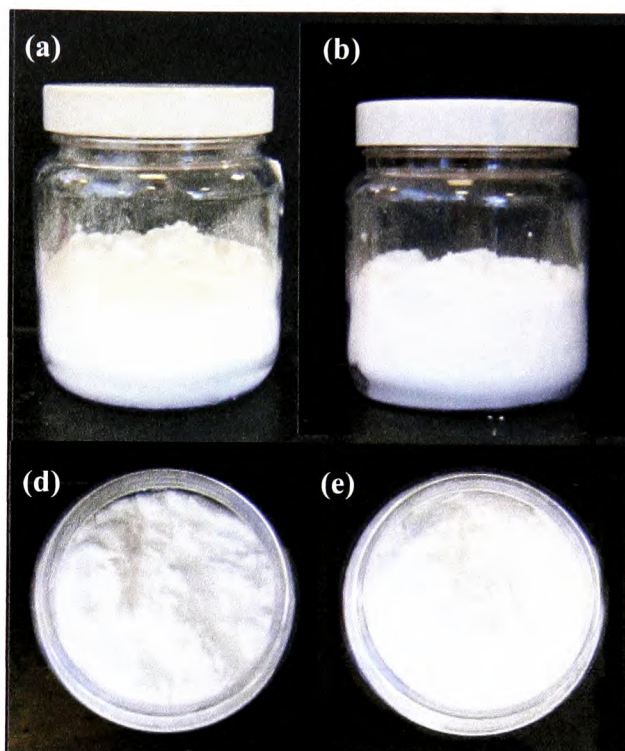
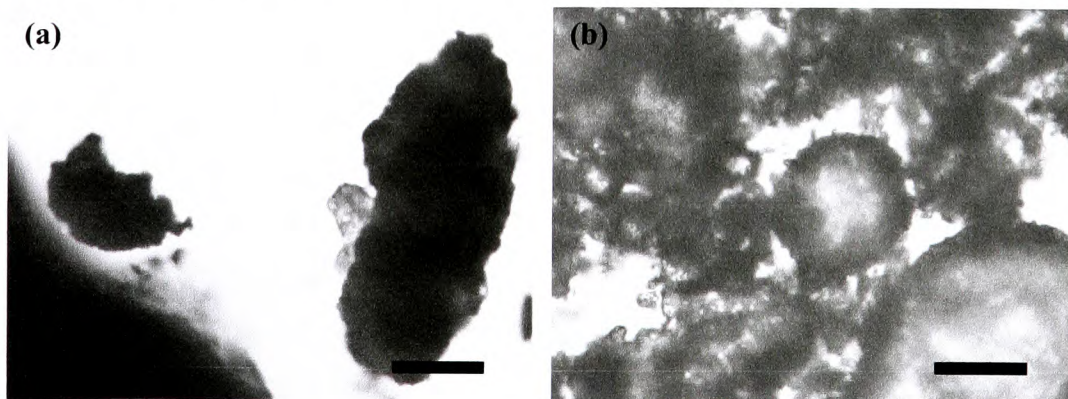


Figure 8.8. Optical microscopy images of 5-minute old tricaprylin-water-air soufflés stabilised with 5 wt.% silica particles at (a) 14% and (b) 20% SiOH. Tricaprylin-in-water emulsions were stabilised by 3 wt.% of 80% SiOH silica particles at $\Phi_o = 0.5$ before dilution to $\Phi_o = 0.05$. Soufflés were made by 30 s homogenisation in a blender jug at 25000 rpm. Scale bars represent 160 μm .



8.3.2 Effect of blending time on powdered emulsions

During blender homogenisation, the tricaprylin-water-air material was observed to change in appearance. Consequently blender homogenisation for different lengths of time was investigated. The products formed displayed different appearances (Figure 8.9): a 40 s blending gives a soufflé with a foam-like aspect, at 20 s the material resembles the soufflé formed with the 30 s blending, whereas the 5 s blending produces a dry material. The powdered material flows similarly to dry water, and can also be shaped into a mountain-like pile (Figure 8.9(g)). Under microscopy, in Figure 8.10, the soufflé and dry material have similar appearances: liquid is encapsulated by particles in non-spherical and irregular oil-in-water-in-air globules. Although few differences can be noted, the dry material exhibits only a dry phase, and oil drops are visible in the liquid capsule (Figure 8.10(d)), hence the oil has effectively been encapsulated within a dry powder.

To render more obvious the presence of oil drops in the emulsion capsules, the production of the powdered emulsion was repeated with Nile red fluorescent dye contained within the tricaprylin oil. Figures 8.10(e) and (f) show the microscopy images with and without UV light: some oil drops can be observed, but they are larger than the initial emulsion drops. Although the large size could be indicating drop aggregates, the second homogenisation (blending) might have affected the emulsion drops by causing their limited coalescence under shear. Although the dye intensity is stronger for the oil drops, the water capsules also appear slightly red, possibly indicating free oil or particle-stabilised oil drops at the capsule surface. The partial destruction of the particle-stabilised oil drops during blender homogenisation may also explain the transition to more foam-like materials with homogenisation time. The destruction of the emulsion drops would reduce the average particle contact angle at the fluid surface, either through the release of hydrophilic particles or free oil from the emulsion drops.

Cryo-SEM micrographs of the frozen powdered emulsion are displayed in Figure 8.11: the dry capsules of emulsion are observed to measure an average of 50 μm , and closer examination enables detection of the round emulsion drops up to 10 μm in diameter under the surface particle layer. The drops seem to be close to the silica capsule surface as expected from their buoyancy.

Figure 8.9. Photographs of 5-minute old tricaprylin-water-air materials stabilised with 5 wt.% silica particles at 14% SiOH. Tricaprylin-in-water emulsions stabilised by 3 wt.% of 80% SiOH silica particles at $\Phi_o = 0.5$ before dilution to $\Phi_o = 0.05$. Soufflés or powdered emulsions were made by (a, d) 40, (b, e) 30 or (c, f-g) 5 seconds homogenisation in a blender jug at 25000 rpm. Photographs show the (a-c) side and (d-f) top of the vessel, and a pile formed of the dry emulsion in (c).

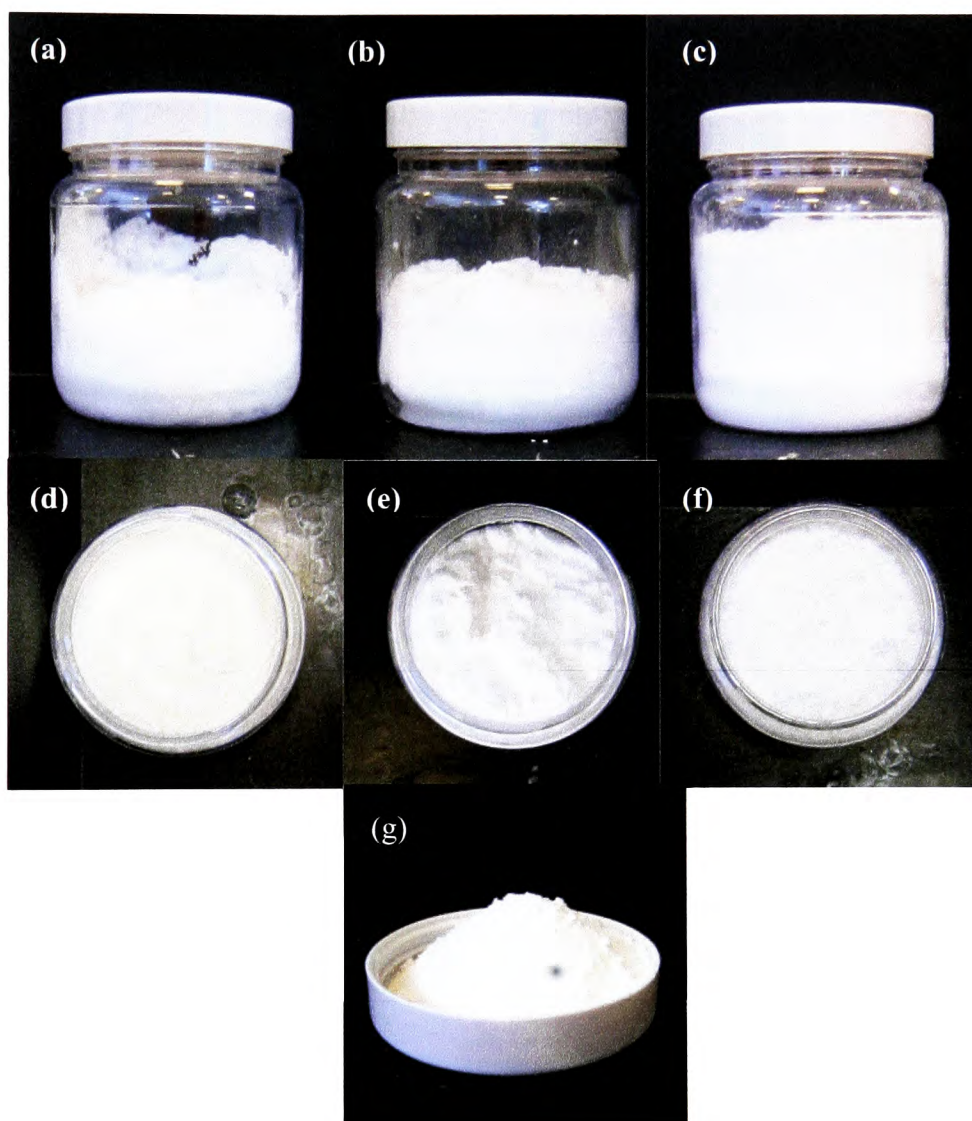


Figure 8.10. Optical microscopy images of 5-minute old tricaprylin-water-air stabilised with 5 wt.% silica particles at 14% SiOH. Tricaprylin-in-water emulsions were stabilised by 3 wt.% of 80% SiOH silica particles at $\Phi_o = 0.5$ before dilution to $\Phi_o = 0.05$. Soufflés or powdered emulsions were made by (a) 40, (b) 20 and (c-f) 5 seconds homogenisation in a blender jug at 25000 rpm. Scale bars represent 160 μm .

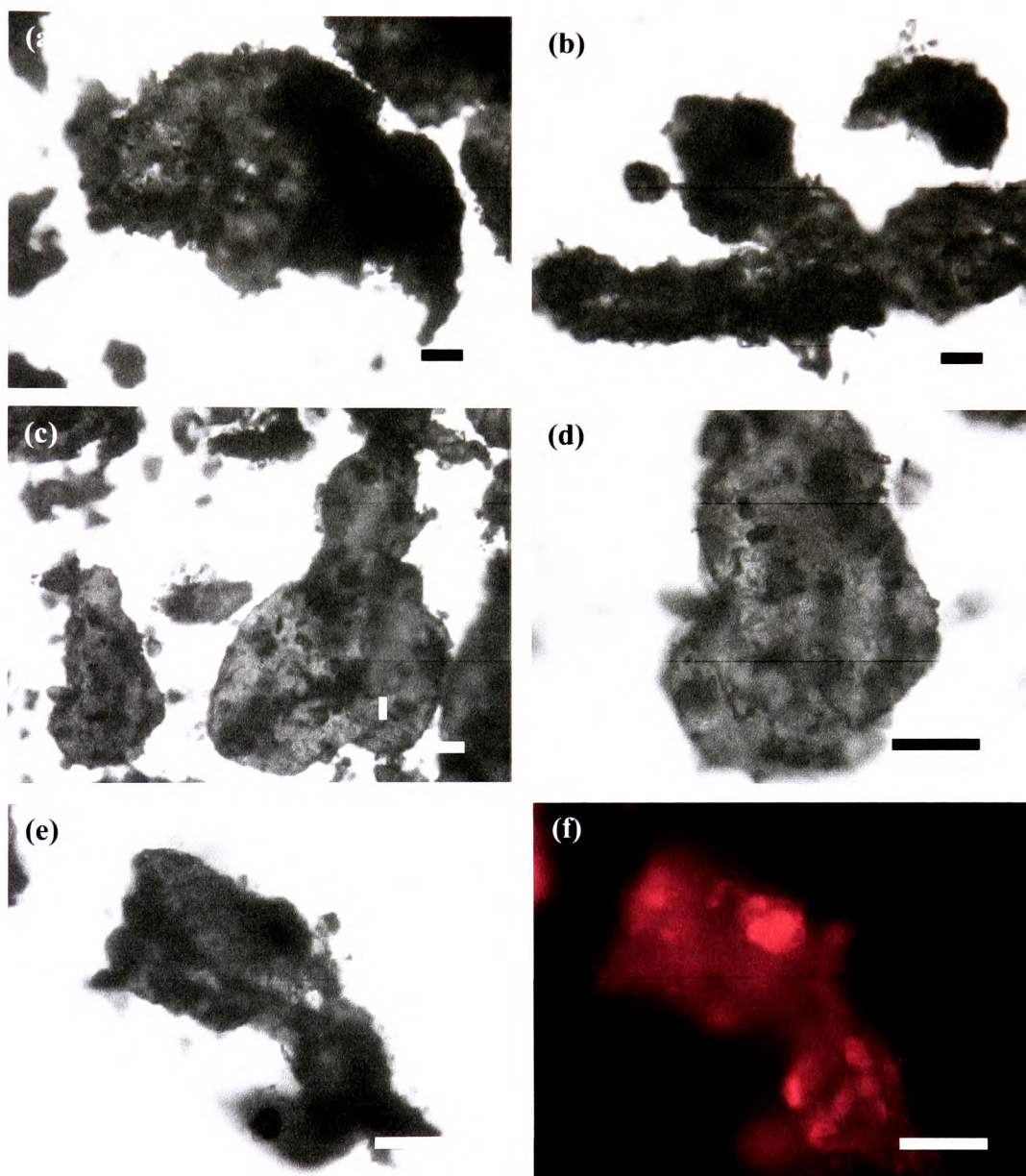
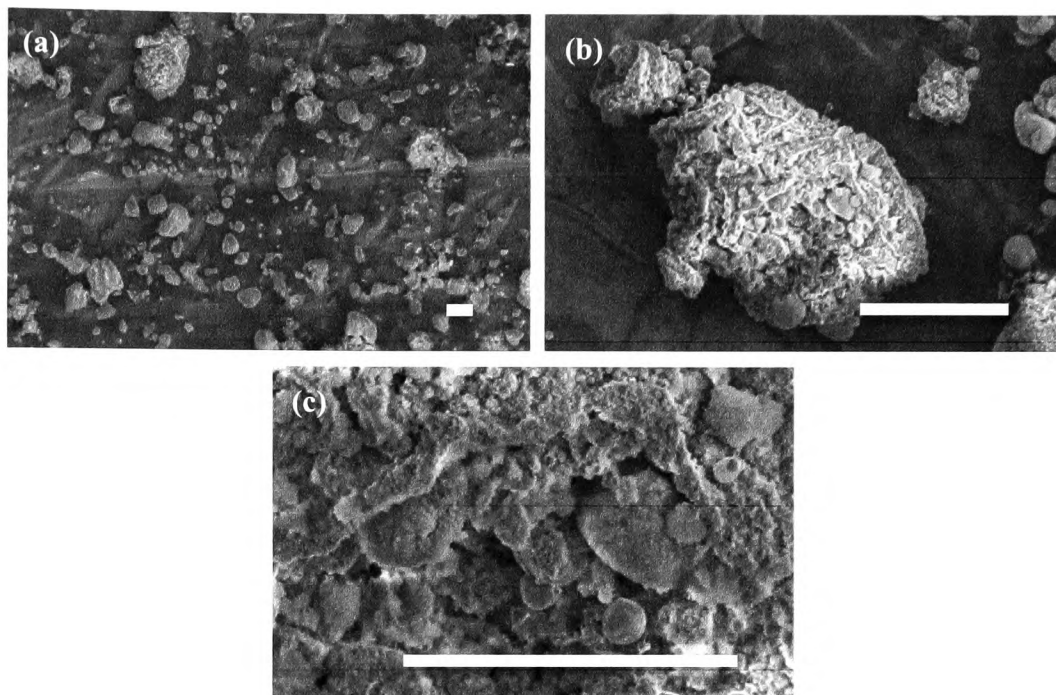


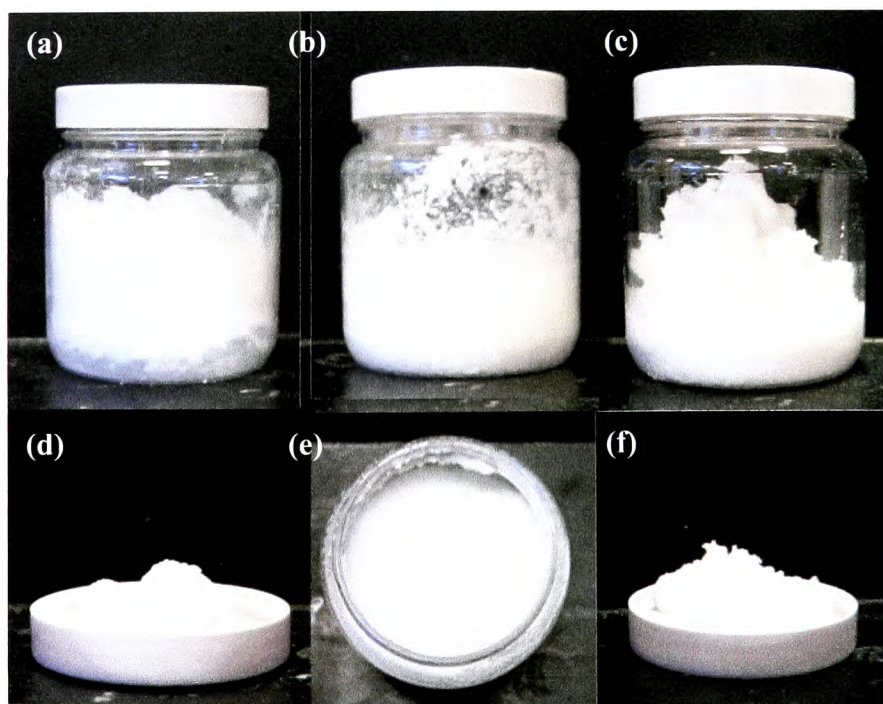
Figure 8.11. Cryo-SEM images of tricaprylin-in-water-in-air capsules stabilised with 5 wt.% silica particles at 14% SiOH. Tricaprylin-in-water emulsions were stabilised by 3 wt.% of 80% SiOH silica particles at $\Phi_o = 0.5$ before dilution to $\Phi_o = 0.05$. Powdered emulsion was made by 5 seconds blending in a blender jug at 25000 rpm. Scale bars represent 50 μm .



8.3.3 Effect of initial oil fraction on powdered emulsions

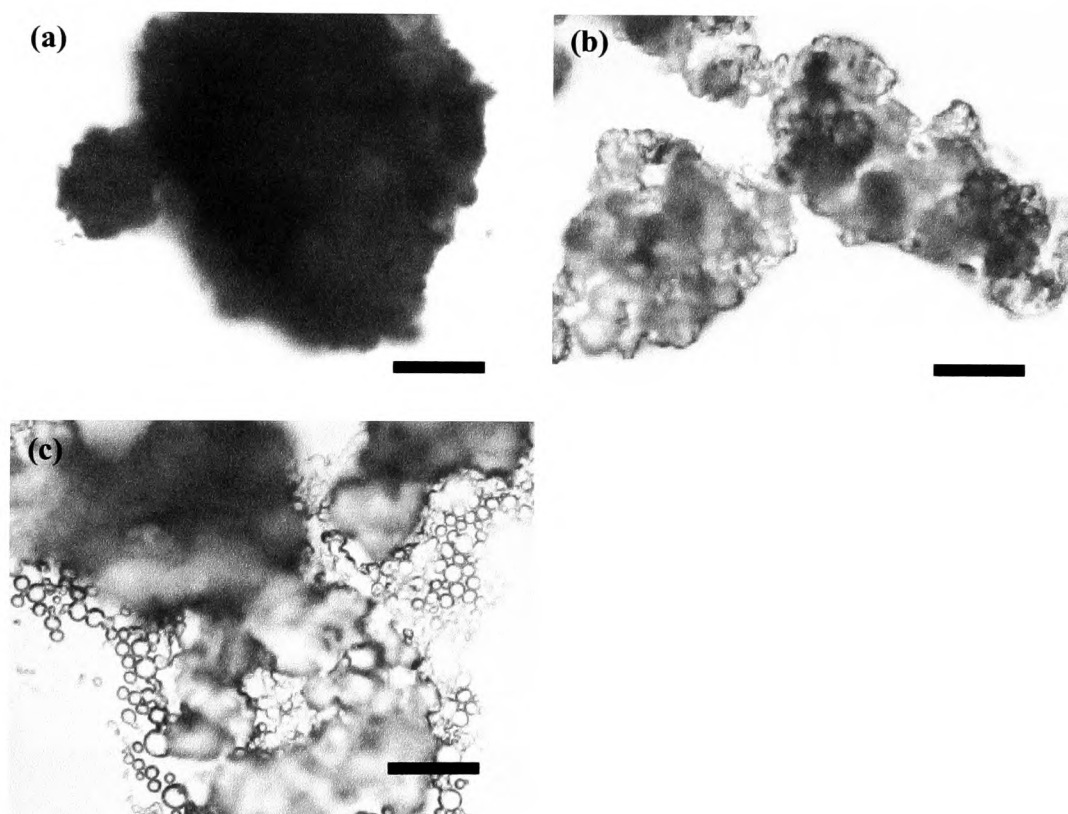
The maximum concentration of oil able to be encapsulated in a powdered emulsion was investigated by reducing the initial emulsion dilution, before blending it with the hydrophobic silica particles. This was meant to increase the oil fraction in the powdered emulsions from 0.05 to 0.5. As Figure 8.12 shows, the resulting materials differed a lot in appearance. The emulsion at $\Phi_o = 0.1$ gave a soufflé-like material with a small volume of dry emulsion at the top and some resolved emulsion at the bottom, similar to the material obtained with 30 s blending in section 8.3.2 (Figure 8.12(a)). Those at $\Phi_o = 0.5$ (non-diluted) and at $\Phi_o = 0.25$ produced emulsion-like materials, which seemed thickened by the silica particles, with a grainy like consistency for the non-diluted emulsion system (Figures 8. 12(b) and (c)).

Figure 8.12. Photographs of 5-minute old tricaprylin-water-air materials stabilised with 5 wt.% silica particles at 14% SiOH. Tricaprylin-in-water emulsions were initially stabilised by 3 wt.% of 80% SiOH silica particles and diluted either to $\Phi_o = 0.1$ (a and d) or $\Phi_o = 0.25$ (b and e) or (c and f) not diluted ($\Phi_o = 0.5$) before being mixed for 5 s in a blender jug at 25000 rpm with the hydrophobic silica particles. Photographs show the (a-c) side or (e) top of the vessels, or (d and f) a pile or the resulting material.



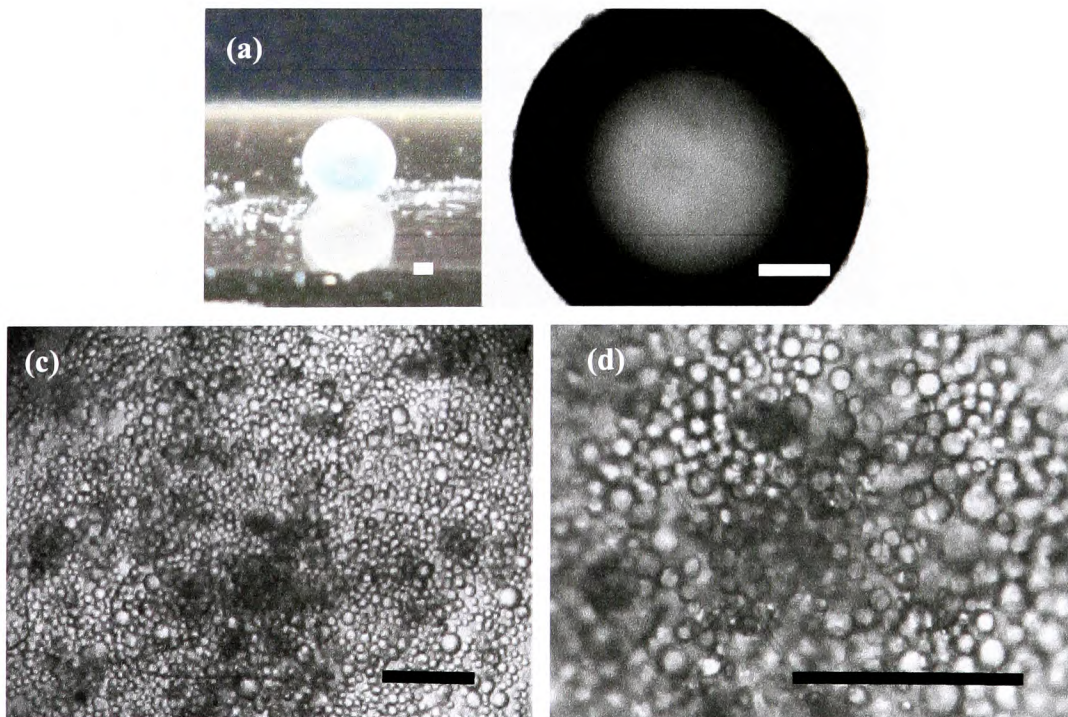
These latter two materials are more likely to be formed as a result of the silica aggregates being wet by the larger volume of tricaprylin in the emulsions, as shown in Figure 8.13. However, the material formed at $\Phi_o = 0.1$ is similar to the soufflé/powdered emulsion in Figure 8.10.

Figure 8.13. Optical microscopy images of 5-minute old tricaprylin-water-air materials stabilised with 5 wt.% silica particles at 14% SiOH. Tricaprylin-in-water emulsions were made with 3 wt.% of 80% SiOH silica particles and diluted either to $\Phi_o = 0.1$ (a) or $\Phi_o = 0.25$ (b) or (c) not diluted ($\Phi_o = 0.5$) before being mixed for 5 s in a blender jug at 25000 rpm with hydrophobic silica particles. Scale bars represent 160 μm .



Although the encapsulation of high oil content proved difficult through blender homogenisation, it was observed to be achievable with liquid marbles: Figure 8.14 displays a photograph and microscopy images of the liquid marble formed by rolling a drop of non-diluted emulsion ($\Phi_o = 0.5$) onto hydrophobic silica particles (14% SiOH). The emulsion drops were observed through the silica particle layer, and they appear unchanged compared with the initial emulsion formed, shown in Figure 8.2(c). The formation of a stable liquid marble with the same systems which gave a thickened emulsion in Figure 8.12(c) is solely due to the method of production: liquid marble preparation does not involve high shear, which can break the particle-stabilised oil drops. Hence there is no free oil to wet the hydrophobic silica which stabilises the liquid marbles, and they remain at the fluid surface. It seems therefore that high oil content powdered emulsions may be possible through utilisation of a lower shear process which leaves the internal oil drops intact.

Figure 8.14. (a) Photograph and (b-d) optical microscopy images of a 5-minute old tricaprylin-in-water-in-air liquid marble stabilised with 14% SiOH silica particles viewed from the (a) side or (b-d) top. The tricaprylin-in-water emulsion was stabilised by 3 wt.% of 80% SiOH silica particles and remained undiluted ($\Phi_o = 0.5$). Scale bars represent 400 μm .



8.4 Conclusions

The production of a powdered emulsion has been achieved by optimising the system composition and homogenisation processes. The oil-in-water emulsion to be encapsulated was optimised by varying the wettability of the stabilising particles used and their concentration: a tricaprylin-in-water emulsion stabilised with 3 wt.% silica particles at 80% SiOH proved ideal due to its complete stability over several days and small emulsion drops. The emulsion was then diluted with Milli-Q water and homogenised using a blender in the presence of 5 wt.% hydrophobic silica particles. The precise hydrophobicity of the silica particles and the time of blending were changed in order to obtain a powdered emulsion: silica particles with low silanol content (14%) and a short blending time (5 s) were found to be required to form stable dry emulsions. Longer homogenisations of around 30 s resulted in a soufflé-like material (consisting of areas of powdered emulsion and excess emulsion) probably through release of internal oil from the emulsion affecting particle desorption at the air-emulsion interface.

Although liquid marbles stabilised with 14% SiOH silica particles can encapsulate an oil-in-water emulsion at $\Phi_o = 0.5$, the equivalent powdered emulsion was not successfully produced by blending. The high shear of the blending, in combination with the increased oil content, probably results in emulsion breakdown and powdered emulsion destabilisation.

8.5 References

1. P. Aussillous and D. Quere, *Nature*, **411**, 924 (2001).
2. B. P. Binks and R. Murakami, *Nat. Mater.*, **5**, 865 (2006).
3. B. O. Carter, D. J. Adams and A. I. Cooper, *Green Chem.*, **12**, 783 (2010).
4. B. O. Carter, W. X. Wang, D. J. Adams and A. I. Cooper, *Langmuir*, **26**, 3186 (2010).
5. M. Dandan and H. Y. Erbil, *Langmuir*, **25**, 8362 (2009).
6. D. Dupin, S. P. Armes and S. Fujii, *J. Am. Chem. Soc.*, **131**, 5386 (2009).
7. R. Murakami and A. Bismarck, *Adv. Funct. Mater.*, **20**, 732 (2010).
8. B. P. Binks and A. Rocher, *J. Colloid Interface Sci.*, **335**, 94 (2009).
9. B. P. Binks and S. O. Lumsdon, *Langmuir*, **16**, 3748 (2000).
10. B. P. Binks and C. P. Whitby, *Langmuir*, **20**, 1130 (2004).

CHAPTER 9 SUMMARY OF CONCLUSIONS AND FUTURE WORK

9.1 Conclusion

This thesis has advanced the understanding of particle behaviour at fluid-fluid interfaces, by studying particle adsorption in systems such as emulsions, foams or other materials, which are stabilised solely by them. The potential toxicity of surfactant-stabilised materials has resulted in the need to investigate other emulsifiers, hence materials stabilised solely by particles have become of great interest. Particle-stabilised material stability depends mainly on the adsorption/desorption of a particle from the fluid interface. This mechanism is linked to the particle wettability, which can in turn be affected by the temperature, the pH, or the liquid type used. This thesis has investigated particle behaviour through six different sections ranging from particle-stabilised emulsions to particle-stabilised foams, including the production of novel materials such as powdered emulsions.

Stimuli-responsive particles, use to produce stimuli-responsive materials has been lately considered of interest particularly for bio-medical applications. The effect of temperature has been studied here and shown to have a strong effect on the stability of microwax particle-stabilised water-in-oil emulsions. Separation of wax-stabilised emulsions has been triggered by increasing the storing temperature of these emulsions: the particles adsorbed to the interface were unable to hinder coalescence when they melted. However, really stable emulsions were observed to form when homogenised at elevated temperature with the same wax particles, as surface-active molecules released from the particles adsorbed at the oil-water interface and stabilised it. Emulsions stabilised with PLGA biodegradable polymer particles were observed to undergo analogous separation, which happen more as an effect of time than as one of temperature. The “PLGA particle-stabilised” oil-in-water emulsions destabilised over time, likely due to degradation of the polymer, ultimately causing desorption of the particle from the interface. It was also observed that modification of the polymer particle surface, by grafting pH-sensitive COOH and NH₂ groups hindered emulsion separation. While the non-modified PLGA particle-stabilised emulsion displayed phase separation, the ones stabilised with the group-modified

particles were stable over a large range of pH for more than two years. The particle modification was believed to slow, or totally hinder, particle degradation. Another stimuli-responsive material investigated was that of emulsions stabilised by sporopollenin particles. The sporopollenin particles, originating from natural *Lycopodium clavatum* spores, were observed to display a change in charge and wettability with pH. This caused an emulsion transitional inversion from oil-in-water at their high natural pH (~ 9.5) to water-in-oil at low pH. The type of oil used was also seen to affect the pH of inversion: affecting the particle contact angle, the tricaprylin gave preferentially water-in-oil emulsion, while the dodecane and isopropyl myristate (IPM) preferred to form oil-in-water. Interestingly, the sporopollenin particles also exhibited preferred orientation around water droplets of sporopollenin-stabilised emulsion: the anisotropic sporopollenins orientate with their hemispherical side toward the oil either for a better packing geometry or due to a wettability difference.

New particle-stabilised material production has also been achieved during this study. An attempt to produce novel emulsion drop architectures was made using emulsion heteroaggregation. Although aggregation of oppositely-charged Ludox-stabilised emulsion drops has been found difficult to obtain, the importance of pH, method used for mixing and excess free particle concentration in the continuous phase has been demonstrated. The pH range over which the emulsions stabilised by Ludox particles were stable was witnessed to be larger for IPM than for dodecane as the oil phase, caused by the change in particle contact angle. The mechanical stirring used to mix these emulsions caused coalescence and so was replaced by a gentle handshaking. In systems containing mixtures of Ludox-stabilised emulsions, an increase in excess particle concentration was witnessed to decrease the stability of the mixture, by enhancing coalescence. Some evidence of drop aggregations was shown when the number ratio of small to large drops was varied. Another example of a new material generated in this study was that of tetrafluoroethylene (TFE) particle-stabilised non-aqueous foam. Oligomeric and polymeric TFE microparticles were observed to disperse in low surface tension oil which wet them, but to stabilise air bubbles when aerated with intermediate surface tension oil, and to form a powder like material with really high surface tension liquids. The produced foams were

stable to coalescence and disproportionation, and large volumes of foam were produced at high particle concentration, in line with observations made of particle-stabilised emulsions. The size and shape of the TFE particles slightly affected the foam formed, as the larger particles stabilised larger bubbles and the smaller particles stabilised larger foam volumes. Freeze fracture electron microscopy was used in order to observe the close-packed arrangement of particles at the air-oil surface.

Finally, production of a powdered emulsion was attempted by following the protocol to make “dry water”. For this purpose, oil-in-water emulsions were produced stabilised by very hydrophilic fumed silica particles. These emulsions were then blended with very hydrophobic particles, resulting in an encapsulation of emulsion drops into particles. However, the blending time was found to be of great importance: a short time of blending produced a dry powder material, while further blending caused the material to change through soufflé-like to a foam-like material. It was observed that encapsulation of high volume fractions of oil within the powdered material was difficult: upon increasing the oil volume fraction the material formed changed from a powdered emulsion to a simple emulsion thickened with particles, the emulsion capsules breaking and releasing the emulsion droplets. However, it was shown that high oil volume fraction macroscopic capsules can be obtained with liquid marbles of the silica particle-stabilised emulsions.

9.2 Future work

As described in Chapter 3, wax-stabilised emulsions were observed to destabilise when the temperature was increased after emulsification. Destabilisation occurred because the melting particles could not hinder coalescence anymore at high temperature. However, increasing the temperature of the emulsion and cooling them down has not been tried, and it is believed that formation of wax capsules of water could be formed that way.¹ An easy production of such robust capsules could be applied in cosmetic products for the slow or targeted release of water soluble active ingredients. The effect of emulsification temperature on emulsions stabilised with triglyceride crystals was investigated, but not the effect of increasing the temperature of the emulsion formed at room temperature. It is believed that the emulsion would

destabilise really quickly at the melting temperature of the crystals. The possibility to form triglycerides capsules from these emulsions could also be investigated.

The stability of emulsions stabilised by the PLGA, PLGA-COOH and PLGA-NH₂ with time was monitored over 24 months, for consistency, the stability of the emulsions made with PLGA particles of high L:G ratio should be monitored over the same length of time, to find out if the L:G ratio affects the emulsion destabilisation. The effect of temperature on the emulsion degradation should also be investigated, as the PLGA particles can be used in pharmaceutical products for drug delivery, and the temperature of the skin (if the product is a topical medication) and that of the body (for the other medications) are different.

The heteroaggregation of oppositely charged emulsion drops was found difficult to achieve, it is believed that more stable emulsions, like the one made for production of the powdered emulsion with fumed silica particles, or smaller drops and higher charge, could enable better heteroaggregation. However, emulsions made with fumed silica particles would only be negatively charged; a charge reversal could be obtained by either Ludox CL particles or positive polyelectrolytes.²

Sporopollenin particles were observed to adsorb at the oil-water and air-water interface, but as they might be porous, it is possible that the sporopollenin particles contain water, oil or both inside, replacing the air. It would be interesting to study if air filled sporopollenins, adsorb differently to the fluid interface compared to water and oil filled particles. As the type of emulsion stabilised with sporopollenins depends on the pH of the dispersion, it might be possible to destabilise a sporopollenin-stabilised emulsion by changing its pH, enabling triggered release of the emulsion dispersed phase; this could also be an additional investigation.^{3, 4} Functionalising the sporopollenin particles, by adding a controlled quantity of charged groups on their surface, might enable control of the pH of inversion of the emulsion type. As the sporopollenin can be used as capsule, it might also be interesting to load them with reactant, and dissolve another reactant in the water phase of the emulsion, to use the emulsion drops as mini-reactors or dual compartment capsules.^{5, 6}

Achieving control over non-aqueous foam stability would be interesting, studying the stability of particles stabilised oil foams as function of parameters like particle dispersion, temperature or addition of oil soluble surfactants might enable to find a way to do it. The powdered emulsion was found to only be stable for low content of oil. It is of importance to find the right parameters or method to encapsulate more oil into the powder, perhaps by using OTFE particles with a lower shear.⁷

9.3 References

1. M. Mellema, W. A. J. Van Benthum, B. Boer, J. Von Harras and A. Visser, *J. Microencapsul.*, 23, 729 (2006).
2. F. Simon, E. S. Dragan and F. Bucatariu, *React. Funct. Polym.*, 68, 1178 (2008).
3. B. P. Binks, R. Murakami, S. P. Armes and S. Fujii, *Langmuir*, 22, 2050 (2006).
4. S. Fujii, D. P. Randall and S. P. Armes, *Langmuir*, 20, 11329 (2004).
5. D. Fiordemondo and P. Stano, *ChemBioChem*, 8, 1965 (2007).
6. H. C. Shum, A. Bandyopadhyay, S. Bose and D. A. Weitz, *Chem. Mat.*, 21, 5548 (2009).
7. R. Murakami and A. Bismarck, *Advanced Functional Materials*, 20, 732 (2010).